frontiers | Research Topics

Women in neuropharmacology 2021

Edited by
Divya Vohora and Nidhi Agarwal

Published in
Frontiers in Pharmacology
Frontiers in Neuroscience

ISSN 1664-8714
ISBN 978-2-8325-2259-2
DOI 10.3389/978-2-8325-2259-2

About Frontiers

Frontiers is more than just an open access publisher of scholarly articles: it is a pioneering approach to the world of academia, radically improving the way scholarly research is managed. The grand vision of Frontiers is a world where all people have an equal opportunity to seek, share and generate knowledge. Frontiers provides immediate and permanent online open access to all its publications, but this alone is not enough to realize our grand goals.

Frontiers journal series

The Frontiers journal series is a multi-tier and interdisciplinary set of open-access, online journals, promising a paradigm shift from the current review, selection and dissemination processes in academic publishing. All Frontiers journals are driven by researchers for researchers; therefore, they constitute a service to the scholarly community. At the same time, the *Frontiers journal series* operates on a revolutionary invention, the tiered publishing system, initially addressing specific communities of scholars, and gradually climbing up to broader public understanding, thus serving the interests of the lay society, too.

Dedication to quality

Each Frontiers article is a landmark of the highest quality, thanks to genuinely collaborative interactions between authors and review editors, who include some of the world's best academicians. Research must be certified by peers before entering a stream of knowledge that may eventually reach the public - and shape society; therefore, Frontiers only applies the most rigorous and unbiased reviews. Frontiers revolutionizes research publishing by freely delivering the most outstanding research, evaluated with no bias from both the academic and social point of view. By applying the most advanced information technologies, Frontiers is catapulting scholarly publishing into a new generation.

What are Frontiers Research Topics?

Frontiers Research Topics are very popular trademarks of the *Frontiers journals series*: they are collections of at least ten articles, all centered on a particular subject. With their unique mix of varied contributions from Original Research to Review Articles, Frontiers Research Topics unify the most influential researchers, the latest key findings and historical advances in a hot research area.

Find out more on how to host your own Frontiers Research Topic or contribute to one as an author by contacting the Frontiers editorial office: frontiersin.org/about/contact

Women in neuropharmacology: 2021

Topic editors
Divya Vohora — Jamia Hamdard University, India
Nidhi Agarwal — Jamia Hamdard University, India

Citation
Vohora, D., Agarwal, N., eds. (2023). *Women in neuropharmacology: 2021*. Lausanne: Frontiers Media SA. doi: 10.3389/978-2-8325-2259-2

The authors declare that the research was conducted in the absence of any commercial or financial relationships that could be construed as a potential conflict of interest

Table of contents

frontiers | Frontiers in Pharmacology

TYPE Editorial
PUBLISHED 12 April 2023
DOI 10.3389/fphar.2023.1198876

OPEN ACCESS

EDITED AND REVIEWED BY
Nicholas M. Barnes,
University of Birmingham,
United Kingdom

*CORRESPONDENCE
Divya Vohora,
divyavohora@gmail.com

RECEIVED 02 April 2023
ACCEPTED 03 April 2023
PUBLISHED 12 April 2023

CITATION
Vohora D and Agarwal N (2023), Editorial: Women in neuropharmacology: 2021. *Front. Pharmacol.* 14:1198876. doi: 10.3389/fphar.2023.1198876

Editorial: Women in neuropharmacology: 2021

Divya Vohora[1]* and Nidhi Agarwal[2]

[1]Neurobehavioral Pharmacology Laboratory, Department of Pharmacology, School of Pharmaceutical Education and Research (SPER), Jamia Hamdard, New Delhi, India, [2]Centre for Translational and Clinical Research, School of Chemical and Life Sciences (SCLS), Jamia Hamdard, New Delhi, India

KEYWORDS

neuropharmacology, neurodegenarative disease, psychiatric diseases, CNS–central nervous system, women in science

Editorial on the Research Topic
Women in neuropharmacology: 2021

Introduction

Neuropharmacology is a field of study focussing on understanding the actions of drugs affecting the nervous system and encompassing all aspects of research including, *in vitro*, *in vivo* or clinical research on drugs that could potentially treat neurological and psychiatric disorders. Considering the complexity of the nervous system and limited understanding of the etiopathogenesis of most neurological diseases particularly neurodegenerative diseases, there is a critical need to encourage research in this direction. Additionally, there are still unmet needs when it comes to drug therapies for these conditions.

Women in Neuropharmacology 2021 is a part of the inaugural series of article collection for the Frontiers in Pharmacology Research Topics with an aim to acknowledge and promote the contributions of woman scientists in all areas of Neuropharmacology. This is because as per UNESCO fact sheet 2020, there is a significant gender gap for women in science and women researchers represent only 30% of the researchers worldwide (UNESCO Institute for Statistics, 2020). This article collection is a small effort to bridge this gap to highlight the important research findings of woman scientists from all over the world. The collection comprises of 5 original research articles, 3 mini reviews and 1 systematic review from woman authors from 7 countries–Brazil, Denmark, Greece, Japan, New Zealand, UK, USA.

The Research Topic covers the diverse areas on Neuropharmacology including identifying or reviewing current targets and challenges associated with drug treatments in neurodegenerative diseases such as Parkinson's disease, Alzheimer's disease and other neurological diseases such as Schizophrenia, neuropathic pain, depression, learning and memory etc. (Figure 1).

The major highlights from the 9 articles are summarized below:

1. Kappa opioid receptor (KOR) agonists were studied in mice for paclitaxel-mediated neuropathic pain by Kelly Paton from Victoria University of Wellington, New Zealand and coworkers. The major highlight of the study was that the authors evaluated sex differences in view of the fact that women have increased pain sensitivity and respond differently to pain medications and that majority of preclinical studies have been

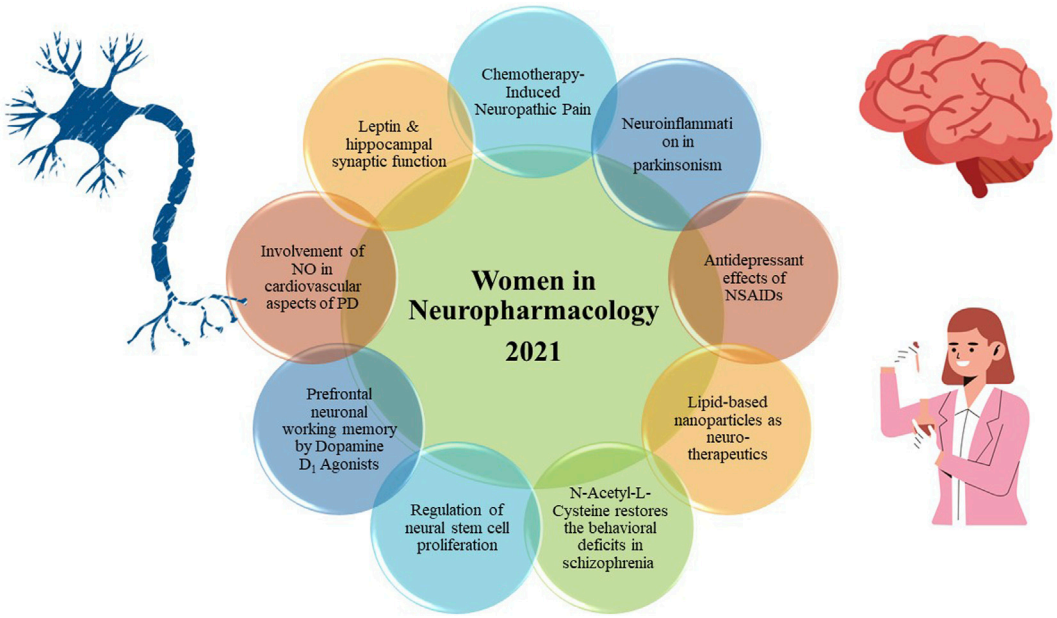

FIGURE 1
Highlights of articles from Women in Neuropharmacology 2021 Collection.

performed in male animals only. The increased antinociceptive effect observed in females was related to a slower elimination in pharmacokinetic studies (Paton et al.). The study indeed complements the recent guidelines by NIH and ARRIVE where researchers must consider sex as a factor while designing, analysis or reporting of research findings, whether preclinical or clinical.

2. Leptin, adipocyte derived hormone, is widely known to have a fundamental role in regulating energy balance. However, over the past several years, leptin role has been reported to be more widespread as leptin receptors are not just restricted to hypothalamus but have been identified in hippocampus and hippocampal synapses. Leptin therefore shows several central actions including precognitive effects. Also, alterations in leptin levels have been linked with several neurodegenerative diseases. Jenni Harvey from University of Dundee, UK highlighted some of these actions and mechanisms thereof through a mini review (Harvey).
3. Yang Yang and coworkers from Penn State College of Medicine, PA, USA (Yang et al.) studied the signalling mechanisms for dopamine D1 receptor agonists at the neuron population level. This is because of the differential effects of D1 agonists on memory exhibiting an inverted-U type response. Their findings suggested that D1-related regulation of memory can be differentially modified by using functionally selective ligands. The authors emphasized that pharmacokinetics and signalling must be considered beyond receptor selectivity.
4. The mini review by Martins-Pinge and coworkers from Universidade Estadual de Londrina- UEL, Londrina, Brazil (Martins-Pinge et al.) presented the role of nitric oxide (NO) in cardiovascular and autonomic dysfunctions observed in Parkinson's disease. Based on the review, the hypothalamic nuclei were reported to be the target for NO alterations.
5. Maria Tsakiri from National and Kapodistrian University of Athens, Athens, Greece (Tsakiri et al.) presented a mini review on lipid-based advanced RNA-delivery platforms including Liposomes and lipoplexes, solid lipid nanoparticles and lipid nanoparticles, their advantages, disadvantages. Though there were challenges, lipidic nanoparticles for RNA delivery demonstrate potential in the treatment of neurodegenerative disorders, such as Alzheimer's disease, or brain tumors like glioblastoma.
6. Bay Richter and coworker from Aarhus University, Denmark (Bay-Richter and Wegener) performed a systematic review of preclinical studies of NSAIDs on depressive-like behavior in rodents whereby 36 meeting the inclusion criteria were reviewed. One of the observations was that majority of the studies were conducted in male animals and very few in female animals again highlighting the need to have future studies conducted in both sexes. Selective COX-2 inhibitors in the stress models provided most robust antidepressant effect as compared to the non-selective ones. The mechanisms suggested were related to attenuation of neuroinflammation, HPA Axis dysregulation and alterations of monoamines.
7. Cunha from Universidade Federal de São Paulo, São Paulo, Brazil and coworkers (Cunha et al.) investigated and proved the role of neuroinflammation in repeated low-dose reserpine-induced model of Parkinson's disease in Wistar rats using immunostaining for astrocytes and microglia markers and cytokines expression. The neuroinflammation was observed in regions involved in the pathophysiology of PD and reversed 20 days later.

8. Lopes-Rocha and co-workers from Universidade Federal do ABC, Brazil (Lopes-Rocha et al.) reported the antipsychotic effects of antioxidant N-acetyl-L-cysteine (NAC) in metilazoximetanol acetate (MAM)-induced neurodevelopmental model of schizophrenia in Wistar rats through a mechanism that involves nitric oxide. Based on the findings, the authors suggested oxidative stress to be a potential target for schizophrenia.
9. Recent research has shed new light on the regulation of NSC proliferation and survival by Protein Arginine Methyl Transferase-1 (PRMT-1). PRMT-1 is necessary for NSC proliferation, and loss of PRMT-1 activity leads to decreased NSC proliferation and survival. The research has important implications for the development of potential therapies for neurological disorders. The research conducted by a team of scientists led by Misuzu Hashimoto at the Gifu University of Japan (Hashimoto et al.) examined NSCs derived from Nestin-Cre mediated *Prmt1*-deficient mouse embryo both *in vitro* and *in vivo*. The study concluded that PRMT1 plays a cell-autonomous role in the survival and proliferation of embryonic NSCs.

Concluding remarks

Research in neuropharmacology is essential for our understanding of the intricate nature of nervous system and developing new treatments for neurological and psychiatric diseases. This article collection highlighted the novel CNS actions of some of the key targets such as leptin, PRMT-1, KOR agonists; the new indications of existing treatments such as NSAIDs in depression, NAC in psychosis, D1 receptor agonists in memory; role of neuroinflammation and NO in animal model and addressing the complications of Parkinson's disease respectively; and lipid-based advanced RNA-delivery platforms for neurodegenerative diseases. Further, one of the articles reported that there might be differential effect of drugs when studied in male and female animal models of disease. So, as far as we encourage to bridge gender gap in science, we must also bridge this gap in experimental research and consider sex as an important biological variable.

Author contributions

All authors listed have made a substantial, direct, and intellectual contribution to the work and approved it for publication.

Acknowledgments

We acknowledge the women neuropharmacologists who contributed articles to this Research Topic. We are grateful to Frontiers Team for initiating the series for encouraging and promoting women researchers.

Conflict of interest

The authors declare that the research was conducted in the absence of any commercial or financial relationships that could be construed as a potential conflict of interest.

Publisher's note

Reference

UNESCO Institute for Statistics (2020). *Women in science, fact sheet No. 60 june 2020 FS/2020/SCI/60*. Available at: http://uis.unesco.org.

frontiers in Pharmacology

ORIGINAL RESEARCH
published: 18 February 2022
doi: 10.3389/fphar.2022.813562

Sex Differences in Kappa Opioid Receptor Agonist Mediated Attenuation of Chemotherapy-Induced Neuropathic Pain in Mice

*Kelly F. Paton[1], Dan Luo[2], Anne C. La Flamme[1,3], Thomas E. Prisinzano[2] and Bronwyn M. Kivell[1]**

[1]School of Biological Sciences, Centre for Biodiscovery, Victoria University of Wellington, Wellington, New Zealand, [2]Department of Pharmaceutical Sciences, University of Kentucky, Lexington, KY, United States, [3]Malaghan Institute of Medical Research, Wellington, New Zealand

Chemotherapy-induced neuropathic pain is a common side effect for cancer patients which has limited effective treatment options. Kappa opioid receptor (KOR) agonists are a promising alternative to currently available opioid drugs due to their low abuse potential. In the current study, we have investigated the effects of Salvinorin A (SalA) analogues, 16-Ethynyl SalA, 16-Bromo SalA and ethyoxymethyl ether (EOM) SalB, and in a preclinical model of paclitaxel-induced neuropathic pain in male and female C57BL/6J mice. Using an acute dose-response procedure, we showed that compared to morphine, 16-Ethynyl SalA was more potent at reducing mechanical allodynia; and SalA, 16-Ethynyl SalA, and EOM SalB were more potent at reducing cold allodynia. In the mechanical allodynia testing, U50,488 was more potent in males and SalA was more potent in females. There were no sex differences in the acute cold allodynia testing. In the chronic administration model, treatment with U50,488 (10 mg/kg) reduced the mechanical and cold allodynia responses to healthy levels over 23 days of treatment. Overall, we have shown that KOR agonists are effective in a model of chemotherapy-induced neuropathic pain, indicating that KOR agonists could be further developed to treat this debilitating condition.

Keywords: paclitaxel, kappa opioid receptor, salvinorin A, chemotherapy-induced neuropathic pain, sex differences

OPEN ACCESS

Edited by:
Divya Vohora,
Jamia Hamdard University, India

Reviewed by:
Enrique Portillo-Salido,
Welab Barcelona, Spain
Vinod Tiwari,
Indian Institute of Technology (BHU), India

****Correspondence:***
Bronwyn M. Kivell
bronwyn.kivell@vuw.ac.nz

Specialty section:
This article was submitted to Neuropharmacology, a section of the journal Frontiers in Pharmacology

Received: *11 November 2021*
Accepted: *25 January 2022*
Published: *18 February 2022*

Citation:
Paton KF, Luo D, La Flamme AC, Prisinzano TE and Kivell BM (2022) Sex Differences in Kappa Opioid Receptor Agonist Mediated Attenuation of Chemotherapy-Induced Neuropathic Pain in Mice. Front. Pharmacol. 13:813562. doi: 10.3389/fphar.2022.813562

INTRODUCTION

Chemotherapy-induced peripheral neuropathy (CIPN) is a common side effect of treating cancer (Sisignano et al., 2014; Addington and Freimer, 2016) with 68% of chemotherapy patients reporting CIPN within the first month of treatment (Seretny et al., 2014). CIPN is often characterized by spontaneous tingling or burning pain, hypersensitivity to mechanical and cold stimuli, and numbness (Forman, 1990; Dougherty et al., 2004). CIPN can be very debilitating, significantly impacting the quality of life and independence of cancer sufferers (Beijers et al., 2014; Mols et al., 2014). Often CIPN is identified as the reason for limiting either the dose or length of chemotherapy treatment and in severe CIPN cases, chemotherapy may be terminated (Holmes et al., 1991; Rowinsky et al., 1993); however, CIPN may persist for months following cessation of chemotherapy (van den Bent et al., 1997). Chemotherapy drugs that induce CIPN include vinca alkaloids, platinum derivatives and taxanes (Jaggi et al., 2011; Sisignano et al., 2014; Ewertz et al., 2015). Paclitaxel is a

taxane chemotherapeutic widely used to treat solid tumors such as ovarian, breast, cervical, prostate, non-small cell lung, gastric, head and neck, Kaposi's sarcoma, and pancreatic cancers (Khanna et al., 2015).

The pathogenesis of paclitaxel-induced neuropathic pain involves dying-back axonal damage. This causes distal sensory axons to degenerate in the peripheral nervous system, and causes sensitization of nociceptive afferents leading to neuropathic pain symptoms in the hands and feet in a "stocking and glove"-type distribution (Forman, 1990; Dougherty et al., 2004). The American Society of Clinical Oncology clinical practice guideline states there are no recommended therapeutics for the prevention of CIPN as there is not sufficient or consistent evidence from any randomized placebo-controlled trials (Hershman et al., 2014; Loprinzi et al., 2020). For the treatment of established CIPN, the serotonin-norepinephrine reuptake inhibitor duloxetine is the only agent which is moderately recommended (Hershman et al., 2014; Loprinzi et al., 2020). Mu opioid receptor (MOR) analgesics, including hydrocodone, morphine, oxycodone, methadone, and fentanyl patches or tramadol are considered a third-line therapy (Finnerup et al., 2015; Grace et al., 2016); however, MOR agonists are still commonly used to treat CIPN, with a recent study finding that 97% of CIPN patients used opioid therapy (Shah et al., 2018).

MOR agonists are associated with many side effects and can induce hyperalgesia (Grace et al., 2016), respiratory depression (Pattinson, 2008; Dahan et al., 2010), tolerance (Chu et al., 2006; Uniyal et al., 2020), and addiction (Compton and Volkow, 2006). In comparison, kappa opioid receptor (KOR) agonists do not have rewarding effects (Vonvoigtlander et al., 1983), and are not associated with respiratory depression (Freye et al., 1983) or gastrointestinal transit (Porreca et al., 1984), and have potential to treat pain (Beck et al., 2019; Paton et al., 2020a). The naturally occurring KOR agonist, Salvinorin A (SalA), has been used as a chemical scaffold to produce analogues with greater metabolic stability and potency. We investigated two analogues with alterations at the carbon-16 position, 16-Ethynyl SalA and 16-Bromo SalA, and one analogue at the carbon-2 position, ethoxymethyl ether Salvinorin B (EOM SalB). We have previously shown that 16-Ethynyl SalA and 16-Bromo SalA have antinociceptive effects in preclinical models of pain in mice, have a longer duration of action than SalA, and have improved side effect profiles (Paton et al., 2020b). Therefore, in the current study we have assessed the effect of 16-Ethynyl SalA, 16-Bromo SalA and EOM SalB in mice with paclitaxel-induced neuropathic pain. Furthermore, the majority of preclinical studies of the paclitaxel-induced neuropathic pain model have used male animals (Naji-Esfahani et al., 2016); however, in chronic pain studies, women typically have increased pain sensitivity and higher prevalence of clinical pain (Mogil, 2012; Bartley and Fillingim, 2013), and respond differently to pain medications (Pieretti et al., 2016). Therefore, we sought to understand the sex differences in the progression of paclitaxel-induced neuropathic pain and the differences in KOR treatment outcomes.

MATERIALS AND METHODS

Animals

Female and male C57BL/6J mice (8 + weeks old) were used for all experiments. Animals were bred and housed at the Victoria University of Wellington (VUW) Animal Facility, Wellington, New Zealand. Animals were originally sourced from the Jackson Laboratories (Bar Harbour, ME, United States). All animals were group-housed (maximum 5 mice/cage) in a temperature (20–22°C) and humidity (55%) controlled environment. The animals were maintained on a 12-h light/dark cycle with lights on at 7 a.m. Access to food and water was provided *ad libitum* except during experimental sessions. For all paclitaxel-induced neuropathic pain experiments, soft paper/pulp-based Carefresh Natural bedding (Masterpet, Lower Hutt, NZ) was used in the home cage to avoid any mechanical stimulation to the paw. Each cage had shredded nesting material as environmental enrichment.

All experimental procedures were undertaken during the light cycle and in presence of white noise. Animals were handled for at least 2 days before testing to acclimatise to handling and prevent stress during experimental procedures. Animals were habituated to the experimental room for 30 min each day. All procedures were carried out with the approval of the VUW Animal Ethics Committee (approval numbers 21480 and 25751). All procedures were carried out in agreement with the New Zealand Animal Welfare Act, 1999.

Drug Preparation

SalA was isolated and purified from *Salvia divinorum* leaves and assessed for purity (>98%) using high-performance liquid chromatography (HPLC) (Munro and Rizzacasa, 2003; Tidgewell et al., 2004). The SalA analogues were synthesized as previously described (Prevatt-Smith et al., 2011; Riley et al., 2014) and tested for purity (>95%) with HPLC. The prototypical KOR agonist U50,488 was purchased from Sigma-Aldrich (St. Louis, MO, United States) and morphine sulphate from Hospira NZ Ltd (Wellington, New Zealand). The compounds were dissolved in a vehicle containing DMSO, Tween-80 (Sigma-Aldrich), and 0.9% saline at a ratio of 2:1:7, respectively. The compounds were delivered at a volume of 10 µl/g of weight via intraperitoneal (i.p.) injection and delivered at 5 µl/g via subcutaneous (s.c.) injection in the dose-response experiments. The KOR antagonist *nor*-BNI (Sigma-Aldrich) was dissolved in 0.9% saline and injected s.c. 24 h before testing to selectively antagonize the KOR, as earlier pre-treatment intervals have been shown to also antagonize the MOR (Endoh et al., 1992; Kishioka et al., 2013).

Induction of Paclitaxel-Induced Neuropathic Pain

Paclitaxel (Taxol, Tocris Bioscience #RDS109750, Bristol, United Kingdom) was made fresh daily by dissolving in absolute ethanol, cremophor EL (Sigma-Aldrich) and 0.9% saline at a ratio of 1:1:18, respectively. Experimental procedures were as previously described (Deng et al., 2015;

Paton et al., 2017; Atigari et al., 2020). Mice were administered paclitaxel 4 mg/kg i.p. injections on four alternate days to give a cumulative dose of 16 mg/kg. Mechanical and cold allodynia were assessed every second day to measure the progression of paclitaxel-induced effects. Mice were placed in transparent plastic chambers upon a metal mesh stand. After a 20 min habituation to the apparatus, each hind paw was measured in duplicate for each type of stimulation, always beginning with mechanical testing. On days with behavioural measurements and a paclitaxel dose, measurements were always taken before the administration of paclitaxel.

Von Frey Filament Procedure

Mechanical allodynia was measured using a 20-piece set of Semmes Weinstein von Frey filaments (#58011, Stoelting, IL, United States) as previously described (Paton et al., 2017; Atigari et al., 2020). Filaments numbered from 2 to 9 were used, with testing always beginning with filament number 5. The filament was applied at a right angle to the plantar surface of the hind paw with enough force to produce a slight bend. The filaments were held for 3 s or until a positive withdrawal response was observed. Mechanical allodynia was measured using a simplified up-down method until 5 filaments had been administered (Bonin et al., 2014). Mechanical allodynia for each animal was calculated by averaging the paw withdrawal thresholds from duplicate values for each hind paw.

Acetone Test

Using a 1 ml syringe, a bubble of acetone was administered to the plantar surface of the hind paw with care not to cause any mechanical stimulation. The amount of time the animal reacted to the stimulus was recorded for 60 s following application. A positive reaction was defined as elevating, licking, biting or shaking of the paw. Two measurements were taken for each hind paw alternately, with 5 min between consecutive applications. Cold allodynia for each animal was calculated by averaging the duration of time spent responding to the acetone across the 4 applications.

Acute Dose-Response in Paclitaxel-Treated Mice

On day 15, the cumulative dose-response effects were assessed in the paclitaxel-treated mice using a within-animals design (Paton et al., 2017; Atigari et al., 2020). The KOR agonists, morphine, or equivalent volumes of the vehicle were administered via s. c. injection every 30 min at increasing concentrations to create cumulative doses, with the mechanical and cold allodynia measured 30 min following each dose. The effects were measured in each hind paw once for each dose.

Chronic Administration of Treatment in Mice With Paclitaxel-Induced Neuropathic Pain

The efficacy and tolerance effects of chronic administration of the KOR agonists were measured in mice with established paclitaxel-induced neuropathic pain. Following the measurements on day 15, animals were assigned to treatment groups to ensure an equivalent average mechanical allodynia score across all groups. The experimenter was blinded to the treatments each animal received. The doses used were based on the ED_{80} value obtained from the mechanical allodynia dose-response results. Animals were given daily i.p. injections starting on day 16. The treatments were as follows: 16-Ethynyl SalA, 3 mg/kg; 16-Bromo SalA, 4 mg/kg; U50,488, 10 mg/kg; morphine, 10 mg/kg; and vehicle. On all the even-numbered days the treatment was given 30 min before mechanical and cold allodynia testing.

Statistical Analysis

GraphPad Prism (version 7.03, GraphPad Software, La Jolla, CA, United States) and SPSS Statistics (version 25, IBM, Armonk, NY, United States) were used to determine statistical significance. Values represented as the mean ± standard error of the mean (SEM) and were considered significant when $p < 0.05$. The data sets were tested for normality using the D'Agostino and Pearson omnibus normality test. Comparison of multiple treatment data was analyzed using one-way analysis of variance (ANOVA) followed by Bonferroni post-tests. Comparisons of multiple effects were analyzed using two-way ANOVA followed by Bonferroni post-tests. Two-way repeated-measures ANOVA was used when one variable was measured over time.

Dose-response data were analyzed by creating a non-linear regression. A four-parameter variable slope with least-squares ordinary fit was used to fit the curve to the data sets. For mechanical allodynia, the top constraint was set no more than 9.5. For cold allodynia, the bottom constraint was set at no less than 0. The extra sum-of-squares F test with the bottom, top, $logED_{50}$ and hillslope parameters was used to compare the treatment curves, and with the null hypothesis that one curve fits all data sets. If the results showed a different curve fit for each data set, then the ED_{50} and E_{max} values were compared with one-way ANOVA analysis.

The effects of treatment, sex and time were analyzed with a three-way repeated-measures mixed ANOVA, with treatment and sex as between-subjects variables, and time as the within-subjects variable. The normality of the data was assessed with the Shapiro-Wilk test using the standardized residuals. The homogeneity of variances was measured using Levene's test of equality of error variances. If the data was non-normal and had unequal variances at some time points, then the data was transformed. The sphericity of the data was tested using Mauchly's test. If the $p < 0.05$, the assumption of sphericity was violated and the Greenhouse-Geisser correction was applied. The Bonferroni correction was applied for multiple families of comparisons and the adjusted α level reported.

RESULTS

This study aimed to understand the effects of KOR agonists (**Figure 1**) for the treatment of paclitaxel-induced neuropathic pain in male and female mice. Initially, we investigated the sex differences throughout the progression of the paclitaxel-induced neuropathic pain model. A three-way repeated-measures mixed ANOVA was run to understand the effects of treatment, sex, and

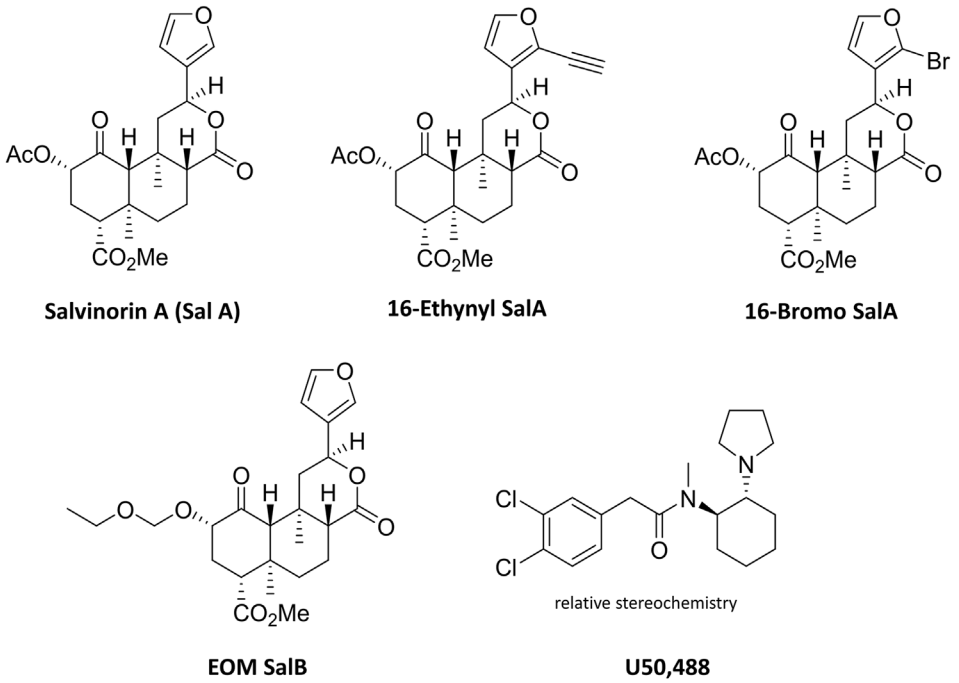

FIGURE 1 | Chemical structures of Salvinorin A, 16-Ethynyl SalA, 16-Bromo SalA, EOM SalB, and U50,488.

time on the mechanical withdrawal thresholds. The three-way interaction of treatment, sex and time was not statistically significant [$F_{(6.183,717.2)} = 2.053$, $p = 0.055$] (**Figure 2A**). There was a statistically significant two-way interaction between treatment and time [$F_{(6.183,717.2)} = 66.771$, $p < 0.0005$] and between treatment and sex [$F_{(1,116)} = 9.744$, $p = 0.002$]. Statistical significance of a simple main effect was accepted at a Bonferroni-adjusted alpha level of 0.006 due to multiple families of comparisons. There was a statistically significant simple main effect of treatment at days 4–15 ($p < 0.006$). The simple main effects of sex were not significant on any day. Overall, this shows that the paclitaxel treatment group was significantly different to the vehicle treatment group, but there were no sex differences.

A three-way repeated-measures mixed ANOVA was run to understand the effects of treatment, sex and time on the reaction times to the cold acetone stimulus. The three-way interaction was statistically significant [$F_{(6.618,767.7)} = 3.284$, $p = 0.002$] (**Figure 2B**). There was not a significant simple two-way interaction of treatment and sex at any time point ($p > 0.006$), however, there was a significant main effect of both treatment and sex on days 2–15 ($p < 0.006$). Overall, this means that there is an effect of paclitaxel treatment and an inherent difference between the sexes reaction to the cold stimulus, however, the effect of paclitaxel on each sex does not change over time.

Cumulative Dose-Response Effects of Kappa Opioid Receptor Agonists

The dose-response effects of the KOR agonists were measured to understand and compare the potency and efficacy of each drug in both sexes. All of the curves were analyzed separated for sex, showing that a different curve fits each data set for the treatment of mechanical [$F_{(22,450)} = 9.915$, $p < 0.0001$] and cold allodynia [$F_{(22,450)} = 13.33$, $p < 0.0001$] (**Figures 2D–G**). The potencies (ED_{50} values) were compared by treatment and sex (**Table 1**). For mechanical allodynia, treatment with U50,488 in males was more potent than females ($p = 0.0136$), whilst the opposite was found with SalA, and with treatment in females significantly more potent than males ($p = 0.0040$). Morphine, 16-Ethynyl SalA, 16-Bromo SalA, and EOM SalB had no significant difference between the sexes. When the male treatment groups were compared to morphine, only 16-Ethynyl SalA was significantly more potent ($p = 0.0152$). When compared to the female morphine treatment group, SalA ($p = 0.0098$) and 16-Ethynyl SalA ($p = 0.0242$) were significantly more potent.

For the treatment of cold allodynia, the two-way ANOVA found no interaction of sex and treatment [$F_{(5,450)} = 0.329$, $p = 0.8955$] (**Table 2**). Therefore, only the data with the combined sexes could be compared, showing SalA ($p = 0.0034$) and 16-Ethynyl SalA ($p < 0.0001$) had significantly more potent antinociceptive effects than morphine.

Antagonism of the Kappa Opioid Receptor

16-Ethynyl SalA, 16-Bromo SalA, and U50,488 were antagonized at the KOR by pre-treating with *nor*-BNI (**Figure 3**). One-way ANOVA analysis of the values at the final dose for 16-Ethynyl SalA, 16-Bromo SalA (10 mg/kg), and U50,488 (20 mg/kg) showed a significant effect of treatment for the mechanical [$F_{(5,51)} = 118.9$, $p < 0.0001$] (**Figure 3A**) and cold allodynia data [$F_{(5,51)} = 73.85$, $p < 0.0001$] (**Figure 3B**). Bonferroni post-

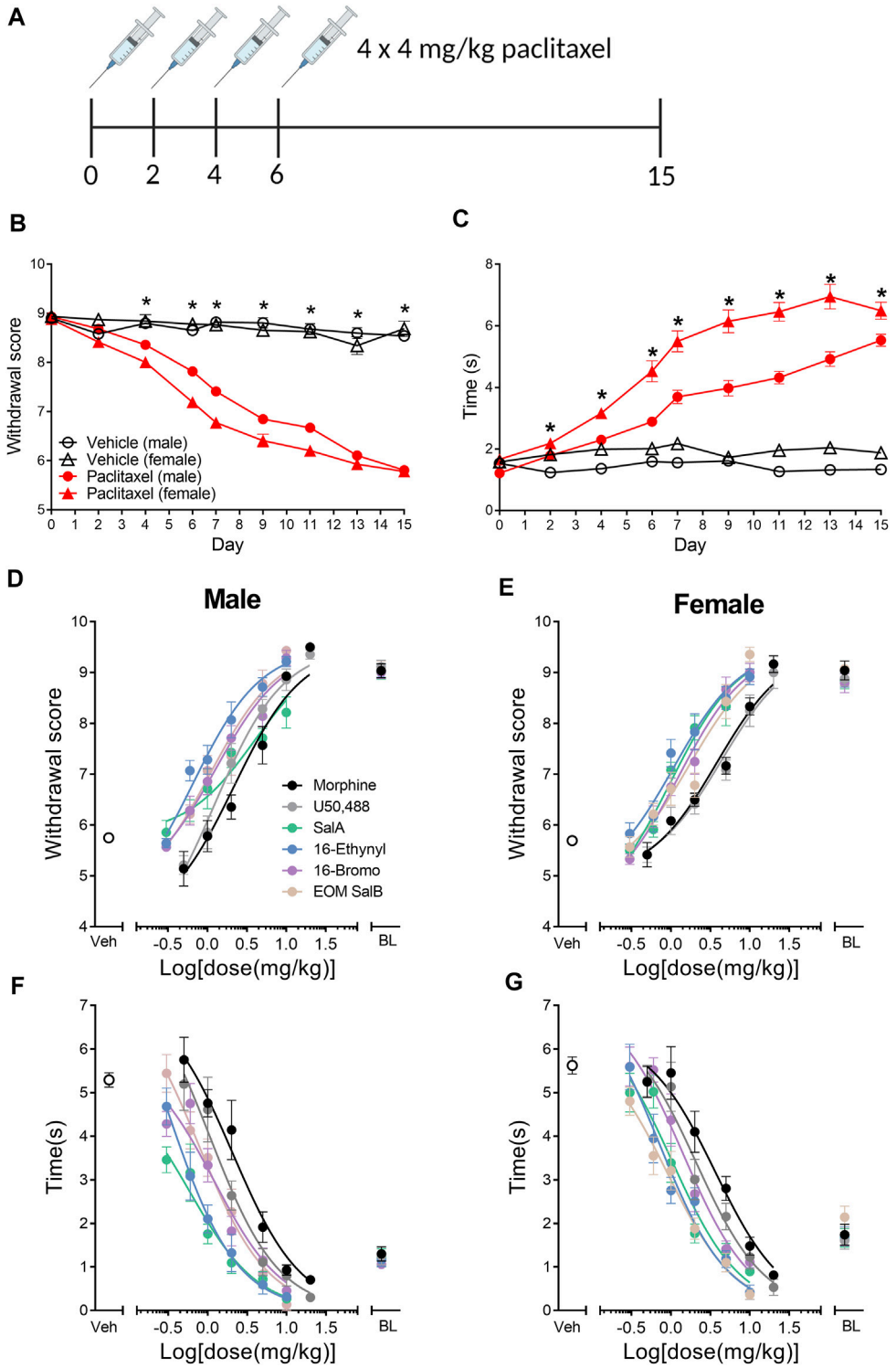

FIGURE 2 | Paclitaxel administration produces mechanical and cold allodynia in male and female C57BL/6J mice. **(A)** Paclitaxel was administered as 4 doses of 4 mg/kg and allodynia measured until day 15. Numbers underneath the timeline represent experimental days. **(B)** Paclitaxel administration produced mechanical allodynia on days 4–15, shown as a reduction in withdrawal score measured using von Frey filaments. There were no sex differences in the withdrawal scores. **(C)** Paclitaxel administration had a significant effect on days 2–15, with an increase in reaction time to a cold acetone stimulus. There was an effect of treatment and sex, and but no interaction of both factors, with females showing an increased reaction time in the vehicle and paclitaxel treatment groups compared to males. Three-way repeated measures mixed ANOVA. *$p < 0.006$. Vehicle-treated $n = 16–18$; paclitaxel-treated males $n = 50$, females $n = 36$. **(D–G)** Dose-response effects of morphine and the KOR agonists comparing male and female mice with established paclitaxel-induced neuropathic pain. Mechanical allodynia was measured in **(D)** males and **(E)** females. Cold allodynia was measured in **(F)** males and **(G)** females. Veh refers to paclitaxel-treated animals treated with vehicle. BL refers to pre-paclitaxel baseline values. $n = 6–8$. Values presented as mean ± SEM. Image in panel **(A)** created using BioRender.com.

TABLE 1 | Dose-response effects of the KOR agonists in female and male mice with established paclitaxel-induced mechanical allodynia. The potency (ED_{50}) of the opioid receptor agonists were measured in mice of both sexes. U50,488 had more potent effects in males compared to females, whereas SalA was more potent in females. When the KOR treatments for each sex were compared to morphine, 16-Ethynyl SalA was significantly more potent in males and females. SalA was more potent than morphine in females only. Non-linear regression analysis. Two-way ANOVA with Bonferroni post-tests. n = 6–7. n.s. = not significant, $^{*}p < 0.05$, $^{**}p < 0.01$.

Opioid receptor agonist	ED_{50} value (mg/kg)		$logED_{50}$ ± SEM		Two-way ANOVA comparisons					
	Male	Female	Male	Female	Male vs female		Male vs. Male treated with morphine		Female vs. Female treated with morphine	
Morphine	2.16	3.83	0.33 ± 0.11	0.58 ± 0.07	>0.9999	n.s.	—		—	
U50,488	1.23	4.38	0.09 ± 0.11	0.64 ± 0.09	0.0255	*	>0.9999	n.s.	>0.9999	n.s.
SalA	3.94	0.99	0.60 ± 0.12	−0.003 ± 0.101	0.0078	**	>0.9999	n.s.	0.0186	*
16-Ethynyl SalA	0.65	1.08	−0.19 ± 0.12	0.03 ± 0.13	>0.9999	n.s.	0.0283	*	0.0447	*
16-Bromo SalA	1.27	1.25	0.10 ± 0.01	0.10 ± 0.08	>0.9999	n.s.	>0.9999	n.s.	0.1636	n.s.
EOM SalB	1.07	1.76	0.031 ± 0.11	0.25 ± 0.11	>0.9999	n.s.	>0.9999	n.s.	>0.9999	n.s.

TABLE 2 | Dose-response effects of the KOR agonists in female and male mice with established paclitaxel-induced cold allodynia. Non-linear regression analysis was used to calculate the potency (ID_{50}) of the opioid receptor agonists in male and female mice. Two-way ANOVA showed there was no significant interaction of treatment and sex. Using the combined sex data, SalA and 16-Ethynyl SalA had more potent antinociceptive effects than morphine. The efficacy of the treatments were not significantly different. One-way ANOVA with Bonferroni post-tests. n = 6–7. n.s. = not significant, $^{**}p < 0.01$, $^{****}p < 0.0001$.

Opioid receptor agonist	ID_{50} value (mg/kg)		$logID_{50}$ ± SEM		ID_{50} value (mg/kg)	$logID_{50}$ ± SEM	p value for ID_{50} compared to morphine	
	Male	Female	Male	Female	Sexes combined	Sexes combined	Sexes combined	
Morphine	2.06	3.64	0.31 ± 0.12	0.56 ± 0.10	2.71	0.43 ± 0.08	—	
U50,488	1.06	2.08	0.03 ± 0.17	0.32 ± 0.12	1.46	0.17 ± 0.10	0.3349	n.s.
SalA	0.60	1.03	−0.22 ± 0.19	0.01 ± 0.12	0.82	−0.09 ± 0.13	0.0011	**
16-Ethynyl SalA	0.31	0.71	−0.51 ± 0.20	−0.15 ± 0.14	0.48	−0.32 ± 0.12	<0.0001	****
16-Bromo SalA	1.20	1.44	0.08 ± 0.13	0.16 ± 0.11	1.31	0.12 ± 0.09	0.1607	n.s.
EOM SalB	0.77	0.90	−0.11 ± 0.14	−0.04 ± 0.12	0.83	−0.08 ± 0.09	0.0021	**

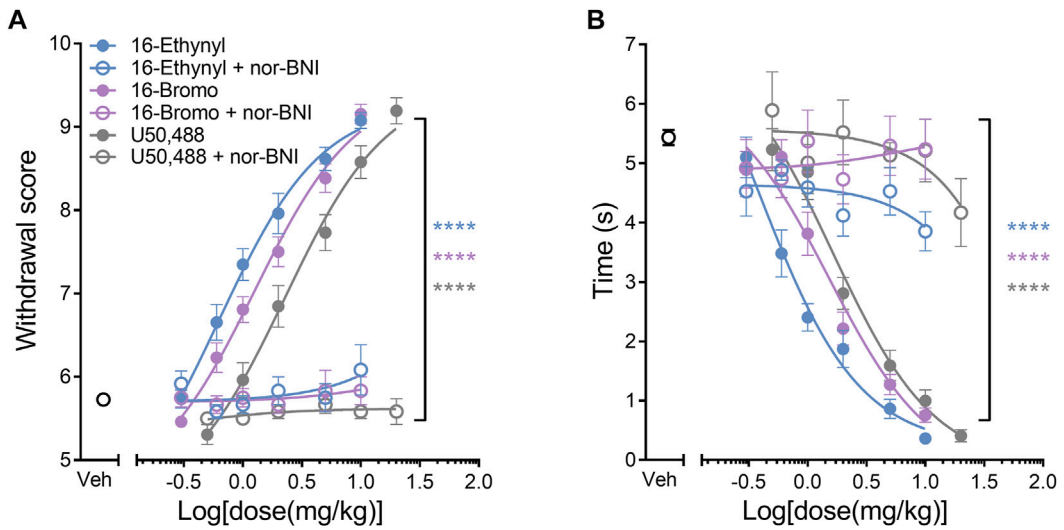

FIGURE 3 | KOR antagonism reduces the antinociceptive effect of the KOR agonists. The selective KOR antagonist *nor*-binaltorphimine (*nor*-BNI, 10 mg/kg) was administered prior to the dose-response procedure. **(A)** Antinociceptive dose-response effects against mechanical allodynia. *Nor*-BNI reduced the antinociceptive effects of the KOR agonists at the highest dose for 16-Ethynyl SalA, 16-Bromo SalA (10 mg/kg) and U50,488 (20 mg/kg) to the mechanical stimulus. **(B)** Antinociceptive dose-response effects against cold allodynia. *Nor*-BNI reduced the antinociceptive effects of the KOR agonists to the cold stimulus. One-way ANOVA with Bonferroni post-tests. Values presented as mean ± SEM. n = 13 for KOR agonist treatment, n = 6 for groups with *nor*-BNI pre-treatment. $^{****}p < 0.0001$ indicates comparison between treatment with and without pre-treatment of *nor*-BNI.

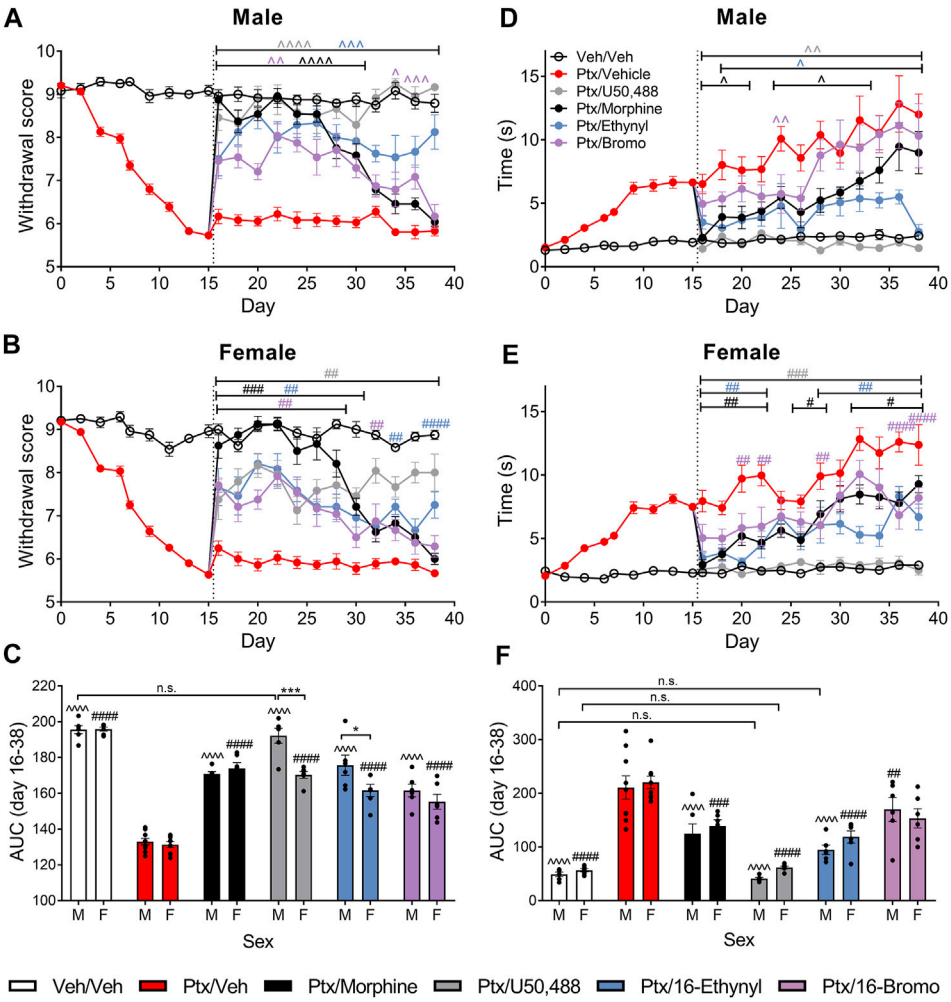

FIGURE 4 | Chronic KOR treatment reduced mechanical and cold allodynia in mice with established paclitaxel (Ptx)-induced neuropathic pain. **(A, B)** Time course of the treatment effects of vehicle (Veh), morphine (10 mg/kg), U50,488 (10 mg/kg), 16-Ethynyl SalA (3 mg/kg), and 16-Bromo SalA (4 mg/kg) on mechanical allodynia in **(A)** males and **(B)** females. **(C)** Area under the curve (AUC) comparison within the male and female animals showed treatments all significantly increased the paclitaxel-induced withdrawal scores, with U50,488 treatment in males improving the mechanical thresholds to vehicle/vehicle levels. Comparison of the sex differences in the treatments found that U50,488 and 16-Ethynyl were more effective in males. **(D, E)** Time course of the treatment effects on cold allodynia in **(D)** males and **(E)** females. **(F)** AUC analysis showed that U50,488 treatment in both sexes and 16-Ethynyl treatment in males reduced the cold stimulus responding time to the same level as vehicle/vehicle controls. Two-way ANOVA with Bonferroni post-tests. n. s. = not significant, $^{\wedge}p < 0.05$, $^{\wedge\wedge}p < 0.01$, $^{\wedge\wedge\wedge}p < 0.005$, $^{\wedge\wedge\wedge\wedge}p < 0{,}001$ for male treatment group compared to male paclitaxel/vehicle group; $^{\#}p < 0.05$, $^{\#\#}p < 0.01$, $^{\#\#\#}p < 0.005$, and $^{\#\#\#\#}p < 0.0001$ for female treatment group compared to female paclitaxel/vehicle group; $^{*}p < 0.05$, $^{***}p < 0.005$ for sex difference within treatment group. Values presented as mean ± SEM, $n = 6–9$.

tests showed that there was a significant difference with pre-treatment of *nor*-BNI for all KOR agonists ($p < 0.0001$). The results show that the antinociceptive actions of the novel SalA analogues are mediated via the KOR.

Effect of Chronic Administration of Kappa Opioid Receptor Agonists on Mechanical Allodynia

We further assessed the effect of the KOR agonists using a chronic administration model, in which treatment began on day 16 post-initiation of paclitaxel-induced neuropathic pain. In male mice, 16-Ethynyl SalA and U50,488 reduced paclitaxel-induced mechanical allodynia on all days evaluated ($p < 0.005$; **Figure 4A**). Morphine treatment had antinociceptive effects on days 16–30, and 16-Bromo SalA on days 16–30 and 34–36 ($p < 0.05$; **Figure 4A**). In the female mice, U50,488 reduced mechanical allodynia at all time points evaluated, whereas, 16-Ethynyl SalA reduced mechanical allodynia at days 16–30, 34, and 38; 16-Bromo SalA at days 16–28, and 32; and morphine at days 16–30 (**Figure 4C**). The area under the curve (AUC) analysis showed that all treatment groups were significantly different to the paclitaxel/vehicle group within each sex ($p < 0.001$; **Figure 4B**). Furthermore, in the males, U50,488 treatment reduced the mechanical withdrawal thresholds to healthy control levels (vehicle/vehicle treatment group; $p > 0.9999$;

Figure 4B). Further investigation into sex differences within each treatment showed that U50,488 and 16-Ethynyl SalA were more effective in male mice than female mice ($p < 0.05$), whereas, all other treatments had no sex differences (**Figure 4C**).

Effect of Chronic Administration of Kappa Opioid Receptor Agonists on Cold Allodynia

In male mice, U50,488 reduced the paclitaxel-induced cold allodynia at all the days evaluated (days 16–38; $p < 0.01$); 16-Ethynyl SalA attenuated cold allodynia at days 18–38; 16-Bromo SalA at day 24; and morphine at days 16–20, 24–28, and day 32 (**Figure 4D**). In the female mice, U50,488 reduced the reaction time at all time points (days 16–38; $p < 0.005$); 16-Ethynyl SalA reduced cold allodynia at days 16–22 and 28–38 ($p < 0.01$); 16-Bromo SalA at days 20–22, 28 and 36–38 ($p < 0.01$); and morphine at days 16–22, 26–28, and 32–38 ($p < 0.05$; **Figure 4E**). In male mice, AUC analysis showed all KOR agonist treatments attenuated thermal nociception; in female mice, all treatment groups except 16-Bromo SalA attenuated thermal nociception when compared to the paclitaxel/vehicle control group (**Figure 4F**). U50,488 (both sexes) and 16-Ethynyl SalA (males only) returned antinociceptive responses to healthy control levels (vehicle/vehicle group). When the sexes were compared within each treatment, there were no significant sex differences (**Figure 4F**).

DISCUSSION

There is an urgent need to develop new treatments for CIPN, as this debilitating condition currently has very limited treatment options (Loprinzi et al., 2020). MOR agonists are often used to alleviate pain; however, these can potentiate pain when used chronically, and have addictive and aversive side effects (Chu et al., 2006; Compton and Volkow, 2006; Pattinson, 2008; Dahan et al., 2010; Roeckel et al., 2016). We have investigated the effect of KOR agonists for the treatment of paclitaxel-induced neuropathic pain due to the reduced abuse potential of KOR agonists, which is an important requirement for these treatments due to the long-term nature of chemotherapy regimens. We have further investigated the sex differences within our experiments due to the over-reliance on male animals used in research, which may not give an accurate representation of both sexes (Clayton and Collins, 2014; Lee, 2018; Shansky and Murphy, 2021).

We initially investigated the effect of sex on the onset of disease in the paclitaxel-induced neuropathic pain model. We showed that paclitaxel administration induces significant mechanical allodynia, with no sex differences at any time points. In contrast, measurements of cold allodynia showed the female mice had a longer reaction time in both the vehicle and paclitaxel groups. This is consistent with a previous study using NMRI mice, which found the paclitaxel-treated female mice had increased paw licking following cold stimulus to the paw between days 7–11, however, measurements on days 13 and 15 were not significantly different to males (Naji-Esfahani et al., 2016). The same study found no sex differences in the development of paclitaxel-induced mechanical allodynia measured using von Frey filaments (Naji-Esfahani et al., 2016). In further studies, there were no differences between the sexes in paclitaxel-induced mechanical allodynia in C57BL/6 mice (Smith et al., 2004); whereas in rats, there were both findings with no sex difference (Hwang et al., 2012) and with females showing greater mechanical hyperalgesia (Wang et al., 2018; Ferrari et al., 2020). Overall, the majority of studies have no inherent sex differences in paclitaxel-induced mechanical allodynia, whereas multiple studies have shown females to have a heightened cold response.

The antinociceptive dose-response effects of the KOR agonists were evaluated alongside morphine to assess the potency of the compounds in both sexes. The mechanical testing showed U50,488 was significantly more potent in males compared to females. It has been shown in previous studies that U50,488 exhibits higher antinociceptive potency in males when measured with the tail withdrawal assay (reviewed in Rasakham and Liu-Chen, 2011). However, in a similar paclitaxel-induced experiment performed in Sprague Dawley rats, acute morphine treatment (2–5 mg/kg i.p.) had the same antinociceptive effects in both sexes with mechanical allodynia (Hwang et al., 2012). We also found that SalA treatment was more potent in females. Interestingly, in rhesus macaques, SalA has sex differences in the pharmacokinetic effects, with females showing a slower elimination from plasma and a larger area under the concentration-time curve following intravenous injection (Schmidt et al., 2005), which may explain the increased antinociceptive effects produced in females. We also showed that 16-Ethynyl SalA was more potent than morphine for treatment of both mechanical and cold allodynia, which is similar to our previous study showing 16-Ethynyl SalA was more potent and efficacious than U50,488 in the warm water tail withdrawal assay (Paton et al., 2020b).

There are few previous studies measuring the effects of KOR agonists in a model of paclitaxel-induced neuropathic pain. We have shown the SalA analogue, β-tetrahydropyran SalB, and the mixed opioid receptor agonist MP1104 have anti-allodynic effects in this model (Paton et al., 2017; Atigari et al., 2020). In an alternative CIPN model, KOR agonist LOR17 was found to alleviate oxaliplatin-induced thermal hypersensitivity to a cold stimulus, and was more potent than U50,488 (Bedini et al., 2020). SalA has also been assessed in other models of neuropathic pain. SalA reduced pain in a sciatic nerve ligature model in male Wistar rats when injected directly into the insular cortex (Coffeen et al., 2018). Furthermore, an extract of *Salvia divinorum*, containing SalA, SalB, and other substances found in the leaves of the plant, reduced mechanical and thermal sciatic nerve ligature neuropathic pain when administered at 100–200 mg/kg i.p. (Simon-Arceo et al., 2017). The effect of KOR agonists in CIPN is an emerging area of research, however, these studies set the groundwork to show that KOR agonists have promise at treating neuropathic pain.

Several studies have assessed the effects of MOR agonists in the paclitaxel-induced neuropathic pain model. In male C57BL/6J mice, previous findings show morphine with an ED_{50} of 6.68 mg/kg against mechanical allodynia and 12.5 mg/kg against cold allodynia (Slivicki et al., 2018), whereas, we found that morphine was 3–6 fold more potent (mechanical allodynia

ED_{50} of 2.16 mg/kg; cold allodynia ED_{50} of 2.06 mg/kg). The effects in both studies were done at 30 min post-injection, however, the dose-response in the Slivicki et al. (2018) study was done over multiple days rather than a cumulative dose-response in one session. Previous work has indicated that discrete versus cumulative dose-response procedures yield the same results (Schechter, 1997). A further difference between the studies is Slivicki et al. (2018) used an electronic von Frey anesthesiometer, whereas the current study used classical von Frey filaments of varying diameter. The electronic von Frey anesthesiometer may give more continuous data, as opposed to the individual von Frey filaments that each exert a discrete maximum force, and the electronic von Frey apparatus is believed to be more sensitive (Cunha et al., 2004).

In the current study, daily 10 mg/kg morphine administration was effective for 15 days against mechanical allodynia, whereas a previous study found morphine was only effective on the first treatment day and was no longer effective 3 days later (Slivicki et al., 2020). In male Sprague Dawley rats, Flatters and Bennett (2004) found an acute treatment of 4 mg/kg morphine was ineffective at treating paclitaxel-induced mechanical allodynia and 8 mg/kg only produced a 50% reversal of mechanical allodynia. A further study in male Sprague Dawley rats found that 4 mg/kg normalized the mechanical withdrawal thresholds to pre-paclitaxel baseline levels (Rahn et al., 2008). This shows there is great variation in the effects of morphine in the paclitaxel-induced neuropathic pain model. Reasons for variations in the results could include the use of different species (mice vs rats), different concentration of paclitaxel, the use of electronic vs. classical von Frey apparatus, and different experimental time points.

In the chronic administration regimen, we showed that U50,488 significantly reversed the effects of paclitaxel over 23 days, with no apparent tolerance effects. In the warm water (55°) tail withdrawal assay in C57BL/6 mice, U50,488 has been shown to cause tolerance effects, however, this was with an escalating dose scheme up to 75 mg/kg i.p. over 4 days (McLaughlin et al., 2004), whereas in the current study we used 10 mg/kg i.p. treatment daily. Interestingly, using a partial spinal nerve ligation model, phosphorylated KOR immunoreactivity was increased in the L4-5 dorsal horn regions of the spinal cord in male C57BL/6 mice and KOR knock-out mice there was increased mechanical allodynia and thermal heat hyperalgesia (Xu et al., 2004). However, due to this endogenous KOR activation in the mice with neuropathic pain, treatment with U50,488 showed increased tolerance compared to sham, and this tolerance effect was absent in prodynorphin or GRK3 knock-out mice (Xu et al., 2004). Furthermore, KOR antagonism with *nor*-BNI in mice and rats led to increased levels of mechanical and thermal allodynia (Obara et al., 2003). In comparing to the current study, because U50,488 does not show the tolerance effects associated with endogenous KOR activation, it could be that the endogenous KOR system is not activated to the same extent in the paclitaxel-induced neuropathic pain model compared to the partial spinal nerve ligation model; however, this effect has not been studied.

Interestingly, the KOR mediates the initial aversive component of paclitaxel-induced neuropathic pain (day 8), with an increase in prodynorphin levels in the nucleus accumbens (Meade et al., 2020). Due to this aversive nature of the pain, it is important to develop treatments that do not have negative side effects. We have previously shown that 16-Bromo SalA does not have anxiogenic effect in the elevated zero maze and the marble burying test; however, 16-Ethynyl SalA did significantly reduce exploratory behaviors in the elevated zero maze but had no effect in the marble burying test (Paton et al., 2020b). Furthermore, the sedative effects of the treatments should be considered, we know that 16-Ethynyl SalA, 16-Bromo SalA, and U50,488 have motor incoordination effects in the rotarod performance test (Paton et al., 2020b; Dunn et al., 2020); however, 16-Bromo SalA and 16-Ethynyl SalA did not reduce spontaneous locomotor activity at lower doses in rats (Riley et al., 2014). Even though the duration of action of these novel SalA analogues is longer than the parent compound (Paton et al., 2020b), the relatively short duration of action and negative side effects may hinder progression of these compounds into a clinical setting. However, these compounds show proof-of-concept that KOR agonists can be used for this form of neuropathic pain. In addition, there has been some progress in developing peripherally-restricted MOR agonists for the treatment of neuropathic pain (Tiwari et al., 2018), so further investigation into the mechanism of action could indicate whether a peripherally-restricted KOR agonist could be developed with no centrally-active side effects.

In conclusion, we have shown that KOR agonists have anti-allodynic effects in a mouse model of CIPN and are more potent than morphine for the treatment of paclitaxel-induced neuropathic pain. We have shown that U50,488 was more potent in male mice; whereas, SalA treatment was more potent in females. In the chronic administration paradigm, treatment with U50,488 reversed the paclitaxel-induced allodynia to healthy levels. Therefore, this study provides evidence that KOR agonists have potential for treating pain conditions associated with chronic neuropathy such as CIPN by reducing allodynia.

DATA AVAILABILITY STATEMENT

The raw data supporting the conclusion of this article will be made available by the authors, without undue reservation.

ETHICS STATEMENT

The animal study was reviewed and approved by the Victoria University of Wellington Animal Ethics Committee.

AUTHOR CONTRIBUTIONS

KP, AL, TP, and BK contributed to the design of the study. DL and TP provided the kappa opioid receptor agonists. KP conducted the experiments and performed the data analysis.

KP wrote the first draft of the manuscript. DL, AL, TP, and BK critically evaluated the manuscript. All authors contributed to the manuscript revision, read and approved the submitted version.

FUNDING

This work was supported by the Health Research Council of New Zealand (Explorer grant number 16/646 to BK), Cancer Society of New Zealand Wellington Division (to BK) and the National Institute of Drug Abuse (Grant number DA018151 to TP). KP received a doctoral scholarship from Victoria University of Wellington.

ACKNOWLEDGMENTS

The authors would like to acknowledge Shaun Graham (Victoria University of Wellington) who built the chambers and stand used to assess allodynia.

REFERENCES

Addington, J., and Freimer, M. (2016). Chemotherapy-induced Peripheral Neuropathy: an Update on the Current Understanding. *F1000Res* 5, F1000 Faculty Rev-1466. doi:10.12688/f1000research.8053.1

Atigari, D. V., Paton, K. F., Uprety, R., Váradi, A., Alder, A. F., Scouller, B., et al. (2021). The Mixed Kappa and delta Opioid Receptor Agonist, MP1104, Attenuates Chemotherapy-Induced Neuropathic Pain. *Neuropharmacology* 185, 108445. doi:10.1016/j.neuropharm.2020.108445

Bartley, E. J., and Fillingim, R. B. (2013). Sex Differences in Pain: a Brief Review of Clinical and Experimental Findings. *Br. J. Anaesth.* 111 (1), 52–58. doi:10.1093/bja/aet127

Beck, T. C., Hapstack, M. A., Beck, K. R., and Dix, T. A. (2019). Therapeutic Potential of Kappa Opioid Agonists. *Pharmaceuticals (Basel)* 12 (2), 95. doi:10.3390/ph12020095

Bedini, A., Di Cesare Mannelli, L., Micheli, L., Baiula, M., Vaca, G., De Marco, R., et al. (2020). Functional Selectivity and Antinociceptive Effects of a Novel KOPr Agonist. *Front. Pharmacol.* 11 (188), 188. doi:10.3389/fphar.2020.00188

Beijers, A., Mols, F., Dercksen, W., Driessen, C., and Vreugdenhil, G. (2014). Chemotherapy-induced Peripheral Neuropathy and Impact on Quality of Life 6 Months after Treatment with Chemotherapy. *J. Community Support. Oncol.* 12 (11), 401–406. doi:10.12788/jcso.0086

Bonin, R. P., Bories, C., and De Koninck, Y. (2014). A simplified up-down method (SUDO) for measuring mechanical nociception in rodents using von Frey filaments. *Mol. Pain* 10 (1), 26. doi:10.1186/1744-8069-10-26

Chu, L. F., Clark, D. J., and Angst, M. S. (2006). Opioid Tolerance and Hyperalgesia in Chronic Pain Patients after One Month of Oral Morphine Therapy: a Preliminary Prospective Study. *J. Pain* 7 (1), 43–48. doi:10.1016/j.jpain.2005.08.001

Clayton, J. A., and Collins, F. S. (2014). Policy: NIH to Balance Sex in Cell and Animal Studies. *Nature* 509 (7500), 282–283. doi:10.1038/509282a

Coffeen, U., Canseco-Alba, A., Simón-Arceo, K., Almanza, A., Mercado, F., León-Olea, M., et al. (2018). Salvinorin A Reduces Neuropathic Nociception in the Insular Cortex of the Rat. *Eur. J. Pain* 22 (2), 311–318. doi:10.1002/ejp.1120

Compton, W. M., and Volkow, N. D. (2006). Major Increases in Opioid Analgesic Abuse in the United States: Concerns and Strategies. *Drug Alcohol Depend* 81 (2), 103–107. doi:10.1016/j.drugalcdep.2005.05.009

Cunha, T. M., Verri, W. A., Jr., Vivancos, G. G., Moreira, I. F., Reis, S., Parada, C. A., et al. (2004). An Electronic Pressure-Meter Nociception Paw Test for Mice. *Braz. J. Med. Biol. Res.* 37 (3), 401–407. doi:10.1590/s0100-879x2004000300018

Dahan, A., Aarts, L., and Smith, T. W. (2010). Incidence, Reversal, and Prevention of Opioid-Induced Respiratory Depression. *Anesthesiology* 112 (1), 226–238. doi:10.1097/ALN.0b013e3181c38c25

Deng, L., Guindon, J., Cornett, B. L., Makriyannis, A., Mackie, K., and Hohmann, A. G. (2015). Chronic Cannabinoid Receptor 2 Activation Reverses Paclitaxel Neuropathy without Tolerance or Cannabinoid Receptor 1-dependent Withdrawal. *Biol. Psychiatry* 77 (5), 475–487. doi:10.1016/j.biopsych.2014.04.009

Dougherty, P. M., Cata, J. P., Cordella, J. V., Burton, A., and Weng, H. R. (2004). Taxol-induced Sensory Disturbance Is Characterized by Preferential Impairment of Myelinated Fiber Function in Cancer Patients. *Pain* 109 (1-2), 132–142. doi:10.1016/j.pain.2004.01.021

Dunn, A., Windisch, K., Ben-Ezra, A., Pikus, P., Morochnik, M., Erazo, J., et al. (2020). Modulation of Cocaine-Related Behaviors by Low Doses of the Potent KOR Agonist Nalfurafine in Male C57BL6 Mice. *Psychopharmacology (Berl)* 237 (8), 2405–2418. doi:10.1007/s00213-020-05543-7

Endoh, T., Matsuura, H., Tanaka, C., and Nagase, H. (1992). Nor-binaltorphimine: a Potent and Selective Kappa-Opioid Receptor Antagonist with Long-Lasting Activity *In Vivo*. *Arch. Int. Pharmacodyn Ther.* 316, 30–42.

Ewertz, M., Qvortrup, C., and Eckhoff, L. (2015). Chemotherapy-induced Peripheral Neuropathy in Patients Treated with Taxanes and Platinum Derivatives. *Acta Oncol.* 54 (5), 587–591. doi:10.3109/0284186X.2014.995775

Ferrari, L. F., Araldi, D., Green, P. G., and Levine, J. D. (2020). Marked Sexual Dimorphism in Neuroendocrine Mechanisms for the Exacerbation of Paclitaxel-Induced Painful Peripheral Neuropathy by Stress. *Pain* 161 (4), 865–874. doi:10.1097/j.pain.0000000000001798

Finnerup, N. B., Attal, N., Haroutounian, S., McNicol, E., Baron, R., Dworkin, R. H., et al. (2015). Pharmacotherapy for Neuropathic Pain in Adults: a Systematic Review and Meta-Analysis. *Lancet Neurol.* 14 (2), 162–173. doi:10.1016/S1474-4422(14)70251-0

Flatters, S. J., and Bennett, G. J. (2004). Ethosuximide Reverses Paclitaxel- and Vincristine-Induced Painful Peripheral Neuropathy. *Pain* 109 (1-2), 150–161. doi:10.1016/j.pain.2004.01.029

Forman, A. (1990). Peripheral Neuropathy in Cancer Patients: Clinical Types, Etiology, and Presentation. Part 2. *Oncology (Williston Park)* 4 (2), 85–89.

Freye, E., Hartung, E., and Schenk, G. K. (1983). Bremazocine: an Opiate that Induces Sedation and Analgesia without Respiratory Depression. *Anesth. Analg* 62 (5), 483–488. doi:10.1213/00000539-198305000-00005

Grace, P. M., Strand, K. A., Galer, E. L., Urban, D. J., Wang, X., Baratta, M. V., et al. (2016). Morphine Paradoxically Prolongs Neuropathic Pain in Rats by Amplifying Spinal NLRP3 Inflammasome Activation. *Proc. Natl. Acad. Sci. U S A.* 113 (24), E3441–E3450. doi:10.1073/pnas.1602070113

Hershman, D. L., Lacchetti, C., Dworkin, R. H., Lavoie Smith, E. M., Bleeker, J., Cavaletti, G., et al. (2014). Prevention and Management of Chemotherapy-Induced Peripheral Neuropathy in Survivors of Adult Cancers: American Society of Clinical Oncology Clinical Practice Guideline. *J. Clin. Oncol.* 32 (18), 1941–1967. doi:10.1200/JCO.2013.54.0914

Holmes, F. A., Walters, R. S., Theriault, R. L., Forman, A. D., Newton, L. K., Raber, M. N., et al. (1991). Phase II Trial of Taxol, an Active Drug in the Treatment of Metastatic Breast Cancer. *J. Natl. Cancer Inst.* 83 (24), 1797–1805. doi:10.1093/jnci/83.24.1797-a

Hwang, B. Y., Kim, E. S., Kim, C. H., Kwon, J. Y., and Kim, H. K. (2012). Gender Differences in Paclitaxel-Induced Neuropathic Pain Behavior and Analgesic Response in Rats. *Korean J. Anesthesiol* 62 (1), 66–72. doi:10.4097/kjae.2012.62.1.66

Jaggi, A. S., Jain, V., and Singh, N. (2011). Animal Models of Neuropathic Pain. *Fundam. Clin. Pharmacol.* 25 (1), 1–28. doi:10.1111/j.1472-8206.2009.00801.x

Khanna, C., Rosenberg, M., and Vail, D. M. (2015). A Review of Paclitaxel and Novel Formulations Including Those Suitable for Use in Dogs. *J. Vet. Intern. Med.* 29 (4), 1006–1012. doi:10.1111/jvim.12596

Kishioka, S., Kiguchi, N., Kobayashi, Y., Yamamoto, C., Saika, F., Wakida, N., et al. (2013). Pharmacokinetic Evidence for the Long-Lasting Effect of Nor-Binaltorphimine, a Potent Kappa Opioid Receptor Antagonist, in Mice. *Neurosci. Lett.* 552, 98–102. doi:10.1016/j.neulet.2013.07.040

Lee, S. K. (2018). Sex as an Important Biological Variable in Biomedical Research. *BMB Rep.* 51 (4), 167–173. doi:10.5483/bmbrep.2018.51.4.034

Loprinzi, C. L., Lacchetti, C., Bleeker, J., Cavaletti, G., Chauhan, C., Hertz, D. L., et al. (2020). Prevention and Management of Chemotherapy-Induced Peripheral Neuropathy in Survivors of Adult Cancers: ASCO Guideline Update. *J. Clin. Oncol.* 38 (28), 3325–3348. doi:10.1200/JCO.20.01399

McLaughlin, J. P., Myers, L. C., Zarek, P. E., Caron, M. G., Lefkowitz, R. J., Czyzyk, T. A., et al. (2004). Prolonged Kappa Opioid Receptor Phosphorylation Mediated by G-Protein Receptor Kinase Underlies Sustained Analgesic Tolerance. *J. Biol. Chem.* 279 (3), 1810–1818. doi:10.1074/jbc.M305796200

Meade, J. A., Alkhlaif, Y., Contreras, K. M., Obeng, S., Toma, W., Sim-Selley, L. J., et al. (2020). Kappa Opioid Receptors Mediate an Initial Aversive Component of Paclitaxel-Induced Neuropathy. *Psychopharmacology (Berl)* 237 (9), 2777–2793. doi:10.1007/s00213-020-05572-2

Mogil, J. S. (2012). Sex Differences in Pain and Pain Inhibition: Multiple Explanations of a Controversial Phenomenon. *Nat. Rev. Neurosci.* 13 (12), 859–866. doi:10.1038/nrn3360

Mols, F., Beijers, T., Vreugdenhil, G., and van de Poll-Franse, L. (2014). Chemotherapy-induced Peripheral Neuropathy and its Association with Quality of Life: a Systematic Review. *Support Care Cancer* 22 (8), 2261–2269. doi:10.1007/s00520-014-2255-7

Munro, T. A., and Rizzacasa, M. A. (2003). Salvinorins D-F, New Neoclerodane Diterpenoids from Salvia Divinorum, and an Improved Method for the Isolation of Salvinorin A. *J. Nat. Prod.* 66 (5), 703–705. doi:10.1021/np0205699

Naji-Esfahani, H., Vaseghi, G., Safaeian, L., Pilehvarian, A. A., Abed, A., and Rafieian-Kopaei, M. (2016). Gender Differences in a Mouse Model of Chemotherapy-Induced Neuropathic Pain. *Lab. Anim.* 50 (1), 15–20. doi:10.1177/0023677215575863

Obara, I., Mika, J., Schafer, M. K., and Przewlocka, B. (2003). Antagonists of the Kappa-Opioid Receptor Enhance Allodynia in Rats and Mice after Sciatic Nerve Ligation. *Br. J. Pharmacol.* 140 (3), 538–546. doi:10.1038/sj.bjp.0705427

Paton, K. F., Atigari, D. V., Kaska, S., Prisinzano, T., and Kivell, B. M. (2020a). Strategies for Developing κ Opioid Receptor Agonists for the Treatment of Pain with Fewer Side Effects. *J. Pharmacol. Exp. Ther.* 375 (2), 332–348. doi:10.1124/jpet.120.000134

Paton, K. F., Biggerstaff, A., Kaska, S., Crowley, R. S., La Flamme, A. C., Prisinzano, T. E., et al. (2020b). Evaluation of Biased and Balanced Salvinorin A Analogs in Preclinical Models of Pain. *Front. Neurosci.* 14 (765), 765. doi:10.3389/fnins.2020.00765

Paton, K. F., Kumar, N., Crowley, R. S., Harper, J. L., Prisinzano, T. E., and Kivell, B. M. (2017). The Analgesic and Anti-inflammatory Effects of Salvinorin A Analogue β-tetrahydropyran Salvinorin B in Mice. *Eur. J. Pain* 21 (6), 1039–1050. doi:10.1002/ejp.1002

Pattinson, K. T. (2008). Opioids and the Control of Respiration. *Br. J. Anaesth.* 100 (6), 747–758. doi:10.1093/bja/aen094

Pieretti, S., Di Giannuario, A., Di Giovannandrea, R., Marzoli, F., Piccaro, G., Minosi, P., et al. (2016). Gender Differences in Pain and its Relief. *Ann. Ist Super Sanita* 52 (2), 184–189. doi:10.4415/ANN_16_02_09

Porreca, F., Mosberg, H. I., Hurst, R., Hruby, V. J., and Burks, T. F. (1984). Roles of Mu, delta and Kappa Opioid Receptors in Spinal and Supraspinal Mediation of Gastrointestinal Transit Effects and Hot-Plate Analgesia in the Mouse. *J. Pharmacol. Exp. Ther.* 230 (2), 341–348.

Prevatt-Smith, K. M., Lovell, K. M., Simpson, D. S., Day, V. W., Douglas, J. T., Bosch, P., et al. (2011). Potential Drug Abuse Therapeutics Derived from the Hallucinogenic Natural Product Salvinorin A. *Medchemcomm* 2 (12), 1217–1222. doi:10.1039/C1MD00192B

Rahn, E. J., Zvonok, A. M., Thakur, G. A., Khanolkar, A. D., Makriyannis, A., and Hohmann, A. G. (2008). Selective Activation of Cannabinoid CB2 Receptors Suppresses Neuropathic Nociception Induced by Treatment with the Chemotherapeutic Agent Paclitaxel in Rats. *J. Pharmacol. Exp. Ther.* 327 (2), 584–591. doi:10.1124/jpet.108.141994

Rasakham, K., and Liu-Chen, L. Y. (2011). Sex Differences in Kappa Opioid Pharmacology. *Life Sci.* 88 (1-2), 2–16. doi:10.1016/j.lfs.2010.10.007

Riley, A. P., Groer, C. E., Young, D., Ewald, A. W., Kivell, B. M., and Prisinzano, T. E. (2014). Synthesis and κ-opioid Receptor Activity of Furan-Substituted Salvinorin A Analogues. *J. Med. Chem.* 57 (24), 10464–10475. doi:10.1021/jm501521d

Roeckel, L. A., Le Coz, G. M., Gavériaux-Ruff, C., and Simonin, F. (2016). Opioid-induced Hyperalgesia: Cellular and Molecular Mechanisms. *Neuroscience* 338, 160–182. doi:10.1016/j.neuroscience.2016.06.029

Rowinsky, E. K., Chaudhry, V., Forastiere, A. A., Sartorius, S. E., Ettinger, D. S., Grochow, L. B., et al. (1993). Phase I and Pharmacologic Study of Paclitaxel and Cisplatin with Granulocyte colony-stimulating Factor: Neuromuscular Toxicity Is Dose-Limiting. *J. Clin. Oncol.* 11 (10), 2010–2020. doi:10.1200/JCO.1993.11.10.2010

Schechter, M. D. (1997). Discrete versus Cumulative Dosing in Dose-Response Discrimination Studies. *Eur. J. Pharmacol.* 326 (2-3), 113–118. doi:10.1016/s0014-2999(97)85404-0

Schmidt, M. D., Schmidt, M. S., Butelman, E. R., Harding, W. W., Tidgewell, K., Murry, D. J., et al. (2005). Pharmacokinetics of the Plant-Derived Kappa-Opioid Hallucinogen Salvinorin A in Nonhuman Primates. *Synapse* 58 (3), 208–210. doi:10.1002/syn.20191

Seretny, M., Currie, G. L., Sena, E. S., Ramnarine, S., Grant, R., MacLeod, M. R., et al. (2014). Incidence, Prevalence, and Predictors of Chemotherapy-Induced Peripheral Neuropathy: A Systematic Review and Meta-Analysis. *Pain* 155 (12), 2461–2470. doi:10.1016/j.pain.2014.09.020

Shah, A., Hoffman, E. M., Mauermann, M. L., Loprinzi, C. L., Windebank, A. J., Klein, C. J., et al. (2018). Incidence and Disease burden of Chemotherapy-Induced Peripheral Neuropathy in a Population-Based Cohort. *J. Neurol. Neurosurg. Psychiatry* 89 (6), 636–641. doi:10.1136/jnnp-2017-317215

Shansky, R. M., and Murphy, A. Z. (2021). Considering Sex as a Biological Variable Will Require a Global Shift in Science Culture. *Nat. Neurosci.* 24 (4), 457–464. doi:10.1038/s41593-021-00806-8

Simon-Arceo, K., González-Trujano, M. E., Coffeen, U., Fernández-Mas, R., Mercado, F., Almanza, A., et al. (2017). Neuropathic and Inflammatory Antinociceptive Effects and Electrocortical Changes Produced by Salvia Divinorum in Rats. *J. Ethnopharmacol* 206, 115–124. doi:10.1016/j.jep.2017.05.016

Sisignano, M., Baron, R., Scholich, K., and Geisslinger, G. (2014). Mechanism-based Treatment for Chemotherapy-Induced Peripheral Neuropathic Pain. *Nat. Rev. Neurol.* 10 (12), 694–707. doi:10.1038/nrneurol.2014.211

Slivicki, R. A., Iyer, V., Mali, S. S., Garai, S., Thakur, G. A., Crystal, J. D., et al. (2020). Positive Allosteric Modulation of CB1 Cannabinoid Receptor Signaling Enhances Morphine Antinociception and Attenuates Morphine Tolerance without Enhancing Morphine- Induced Dependence or Reward. *Front. Mol. Neurosci.* 13 (54), 54. doi:10.3389/fnmol.2020.00054

Slivicki, R. A., Saberi, S. A., Iyer, V., Vemuri, V. K., Makriyannis, A., and Hohmann, A. G. (2018). Brain-Permeant and -Impermeant Inhibitors of Fatty Acid Amide Hydrolase Synergize with the Opioid Analgesic Morphine to Suppress Chemotherapy-Induced Neuropathic Nociception without Enhancing Effects of Morphine on Gastrointestinal Transit. *J. Pharmacol. Exp. Ther.* 367 (3), 551–563. doi:10.1124/jpet.118.252288

Smith, S. B., Crager, S. E., and Mogil, J. S. (2004). Paclitaxel-induced Neuropathic Hypersensitivity in Mice: Responses in 10 Inbred Mouse Strains. *Life Sci.* 74 (21), 2593–2604. doi:10.1016/j.lfs.2004.01.002

Tidgewell, K., Harding, W. W., Schmidt, M., Holden, K. G., Murry, D. J., and Prisinzano, T. E. (2004). A Facile Method for the Preparation of Deuterium Labeled Salvinorin A: Synthesis of [2,2,2-2H3]-Salvinorin A. *Bioorg. Med. Chem. Lett.* 14 (20), 5099–5102. doi:10.1016/j.bmcl.2004.07.081

Tiwari, V., Anderson, M., Yang, F., Tiwari, V., Zheng, Q., He, S. Q., et al. (2018). Peripherally Acting μ-Opioid Receptor Agonists Attenuate Ongoing Pain-Associated Behavior and Spontaneous Neuronal Activity after Nerve Injury in Rats. *Anesthesiology* 128 (6), 1220–1236. doi:10.1097/ALN.0000000000002191

Uniyal, A., Gadepalli, A., Kotiyal, A., and Tiwari, V. (2020). Underpinning the Neurobiological Intricacies Associated with Opioid Tolerance. *ACS Chem. Neurosci.* 11 (6), 830–839. doi:10.1021/acschemneuro.0c00019

van den Bent, M. J., van Raaij-van den Aarssen, V. J., Verweij, J., Doorn, P. A., and Sillevis Smitt, P. A. (1997). Progression of Paclitaxel-Induced Neuropathy Following Discontinuation of Treatment. *Muscle Nerve* 20 (6), 750–752. doi:10.1002/(sici)1097-4598(199706)20:6<750:aid-mus15>3.0.co;2-y

Vonvoigtlander, P. F., Lahti, R. A., and Ludens, J. H. (1983). U-50,488: a Selective and Structurally Novel Non-mu (Kappa) Opioid Agonist. *J. Pharmacol. Exp. Ther.* 224 (1), 7–12.

Wang, Y. C., Li, N., Zhao, Y., and Zhang, L. J. (2018). Effects of Female Sex Hormones on Chemotherapeutic Paclitaxel-Induced Neuropathic Pain and Involvement of Inflammatory Signal. *J. Biol. Regul. Homeost Agents* 32 (5), 1157–1163.

Xu, M., Petraschka, J. P., McLaughlin, M. G., Czyzyk, T. A., Termanr, G. W., Chavkin, C., et al. (2004). Neuropathic Pain Activates the Endogenous Kappa Opioid System in Mouse Spinal Cord and Induces Opioid Receptor Tolerance. *J. Neurosci.* 24 (19), 4576–4584. doi:10.1523/JNEUROSCI.5552-03.2004

Conflict of Interest: The authors declare that the research was conducted in the absence of any commercial or financial relationships that could be construed as a potential conflict of interest.

Publisher's Note: All claims expressed in this article are solely those of the authors and do not necessarily represent those of their affiliated organizations, or those of the publisher, the editors and the reviewers. Any product that may be evaluated in this article, or claim that may be made by its manufacturer, is not guaranteed or endorsed by the publisher.

frontiers | Frontiers in Pharmacology

SYSTEMATIC REVIEW
published: 08 June 2022
doi: 10.3389/fphar.2022.909981

Antidepressant Effects of NSAIDs in Rodent Models of Depression—A Systematic Review

Cecilie Bay-Richter and Gregers Wegener*

Translational Neuropsychiatry Unit, Department of Clinical Medicine, Aarhus University, Aarhus, Denmark

In recent years much focus has been on neuroimmune mechanisms of depression. As a consequence, many preclinical and clinical trials have been performed examining potential antidepressant effects of several anti-inflammatory drugs. The results of such trials have been varied. With the current manuscript we wished to elucidate the effects of non-steroidal anti-inflammatory drugs (NSAIDs) on depressive-like behaviour in rodent models of depression by performing a systematic review of the available literature. We performed a systematic literature search in PubMed for rodent models of depression where NSAIDs were administered and a validated measure of depressive-like behaviour was applied. 858 studies were initially identified and screened using Covidence systematic review software. Of these 36 met the inclusion criteria and were included. The extracted articles contained data from both rat and mouse studies but primarily male animals were used. Several depression models were applied and 17 different NSAIDs were tested for antidepressant effects. Our results suggest that stress models are the best choice when examining antidepressant effects of NSAIDs. Furthermore, we found that rat models provide a more homogenous response than mouse models. Intriguingly, the use of female animals was only reported in three studies and these failed to find antidepressant effects of NSAIDs. This should be explored further. When comparing the different classes of NSAIDs, selective COX-2 inhibitors were shown to provide the most stable antidepressant effect compared to non-selective COX-inhibitors. Suggested mechanisms behind the antidepressant effects were attenuation of neuroinflammation, HPA-axis dysregulation and altered monoamine expression.

Keywords: depression, animal model, behaviour, non-steroidal anti-inflammatory drug, neuroinflammation

OPEN ACCESS

Edited by:
Divya Vohora,
Jamia Hamdard University, India

Reviewed by:
Laura Musazzi,
University of Milano Bicocca, Italy
Raquel Romay-Tallon,
University of Illinois at Chicago, United States

****Correspondence:***
Cecilie Bay-Richter
cbr@clin.au.dk

Specialty section:
This article was submitted to Neuropharmacology, a section of the journal Frontiers in Pharmacology

Received: *31 March 2022*
Accepted: *12 May 2022*
Published: *08 June 2022*

Citation:
Bay-Richter C and Wegener G (2022) Antidepressant Effects of NSAIDs in Rodent Models of Depression—A Systematic Review. Front. Pharmacol. 13:909981. doi: 10.3389/fphar.2022.909981

1 INTRODUCTION

Depression is a common psychiatric disease with high personal and socio-economical costs. Traditionally, monoamines have been considered to play a significant role in the disease and therefore, most antidepressant treatments target these neurotransmitter systems. However, only approximately half of the patients experience sufficient symptom relief. This indicates that additional biological mechanisms play a role in the aetiology of depression (Williams et al., 2010). More and more evidence point to the role of inflammation in the pathophysiology of the disease. It is known that cancer patients without psychiatric history who receive treatment with interferons are at increased risk of developing depression (Capuron et al., 2000; Raison et al., 2005). Furthermore, depressive symptoms appear in animal models when cytokine levels are experimentally elevated, for

example, by injections of the bacterial endotoxin lipopolysaccharide (Bay-Richter et al., 2011) or by poly I:C, which simulates a viral infection (Gibney et al., 2013). Interestingly, depressed patients have, in some studies, been shown to have elevated plasma levels of pro-inflammatory cytokines (Hestad et al., 2003), and it has been suggested that cytokine levels correlate with the severity of depression (Sha et al., 2022). Furthermore, the HPA axis is known to be dysregulated in depression. The negative cortisol feedback to the hypothalamus, pituitary and immune system is impaired. This leads to continual activation of the HPA axis and excess cortisol release. Cortisol receptors become desensitized, leading to increased activity of the pro-inflammatory immune mediators and disturbances in neurotransmitter transmission. Approximately 50% of patients suffering from MDD experience elevated cortisol secretion (Blackburn-Munro and Blackburn-Munro, 2001). Interestingly, some studies have shown that traditional antidepressant drugs can reduce inflammation (Hannestad et al., 2011; Cattaneo et al., 2013).

Because of the above evidence, a natural next step would be to assess the antidepressant effects of anti-inflammatory drugs. Clinical trials have been performed to evaluate the efficacy of anti-inflammatory drugs on depressive symptomatology. Specifically, three double-blind, placebo controlled studies have been performed to examine the putative antidepressant effects of add-on treatment with celecoxib. All three studies showed a significant impact of celecoxib compared to monotherapy with the antidepressants, which were either reboxetine (a noradrenaline reuptake inhibitor) (Muller et al., 2006), fluoxetine (an SSRI) (Akhondzadeh et al., 2009), or sertraline (an SSRI) (Abbasi et al., 2012). Only a few clinical studies using NSAIDs as monotherapy have been performed. Of the few done, one study found that celecoxib, naproxen, and ibuprofen improve depressive symptomatology compared to placebo (Iyengar et al., 2013). On the contrary, Fields et al. (2012) found no effect of celecoxib or naproxen on depressive symptoms in persons above 70 years old. Similarly, Berk et al. (2020) found low-dose aspirin not to prevent depression in individuals older than 70 years old. A large randomised controlled trial failed to demonstrate an effect of minocycline and celecoxib on depressive symptoms in patients with bipolar depression (Husain et al., 2020). This significant heterogeneity of results has sparked debate as to the underlying course of the results. Why do anti-inflammatory drugs have an effect in some studies and not in others? It has, for example, been suggested that the anti-inflammatory treatment should only be applied in subgroups of patients who are known to have inflammation (Miller and Pariante, 2020).

NSAIDs exert anti-inflammatory effects by inhibiting pro-inflammatory cytokines through inhibitory effects on the COX-enzymes. Depending on chemical structure, the drug can be either non-selective for the COX-enzymes, have a preference for COX-2 or be selective for COX-2 exclusively. In the current review, we wish to present an overview of the preclinical results which exist so far using validated measures of depressive-like behaviour and NSAIDs as intervention. We will evaluate the importance of the depression model, animal species, sex, drug, dose, and treatment regimen. Furthermore, we provide an overview of the potential mechanisms for the antidepressant effects of NSAIDs, as highlighted in the included articles.

2 MATERIALS AND METHODS

2.1 Search Strategy and Selection Criteria

We searched the PubMed database for studies on the effects of NSAIDs on depressive-like behaviour in rodents. The search was performed on 28th October 2021. Only primary articles published in peer-reviewed journals in English using an FDA approved NSAID and a validated measure of depressive-like behaviour such as forced swim test (FST)/tail suspension test (TST) or sucrose preference test (SPT). Opinion articles, commentaries, reviews, and other articles without original data were excluded.

2.2 Search String

We used a combined set of keywords to perform the PubMed search. These were: ("depres*"[Title/Abstract] OR "swim test"[Title/Abstract] OR "sucrose preference"[Title/Abstract] OR "porsolt"[Title/Abstract] OR "forced swim"[Title/Abstract] OR ("depressive disorder"[MeSH Terms] OR "depression"[MeSH Terms]) OR "depressive disorder"[MeSH Terms]) AND ("anti inflammatory drugs"[Title/Abstract] OR "anti inflammatory drug*"[Title/Abstract] OR "nsaid*"[Title/Abstract] OR "anti inflammatory agents, non steroidal"[MeSH Terms] OR "anti inflammatory agents"[MeSH Terms]) AND ("mouse"[Title/Abstract] OR "mice"[Title/Abstract] OR "rat"[Title/Abstract] OR "rats"[Title/Abstract] OR "muridae"[Title/Abstract] OR "mice"[MeSH Terms] OR "rats"[MeSH Terms]).

2.3 Study Selection and Data Extraction

Study selection and data extraction were performed using Covidence systematic review software (Veritas Health Innovation, Australia). Title/abstract screening and full-text screenings were performed by CBR. In cases of doubt during either title/abstract screening or full-text screening, the study was forwarded to a second reviewer (GW), who made the final decision. We included rodent studies that used an FDA approved NSAID to reverse depressive-like behaviour. The depressive-like behaviour could be produced by the behavioural test itself (e.g., FST) or by a range of inducers, including genetic models, inflammation and stress. We excluded studies using anti-inflammatory drugs that did not belong to the NSAID class or were not FDA approved. Furthermore, studies were excluded when the induction of depression was unclear (for example, in cases where immobility in the FST was confounded by general hypolocomotion). Additionally, the included studies had to contain a behavioural outcome measure of depression. Following descriptive variables were extracted for each study and presented in **Supplementary Table S1**: Reference, Primary aim of the study, Sex, strain and species,

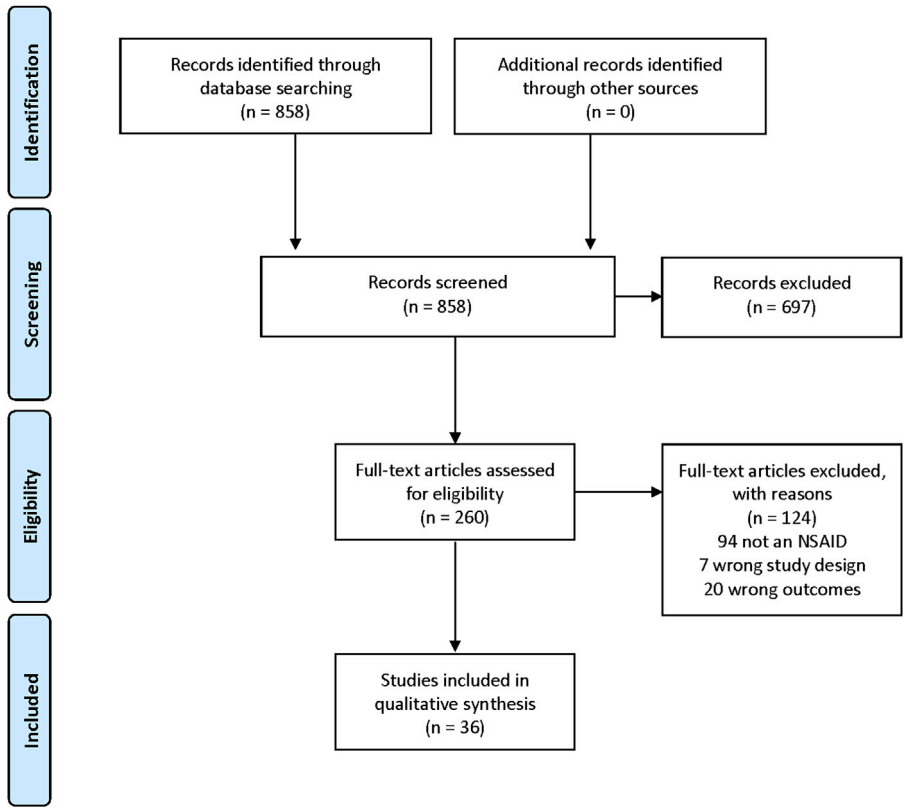

FIGURE 1 | Study selection (PRISMA flow chart).

Age and/or bodyweight, Depression model, Pharmacological intervention, and Main findings.

3 RESULTS

The search resulted in 858 references. Of these, 697 were excluded as irrelevant during the title-abstract screening. Mostly these references used a pharmaceutical intervention that was not classified as an NSAID. 260 articles were full-text screened. Of these, 124 were excluded; 94 because the intervention was not an NSAID, 7 had a wrong study design (e.g., where depressive-like behaviour could not be differentiated from locomotor abnormalities), and 20 had wrong outcomes (most often, no behavioural measure of depressive-like behaviour). In total, 36 references were included in this review (**Supplementary Table S1**). The study selection process is illustrated in **Figure 1**. The extracted articles contain data on both rat and mouse studies. 13 studies used Sprague-Dawley (S-D) rats, 7 Wistar, 1 study used HIV-1 rats and 17 studies used different mouse strains, both inbred, outbred and genetically modified. Only three studies reported the use of female animals. The depression models used to induce a depressive state ranged from stress models [e.g., chronic mild stress (CMS)] to pain models (e.g. CFA injections), to inflammation models (e.g. LPS) to a range of genetic models (e.g. HIV-1 rats) and diet-related models. Also, the FST alone in some studies served to detect antidepressant activity. The depression models were primarily stress-related (17 studies) or inflammation-related (9 studies). The remaining 11 studies used models of pain, neurodegeneration, diet, somatic disease or chemotherapy. 17 different NSAIDs were used, belonging to several NSAID groups. Most commonly used were the selective COX-2 inhibitor celecoxib (11 studies) and the non-selective COX inhibitor ibuprofen (8 studies). Drugs were administered in different doses, for different lengths of time and using different routes of administration (most commonly p.o. or i.p.). The results are presented according to the chemical classification of the NSAID.

3.1 Carboxylic Acids

The carboxylic acids include salicylates (e.g., acetylsalicylic acid), fenamates (e.g., mefenamic acid), indole acetates (e.g., indomethacin), phenylacetates (e.g., diclofenac) and the propionates (e.g., ibuprofen). Typical of these NSAIDs is that they are non-selective COX-inhibitors.

3.1.1 Propionates

Ibuprofen was used in 8 studies. One study found no effect on lupus-induced despair. Here, ibuprofen was administered to MRL-lpr mice in food for 14 weeks (Ballok et al., 2006). One study found ibuprofen to have an antidepressant-like effect on FST-induced despair (50 but not 75 mg/kg) as well as reducing

interferon (IFN)-α induced despair and anhedonia in male mice (Mesripour et al., 2019). Another study found ibuprofen not to affect FST-induced despair but indeed to decrease tumour induced despair using female mice (Norden et al., 2015). Qadeer et al. (2018) found no effect on FST induced despair in Wistar rats but significantly decreased stress-induced distress. BCG-induced despair was also shown to be reduced in mice (Saleh et al., 2014). Salmani et al. (2021) shoved that ibuprofen decreased FST induced despair but had no effect on LPS-induced despair in male BALB/c mice. Seo et al. (2019) found ibuprofen to reduce stress-induced despair. When co-administered, Warner-Schmidt et al. (2011) reported that ibuprofen reversed the antidepressant effects of several traditional antidepressant drugs.

Naproxen was used in 2 studies. Both studies found no effect on FST induced despair in female and male C57BL/6 mice (Warner-Schmidt et al., 2011; Pavlock et al., 2021). Warner-Schmidt et al. (2011) even showed that naproxen reversed the antidepressant effects of citalopram.

One study examined the effect of ketoprofen and found it to reduce swim stress-induced despair (Guevara et al., 2015). Flurbiprofen did not add any antidepressant effect when co-administered with fluoxetine (Alboni et al., 2018).

3.1.2 Indole Acetates

Five studies examined the effects of indomethacin. Deak et al. (2005) found no impact on FST-induced despair in male S-D rats. On the contrary Mesripour et al. (2019) found indomethacin to reverse FST-induced despair and improve IFN-α induced despair and anhedonia in male albino mice. Perveen et al. (2018) also found indomethacin to reverse FST induced despair and CMS induced despair in male S-D rats. Stachowicz (2020) reported indomethacin not to affect FST or TST induced despair but to improve the antidepressant effect of imipramine when given in combination in CD1 and C57/BL6 mice.

3.1.3 Phenyl Acetates

Diclofenac was examined in three studies. Borges et al. (2014) found diclofenac to reduce monoarthritis-induced despair in male S-D rats, and De La Garza et al. (2005) showed the same for LPS induced despair in male Wistar rats. Perveen et al. (2018) reported that diclofenac reduced FST- and stress-induced despair in male S-D rats.

3.1.4 Salicylates

Acetylsalicylic acid (ASA) was used in 4 studies. Alboni et al. (2018); Brunello et al. (2006) both showed that in co-administration with fluoxetine, ASA decreased stress-induced depressive-like behaviour in male S-D rats. Alone, ASA had no antidepressant effect (Brunello et al., 2006; Warner-Schmidt et al., 2011). On the contrary (Guan et al., 2014) found ASA monoadministration to have antidepressant effects in the FST in male S-D rats. Warner-Schmidt et al. (2011) even showed that ASA attenuated the antidepressant effects of citalopram.

3.1.5 Fenamates

Mefenamic acid reduced CMS-induced anhedonia and despair in male C57/BL6 mice (Feng et al., 2020).

3.2 Diaryl Heterocyclic Compounds

Celecoxib was used in 10 studies and was, therefore, the most frequently used NSAID included in this review. Belonging to the same drug group was rofecoxib which was used in one study. Common to these drugs is their selectivity as specific inhibitors of the COX-2 enzyme.

Alboni et al. (2018) found a non-significant tendency of celecoxib to increase the antidepressant effects of fluoxetine when coadministered. de Munter et al. (2020) showed that celecoxib did not affect FST-induced despair in WT mice but in a genetic model of frontotemporal lobar degeneration (FUS[1-359]-tg mice) the drug reduced despair. There was also a tendency for celecoxib to reduce IFN-α induced despair in male S-D rats (Fischer et al., 2015). Guo et al. (2009) found celecoxib to reduce CMS-induced anhedonia in male S-D rats and Kurhe et al. (2014) showed reduced despair and anhedonia in a high-fat diet model of depression in swiss albino mice. Maciel et al. (2013) reported that celecoxib could reduce despair-like behaviour induced by peripheral inflammation and Mesripour et al. (2019) showed that celecoxib had antidepressant effects in FST and reduced IFN-α induced despair and anhedonia. Further, celecoxib reduced Aβ-induced despair (Morgese et al., 2018) and CMS-induced anhedonia in male Wistar rats (Santiago et al., 2014). In the same study, celecoxib was found to have antidepressant effects in the FST. Song et al. (2019) did not find antidepressant effects in the FST after celecoxib treatment but did show celecoxib to reduce stress- and LPS-induced despair. Rofecoxib had antidepressant effects in an Nrf2 KO model of depression (Martín-de-Saavedra et al., 2013).

3.3 Enolic Acid Derivatives

The enolic acid derivatives (oxicams) include both preferential COX-2 inhibitors such as meloxicam, but also non-selective COX-inhibitors such as lornoxicam and piroxicam. Four studies examined meloxicam. Meloxicam was reported to improve repeated swim stress-induced despair in male S-D rats and reduce CMS-induced anhedonia in S-D rats (Guevara et al., 2015; Luo et al., 2017). Nemeth and colleagues found meloxicam to improve microembolism-induced despair but not HIV-induced despair in rats (Nemeth et al., 2014; Nemeth et al., 2016). Santiago and colleagues found a single dose of piroxicam to reduce FST-induced despair. Further, the drug reversed CMS-induced anhedonia and 6-OHDA-induced despair and anhedonia in male Wistar rats (Santiago et al., 2014; Santiago et al., 2015). Lornoxicam did not affect neuropathic pain induced despair (Hu et al., 2010).

3.4 Sulphonanilides

The preferential COX-2 inhibitor nimesulide was used in two studies. Both studies found nimesulide to reverse stress-induced despair in male S-D rats and male albino Laca mice (Singh et al., 2017; Luo et al., 2020).

4 DISCUSSION

In summary, we identified and included 36 studies which met the inclusion criteria. The studies included examinations of both rats and mice. Inbred, outbred as well as genetically modified animals were used. Antidepressant effects of the NSAIDs alone were examined in the FST and/or TST in some studies. Still, most studies examined whether an NSAID drug could reverse experimentally induced depressive-like behaviour.

4.1 Depression Model

Thirteen studies examined the antidepressant effects of the NSAID in the FST without further manipulations of the animals (Yamano et al., 2000; Deak et al., 2005; Warner-Schmidt et al., 2011; Guan et al., 2014; Santiago et al., 2014; Norden et al., 2015; Perveen et al., 2018; Qadeer et al., 2018; Mesripour et al., 2019; Song et al., 2019; Stachowicz, 2020; Pavlock et al., 2021; Salmani et al., 2021). ASA, Celecoxib, ibuprofen, piroxicam, and indomethacin were shown to have antidepressant effects (Guan et al., 2014; Santiago et al., 2014; Perveen et al., 2018; Mesripour et al., 2019; Salmani et al., 2021). Other studies showed no antidepressant effects in the FST of ibuprofen, celecoxib, indomethacin, ASA or naproxen (Yamano et al., 2000; Warner-Schmidt et al., 2011; Norden et al., 2015; Qadeer et al., 2018; Song et al., 2019; Stachowicz, 2020; Pavlock et al., 2021).

In all studies, independent of the depression model, 29 out of 36 reported antidepressant effects of NSAIDs. The models used were either stress-induced depressive-like behaviour (15 of 29) (Brunello et al., 2006; Guo et al., 2009; Guan et al., 2014; Santiago et al., 2014; Guevara et al., 2015; Luo et al., 2017; Singh et al., 2017; Alboni et al., 2018; Perveen et al., 2018; Qadeer et al., 2018; Seo et al., 2019; Song et al., 2019; Feng et al., 2020; Luo et al., 2020; Stachowicz, 2020), 5 studies were directly related to inflammation (De La Garza et al., 2005; Saleh et al., 2014; Fischer et al., 2015; Mesripour et al., 2019; Salmani et al., 2021), 8 studies used different disease models (Maciel et al., 2013; Martín-de-Saavedra et al., 2013; Borges et al., 2014; Norden et al., 2015; Santiago et al., 2015; Nemeth et al., 2016; Morgese et al., 2018; de Munter et al., 2020) and a single study used diet-induced depression (Kurhe et al., 2014). Six studies failed to find antidepressant effects of NSAIDs. The models used were either stress-induced (by FST) (Deak et al., 2005), inflammation-induced (Yamano et al., 2000) or related to a disease (Ballok et al., 2006; Hu et al., 2010; Nemeth et al., 2014; Pavlock et al., 2021). A single study found antidepressant drugs to reverse the antidepressant effects of several antidepressant drugs in mice (Warner-Schmidt et al., 2011).

Intriguingly, the only stress-related model which fails to find antidepressant effects of NSAIDs is the FST alone (Deak et al., 2005). Of the 29 studies reporting antidepressant effects, 13 use stress models, primarily CMS. All studies using CMS report antidepressant effects of the NSAIDs. Therefore, stress models, in particular CMS models, appear to be a good choice when examining the antidepressant effects of NSAIDs. This may also have clinical relevance; NSAIDs may be better at treating depression related to stress than other types of depressive illness. This could be important as more and more people suffer from stress-related depression, and this has severe socioeconomic as well as personal consequences (Yang et al., 2015).

4.2 Species and Sex

Rats were used in 21 studies, whereas 15 used different mouse strains. The most frequently used strain was the S-D rat (used in 13 studies). In the 12 studies which examined antidepressant effects in the FST mice and rats were test subjects both in the studies showing antidepressant activity of NSAIDs as well as studies failing to find an effect. Intriguingly, 5 out of 7 studies failing to find antidepressant effects of NSAIDs in the FST without other manipulations were performed on mice. This pattern is similar when looking at all models; Of the 29 studies showing antidepressant properties of NSAIDs, 11 studies used mice (38%). Out of the 7 studies that failed to find an antidepressant activity, 5 studies used mice (71%). The rat studies which failed to report antidepressant effects used the FST alone and a model of neuropathic pain. The mouse models without antidepressant effects used inflammation models, different disease models, and FST alone. As the same or similar models are also used in studies that report antidepressant effects of the NSAIDs, it seems unlikely that methodological differences cause the species difference. The same applies to the drugs used; several different classes of NSAIDs were used in both mice and rats (see **Supplementary Table S1**). In summary, it appears that rat models are better at detecting antidepressant properties using the FST. This is in line with previous research (Borsini and Meli, 1988).

Of the 6 studies failing to show antidepressant effects of NSAIDs, one study used IFN-α to induce a depressive state in mice. In this study, indomethacin could not reverse the depressive-like behaviour (Yamano et al., 2000). Interestingly, Mesripour et al. (2019) also studied the effects of indomethacin after IFN-α-induced depression. Here, indomethacin was able to reverse IFN-α-induced despair and anhedonia. The groups used different mouse strains; ddY mice vs. non-specified albino mice. While ddY is sometimes used as a general purpose model, it is also known that the mouse develops spontaneous IgA nephropathy (Imai et al., 1985), which could affect the result.

Intriguingly, all studies reporting the use of female animals failed to detect the antidepressant properties of NSAIDs. Preclinical work has traditionally been performed exclusively in male animals. Still, more and more research suggests that disease progression and therapeutic drug response may vary substantially between the sexes (see LeGates et al. (2019) for review). An important goal of future research will be to explore potential sex differences further, and future studies should therefore include both male and female animals when examining drug effects of e.g., NSAIDs.

4.3 Drug, Dose and Treatment Regiment

Two studies examined the effect of indomethacin on IFN-α—induced depression in mice and found conflicting evidence (Yamano et al., 2000; Mesripour et al., 2019). Apart from the different mouse strains used, as described above, the studies also used different doses, routes of administration and lengths of treatment. Yamano et al. (2000), who failed to find an effect of indomethacin, used 10 mg/kg, s.c. for 7 days Mesripour et al. (2019)

found an effect of a single injection of 25 mg/kg i.p indomethacin 30 min before the FST. One explanation for the discrepancy could therefore be the chosen dose. It should, however, be noted that both Perveen et al. (2018) also reported on effects of indomethacin on stress-induced despair. Here, 7 days of treatment with 7.5 mg/kg indomethacin had antidepressant properties in the FST in male rats (Perveen et al., 2018), whereas, for mice, 2 mg/kg indomethacin for 7 or 14 days was not able to produce antidepressant effects in the FST (Stachowicz, 2020). Mice likely require a larger dose than rats as smaller animals have higher metabolic rates and higher physiological processes (Nair and Jacob, 2016).

Surprisingly, Warner-Schmidt et al. (2011) reported that ibuprofen reversed the antidepressant effects of citalopram, fluoxetine, imipramine, and desipramine and that naproxen and ASA reversed the effect of citalopram in C57Bl6 mice. The only other included study examining the effect of NSAIDs and antidepressants on antidepressant effects was (Stachowicz, 2020), who reported that indomethacin improved the antidepressant effect of imipramine when administered together. A difference between the two studies is the use of different NSAIDs. Where ibuprofen is a propriate, indomethacin belongs to the indole acetates.

Interestingly, all studies applying selective COX-2 inhibitors (celecoxib and rofecoxib) reported antidepressant effects of these drugs (Guo et al., 2009; Maciel et al., 2013; Martín-de-Saavedra et al., 2013; Kurhe et al., 2014; Santiago et al., 2014; Fischer et al., 2015; Alboni et al., 2018; Morgese et al., 2018; Mesripour et al., 2019; Song et al., 2019; de Munter et al., 2020; Feng et al., 2020). It has previously been reported that selective COX-2 inhibitors may be more effective in relieving depression than non-selective COX-inhibitors (Baune, 2017).

4.4 Mechanisms

In many of the studies, neurobiological mechanisms which may underlie the antidepressant effects of the NSAID are examined. Eight studies which reported antidepressant effects of NSAIDs have examined neuroinflammation in animals. Five of these report that NSAIDs lead to decreased neuroinflammation (Maciel et al., 2013; Norden et al., 2015; Song et al., 2019; de Munter et al., 2020; Feng et al., 2020) either measured as normalisation of microgliosis or cytokine expression in the brain. De La Garza et al. (2005) and Guan et al. (2014) examined peripheral cytokines but reported conflicting results. Guan et al. (2014) found blood levels of TNF-a and IL-6 normalised after ASA treatment, whereas De La Garza et al. (2005) found no effect of diclofenac on LPS-induced elevation of plasma IL-1β. Of the studies which failed to find antidepressant effects of NSAIDs, three examined neuroinflammation. Ballok et al. (2006) reported that ibuprofen neither affects lupus-induced despair nor microgliosis. For this study, it should be noted that ibuprofen is provided in the food, and no measure of the actual dose is reported. Nemeth et al. (2014) and Warner-Schmidt et al. (2011) showed that neuroinflammation is decreased by meloxicam and ibuprofen without having an antidepressant effect. It therefore appears that reversal of neuroinflammation could be an essential player in the anti-inflammatory effects of NSAIDs, as has often been suggested (Leonard and Song, 1999; Hestad et al., 2003; Thomas et al., 2005), but caution should be taken before drawing such conclusion.

As described in the introduction, depression is often associated with dysregulation of the HPA-axis, which is linked to neuroinflammation (Holsboer, 2003), and several preclinical studies have shown that depressive-like behaviour is associated with elevated levels of CORT (McEwen, 2005; Pariante and Lightman, 2008). CORT expression was examined in four of the studies reporting antidepressant effects of NSAIDs. Three of these showed that meloxicam, ibuprofen, indomethacin and diclofenac normalised plasma CORT levels (Guevara et al., 2015; Perveen et al., 2018; Seo et al., 2019). Guan et al. (2014) reported that while ASA had antidepressant effects, the drug did not attenuate CORT levels. None of the studies which failed to find antidepressant properties of NSAIDs measured CORT. In summary, there is some evidence that CORT plays a role in the antidepressant activity of NSAIDs.

Monoamines are the main targets of classical antidepressants. Here, three studies reported how piroxicam and celecoxib could reverse both despair but also normalise the monoamine expression in the brain (Santiago et al., 2014; Morgese et al., 2018).

5 CONCLUSION

In summary, we found that antidepressant effects of NSAIDs was studied in several different depression models, using both mouse- and rat strains but primarily using male animals. Seventeen different NSAIDs were examined for potential antidepressant effects. The results showed that stress models using selective COX-2 inhibitors provided the most robust antidepressant response. This may have clinical implications as it could be speculated that patients with stress-related depression are more likely to benefit from NSAID treatment than other types of depression and that the most efficient treatment would be selective COX-2 inhibitors such as celecoxib and rofecoxib.

DATA AVAILABILITY STATEMENT

The original contributions presented in the study are included in the article/Supplementary Material, further inquiries can be directed to the corresponding author.

AUTHOR CONTRIBUTIONS

CBR and GW contributed to conception and design of the study. CBR performed the data-extraction and wrote the first draft of the manuscript. Both authors contributed to manuscript revision, read, and approved the submitted version.

SUPPLEMENTARY MATERIAL

The Supplementary Material for this article can be found online at: https://www.frontiersin.org/articles/10.3389/fphar.2022.909981/full#supplementary-material

REFERENCES

Abbasi, S. H., Hosseini, F., Modabbernia, A., Ashrafi, M., and Akhondzadeh, S. (2012). Effect of Celecoxib Add-On Treatment on Symptoms and Serum IL-6 Concentrations in Patients with Major Depressive Disorder: Randomized Double-Blind Placebo-Controlled Study. *J. Affect Disord.* 141, 308–314. doi:10.1016/j.jad.2012.03.033

Akhondzadeh, S., Jafari, S., Raisi, F., Nasehi, A. A., Ghoreishi, A., Salehi, B., et al. (2009). Clinical Trial of Adjunctive Celecoxib Treatment in Patients with Major Depression: a Double Blind and Placebo Controlled Trial. *Depress Anxiety* 26, 607–611. doi:10.1002/da.20589

Alboni, S., Benatti, C., Capone, G., Tascedda, F., and Brunello, N. (2018). Neither all Anti-inflammatory Drugs Nor All Doses Are Effective in Accelerating the Antidepressant-like Effect of Fluoxetine in an Animal Model of Depression. *J. Affect Disord.* 235, 124–128. doi:10.1016/j.jad.2018.04.063

Ballok, D. A., Ma, X., Denburg, J. A., Arsenault, L., and Sakic, B. (2006). Ibuprofen Fails to Prevent Brain Pathology in a Model of Neuropsychiatric Lupus. *J. Rheumatol.* 33, 2199–2213.

Baune, B. T. (2017). Are Non-steroidal Anti-inflammatory Drugs Clinically Suitable for the Treatment of Symptoms in Depression-Associated Inflammation? *Curr. Top. Behav. Neurosci.* 31, 303–319. doi:10.1007/7854_2016_19

Bay-Richter, C., Janelidze, S., Hallberg, L., and Brundin, L. (2011). Changes in Behaviour and Cytokine Expression upon a Peripheral Immune Challenge. *Behav. Brain Res.* 222, 193–199. doi:10.1016/j.bbr.2011.03.060

Berk, M., Woods, R. L., Nelson, M. R., Shah, R. C., Reid, C. M., Storey, E., et al. (2020). Effect of Aspirin vs Placebo on the Prevention of Depression in Older People: A Randomized Clinical Trial. *JAMA Psychiatry* 77, 1012–1020. doi:10.1001/jamapsychiatry.2020.1214

Blackburn-Munro, G., and Blackburn-Munro, R. E. (2001). Chronic Pain, Chronic Stress and Depression: Coincidence or Consequence? *J. Neuroendocrinol.* 13, 1009–1023. doi:10.1046/j.0007-1331.2001.00727.x

Borges, G., Neto, F., Mico, J. A., and Berrocoso, E. (2014). Reversal of Monoarthritis-Induced Affective Disorders by Diclofenac in Rats. *Anesthesiology* 120, 1476–1490. doi:10.1097/ALN.0000000000000177

Borsini, F., and Meli, A. (1988). Is the Forced Swimming Test a Suitable Model for Revealing Antidepressant Activity? *Psychopharmacol. Berl.* 94, 147–160. doi:10.1007/BF00176837

Brunello, N., Alboni, S., Capone, G., Benatti, C., Blom, J. M., Tascedda, F., et al. (2006). Acetylsalicylic Acid Accelerates the Antidepressant Effect of Fluoxetine in the Chronic Escape Deficit Model of Depression. *Int. Clin. Psychopharmacol.* 21, 219–225. doi:10.1097/00004850-200607000-00004

Capuron, L., Ravaud, A., and Dantzer, R. (2000). Early Depressive Symptoms in Cancer Patients Receiving Interleukin 2 And/or Interferon Alfa-2b Therapy. *J. Clin. Oncol.* 18, 2143–2151. doi:10.1200/JCO.2000.18.10.2143

Cattaneo, A., Gennarelli, M., Uher, R., Breen, G., Farmer, A., Aitchison, K. J., et al. (2013). Candidate Genes Expression Profile Associated with Antidepressants Response in the GENDEP Study: Differentiating between Baseline 'predictors' and Longitudinal 'targets'. *Neuropsychopharmacology* 38, 377–385. doi:10.1038/npp.2012.191

De La Garza, R., 2nd, Asnis, G. M., Fabrizio, K. R., and Pedrosa, E. (2005). Acute Diclofenac Treatment Attenuates Lipopolysaccharide-Induced Alterations to Basic Reward Behavior and HPA axis Activation in Rats. *Psychopharmacol. Berl.* 179, 356–365. doi:10.1007/s00213-004-2053-x

de Munter, J., Babaevskaya, D., Wolters, E. C., Pavlov, D., Lysikova, E., V Kalueff, A., et al. (2020). Molecular and Behavioural Abnormalities in the FUS-Tg Mice Mimic Frontotemporal Lobar Degeneration: Effects of Old and New Anti-inflammatory Therapies. *J. Cell Mol. Med.* 24, 10251–10257. doi:10.1111/jcmm.15628

Deak, T., Bellamy, C., D'Agostino, L. G., Rosanoff, M., McElderry, N. K., and Bordner, K. A. (2005). Behavioral Responses during the Forced Swim Test Are Not Affected by Anti-inflammatory Agents or Acute Illness Induced by Lipopolysaccharide. *Behav. Brain Res.* 160, 125–134. doi:10.1016/j.bbr.2004.11.024

Feng, X., Fan, Y., and Chung, C. Y. (2020). Mefenamic Acid Can Attenuate Depressive Symptoms by Suppressing Microglia Activation Induced upon Chronic Stress. *Brain Res.* 1740, 146846. doi:10.1016/j.brainres.2020.146846

Fields, C., Drye, L., Vaidya, V., Lyketsos, C., and Group, A. R. (2012). Celecoxib or Naproxen Treatment Does Not Benefit Depressive Symptoms in Persons Age 70 and Older: Findings from a Randomized Controlled Trial. *Am. J. Geriatr. Psychiatry* 20, 505–513. doi:10.1097/JGP.0b013e318227f4da

Fischer, C. W., Eskelund, A., Budac, D. P., Tillmann, S., Liebenberg, N., Elfving, B., et al. (2015). Interferon-alpha Treatment Induces Depression-like Behaviour Accompanied by Elevated Hippocampal Quinolinic Acid Levels in Rats. *Behav. Brain Res.* 293, 166–172. doi:10.1016/j.bbr.2015.07.015

Gibney, S. M., McGuinness, B., Prendergast, C., Harkin, A., and Connor, T. J. (2013). Poly I:C-induced Activation of the Immune Response Is Accompanied by Depression and Anxiety-like Behaviours, Kynurenine Pathway Activation and Reduced BDNF Expression. *Brain Behav. Immun.* 28, 170–181. doi:10.1016/j.bbi.2012.11.010

Guan, X. T., Shao, F., Xie, X., Chen, L., and Wang, W. (2014). Effects of Aspirin on Immobile Behavior and Endocrine and Immune Changes in the Forced Swimming Test: Comparison to Fluoxetine and Imipramine. *Pharmacol. Biochem. Behav.* 124, 361–366. doi:10.1016/j.pbb.2014.07.002

Guevara, C., Fernandez, A. C., Cardenas, R., and Suarez-Roca, H. (2015). Reduction of Spinal PGE2 Concentrations Prevents Swim Stress-Induced Thermal Hyperalgesia. *Neurosci. Lett.* 591, 110–114. doi:10.1016/j.neulet.2015.02.035

Guo, J. Y., Li, C. Y., Ruan, Y. P., Sun, M., Qi, X. L., Zhao, B. S., et al. (2009). Chronic Treatment with Celecoxib Reverses Chronic Unpredictable Stress-Induced Depressive-like Behavior via Reducing Cyclooxygenase-2 Expression in Rat Brain. *Eur. J. Pharmacol.* 612, 54–60. doi:10.1016/j.ejphar.2009.03.076

Hannestad, J., DellaGioia, N., and Bloch, M. (2011). The Effect of Antidepressant Medication Treatment on Serum Levels of Inflammatory Cytokines: a Meta-Analysis. *Neuropsychopharmacology* 36, 2452–2459. doi:10.1038/npp.2011.132

Hestad, K. A., Tønseth, S., Støen, C. D., Ueland, T., and Aukrust, P. (2003). Raised Plasma Levels of Tumor Necrosis Factor Alpha in Patients with Depression: Normalization during Electroconvulsive Therapy. *J. ECT* 19, 183–188. doi:10.1097/00124509-200312000-00002

Holsboer, F. (2003). High-quality Antidepressant Discovery by Understanding Stress Hormone Physiology. *Ann. N. Y. Acad. Sci.* 1007, 394–404. doi:10.1196/annals.1286.038

Hu, Y., Yang, J., Hu, Y., Wang, Y., and Li, W. (2010). Amitriptyline rather Than Lornoxicam Ameliorates Neuropathic Pain-Induced Deficits in Abilities of Spatial Learning and Memory. *Eur. J. Anaesthesiol.* 27, 162–168. doi:10.1097/EJA.0b013e328331a3d5

Husain, M. I., Chaudhry, I. B., Khoso, A. B., Husain, M. O., Hodsoll, J., Ansari, M. A., et al. (2020). Minocycline and Celecoxib as Adjunctive Treatments for Bipolar Depression: a Multicentre, Factorial Design Randomised Controlled Trial. *Lancet Psychiatry* 7, 515–527. doi:10.1016/S2215-0366(20)30138-3

Imai, H., Nakamoto, Y., Asakura, K., Miki, K., Yasuda, T., and Miura, A. B. (1985). Spontaneous Glomerular IgA Deposition in ddY Mice: an Animal Model of IgA Nephritis. *Kidney Int.* 27, 756–761. doi:10.1038/ki.1985.76

Iyengar, R. L., Gandhi, S., Aneja, A., Thorpe, K., Razzouk, L., Greenberg, J., et al. (2013). NSAIDs Are Associated with Lower Depression Scores in Patients with Osteoarthritis. *Am. J. Med.* 126, 1017–1018. e1011. doi:10.1016/j.amjmed.2013.02.037

Kurhe, Y., Mahesh, R., and Gupta, D. (2014). Effect of a Selective Cyclooxygenase Type 2 Inhibitor Celecoxib on Depression Associated with Obesity in Mice: an Approach Using Behavioral Tests. *Neurochem. Res.* 39, 1395–1402. doi:10.1007/s11064-014-1322-2

LeGates, T. A., Kvarta, M. D., and Thompson, S. M. (2019). Sex Differences in Antidepressant Efficacy. *Neuropsychopharmacology* 44, 140–154. doi:10.1038/s41386-018-0156-z

Leonard, B. E., and Song, C. (1999). Stress, Depression, and the Role of Cytokines. *Adv. Exp. Med. Biol.* 461, 251–265. doi:10.1007/978-0-585-37970-8_14

Luo, W., Luo, Y., and Yang, J. (2020). Proteomics-based Screening of the Target Proteins Associated with Antidepressant-like Effect and Mechanism of Nimesulide. *Sci. Rep.* 10, 11052. doi:10.1038/s41598-020-66420-z

Luo, Y., Kuang, S., Li, H., Ran, D., and Yang, J. (2017). cAMP/PKA-CREB-BDNF Signaling Pathway in hippocampus Mediates Cyclooxygenase 2-induced Learning/memory Deficits of Rats Subjected to Chronic Unpredictable Mild Stress. *Oncotarget* 8, 35558–35572. doi:10.18632/oncotarget.16009

Maciel, I. S., Silva, R. B., Morrone, F. B., Calixto, J. B., and Campos, M. M. (2013). Synergistic Effects of Celecoxib and Bupropion in a Model of Chronic

Inflammation-Related Depression in Mice. *PLoS One* 8, e77227. doi:10.1371/journal.pone.0077227

Martín-de-Saavedra, M. D., Budni, J., Cunha, M. P., Gómez-Rangel, V., Lorrio, S., Del Barrio, L., et al. (2013). Nrf2 Participates in Depressive Disorders through an Anti-inflammatory Mechanism. *Psychoneuroendocrinology* 38, 2010–2022.

McEwen, B. S. (2005). Glucocorticoids, Depression, and Mood Disorders: Structural Remodeling in the Brain. *Metabolism* 54, 20–23. doi:10.1016/j.metabol.2005.01.008

Mesripour, A., Shahnooshi, S., and Hajhashemi, V. (2019). Celecoxib, Ibuprofen, and Indomethacin Alleviate Depression-like Behavior Induced by Interferon-Alfa in Mice. *J. Complement. Integr. Med.* 17. doi:10.1515/jcim-2019-0016

Miller, A. H., and Pariante, C. M. (2020). Trial Failures of Anti-inflammatory Drugs in Depression. *Lancet Psychiatry* 7, 837. doi:10.1016/S2215-0366(20)30357-6

Morgese, M. G., Schiavone, S., Bove, M., Mhillaj, E., Tucci, P., and Trabace, L. (2018). Sub-chronic Celecoxib Prevents Soluble Beta Amyloid-Induced Depressive-like Behaviour in Rats. *J. Affect Disord.* 238, 118–121. doi:10.1016/j.jad.2018.05.030

Müller, N., Schwarz, M. J., Dehning, S., Douhe, A., Cerovecki, A., Goldstein-Müller, B., et al. (2006). The Cyclooxygenase-2 Inhibitor Celecoxib Has Therapeutic Effects in Major Depression: Results of a Double-Blind, Randomized, Placebo Controlled, Add-On Pilot Study to Reboxetine. *Mol. Psychiatry* 11, 680–684. doi:10.1038/sj.mp.4001805

Nair, A. B., and Jacob, S. (2016). A Simple Practice Guide for Dose Conversion between Animals and Human. *J. Basic Clin. Pharm.* 7, 27–31. doi:10.4103/0976-0105.177703

Nemeth, C. L., Glasper, E. R., Harrell, C. S., Malviya, S. A., Otis, J. S., and Neigh, G. N. (2014). Meloxicam Blocks Neuroinflammation, but Not Depressive-like Behaviors, in HIV-1 Transgenic Female Rats. *PLoS One* 9, e108399. doi:10.1371/journal.pone.0108399

Nemeth, C. L., Miller, A. H., Tansey, M. G., and Neigh, G. N. (2016). Inflammatory Mechanisms Contribute to Microembolism-Induced Anxiety-like and Depressive-like Behaviors. *Behav. Brain Res.* 303, 160–167. doi:10.1016/j.bbr.2016.01.057

Norden, D. M., McCarthy, D. O., Bicer, S., Devine, R. D., Reiser, P. J., Godbout, J. P., et al. (2015). Ibuprofen Ameliorates Fatigue- and Depressive-like Behavior in Tumor-Bearing Mice. *Life Sci.* 143, 65–70. doi:10.1016/j.lfs.2015.10.020

Pariante, C. M., and Lightman, S. L. (2008). The HPA axis in Major Depression: Classical Theories and New Developments. *Trends Neurosci.* 31, 464–468. doi:10.1016/j.tins.2008.06.006

Pavlock, S., McCarthy, D. M., Kesarwani, A., Jean-Pierre, P., and Bhide, P. G. (2021). Hippocampal Neuroinflammation Following Combined Exposure to Cyclophosphamide and Naproxen in Ovariectomized Mice. *Int. J. Neurosci.*, 1–10. doi:10.1080/00207454.2021.1896508

Perveen, T., Emad, S., Haider, S., Sadaf, S., Qadeer, S., Batool, Z., et al. (2018). Role of Cyclooxygenase Inhibitors in Diminution of Dissimilar Stress-Induced Depressive Behavior and Memory Impairment in Rats. *Neuroscience* 370, 121–129. doi:10.1016/j.neuroscience.2017.11.014

Qadeer, S., Emad, S., Perveen, T., Yousuf, S., Sheikh, S., Sarfaraz, Y., et al. (2018). Role of Ibuprofen and Lavender Oil to Alter the Stress Induced Psychological Disorders: A Comparative Study. *Pak J. Pharm. Sci.* 31, 1603–1608.

Raison, C. L., Demetrashvili, M., Capuron, L., and Miller, A. H. (2005). Neuropsychiatric Adverse Effects of Interferon-Alpha: Recognition and Management. *CNS Drugs* 19, 105–123. doi:10.2165/00023210-200519020-00002

Saleh, L. A., Hamza, M., El Gayar, N. H., Abd El-Samad, A. A., Nasr, E. A., and Masoud, S. I. (2014). Ibuprofen Suppresses Depressive like Behavior Induced by BCG Inoculation in Mice: Role of Nitric Oxide and Prostaglandin. *Pharmacol. Biochem. Behav.* 125, 29–39. doi:10.1016/j.pbb.2014.07.013

Salmani, H., Hosseini, M., Baghcheghi, Y., and Samadi-Noshahr, Z. (2021). The Brain Consequences of Systemic Inflammation Were Not Fully Alleviated by Ibuprofen Treatment in Mice. *Pharmacol. Rep.* 73, 130–142. doi:10.1007/s43440-020-00141-y

Santiago, R. M., Barbiero, J., Martynhak, B. J., Boschen, S. L., da Silva, L. M., Werner, M. F., et al. (2014). Antidepressant-like Effect of Celecoxib Piroxicam in Rat Models of Depression. *J. Neural Transm. (Vienna)* 121, 671–682. doi:10.1007/s00702-014-1159-5

Santiago, R. M., Tonin, F. S., Barbiero, J., Zaminelli, T., Boschen, S. L., Andreatini, R., et al. (2015). The Nonsteroidal Antiinflammatory Drug Piroxicam Reverses the Onset of Depressive-like Behavior in 6-OHDA Animal Model of Parkinson's Disease. *Neuroscience* 300, 246–253. doi:10.1016/j.neuroscience.2015.05.030

Seo, M. K., Lee, J. G., and Park, S. W. (2019). Effects of Escitalopram and Ibuprofen on a Depression-like Phenotype Induced by Chronic Stress in Rats. *Neurosci. Lett.* 696, 168–173. doi:10.1016/j.neulet.2018.12.033

Sha, Q., Madaj, Z., Keaton, S., Escobar Galvis, M. L., Smart, L., Krzyzanowski, S., et al. (2022). Cytokines and Tryptophan Metabolites Can Predict Depressive Symptoms in Pregnancy. *Transl. Psychiatry* 12, 35. doi:10.1038/s41398-022-01801-8

Singh, B., Mourya, A., Sah, S. P., and Kumar, A. (2017). Protective Effect of Losartan and Ramipril against Stress Induced Insulin Resistance and Related Complications: Anti-inflammatory Mechanisms. *Eur. J. Pharmacol.* 801, 54–61. doi:10.1016/j.ejphar.2017.02.050

Song, Q., Feng, Y. B., Wang, L., Shen, J., Li, Y., Fan, C., et al. (2019). COX-2 Inhibition Rescues Depression-like Behaviors via Suppressing Glial Activation, Oxidative Stress and Neuronal Apoptosis in Rats. *Neuropharmacology* 160, 107779. doi:10.1016/j.neuropharm.2019.107779

Stachowicz, K. (2020). Indomethacin, a Nonselective Cyclooxygenase Inhibitor, Does Not Interact with MTEP in Antidepressant-like Activity, as Opposed to Imipramine in CD-1 Mice. *Eur. J. Pharmacol.* 888, 173585. doi:10.1016/j.ejphar.2020.173585

Thomas, A. J., Davis, S., Morris, C., Jackson, E., Harrison, R., and O'Brien, J. T. (2005). Increase in Interleukin-1beta in Late-Life Depression. *Am. J. Psychiatry* 162, 175–177. doi:10.1176/appi.ajp.162.1.175

Warner-Schmidt, J. L., Vanover, K. E., Chen, E. Y., Marshall, J. J., and Greengard, P. (2011). Antidepressant Effects of Selective Serotonin Reuptake Inhibitors (SSRIs) Are Attenuated by Antiinflammatory Drugs in Mice and Humans. *Proc. Natl. Acad. Sci. U. S. A.* 108, 9262–9267. doi:10.1073/pnas.1104836108

Williams, J. M., Russell, I. T., Crane, C., Russell, D., Whitaker, C. J., Duggan, D. S., et al. (2010). Staying Well after Depression: Trial Design and Protocol. *BMC Psychiatry* 10, 23. doi:10.1186/1471-244X-10-23

Yamano, M., Yuki, H., Yasuda, S., and Miyata, K. (2000). Corticotropin-releasing Hormone Receptors Mediate Consensus Interferon-Alpha YM643-Induced Depression-like Behavior in Mice. *J. Pharmacol. Exp. Ther.* 292, 181–187.

Yang, L., Zhao, Y., Wang, Y., Liu, L., Zhang, X., Li, B., et al. (2015). The Effects of Psychological Stress on Depression. *Curr. Neuropharmacol.* 13, 494–504. doi:10.2174/1570159x1304150831150507

Conflict of Interest: The authors declare that the research was conducted in the absence of any commercial or financial relationships that could be construed as a potential conflict of interest.

frontiers | Frontiers in Neuroscience

ORIGINAL RESEARCH
published: 16 June 2022
doi: 10.3389/fnins.2022.898051

Dose-Dependent Regulation on Prefrontal Neuronal Working Memory by Dopamine D_1 Agonists: Evidence of Receptor Functional Selectivity-Related Mechanisms

Yang Yang[1,2], Susan D. Kocher[1], Mechelle M. Lewis[1,2,3] and Richard B. Mailman[1,2,3]**

[1] Department of Pharmacology, Penn State Milton S. Hershey Medical Center, Penn State College of Medicine, Hershey, PA, United States, [2] Translational Brain Research Center, Penn State Milton S. Hershey Medical Center, Penn State College of Medicine, Hershey, PA, United States, [3] Department of Neurology, Penn State Milton S. Hershey Medical Center, Penn State College of Medicine, Hershey, PA, United States

OPEN ACCESS

Edited by:
Divya Vohora,
Jamia Hamdard University, India

Reviewed by:
Jonathan D. Urban,
ToxStrategies, Inc., United States
Amy F. T. Arnsten,
Yale University, United States
Susheel Vijayraghavan,
Western University, Canada

***Correspondence:**
Yang Yang
yangyang@psu.edu
Richard B. Mailman
rmailman@psu.edu

Specialty section:
This article was submitted to Neuropharmacology, a section of the journal Frontiers in Neuroscience

Received: *16 March 2022*
Accepted: *31 May 2022*
Published: *16 June 2022*

Citation:
Yang Y, Kocher SD, Lewis MM and Mailman RB (2022) Dose-Dependent Regulation on Prefrontal Neuronal Working Memory by Dopamine D_1 Agonists: Evidence of Receptor Functional Selectivity-Related Mechanisms. Front. Neurosci. 16:898051. doi: 10.3389/fnins.2022.898051

Low doses of dopamine D_1 agonists improve working memory-related behavior, but high doses eliminate the improvement, thus yielding an 'inverted-U' dose-response curve. This dose-dependency also occurs at the single neuron level in the prefrontal cortex where the cellular basis of working memory is represented. Because signaling mechanisms are unclear, we examined this process at the neuron population level. Two D_1 agonists (2-methyldihydrexidine and CY208,243) having different signaling bias were tested in rats performing a spatial working memory-related T-maze task. 2-Methyldihydrexidine is slightly bias toward D_1-mediated β-arrestin-related signaling as it is a full agonist at adenylate cyclase and a super-agonist at β-arrestin recruitment, whereas CY208,243 is slightly bias toward D_1-mediated cAMP signaling as it has relatively high intrinsic activity at adenylate cyclase, but is a partial agonist at β-arrestin recruitment. Both compounds had the expected inverted U dose-dependency in modulating prefrontal neuronal activities, albeit with important differences. Although CY208,243 was superior in improving the strength of neuronal outcome sensitivity to the working memory-related choice behavior in the T-maze, 2-methyldihydrexidine better reduced neuron-to-neuron variation. Interestingly, at the neuron population level, both drugs affected the percentage, uniformity, and ensemble strength of neuronal sensitivity in a complicated dose-dependent fashion, but the overall effect suggested higher efficiency and potency of 2-methyldihydrexidine compared to CY208,243. The differences between 2-methyldihydrexidine and CY208,243 may be related to their specific D_1 signaling. These results suggest that D_1-related dose-dependent regulation of working memory can be modified differentially by functionally selective ligands, theoretically increasing the balance between desired and undesired effects.

Keywords: dopamine D1 agonist, dose response analysis, prefrontal cortex, working memory, functional selectivity/biased agonism

INTRODUCTION

The prefrontal cortex (PFC) subserves higher-order cognitive function, and its neuron activities represent the cellular basis of working memory (WM) (Goldman-Rakic, 1995, 2011; Kesner and Churchwell, 2011; Caetano et al., 2012; Laubach et al., 2015; Yang and Mailman, 2018). Dopamine D_1 receptors (D_1Rs) play important roles in the PFC (Murphy et al., 1996a; Lidow et al., 2003; Arnsten et al., 2015), and D_1 agonists cause marked cognitive improvement in laboratory animals (Arnsten et al., 1994, 2017; Murphy et al., 1996b; Cai and Arnsten, 1997; Zahrt et al., 1997; Vijayraghavan et al., 2007; Wang et al., 2019; Yang et al., 2021) and in humans (Mu et al., 2007; Rosell et al., 2015; Huang et al., 2020). In animal studies where dose can be manipulated, low doses of dopamine D_1 agonists improve working memory-related behavior, but high doses eliminate the improvement, thus yielding an 'inverted-U' dose-response curve (Arnsten et al., 1994; Cai and Arnsten, 1997; Zahrt et al., 1997; Vijayraghavan et al., 2007; Yang et al., 2021). In monkeys performing spatial WM (sWM) tasks, low doses of D_1 agonists enhanced spatial tuning of a single PFC neuron by increasing responses to preferred directions or suppressing responses to non-preferred directions. Conversely, high doses changed the firing for all directions, eroding tuning (Vijayraghavan et al., 2007; Wang et al., 2019). These dose-dependent sculpting actions at the single neuron level could be the cellular basis of the inverted-U dose response of D_1 agonists at the behavioral level. Alternately, neural ensembles in the PFC may be more important than single neurons (Jung et al., 1998; Baeg et al., 2003; Horst and Laubach, 2012; Yang et al., 2014; Bolkan et al., 2017; Murray et al., 2017; Spaak et al., 2017; Yang and Mailman, 2018; De Falco et al., 2019). This makes the dose-dependent analysis of D_1 action at the neuron population level of special importance at both the basic and translational levels.

The pattern of signal transduction mediated by a drug acting at single receptor (commonly called *functional selectivity* or *biased signaling*) is recognized to be of heuristic importance, but also offers the possibility of developing novel therapies (Urban et al., 2007; Kenakin, 2012). Cyclic AMP (cAMP) is the canonical intracellular messenger mediated by D_1Rs, and a key player in dose-dependent regulation at the single neuron level in the PFC (Vijayraghavan et al., 2007). G protein-independent β-arrestin-related signaling also may be critical (Urs et al., 2011, 2015; Liu et al., 2015; Yang et al., 2021). β-Arrestin, besides functions for receptor desensitization and internalization, also acts as a multifunctional signal transducer by serving as an adaptor/scaffold to connect the activated receptors with diverse signaling pathways within the cell (Yang, 2021). We hypothesize that both cAMP and β-arrestin are involved in the dose-dependent regulation of D_1 agonists, as are other D_1R-mediated signaling such as opening/closing of ion channels (Paspalas et al., 2013; Arnsten, 2015; Arnsten et al., 2015; Gamo et al., 2015). Our underlying premise was that functionally selective/biased D_1 agonists differ in their dose-response characteristics based on differential engagement of alternate signaling pathways. We used two D_1 selective agonists (2-methyldihydrexidine and CY208,243) that contrast in their signaling bias (Yang et al., 2021) to compare dose-response effects in a rodent sWM task. 2-Methyldihydrexidine has modest bias toward D_1-mediated β-arrestin-related signaling as it is a full agonist at adenylate cyclase and a super-agonist (activity greater than dopamine) at β-arrestin recruitment, whereas CY208,243 is slightly bias toward D_1-mediated cAMP signaling with relatively high intrinsic activity at adenylate cyclase, but only partial agonism at β-arrestin recruitment. We probed three aspects of neuron population dynamics in the PFC: percentage; uniformity; and ensemble strength of neuronal sensitivity (see Methods). The results indicate that D_1 agonists affect neuron population dynamics in the PFC in a complicated dose-dependent manner. These data also suggest that functional selectivity can be a promising strategy for the discovery of novel D_1 ligands that may have an improved therapeutic index for cognition.

MATERIALS AND METHODS

Subjects

All animal care and surgical procedures were in accordance with the National Institutes of Health Guide for the Care and Use of Laboratory Animals and Penn State Hershey Animal Resources Program, and were reviewed and approved by the local IACUC. A total of six male Sprague-Dawley rats (Charles River Laboratories) weighing 226–350 g when received were housed individually and maintained on a 12-h light-dark cycle with water continuously available. They were fed a limited diet of Bio-Serv rat chow (5 g/100 g) to maintain their body weight at 90–95% of free-feeding body weight for motivation purposes. Highly palatable rewards (chocolate flavored sucrose, Bio-Serv) were used during testing.

Drug Preparation and Administration

2-Methyldihydrexidine (2MDHX) was synthesized by modifications of published procedures (Yang et al., 2021) whereas CY208,243 (CY208) was purchased from Tocris (Minneapolis, MN, United States). Both compounds were of >97% purity. Stock solutions of 100 mM 2MDHX and CY208 were made in DMSO and stored at −80°C in the dark. For use, they were diluted in 0.1% ascorbic acid vehicle using a dose range (1, 10, 100, and 10,000 nmol/kg) suggested by prior experiments (Yang et al., 2021). Working solutions were prepared on the day of experiments, and injected subcutaneously under brief ca. 4% isoflurane anesthesia. Rats recovered within a minute, and then were placed in the test arena to habituate to the environment. The behavioral task and electrophysiological recording started ca. 20 min later. The order of drug condition was randomly assigned and the interval between two drug conditions was at least 5 days.

Microwire Electrode Array Implantation in Medial Prefrontal Cortex

Rats were given 1 week of full access to food before unilateral implantation of a microwire electrode into the right medial PFC (mPFC) (Yang and Mailman, 2018). Animal weights were all over 350 g when craniotomy surgeries were performed. After initial anesthesia with ca. 4% isoflurane, a continuous 0.5–2% isoflurane

anesthesia was maintained during the surgery. The animal was fixed on a stereotactic frame and ophthalmic antibiotic ointment was applied to prevent the eyes from desiccation. The incised site was disinfected and subcutaneously injected by drops of bupivacaine. The skull surface was exposed and adjusted to lie flat between Bregma and Lambda. Four small holes were drilled for anchor screws including one that served as a ground for the electrode. A 2.5 mm × 2.5 mm bone window was made above the mPFC and the dura mater carefully was removed. A microwire electrode array targeting the mPFC was lowered vertically to a depth of 3.5 mm from the brain surface at 3.0 mm rostral to bregma and 0.4 mm lateral to bregma. The microwire electrode array was made with 25 μm stainless steel wire coated by polyimide (H-ML), which has an impedance between 600 and 900 kΩ, arranged in a 2 × 4 configuration with 250 μm between electrodes (MicroProbes). The array was positioned with its long axis parallel to the anterior-posterior plane. After electrode placement, the craniotomy was sealed with dental cement and wound margins were daubed with antibiotic ointment. Rats were given enrofloxacin (5 mg/kg, Baytril, Bio-Serv) and carprofen (20 mg/kg, Rimadyl, Bio-Serv) tablets for 3 days, and had full access to food for at least 1 week.

Delayed Alternation Response Task in the T-Maze

Rats individually were trained in a T-maze and acclimated with the electrophysiological recording setup (Yang and Mailman, 2018). A standard T-maze was utilized that had one start runway (56 cm long, 10 cm wide and 18 cm high) and two finish arms (41 cm long, 10 cm wide and 18 cm high). The maze was made of acrylic polycarbonate with a black floor and clear sides for better video and electrophysiological recordings. A CCD camera (30 frames/second, STC-TB33USB-AS, SenTech) was hung over the top of the maze and connected to a Limelight video recording system (Actimetrics, Coulbourn Instruments) to monitor simultaneously the animal's free movement in the maze. Pre-defined grids (**Figure 1A**) indicated the animal's behavior (passed grids). The Limelight system sent out a TTL (+5V) signal to mark the reference time (RT), referring to the time for choice behavior (passed a grid).

Rats were habituated to all procedures and tested by a single person. To administer drugs and connect the electrophysiological recording cables, rats were anesthetized briefly with ca. 4% isoflurane. They recovered within a minute and were placed in the recording arena to habituate to the environment. The delayed alternation response (DAR) task started after ca. 20 min and began when the animal was placed in the start box of the T-maze. The start box is located in the lower section of the start runway and cordoned off by a solid gate. After the tester raised the gate, the rat needed to run to the intersection of the T and make a choice of turning down the left or right arm of the maze. This first choice always was rewarded with a hand-fed food reward at the end of the finish arm. Then the rat gently was returned to the start box and remained there for a predetermined fixed delay (5 s), as this is the general temporal scale of WM tasks. After the delay elapsed, the gate was raised, and the task was repeated. For each trial, rats needed to run to the intersection, make a choice, and reach the end of the arm in less than 1 min, otherwise the trial was aborted, and the DAR task restarted. This continued for ca. 40 min to be considered a complete test session. The rats were trained to visit the two arms of the maze alternatively, and were rewarded only after a correct choice. During the entire procedure, the tester minimized any possible cues that might affect choice.

All rats were well-trained for the task. They made correct choice >60% during the vehicle control condition after which they underwent multiple test sessions to evaluate drug effects. Each session had ca. 20 trials (range 8–97). There was a minimum of 5 days of drug washout between any two drug test sessions.

Electrophysiological Recordings

Neural recordings were collected during DAR task using the OmniPlex Neural Data Acquisition System (Plexon) that also recorded the RT signal from Limelight, which enable synchronization of neural and behavioral recordings. Wideband and spike signals were recorded for later off-line analysis. The wideband signal was digitized at 40 kHz. A highpass filter with a cutoff of 250 Hz yielded the continuous spike signal that was sampled at the same 40 kHz rate as the original wideband signal. Artifacts due to cable noise and devices were removed during off-line analysis.

Action potentials were detected and sorted both on- and off-line *via* the Offline Sorter (Plexon) to get better unit isolation results. Waveforms from multiple units were sorted by means of voltage-time threshold windows and a two principal components (PCs) contour template algorithm (PCA). The degree to which the waveform clusters are separated in the 2D projection of two PCs was determined by a Multivariate ANOVA test. Significance ($\alpha < 0.05$) indicated that each waveform cluster had a different location in 2D space and that the clusters were well separated. Then, each well-separated waveform cluster was assigned as a single unit. The same sorting method was implemented throughout all recording sessions, ensuring the sorting stability of the waveform of a single neuron.

Once experiments were complete, rats were euthanized by an overdose of isoflurane *via* inhalation, combined with incising the diaphragm to create a pneumothorax. After perfused with 10% formalin, the dissected brains were fixed with 10% formalin and dehydrated with a 30% sucrose solution, and then sectioned coronally (50 μm) using a cryostat microtome. The brain slices were used to identify electrode recording sites and trajectories that were observed under a microscope. The slices were stained with cresyl violet to verify the detailed structures. The locations of the tips were determined based on the rat brain atlas (Paxinos and Watson, 2013) and were confirmed to be in the mPFC of all rats, including the sub-regions of both prelimbic cortex and infralimbic cortex.

Experimental Design and Statistical Analyses

Each rat underwent multiple (3–13) test sessions, and during each session, one drug (2MDHX or CY208) at one dose (1, 10, 100, or 10,000 nmol/kg) or vehicle was administered. The vehicle session

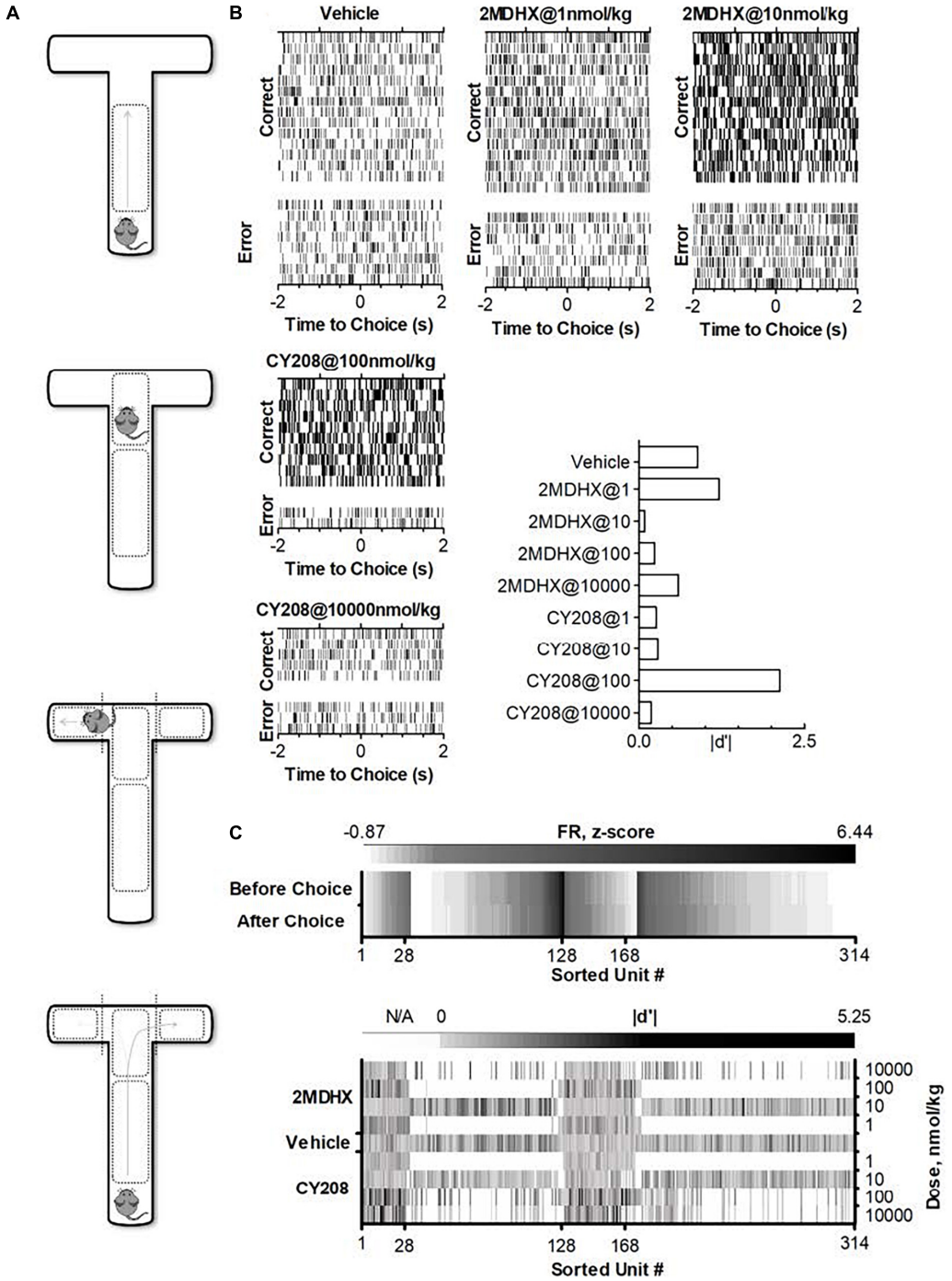

FIGURE 1 | Experimental paradigm and single neuron activities after administration of D_1 agonists 2MDHX or CY208. **(A)** Standard T-maze. Pre-defined zones and grids were used to indicate an animal's behavior as making a choice (passed grids). **(B)** A single neuron example shows the dose response after 2MDHX or CY208 administration. Rasters indicate individual spikes. Trials are organized by correct vs. error outcome. For better illustration, only example trials for five drug conditions were shown, but this neuron was tested for all eight drug conditions. The effect on outcome sensitivity by different doses of drug was summarized in the histogram at the lower-right corner. Note CY208 (at 100 nmol/kg) increased its sensitivity strength better than 2MDHX (at 1 nmol/kg), but its "optimal" and "detrimental" doses of 2MDHX (1 and 10 nmol/kg, respectively) were both lower than CY208 (100 and 10,000 nmol/kg, respectively). **(C)** Summary of all recorded single neurons. Top panel shows firing rate (FR, z-score) during control conditions where vehicle was administered. Note that units #1–128 are prospective-encoding-neurons that have a higher FR before the WM-related choice behavior during the DAR task (i.e., top row has darker color). Conversely, units #129–314 are retrospective-encoding-neurons that have a higher FR after the choice (i.e., bottom row has darker color). The bottom panel shows the strength of outcome sensitivity (|*d'*|) during each drug condition (2MDHX/CY208 @ 1/10/100/10,000 nmol/kg). N/A means data not available as this drug condition was not tested. Only 28 prospective-encoding-neurons (units #1–28) and 40 retrospective-encoding-neurons (units #129–168) were tested for all eight drug conditions.

TABLE 1 | Experimental design.

	Number of neurons recorded	2MDHX (nmol/kg)				CY208 (nmol/kg)			
Rat ID		**1**	**10**	**100**	**10000**	**1**	**10**	**100**	**10000**
1	45		x				x		
2	9	x		x				x	
3	41		x				x		
4	76	xx	xx	x	x	xxx	x	x	x
5	74		x				x		
6	69		x		x		x	x	x

A total of six rats were used. They were first tested after administration of vehicle (control condition), and then after administration of 2MDHX or CY208 at 1, 10, 100, or 10,000 nmol/kg in a randomized order. Because of the challenge to long-term persistent chronic electrophysiological recording, only one rat (#4) completed all eight drug conditions, and others completed two to five drug conditions. "x" indicates completed drug session. Double or triple "x" indicates repeated sessions after first round of eight drug conditions.

was always the first, and then our intention was to perform all eight drug conditions in a randomized order. The long-term persistent chronic electrophysiological recording, however, posed a challenge to complete all eight drug conditions, mostly because of the loose microwire electrode array during this long-time process. Eventually one rat completed all drug conditions and even repeated a few, but all others only completed two to five drug conditions (**Table 1**). To study the neuronal mechanisms, single neurons were recorded from each rat. Number of neurons tested in each drug condition was shown in **Table 2**. The data were organized based on drug conditions (Vehicle/2MDHX/CY208 @ 1/10/100/10,000 nmol/kg). As detailed below, we used a combination of MATLAB 2017 (MathWorks, Natick, MA, United States), SPSS (IBM, Armonk, NY, United States), and Prism (GraphPad, La Jolla, CA, United States) for data analysis. All data are reported as mean ± SD (*sd* used below for clarity) unless otherwise specified.

For each neuron, spike counts, i.e., firing rate (FR), were binned around choice (RT, ± 2 s) in each trial, similarly as reported in a previous study (Yang and Mailman, 2018). Each neuron then was classified as either a "prospective-encoding-neuron" or a "retrospective-encoding-neuron" based on the FR before and after the choice behavior during the DAR task, where:

$$Neuron\ Type = \begin{cases} prospective-encoding-neuron, & mean_{before} > mean_{after} \\ retrospective-encoding-neuron, & mean_{before} < mean_{after} \end{cases}$$

Neuronal sensitivity to correct or error outcome, "neuronal-outcome-sensitivity," then was scaled by calculating the sensitivity index (d'), defined as the ability to distinguish error from correct choice based on the FR, where $d' = (mean_{error} - mean_{correct}) / \sqrt{\left(sd^2_{error} + sd^2_{correct}\right)/2}$.

A positive d' indicates an error outcome sensitivity, whereas a negative d' reflects a correct outcome sensitivity, which classifies neurons into two groups:

$$Neuron\ Type = \begin{cases} correct-sensitive-neuron, & d' < 0 \\ error-sensitive-neuron, & d' > 0 \end{cases}$$

TABLE 2 | Data cohort.

Drug condition	**Number of neurons (Prospective/Retrospective)**		
1 nmol/kg			
2MDHX	35/50		
CY208	30/46		
		30/46	*Tested both drugs*
10 nmol/kg			
2MDHX	123/182		
CY208	117/170		
		117/170	*Tested both drugs*
100 nmol/kg			
2MDHX	35/50		
CY208	60/94		
		35/50	*Tested both drugs*
10,000 nmol/kg			
2MDHX	49/78		
CY208	53/84		
		49/78	*Tested both drugs*
		28/40	*Tested all eight drug conditions*
		128/186	***Total***

Neuron activity in the PFC first was recorded after administration of vehicle (control condition), and then after administration of 2MDHX or CY208 at 1, 10, 100, or 10,000 nmol/kg. Single neurons recorded during the same drug condition were pooled together for analysis of neuron population dynamics.

The absolute value of d' reflects the strength of the sensitivity (i.e., higher or lower values suggest greater or less sensitivity, respectively).

For neurons tested both 2MDHX and CY208 at all four doses (1, 10, 100, and 10,000 nmol/kg), the dose for each neuron that led to the largest increase in sensitivity strength was defined as an "optimal" dose for this neuron, whereas the dose that led to the smallest increase or the largest decrease in sensitivity strength was defined as a "detrimental" dose. The median of the optimal and detrimental dose for all these neurons then was calculated and the Wilcoxon matched-pairs signed rank test was used to evaluate if there was a difference between 2MDHX and CY208. The mean sensitivity strength for all neurons also was calculated and repeated ANOVA was used to evaluate whether there was a significant difference among drug conditions (Vehicle/2MDHX/CY208 @ optimal/detrimental dose). The neuron-to-neuron variation, regarding their sensitivity strength, was measured by coefficient of variation (CV) where CV = SD/mean.

Neuronal population dynamics on the dataset that included all recorded neurons then were analyzed. Neurons recorded during the same drug condition (vehicle/2MDHX/CY208 @ 1/10/100/10,000 nmol/kg) were pooled together and three measurements of neuron population dynamics were calculated: percentage, uniformity, and ensemble neuronal sensitivity. *(1)* Percentage. There are two types of neurons based on their sensitivities: "correct-sensitive-neurons" and "error-sensitive-neurons" (see above the definition). The percentage of each group among the whole neuron population was calculated. Fisher's

TABLE 3 | Definition of the integrated population dynamics index $\sum_{i=1}^{12} F_i \log V_{i\ (drug)}/V_{i\ (\ vehicle)}$.

I			F	Functional meaning for modulation of behavioral performance during the DAR task.
T	O	Measurement		
Prospective	Correct	Percentage (%)	**1**	More prospective-correct-neurons to modulate correct outcomes
		Uniformity (H)	**−1**	More homogenous prospective-correct-neurons for correct outcomes
		Ensemble sensitivity (d′)	**1**	Greater correct sensitivity prospectively for correct outcomes
	Error	Percentage (%)	**−1**	Less prospective-error-neurons to limit error outcomes
		Uniformity (H)	**1**	More heterogeneous prospective-error-neurons to limit error outcomes
		Ensemble sensitivity (d′)	**−1**	Less error sensitivity prospectively to limit error outcomes
Retrospective	Correct	Percentage (%)	**1**	More retrospective-correct-neurons for correct outcomes
		Uniformity (H)	**−1**	More homogeneity retrospective-correct-neurons for feedback adjustment
		Ensemble sensitivity (d′)	**1**	Greater correct sensitivity retrospectively for feedback adjustment
	Error	Percentage (%)	**−1**	Less retrospective-error-neurons to limit error outcomes
		Uniformity (H)	**−1**	More homogeneity retrospective-error-neurons for feedback adjustment
		Ensemble sensitivity (d′)	**1**	Greater sensitivity retrospectively for feedback adjustment

We defined this index to integrate all three measurements of neuron population dynamics (percentage, uniformity, and ensemble sensitivity), and combine them with the consideration of temporal encoding (prospective and retrospective) and event sensitivity (correct- and error-sensitive). V is the value of a population measurement (percentage, uniformity, or ensemble sensitivity) during the vehicle session or after drug administration. F is the functional index of a population measurement, which is either 1 or −1, and indicates an increase (as 1) or a decrease (as −1) of this measurement suggesting a modulation to improve behavioral performance during the DAR. Note the uniformity is calculated by H and the increase of H indicates a decrease of uniformity and vice versa. Therefore, for the uniformity, 1 and −1 indicate an increase (as 1) and a decrease (as −1) of H, which correlates to a decrease (as 1) and an increase (as −1) of uniformity. T, temporal encoding; O, outcome sensitivity.

exact test was used to evaluate whether the percentage differed significantly for drug vs. vehicle. *(2)* Uniformity indicates how homogenous or heterogeneous a group of neurons is regarding their sensitivity. In other words, it measures the diversity of the d' among a group of neurons. To analyze uniformity, a d' proportion distribution of a group of neurons first was calculated using a 0.1-bin and the uniformity then was estimated by the index $H = -\sum_{i=1}^{s} p_i \ln p_i$, where p_i is the proportion in the i^{th} bin of the d' proportion distribution and s is the number of bins. A low H indicates a homogenous population whereas a high H indicates a heterogeneous one (Barnes et al., 2005; Thorn et al., 2010; Dorval et al., 2015). ANOVA was used to evaluate whether the uniformity differed significantly after drug administration. *(3)* Ensemble neuronal sensitivity refers to whether a group of neurons integrate their individual neuronal sensitivity to associate with certain (correct/error) information. To analyze the ensemble sensitivity, the median (including its interquartile range) of d' was calculated for correct- and error-sensitive neurons, respectively. Median values farther from zero indicated a higher strength of ensemble sensitivity, whereas those closer to zero indicated a lower strength. The Mann-Whitney test was used to evaluate whether the ensemble sensitivity differed significantly after drug administration.

Finally, we defined a population dynamics index that integrated temporal encoding (prospective and retrospective), outcome sensitivity (correct- and error-sensitive), and three population measurements (percentage, uniformity, and ensemble sensitivity) together. The index was defined as $\sum_{i=1}^{12} F_i \log(V_{i\ (drug)}/V_{i\ (vehicle)})$, where V is the value of a population measurement (percentage, uniformity, or ensemble sensitivity) during the vehicle session or after drug administration, and F is the functional index of this population measurement. As shown in **Table 3**, we defined the functional index of each population measurement as 1 or −1 based on its physiological meaning to best modulate the DAR task performance.

RESULTS

Dose Response of D_1 Agonists 2-Methyldihydrexidine and CY208 on Neurons Tested All Four Doses

A total of 314 neurons were recorded in the mPFC. An example neuron was showed in **Figure 1B**, and the summary of all recorded neurons was in **Figure 1C** and **Table 2**. Among all recorded neurons, 128 neurons were prospective-encoding-neurons as having higher FR before the choice behavior during the DAR task, whereas 186 neurons were retrospective-encoding-neurons as having higher FR after choice. All neurons were tested during multiple drug conditions, but only 28 prospective-encoding-neurons and 40 retrospective-encoding-neurons were tested for all eight drug conditions (2MDHX/CY208 @ 1/10/100/10,000 nmol/kg). Both 2MDHX and CY208 significantly increased sensitivity strength $|d'|$ of these 68 neurons at one of four testing doses, and this "optimal" dose was lower when 2MDHX was administered (prospective-encoding-neurons, $P_{2MDHX,CY208} = 0.007$; retrospective-encoding-neurons, $P_{2MDHX,CY208} < 0.0001$; **Figure 2A**). The increased sensitivity strength was greater for CY208 compared to 2MDHX (**Figure 2B** and **Table 4**). Neuron-to-neuron variation, as measured by CV, was decreased by both drugs but the effect was greater for 2MDHX (**Figure 2C** and **Table 4**). Both drugs also tended to decrease sensitivity

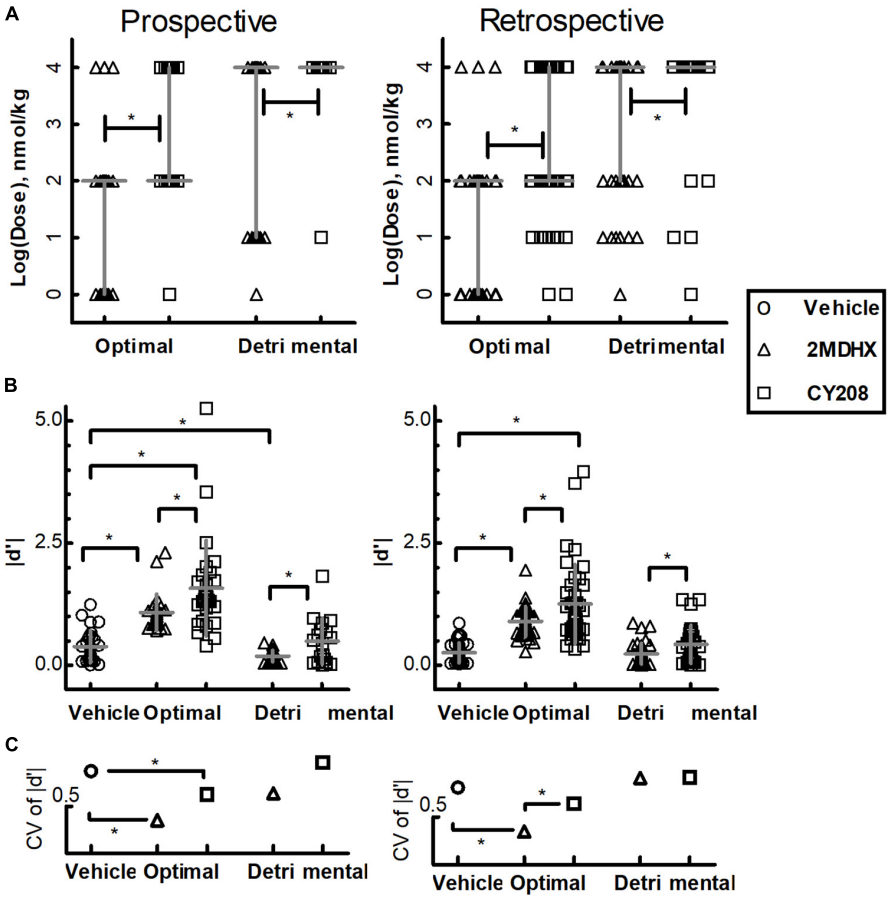

FIGURE 2 | Summary of the effects of D_1 agonists 2MDHX and CY208 on neurons tested all four doses. **(A)** 2MDHX and CY208 had different optimal and detrimental doses causing maximal increases or decreases in the sensitivity strength of a neuron. See the detailed definitions of optimal and detrimental doses in the Methods. Lines indicate median and interquartile ranges for all prospective- and retrospective-encoding-neurons. Triangles and squares represent each single neuron, and the triangles indicate the 2MDHX and the squares indicate CY208 drug conditions, respectively. Note that both optimal and detrimental doses were lower for 2MDHX compared to CY208 for both prospective- and retrospective-encoding-neurons. *Indicates $P < 0.05$. **(B)** The maximal increase in sensitivity strength at the optimal dose was significantly higher after CY208 administration compared to 2MDHX, and the maximal decrease at the detrimental dose was significantly less by CY208. Lines indicate the average (mean ± SD). Circles indicate the vehicle condition. **(C)** The neuron-to-neuron variation (CV) regarding sensitivity strength was decreased at the optimal dose. Note the decrease in CV was greater by 2MDHX, especially for retrospective-encoding-neurons.

strength at a higher dose, and this "detrimental" dose was lower when 2MDHX was administered (prospective neurons, $P_{2MDHX,CY208} = 0.008$; retrospective neurons, $P_{2MDHX,CY208} = 0.025$; **Figure 2A**). The decrease in sensitivity strength was significant only for prospective-encoding-neurons after 2MDHX administration (**Figure 2B** and **Table 4**). There was a trend to increase neuron-to-neuron variation, particularly for CY208 (**Figure 2C** and **Table 4**).

Dose Response of 2-Methyldihydrexidine on Pooled Neuron Population

We pooled neurons tested in the same drug condition together and then analyzed drug effects on the neuron population dynamics comparing to vehicle condition. For prospective-encoding-neurons, 2MDHX increased the percentage of correct-sensitive-neurons at 1 nmol/kg, but it was not statistically significant (**Figure 3A** and **Table 5**). At higher doses, 2MDHX significantly decreased the percentage of correct-sensitive-neurons (10–10,000 nmol/kg; **Figures 3B–D** and **Table 5**). Uniformity of the correct-sensitive-neurons, as measured by H, did not change at lower doses (1–100 nmol/kg; **Figures 3A–C** and **Table 5**), but became slightly more homogeneous (i.e., decreased H) at 10,000 nmol/kg (**Figure 3D** and **Table 5**). The ensemble sensitivity of the correct-neurons, as measured by median of d', was increased at 1 nmol/kg (**Figure 3A** and **Table 5**), but at higher doses the increase became not statistically significant (10–10,000 nmol/kg; **Figures 3B–D** and **Table 5**). For error-sensitive-neurons, their uniformity (H) was not changed at 1 nmol/kg (**Figure 3A** and **Table 5**) but became more homogeneous (i.e., decreased H) at 10 nmol/kg (**Figure 3B** and **Table 5**). At higher doses, however, the uniformity became more heterogeneous (i.e., increased H; 100–10,000 nmol/kg; **Figures 3C,D** and **Table 5**). The ensemble sensitivity (d') of the error-neurons tended to decrease at lower doses (1–10 nmol/kg;

TABLE 4 | Effects of 2MDHX and CY208 on neurons tested all four doses.

D	N		Sensitivity strength |d′|			Variation (CV, %)		
			Vehicle	2MDHX	CY208	Vehicle	2MDHX	CY208
Optimal	Pro		0.38 ± 0.33	1.08 ± 0.38	1.58 ± 0.98	87	35	62
		2MDHX	<0.001*		0.02*	<0.001*		0.097
		CY208	<0.001*	0.02*		0.027	0.097	
	Retro		0.25 ± 0.21	0.89 ± 0.32	1.25 ± 0.81	82	35	65
		2MDHX	<0.001*		0.013*	<0.001*		0.021*
		CY208	<0.001*	0.013*		0.058	0.021*	
Detrimental	Pro		0.38 ± 0.33	0.19 ± 0.12	0.49 ± 0.47	87	64	97
		2MDHX	0.007*		0.016*	0.163		0.19
		CY208	0.391	0.016*		0.802	0.19	
	Retro		0.25 ± 0.21	0.23 ± 0.22	0.42 ± 0.39	82	92	93
		2MDHX	0.665		0.029*	0.925		0.811
		CY208	0.048*	0.029*		0.721	0.811	

*Total of 28 prospective-encoding-neurons and 40 retrospective-encoding-neurons were tested for all eight drug conditions (2MDHX/CY208 @ 1/10/100/10,000 nmol/kg). Both 2MDHX and CY208 increased sensitivity strength |d′| and decreased neuron-to-neuron variation (i.e., decreased CV) of these neurons at an "optimal" dose, with CY208 having better effect on |d′| and 2MDHX having better effect on CV. Conversely, at a higher "detrimental" dose, only 2MDHX significantly decreased |d′|. Table shows mean ± SD on the first row of each section and p-values of repeated ANOVA on the second and third rows. D, dose (nmol/kg); N, neuron type (prospective-neuron, retrospective-neuron); Pro: prospective; Retro: retrospective. *Indicates significance.*

Figures 3A,B and **Table 5**), but increased slightly at higher doses (100–10,000 nmol/kg; **Figures 3C,D** and **Table 5**).

For retrospective-encoding-neurons, 2MDHX increased the percentage of correct-sensitive-neurons at 1 nmol/kg (**Figure 3E** and **Table 5**), decreased it at 10 nmol/kg (**Figure 3F** and **Table 5**), and had no significant effects at higher doses (100–10,000 nmol/kg; **Figures 3G,H** and **Table 5**). Uniformity (H) of the correct-sensitive-neurons became more heterogeneous (i.e., increased H) at most tested doses (1, 100, and 10,000 nmol/kg; **Figures 3E,G,H** and **Table 5**), except at 10 nmol/kg where the effect was not significant (**Figure 3F** and **Table 5**). The ensemble sensitivity (d') of the correct-neurons increased at most tested doses (1, 100, and 10,000 nmol/kg; **Figures 3E,G,H** and **Table 5**), except at 10 nmol/kg where the effect was not significant (**Figure 3F** and **Table 5**). For error-sensitive-neurons, their uniformity (H) tended to be more homogeneous (i.e., decreased H) at lower doses (1–10 nmol/kg; **Figures 3E,F** and **Table 5**), but became more heterogeneous (i.e., increased H) at higher doses (100–10,000 nmol/kg; **Figures 3G,H** and **Table 5**). The ensemble sensitivity (d') of the error-neurons did not change significantly at lower doses (1–100 nmol/kg; **Figures 3E–G** and **Table 5**), but was increased at 10,000 nmol/kg (**Figure 3H** and **Table 5**).

Dose Response of CY208 on Pooled Neuron Population

For prospective-encoding-neurons, CY208 decreased the percentage of correct-sensitive-neurons at most tested doses (1, 10, and 10,000 nmol/kg; **Figures 4A,B,D** and **Table 6**), and only increased it at 100 nmol/kg (**Figure 4C** and **Table 6**). Uniformity (H) of the correct-sensitive-neurons became more homogenous (i.e., decreased H) at most tested doses (1, 10, and 10,000 nmol/kg; **Figures 4A,B,D** and **Table 6**), excepted at 100 nmol/kg where it became more heterogeneous (i.e., increased H; **Figure 4C** and **Table 6**). The ensemble sensitivity (d') of correct-neurons was decreased at most tested doses, especially 10 nmol/kg (1, 10, and 10,000 nmol/kg; **Figures 4A,B,D** and **Table 6**), except at 100 nmol/kg where it was increased (**Figure 4C** and **Table 6**). For error-sensitive-neurons, their uniformity (H) was not changed at lower doses (1–100 nmol/kg; **Figures 4A–C** and **Table 6**) but became more heterogeneous (i.e., increased H) at 10,000 nmol/kg (**Figure 4D** and **Table 6**). The ensemble sensitivity (d') of error-neurons did not change at any tested dose (**Figures 4A–D** and **Table 6**).

For retrospective-encoding-neurons, CY208 at lower doses had no significant effect on the percentage of correct-sensitive-neurons (1–100 nmol/kg; **Figures 4E–G** and **Table 6**), but decreased it at 10,000 nmol/kg (**Figure 4H** and **Table 6**). Uniformity (H) of the correct-sensitive-neurons became more homogeneous (i.e., decreased H) at 1 nmol/kg (**Figure 4E** and **Table 6**), but at higher doses it became heterogeneous (i.e., increased H) though not significantly (10–10,000 nmol/kg; **Figures 4F–H** and **Table 6**). The ensemble sensitivity (d') of correct-neurons tended to decrease at 1 nmol/kg (**Figure 4E** and **Table 6**), but was increased at higher doses, especially 100 nmol/kg (10–10,000 nmol/kg; **Figures 4F–H** and **Table 6**). For error-sensitive-neurons, their uniformity (H) became more homogeneous (i.e., decreased H) at 1 nmol/kg though not significantly (**Figure 4E** and **Table 6**), but at higher doses it became more heterogeneous (i.e., increased H; 10–10,000 nmol/kg; **Figures 4F–H** and **Table 6**). The ensemble sensitivity (d') for error-neurons was increased, but only achieved significance at higher doses (**Figures 4E–H** and **Table 6**).

Comparison Between 2-Methyldihydrexidine and CY208

To investigate whether there was a difference between 2MDHX and CY208 affecting neuron population dynamics, we analyzed

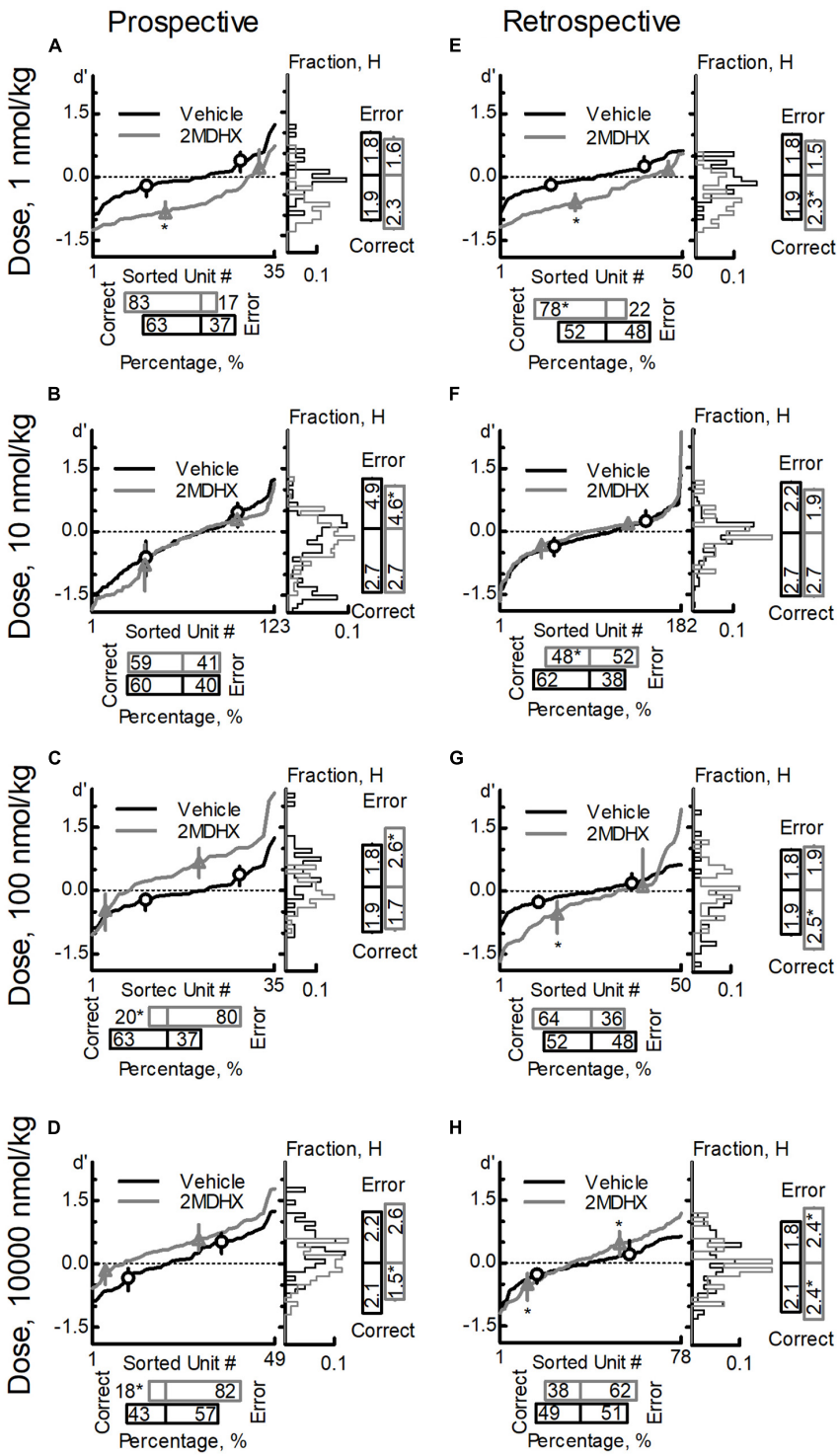

FIGURE 3 | Effects of 2MDHX on neuron population dynamics engaged in the sWM-related DAR task. Three measurements of population dynamics (ensemble sensitivity, uniformity, and percentage) were evaluated for the effects of 2MDHX at four doses: 1 nmol/kg **(A,E)**, 10 nmol/kg **(B,F)**, 100 nmol/kg **(C,G)**, and 10,000 nmol/kg **(D,H)**. All calculations are based on the neuronal-outcome-sensitivity (d') of each neuron in the group (refer to the Methods for detailed definitions of each measurement). The lines in each panel show the value of d' for each neuron. The circle (vehicle) and up-pointed-triangle (2MDHX) on the lines indicate the median and interquartile range of the correct- or error-sensitive-neurons, respectively, which is the indicator of ensemble sensitivity for the population. A histogram of the d' distribution is shown on the right of each panel. The vertical bars on the right indicate the uniformity level of a population (H), and the horizontal bars at the bottom indicate the percentage of correct- or error-sensitive-neurons. *Indicates $P < 0.05$ for the comparison between vehicle (black, circle) and 2MDHX (gray, up-pointed-triangle) conditions. **(A–D)** show the results for prospective-encoding-neurons and **(E,F)** show the results for retrospective-encoding-neurons. Note the variable effects of different doses of 2MDHX on the three parameters.

TABLE 5 | Effects of 2MDHX on neuron population dynamics.

Neuron Type		Dose	Percentage (%)			Uniformity (H)			Ensemble sensitivity (d′)		
			Vehicle	2MDHX	*p*	Vehicle	2MDHX	*p*	Vehicle	2MDHX	*p*
Prospective	Correct	1	63	83	0.1055	1.90 ± 0.03	2.27 ± 0.01	0.0686	−0.21 (−0.47, −0.09)	−0.84 (−0.99, −0.60)	<0.0001*
		10	60	59	1	2.69 ± 0.003	2.70 ± 0.01	0.9891	−0.60 (−1.0, −0.22)	−0.77 (−1.4, −0.30)	0.0938
		100	63	20	0.0006*	1.90 ± 0.03	1.75 ± 0.09	0.6644	−0.21 (−0.47, −0.09)	−0.47 (−0.93, −0.08)	0.2732
		10,000	43	18	0.0152*	2.11 ± 0.02	1.52 ± 0.05	0.0463*	−0.34 (−0.63, −0.11)	−0.15 (−0.49, −0.04)	0.2393
	Error	1	37	17	0.1055	1.84 ± 0.04	1.56 ± 0.10	0.46	0.38 (0.12, 0.58)	0.22 (0.05, 0.63)	0.5107
		10	40	41	1	2.20 ± 0.01	1.89 ± 0.01	0.0425*	0.47 (0.12, 0.68)	0.30 (0.17, 0.39)	0.0642
		100	37	80	0.0006*	1.84 ± 0.04	2.55 ± 0.02	0.0071*	0.38 (0.12, 0.58)	0.68 (0.31, 1.0)	0.0586
		10,000	57	82	0.0152*	2.21 ± 0.02	2.56 ± 0.01	0.0503	0.53 (0.25, 0.73)	0.58 (0.32, 0.93)	0.2811
Retrospective	Correct	1	52	78	0.0113*	1.86 ± 0.02	2.30 ± 0.01	0.0112*	−0.25 (−0.42, −0.09)	−0.63 (−0.84, −0.44)	<0.0001*
		10	62	48	0.0114*	2.39 ± 0.01	2.32 ± 0.01	0.5123	−0.34 (−0.56, −0.15)	−0.31 (−0.61, −0.20)	0.8069
		100	52	64	0.3111	1.86 ± 0.02	2.49 ± 0.02	0.0017*	−0.22 (−0.36, −0.08)	−0.50 (−0.96, −0.21)	0.0012*
		10,000	49	38	0.1055	2.06 ± 0.01	2.40 ± 0.01	0.0445*	−0.25 (−0.46, −0.12)	−0.47 (−0.86, −0.23)	0.0142*
	Error	1	48	22	0.0113*	1.77 ± 0.02	1.47 ± 0.05	0.2563	0.22 (0.11, 0.44)	0.14 (0.05, 0.33)	0.2202
		10	38	52	0.0114*	1.99 ± 0.01	1.89 ± 0.01	0.4015	0.26 (0.12, 0.50)	0.20 (0.10, 0.32)	0.0663
		100	48	36	0.3111	1.77 ± 0.02	1.91 ± 0.05	0.5954	0.22 (0.11, 0.44)	0.15 (0.10, 1.03)	0.8688
		10,000	51	62	0.1055	1.79 ± 0.01	2.38 ± 0.01	<0.0001*	0.23 (0.12, 0.55)	0.49 (0.20, 0.76)	0.0072*

*Neurons tested in the same dose were pooled together for analyzing 2MDHX's effects on the population dynamics comparing to vehicle. Percentage of correct- or error-sensitive-neuron, uniformity (H) and ensemble (d′) of the population, regarding its neuronal-outcome-sensitivity were examined (see Methods for details). The p-values were from Fisher's exact test (Percentage), ANOVA (Uniformity), and Mann-Whitney test (Ensemble sensitivity). Doses are in nmol/kg. *Indicates significance.*

the neurons that were tested for both drugs at a dose. For prospective-encoding-neurons, there was more correct-sensitive-neurons after administration of 2MDHX at lower doses compared to CY208 (1–10 nmol/kg, **Table 7**), whereas at higher doses, it was after administration of CY208 that there was more correct-sensitive-neurons (100–10,000 nmol/kg, **Table 7**). Uniformity (H) of the correct-sensitive neurons was more homogenous (i.e., decreased H) after administration of CY208 at lower doses compared to 2MDHX (1–10 nmol/kg, **Table 7**), whereas at higher doses, it was after administration of 2MDHX that uniformity of the correct-sensitive neurons was more homogenous (100–10,000 nmol/kg, **Table 7**). The ensemble sensitivity (d') of correct-neurons was higher after administration of 2MDHX at lower doses compared to CY208 (1–10 nmol/kg, **Table 7**), whereas at higher doses, it was after CY208 administration that the ensemble sensitivity of correct-neurons trended higher (100–10,000 nmol/kg, **Table 7**). For error-sensitive neurons, uniformity (H) was more heterogeneous (i.e., increased H) after administration of CY208 at lower doses compared to 2MDHX (1–10 nmol/kg, **Table 7**), whereas at higher doses, it was after 2MDHX administration that uniformity of error-sensitive neurons was more heterogeneous (100–10,000 nmol/kg, **Table 7**). Regarding the ensemble sensitivity (d') of the error-neurons, there was no significant difference between 2MDHX and CY208 at all tested doses (**Table 7**).

For retrospective-encoding-neurons, there were more correct-sensitive-neurons after administration of 2MDHX at 1 nmol/kg compared to CY208 (**Table 7**), but not at any other tested dose (10–10,000 nmol/kg, **Table 7**). Uniformity (H) of the correct-sensitive neurons was more homogenous (i.e., decreased H) after administration of CY208 at 1 nmol/kg compared to 2MDHX (**Table 7**), but not at any other tested dose (10–10,000 nmol/kg, **Table 7**). The ensemble sensitivity (d') of the correct-neurons was higher after administration of 2MDHX at 1 nmol/kg compared to CY208 (**Table 7**), but not at any other tested dose (10–10,000 nmol/kg, **Table 7**). For error-sensitive-neurons, their uniformity (H) was more homogenous (i.e., decreased H) after administration of 2MDHX compared to CY208, especially at 10 and 100 nmol/kg (**Table 7**). The ensemble sensitivity (d') for error-neurons was higher after CY208 administration compared to 2MDHX, especially at lower doses (**Table 7**).

Finally, we calculated a population dynamics index that integrates three measurements (percentage, uniformity, and ensemble sensitivity) together and combines outcome sensitivity and temporal encoding. Both 2MDHX and CY208 had dose-dependent effects on population index, with lower doses (2MDHX, 1 nmol/kg; CY208, 100 nmol/kg; **Figure 5**) having a positive impact (i.e., higher value of the index) that diminished at higher doses (2MDHX, 10, 100, and 10000 nmol/kg; CY208, 10000 nmol/kg). The results also suggested that 2MDHX had a larger impact compared to CY208 (2MDHX vs. CY208 = 4.0 vs. 3.4), implying 2MDHX had a higher efficiency. In addition, the index dose response curve of 2MDHX was shifted to lower doses compared to CY208, suggesting a higher potency for 2MDHX.

DISCUSSION

D_1 Dose-Dependency of Prefrontal Cortex Neuronal Activities

This study tested D_1 agonists in a sWM-related T-maze task. By using a wide range of log-spaced doses, we assessed the dose-dependency of PFC neuronal population activities related to sWM. There were complicated dose-response effects at the

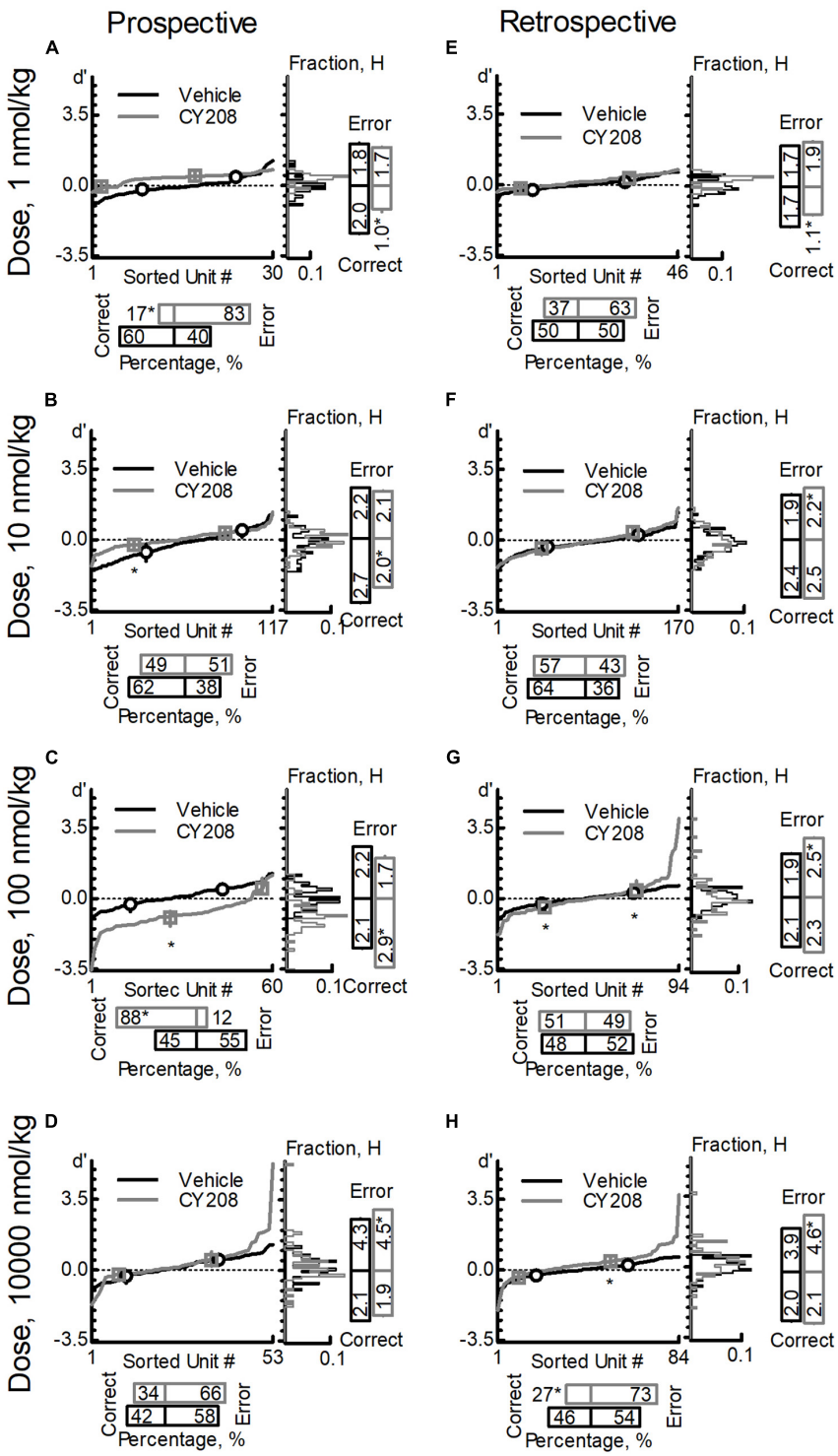

FIGURE 4 | Effects of CY208 on neuron population dynamics engaged in the sWM-related DAR task. Similar to **Figure 3**, three measurements of population dynamics (ensemble sensitivity, uniformity, and percentage) were evaluated for the effects of CY208 at four doses: 1 nmol/kg **(A,E)**, 10 nmol/kg **(B,F)**, 100 nmol/kg **(C,G)**, and 10,000 nmol/kg **(D,H)**. All calculations are based on the neuronal-outcome-sensitivity (d') of each neuron in the group (refer to the Methods for the detailed definition of each measurement). The lines in each panel show the value of d' for each neuron. The circle (vehicle) and square (CY208) on the lines indicate the median and interquartile range of the correct- or error-sensitive-neurons, respectively, an indicator of the ensemble sensitivity for the population. The histogram of d' distribution is shown on the right of each panel. The vertical bars on the right indicate the uniformity level of a population (H), and the horizontal bars at the bottom indicate the percentage of correct- or error-sensitive-neurons. *Indicates $P < 0.05$ for the comparison between vehicle (black, circle) and CY208 (gray, square) conditions. **(A–D)** show the results for prospective-encoding-neurons and **(E,F)** show the results for retrospective-encoding-neurons. Note the variable effects of CY208 at different dose on three measurements.

TABLE 6 | Effects of CY208 on neuron population dynamics.

Neuron Type		Dose	Percentage (%)			Uniformity (H)			Ensemble sensitivity (d′)		
			Vehicle	CY208	*p*	Vehicle	CY208	*p*	Vehicle	CY208	*p*
Prospective	Correct	1	60	17	0.0012*	1.99 ± 0.02	0.95 ± 0.14	0.0419*	−0.22 (−0.50, −0.11)	−0.09 (−0.27, −0.09)	0.1679
		10	62	49	0.0655	2.69 ± 0.004	2.04 ± 0.01	<0.0001*	−0.62 (−1.1, −0.23)	−0.25 (−0.44, −0.13)	<0.0001*
		100	45	88	<0.0001*	2.07 ± 0.02	2.87 ± 0.01	<0.0001*	−0.22 (−0.59, −0.09)	−0.88 (−1.3, −0.58)	<0.0001*
		10,000	42	34	0.548	2.10 ± 0.02	1.88 ± 0.03	0.3378	−0.28 (−0.63, −0.12)	−0.21 (−0.50, −0.15)	0.9242
	Error	1	40	83	0.0012*	1.82 ± 0.05	1.67 ± 0.02	0.58	0.39 (0.12, 0.59)	0.48 (0.38, 0.56)	0.3899
		10	38	51	0.0655	2.20 ± 0.01	2.06 ± 0.01	0.3513	0.47 (0.11, 0.68)	0.34 (0.23, 0.48)	0.2478
		100	55	12	<0.0001*	2.23 ± 0.02	1.75 ± 0.09	0.1628	0.52 (0.25, 0.72)	0.55 (0.42, 1.1)	0.2262
		10,000	58	66	0.548	2.21 ± 0.02	2.61 ± 0.01	0.0268*	0.53 (0.25, 0.73)	0.52 (0.21, 0.92)	0.7383
Retrospective	Correct	1	50	37	0.293	1.67 ± 0.02	1.15 ± 0.03	0.0193*	−0.20 (−0.34, −0.08)	−0.12 (−0.20, −0.07)	0.0848
		10	4	57	0.2677	2.40 ± 0.01	2.46 ± 0.004	0.5873	−0.35 (−0.60, −0.17)	−0.43 (−0.76, −0.20)	0.1396
		100	48	51	0.7706	2.07 ± 0.01	2.30 ± 0.0	0.1115	−0.25 (−0.49, −0.11)	−0.45 (−0.72, −0.15)	0.0181*
		10,000	46	27	0.0161*	2.05 ± 0.01	2.13 ± 0.03	0.6988	−0.25 (−0.45, −0.11)	−0.35 (−0.54, −0.14)	0.4145
	Error	1	50	63	0.293	1.75 ± 0.02	1.93 ± 0.01	0.355	0.19 (0.11, 0.45)	0.38 (0.16, 0.51)	0.2036
		10	96	43	0.2677	1.94 ± 0.01	2.23 ± 0.01	0.0209*	0.23 (0.12, 0.52)	0.36 (0.17, 0.61)	0.0815
		100	52	49	0.7706	1.89 ± 0.004	2.54 ± 0.01	<0.0001*	0.27 (0.13, 0.47)	0.41 (0.13, 0.87)	0.0464*
		10,000	54	73	0.0161*	1.87 ± 0.01	2.45 ± 0.01	<0.0001*	0.27 (0.12, 0.51)	0.44 (0.25, 0.71)	0.0058*

*Similar to **Table 5**, neurons tested in the same dose were pooled together for analyzing CY208's effects on the population dynamics comparing to vehicle. Percentage of correct- or error-sensitive-neuron, uniformity (H) and ensemble (d′) of the population were examined (see Methods for details). The p-values were from Fisher's exact test (Percentage), ANOVA (Uniformity), and Mann-Whitney test (Ensemble sensitivity). Dose are expressed in nmol/kg. *Indicates significance.*

TABLE 7 | Compare effects of 2MDHX with CY208 on neuron population dynamics.

Neuron Type		Dose	Percentage (%)			Uniformity (H)			Ensemble sensitivity (d′)		
			2MDHX	CY208	*p*	2MDHX	CY208	*p*	2MDHX	CY208	*p*
Prospective	Correct	1	90	17	<0.0001*	2.24 ± 0.02	0.95 ± 0.10	0.0089*	−0.85 (−0.99, −0.65)	−0.09 (−0.27, −0.09)	0.0009*
		10	62	49	0.0482*	2.70 ± 0.0	2.04 ± 0.01	<0.0001*	−0.77 (−1.4, −0.30)	−0.25 (−0.44, −0.13)	<0.0001*
		100	20	89	<0.0001*	1.75 ± 0.09	2.91 ± 0.02	0.0055*	−0.46 (−0.93, −0.08)	−0.93 (−1.33, −0.52)	0.0707
		10,000	18	31	0.2399	1.52 ± 0.05	1.96 ± 0.03	0.1644	−0.15 (−0.49, −0.04)	−0.22 (−0.86, −0.18)	0.2105
	Error	1	10	83	<0.0001*	1.10 ± 0.11	1.67 ± 0.02	0.1919	0.60 (0.06, 0.73)	0.48 (0.38, 0.56)	0.6031
		10	38	51	0.0482*	1.74 ± 0.01	2.06 ± 0.01	0.0355*	0.29 (0.17, 0.37)	0.34 (0.23, 0.48)	0.0631
		100	80	11	<0.0001*	2.55 ± 0.02	1.39 ± 0.16	0.0394*	0.68 (0.31, 1.01)	0.48 (0.36, 0.94)	0.9319
		10,000	82	69	0.2399	2.56 ± 0.01	2.61 ± 0.01	0.7279	0.58 (0.32, 0.93)	0.54 (0.18, 0.93)	0.6371
Retrospective	Correct	1	76	37	0.0003*	2.26 ± 0.01	1.15 ± 0.03	<0.0001*	−0.66 (−0.85, −0.49)	−0.12 (−0.20, −0.07)	<0.0001*
		10	46	57	0.0506	2.32 ± 0.01	2.46 ± 0.004	0.2125	−0.31 (−0.62, −0.18)	−0.43 (−0.76, −0.20)	0.1753
		100	64	52	0.3111	2.49 ± 0.02	2.36 ± 0.02	0.5021	−0.50 (−0.96, −0.21)	−0.55 (−0.82, −0.29)	0.9191
		10,000	38	28	0.2343	2.40 ± 0.01	2.16 ± 0.03	0.2742	−0.47 (−0.86, −0.23)	−0.36 (−0.56, −0.14)	0.162
	Error	1	24	63	0.0003*	1.47 ± 0.05	1.93 ± 0.01	0.0824	0.14 (0.05, 0.33)	0.38 (0.16, 0.51)	0.0366*
		10	54	43	0.0506	1.79 ± 0.01	2.23 ± 0.01	0.0004*	0.19 (0.10, 0.29)	0.36 (0.17, 0.61)	<0.0001*
		100	36	48	0.3111	1.91 ± 0.05	2.67 ± 0.02	0.0073*	0.15 (0.10, 1.03)	0.67 (0.28, 1.15)	0.0732
		10,000	62	72	0.2343	2.38 ± 0.01	2.46 ± 0.01	0.5311	0.49 (0.20, 0.76)	0.46 (0.25, 0.74)	0.8679

*To investigate whether 2MDHX and CY208 affected neuron population dynamics differently, we analyzed the neurons that were tested for both drugs at a same dose. Similar to **Tables 5**, **6**, percentage of correct- or error-sensitive-neuron, uniformity (H) and ensemble (d′) of the population were examined (see Methods for details). The p-values were from Fisher's exact test (Percentage), ANOVA (Uniformity), and Mann-Whitney test (Ensemble sensitivity). Doses are in nmol/kg. *Indicates significance.*

neuron population level, but overall it followed an inverted-U curve, consistent with the dose response at the single neuron level reported previously using other D_1 agents and cognitive-related tasks (Vijayraghavan et al., 2007; Wang et al., 2019). Our data support the hypothesis that D_1 dose-dependent effects on cognition were represented not only by single neuron activities, but also by neuron population dynamics in the PFC that eventually propagates to the behavioral level (Yang et al., 2021).

Two prior studies examined the D_1 dose-dependency at the single neuron level in the non-human primate PFC that maintain a persistent firing to represent active maintenance of the sWM. Their overall conclusion was that D_1 agonists improve single neuron activities through a "sculpting action" (Vijayraghavan et al., 2007; Wang et al., 2019). In our experimental paradigm, the neuronal population activities represent strategic encoding of the choice behavior in the T-maze task that reflects flexible

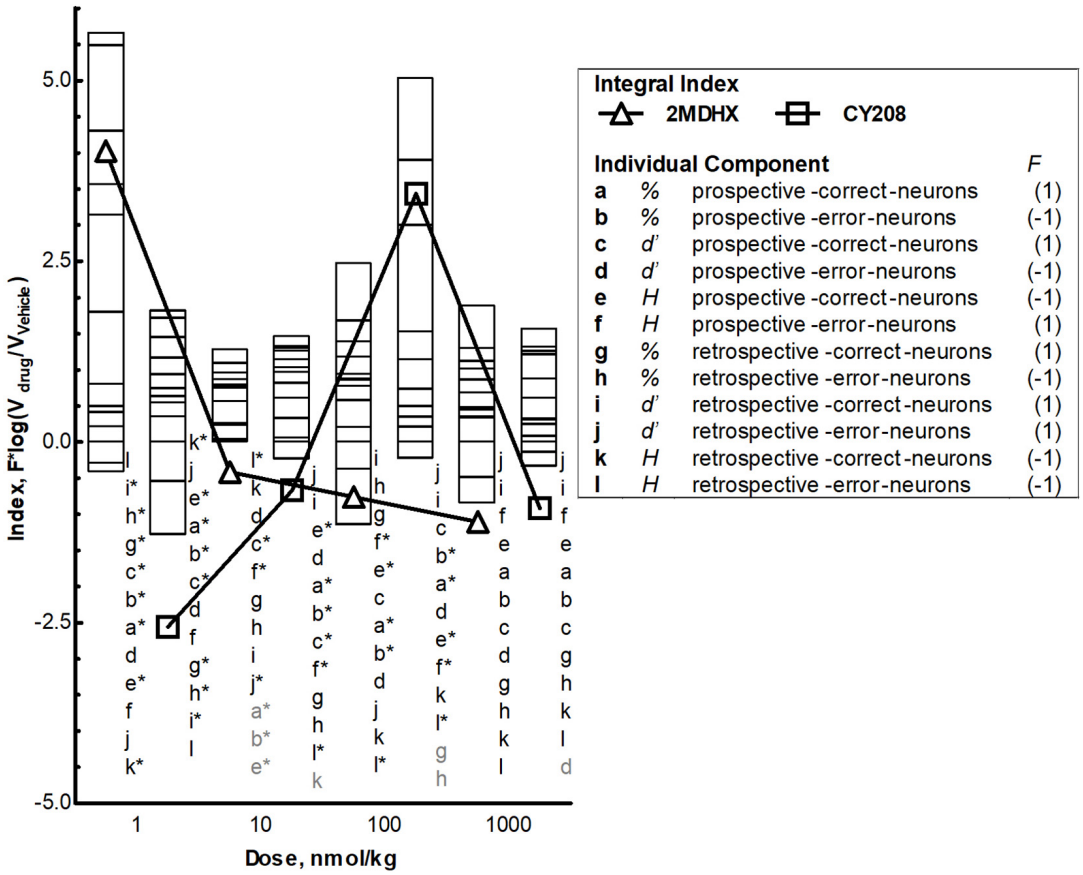

FIGURE 5 | Integrated effects and comparison between 2MDHX and CY208. An integrated population dynamics index, $\sum_{i=1}^{12} F_i \log(V_{i\ (drug)}/V_{i\ (vehicle)})$, was defined to combine all three measurements [percentage (abgh), uniformity (efkl), and ensemble sensitivity (cdij)] with the temporal encoding [prospective (a–f) and retrospective (g–l)] and event sensitivity [correct (acegik) and error (bdfhjl)]. These 12 letters (a–l) represent each component of the integrated index, and the number 1/–1 next to the letter indicates the value of functional index (F) for this component (refer to the Methods for details). Stacked bars show the value of each component at four doses (1, 10, 100, and 10,000 nmol/kg), and triangles and squares show the value of integral index, with triangles indicate the 2MDHX and squares indicate CY208, respectively. The letters next to the bars indicate the order of the stacked bars, and the gray colored letters indicate that the value of these components was too small to be illustrated by the stacked bar. The * next to the letter indicates $P < 0.05$ for the comparison between 2MDHX and CY208 for this component. Note the inverted-*U* curve of the integral index for CY208, the higher integral index values for 2MDHX compared to CY208, and the shift to lower doses of the integral index curve for 2MDHX compared to CY208.

updating of the sWM (Yang and Mailman, 2018). Our data showed that the drug effects on outcome-sensitivity of the group of neurons tested all four doses, although was from only one animal, paralleled this "sculpting action," such that increased sensitivity at an "optimal" dose was decreased at higher, "detrimental," doses. The inconsistencies between the two compounds, however, are intriguing. Specifically, CY208 was superior at improving sensitivity strength at an optimal dose and maintaining it at higher doses, but 2MDHX deceased neuron-to-neuron variation more. These results highlight the importance for examining dose-dependency not only at the single neuron, but also neuron population level, as neuron-to-neuron variation reflects neuron population dynamics. Moreover, the fact that the PFC contains dynamic neural activities (Yang and Mailman, 2018; De Falco et al., 2019; Kaminski and Rutishauser, 2019) suggests that the pattern of dose-dependency at the single neuron level is dissimilar from that at the neuron population level. Indeed, compared to single neuron activities reported previously (Vijayraghavan et al., 2007; Wang et al., 2019), neuron population dynamics reported in current study are dose-dependent, but their pattern is relatively irregular and does not match the typical inverted-U curves.

In the current study, we focused on three aspects of neuron population dynamics: percentage; uniformity; and ensemble sensitivity. We pooled all recorded neurons together and analyzed. Our hypothesis was that optimal doses of D_1 agonists will increase the population of prospective-encoding-correct-sensitive-neurons with strengthened uniformity and ensemble sensitivity and decrease the population of prospective-encoding-error-sensitive-neurons with decreased uniformity and ensemble sensitivity, leading to a greater probability for a correct outcome. Concomitantly, D_1 agonists also should increase the uniformity

and ensemble sensitivity of retrospective-encoding-neurons, with either correct or error sensitivity, leading to better feedback adjustment. Our results were partially consistent, albeit the dose response curves are more complex. It is puzzling that none of the measurements at the neuron population level showed a clear inverted-U/biphasic dose response curve as occurred at the single neuron level (Vijayraghavan et al., 2007; Wang et al., 2019). It is possible that the modest data sample (minimum of n = 30 neurons) was insufficient to detect this. Another possibility is that the high plasticity in the PFC (De Falco et al., 2019; Singh et al., 2019) results in highly variable dose-response curves, although this seems unlikely because all drug tests were performed after rats were well trained for the task. The third explanation is that diverse single neuron activities in the PFC (Yang and Mailman, 2018; De Falco et al., 2019; Kaminski and Rutishauser, 2019) could contribute to this complicated neural modulation at the population level. Our data indeed showed different neuron population among individual rats. This difference potentially may represent different cognitive ability of each individual rats for performing DAR task. It is noteworthy that further analysis showed that although there were irregular patterns over the dose range for each individual measurement, integrating all three measures for every neuron population revealed a relatively clear dose-dependency, that is, the integrated population index was higher at an "optimal" dose and became lower at a higher "detrimental" dose. Although the findings of the current study are complicated, they are the first step in creating a useful model for D_1-related dose-dependent regulation of cognition. Future studies should focus on additional aspects of neuron population dynamics and other behavioral tasks evaluating different domains of WM.

Differences Between 2-Methyldihydrexidine and CY203

There were some striking differences between the effects of 2MDHX and CY208 on PFC neuronal population activities during the sWM task. Overall, 2MDHX had greater effects on integrated neuron population dynamics since its maximum index was higher (implying better efficiency), and the dose response curve of the index was shifted to lower doses (suggesting higher potency). The higher potency of 2MDHX was consistent for the group of neurons tested all four doses, such that the optimal dose for improving neuronal sensitivity was lower after 2MDHX administration compared to CY208. The efficiency of 2MDHX, however, was not greater for this group of neurons. The sensitivity strength was improved less by 2MDHX compared to CY208, although 2MDHX reduced the neuron-to-neuron variation more. Both 2MDHX and CY208 had variable effects on neuron population dynamics and neither showed consistent improvement on the three measurements (percentage; uniformity; and ensemble strength of sensitivity). The overall impression was that 2MDHX was better at increasing the percentage of correct-sensitive-neurons and ensemble sensitivity, whereas CY208 was better at modulating uniformity. For retrospective encoding that may represent a perdurance of activity related to previous choice and could be potentially important for neural feedback adjustment, 2MDHX was better at modulating uniformity, and CY208 was better at increasing the ensemble sensitivity. How these differences at the neuronal population level propagate to behavior is an unsolved question, but it could be proposed that the difference between 2MDHX and CY208, regarding their effects on the time to make the choice in the DAR task as reported in our previous publication (Yang et al., 2021), is one of the behaviors manifested from these neuronal population differences.

It is unclear whether these dissimilarities were due to ligand differences in D_1R signaling bias or some other mechanism. In many pharmacological studies, the drug doses used are likely to engage secondary targets (Lee et al., 2014). We believe off-target effects in the current study can be ruled out by the sensitivity of PFC D_1Rs that allowed the use of very low drug doses. Fractional receptor occupancy would be very low based on the apparent affinities of 2MDHX and CY208 for the D_1R (Markstein et al., 1992; Knoerzer et al., 1995). Indeed, the doses used in the current study were far lower than those from an earlier report that concluded such effects occurred *via* the D_1R (Isacson et al., 2004).

Our working hypothesis is that D_1R functional selectivity is the major mechanism underlying these dissimilarities between 2MDHX and CY208, i.e., 2MDHX has full intrinsic activity at cAMP and $>>$ 100% at β-arrestin signaling, whereas CY208 has high intrinsic activity at cAMP signaling, but partial agonist activity at β-arrestin signaling (Yang et al., 2021). The difference between 2MDHX and CY208 could be interpreted in several ways: (1) D_1-mediated β-arrestin signaling has a major influence on the potency of the dose-response since higher activity (by 2MDHX) leads to higher potency (i.e., the optimal dose for improving neuronal-sensitivity was lower); (2) cAMP signaling may have more influence on the efficiency of the dose-response since higher activity (by CY208) leads to higher efficiency (i.e., more improvement on neuronal-sensitivity); (3) dose-dependency at the neuron population level in the PFC is a result of balancing cAMP and β-arrestin signaling; and/or (4) differential bias at another signaling pathway is involved.

Our data suggest but does not provide direct evidence that D_1-mediated cAMP and/or β-arrestin signaling cooperate to regulate the dose-dependency of sWM-related neural activities in the PFC. Although both pathways are important modulators of dopamine function (Vijayraghavan et al., 2007; Wang et al., 2019; Yang et al., 2021), other signaling pathways modulated by the D_1Rs also may contribute. In addition, factors other than signaling bias (e.g., pharmacokinetics or metabolite formation) can complicate the results and account for the dose-dependent response of PFC neural activities. Moreover, there are no known ligands that have marked selectivity for the D_1 vs. the highly homologous D_5 dopamine receptor. We have used the term "D_1," but are keenly aware that D_5 mechanisms may contribute. Future studies should consider alternate models, other aspects of neural activity, and advanced techniques to gain improved insight into how functional selectivity may modify D_1-related dose-dependency and relate to enhanced therapeutics.

Conclusion: Clinical Implications

Marked cognitive improvement by D_1 agonists has been a consistent finding in animal models (Arnsten et al., 1994, 2017; Murphy et al., 1996b; Cai and Arnsten, 1997; Zahrt et al., 1997; Vijayraghavan et al., 2007; Wang et al., 2019; Yang et al., 2021). The recent and ongoing clinical testing of several D_1 agonists of a novel chemotype (Gray et al., 2018; Sohur et al., 2018; Balice-Gordon et al., 2020; Huang et al., 2020) suggests D_1 agonists can be used safely and for long periods. On the other hand, one of these later compounds (the D_1 agonist PF-06412562) failed to improve cognition and motivation (Balice-Gordon et al., 2020). This compound (and several other ones) differs, however, from earlier experimental compounds in having low intrinsic activity at cAMP signaling and no intrinsic activity at β-arrestin recruitment. Earlier studies with compounds of high intrinsic activity did suggest beneficial effects of D_1 agonists in most (Mu et al., 2007; Rosell et al., 2015; Huang et al., 2020), but not all studies (Girgis et al., 2016). These data underscore how pharmacological properties, from pharmacokinetics to signaling (Mailman and Murthy, 2010; Boyd and Mailman, 2012; Arnsten et al., 2017), must be considered above and beyond receptor selectivity. Not only does the current study highlight the crucial influence caused by the functional selectivity of drugs, it also may affect interpretation of an ongoing trial utilizing PF-06412562 (Krystal, 2019) and, as importantly, underscore the importance of detailed physiological mechanisms of D_1 ligands.

DATA AVAILABILITY STATEMENT

The raw data supporting the conclusion of this article will be made available by the authors, without undue reservation.

ETHICS STATEMENT

The animal study was reviewed and approved by the Institutional Animal Care and Use Committee (IACUC) Milton S Hershey Medical Center Penn State College of Medicine. All animal care and surgical procedures were in accordance with the National Institutes of Health Guide for the Care and Use of Laboratory Animals and Penn State Hershey Animal Resources Program.

AUTHOR CONTRIBUTIONS

YY and RM contributed to conception and design of the study. YY and SK conducted the experiments. YY performed the data analysis and wrote the first draft of the manuscript. All authors contributed to manuscript revision, read, and approved the submitted version.

FUNDING

This work was supported by the Brain & Behavior Research Foundation Young Investigator Award (19469), Children's Miracle Network Research Grant (2017–2018 #10, 2022–2023), the National Institutes of Health (R01 NS105471, RF1 AG071675), and the Penn State Translational Brain Research Center.

ACKNOWLEDGMENTS

The authors wish to thank Natalia Loktionova for her invaluable technical support, and Professor Xuemei Huang for her insight about these results.

REFERENCES

Arnsten, A. F. (2015). Stress weakens prefrontal networks: molecular insults to higher cognition. *Nat. Neurosci.* 18, 1376–1385. doi: 10.1038/nn.4087

Arnsten, A. F., Cai, J. X., Murphy, B. L., and Goldman-Rakic, P. S. (1994). Dopamine D1 receptor mechanisms in the cognitive performance of young adult and aged monkeys. *Psychopharmacology (Berl)* 116, 143–151.

Arnsten, A. F., Girgis, R. R., Gray, D. L., and Mailman, R. B. (2017). Novel dopamine therapeutics for cognitive deficits in schizophrenia. *Biol. Psychiatry* 81, 67–77. doi: 10.1016/j.biopsych.2015.12.028

Arnsten, A. F., Wang, M., and Paspalas, C. D. (2015). Dopamine's actions in primate prefrontal cortex: challenges for treating cognitive disorders. *Pharmacol. Rev.* 67, 681–696. doi: 10.1124/pr.115.010512

Baeg, E. H., Kim, Y. B., Huh, K., Mook-Jung, I., Kim, H. T., and Jung, M. W. (2003). Dynamics of population code for working memory in the prefrontal cortex. *Neuron* 40, 177–188. doi: 10.1016/S0896-6273(03)00597-X

Balice-Gordon, R., Honey, G. D., Chatham, C., Arce, E., Duvvuri, S., Naylor, M. G., et al. (2020). A neurofunctional domains approach to evaluate D1/D5 dopamine receptor partial agonism on cognition and motivation in healthy volunteers with low working memory capacity. *Int. J. Neuropsychopharmacol.* 23, 287–299. doi: 10.1093/ijnp/pyaa007

Barnes, T. D., Kubota, Y., Hu, D., Jin, D. Z., and Graybiel, A. M. (2005). Activity of striatal neurons reflects dynamic encoding and recoding of procedural memories. *Nature* 437, 1158–1161. doi: 10.1038/nature04053

Bolkan, S. S., Stujenske, J. M., Parnaudeau, S., Spellman, T. J., Rauffenbart, C., Abbas, A. I., et al. (2017). Thalamic projections sustain prefrontal activity during working memory maintenance. *Nat. Neurosci.* 20, 987–996. doi: 10.1038/nn.4568

Boyd, K. N., and Mailman, R. B. (2012). Dopamine receptor signaling and current and future antipsychotic drugs. *Handb. Exp. Pharmacol.* 212, 53–86. doi: 10.1007/978-3-642-25761-2_3

Caetano, M. S., Horst, N. K., Harenberg, L., Liu, B., Arnsten, A. F., and Laubach, M. (2012). Lost in transition: aging-related changes in executive control by the medial prefrontal cortex. *J. Neurosci.* 32, 3765–3777. doi: 10.1523/JNEUROSCI.6011-11.2012

Cai, J. X., and Arnsten, A. F. (1997). Dose-dependent effects of the dopamine D1 receptor agonists A77636 or SKF81297 on spatial working memory in aged monkeys. *J. Pharmacol. Exp. Ther.* 283, 183–189.

De Falco, E., An, L., Sun, N., Roebuck, A. J., Greba, Q., Lapish, C. C., et al. (2019). The rat medial prefrontal cortex exhibits flexible neural activity states during the performance of an odor span task. *eNeuro* 6:ENEURO.424-18. doi: 10.1523/ENEURO.0424-18.2019

Dorval, A. D., Muralidharan, A., Jensen, A. L., Baker, K. B., and Vitek, J. L. (2015). Information in pallidal neurons increases with parkinsonian severity. *Parkinsonism Relat. Disord.* 21, 1355–1361. doi: 10.1016/j.parkreldis.2015.09.045

Gamo, N. J., Lur, G., Higley, M. J., Wang, M., Paspalas, C. D., Vijayraghavan, S., et al. (2015). Stress impairs prefrontal cortical function *via* D1 dopamine

receptor interactions with hyperpolarization-activated cyclic nucleotide-gated channels. *Biol. Psychiatry* 78, 860–870. doi: 10.1016/j.biopsych.2015.01.009

Girgis, R. R., Van Snellenberg, J. X., Glass, A., Kegeles, L. S., Thompson, J. L., Wall, M., et al. (2016). A proof-of-concept, randomized controlled trial of DAR-0100A, a dopamine-1 receptor agonist, for cognitive enhancement in schizophrenia. *J. Psychopharmacol.* 30, 428–435. doi: 10.1177/0269881116636120

Goldman-Rakic, P. S. (1995). Cellular basis of working memory. *Neuron* 14, 477–485. doi: 10.1016/0896-6273(95)90304-6

Goldman-Rakic, P. S. (2011). "Circuitry of primate prefrontal cortex and regulation of behavior by representational memory," in *Comprehensive Physiology*, ed. R. Terjung (Hoboken, NJ: John Wiley & Sons), 373–417. doi: 10.1002/cphy.cp010509

Gray, D. L. F., Zhang, L., Davoren, J., Dounay, A. B., Viktorovich, I., Lee, C., et al. (2018). *Heteroaromatic Compounds and Their use as Dopamine D1 Ligands. Us-9617275-B2*. New York, NY: Pfizer.

Horst, N. K., and Laubach, M. (2012). Working with memory: evidence for a role for the medial prefrontal cortex in performance monitoring during spatial delayed alternation. *J. Neurophysiol.* 108, 3276–3288. doi: 10.1152/jn.01192.2011

Huang, X., Lewis, M. M., Van Scoy, L. J., De Jesus, S., Eslinger, P. J., Arnold, A. C., et al. (2020). The D1/D5 dopamine partial agonist PF-06412562 in advanced-stage parkinson's disease: a feasibility study. *J. Parkinsons Dis.* 10, 1515–1527. doi: 10.3233/JPD-202188

Isacson, R., Kull, B., Wahlestedt, C., and Salmi, P. (2004). A 68930 and dihydrexidine inhibit locomotor activity and d-amphetamine-induced hyperactivity in rats: a role of inhibitory dopamine D(1/5) receptors in the prefrontal cortex? *Neuroscience* 124, 33–42. doi: 10.1016/j.neuroscience.2003.11.016

Jung, M. W., Qin, Y., McNaughton, B. L., and Barnes, C. A. (1998). Firing characteristics of deep layer neurons in prefrontal cortex in rats performing spatial working memory tasks. *Cereb. Cortex* 8, 437–450.

Kaminski, J., and Rutishauser, U. (2019). Between persistently active and activity-silent frameworks: novel vistas on the cellular basis of working memory. *Ann. N. Y. Acad. Sci.* 1464, 64–75. doi: 10.1111/nyas.14213

Kenakin, T. (2012). The potential for selective pharmacological therapies through biased receptor signaling. *BMC Pharmacol. Toxicol.* 13:3. doi: 10.1186/2050-6511-13-3

Kesner, R. P., and Churchwell, J. C. (2011). An analysis of rat prefrontal cortex in mediating executive function. *Neurobiol. Learn. Mem.* 96, 417–431. doi: 10.1016/j.nlm.2011.07.002

Knoerzer, T. A., Watts, V. J., Nichols, D. E., and Mailman, R. B. (1995). Synthesis and biological evaluation of a series of substituted benzo[a]phenanthridines as agonists at D1 and D2 dopamine receptors. *J. Med. Chem.* 38, 3062–3070.

Krystal, J. (2019). *A Translational and Neurocomputational Evaluation of a D1R Partial Agonist for Schizophrenia [Online]*. Bethesda, MD: National Institutes of Health.

Laubach, M., Caetano, M. S., and Narayanan, N. S. (2015). Mistakes were made: neural mechanisms for the adaptive control of action initiation by the medial prefrontal cortex. *J. Physiol. Paris* 109, 104–117. doi: 10.1016/j.jphysparis.2014.12.001

Lee, S. M., Yang, Y., and Mailman, R. B. (2014). Dopamine D1 receptor signaling: does GalphaQ-phospholipase C actually play a role? *J. Pharmacol. Exp. Ther.* 351, 9–17. doi: 10.1124/jpet.114.214411

Lidow, M. S., Koh, P. O., and Arnsten, A. F. (2003). D1 dopamine receptors in the mouse prefrontal cortex: immunocytochemical and cognitive neuropharmacological analyses. *Synapse* 47, 101–108. doi: 10.1002/syn.10143

Liu, X., Ma, L., Li, H. H., Huang, B., Li, Y. X., Tao, Y. Z., et al. (2015). beta-Arrestin-biased signaling mediates memory reconsolidation. *Proc. Natl. Acad. Sci. U.S.A.* 112, 4483–4488. doi: 10.1073/pnas.1421758112

Mailman, R. B., and Murthy, V. (2010). Ligand functional selectivity advances our understanding of drug mechanisms and drug discovery. *Neuropsychopharmacology* 35, 345–346. doi: 10.1038/npp.2009.117

Markstein, R., Seiler, M. P., Jaton, A., and Briner, U. (1992). Structure activity relationship and therapeutic uses of dopaminergic ergots. *Neurochem. Int.* 20, 211S–214S. doi: 10.1016/0197-0186(92)90241-I

Mu, Q. W., Johnson, K., Morgan, P. S., Grenesko, E. L., Molnar, C. E., Anderson, B., et al. (2007). A single 20 mg dose of the full D-1 dopamine agonist dihydrexidine (DAR-0100) increases prefrontal perfusion in schizophrenia. *Schizophr. Res.* 94, 332–341. doi: 10.1016/j.schres.2007.03.033

Murphy, B. L., Arnsten, A. F., Goldman-Rakic, P. S., and Roth, R. H. (1996a). Increased dopamine turnover in the prefrontal cortex impairs spatial working memory performance in rats and monkeys. *Proc. Natl. Acad. Sci. U.S.A.* 93, 1325–1329.

Murphy, B. L., Arnsten, A. F., Jentsch, J. D., and Roth, R. H. (1996b). Dopamine and spatial working memory in rats and monkeys: pharmacological reversal of stress-induced impairment. *J. Neurosci.* 16, 7768–7775.

Murray, J. D., Bernacchia, A., Roy, N. A., Constantinidis, C., Romo, R., and Wang, X. J. (2017). Stable population coding for working memory coexists with heterogeneous neural dynamics in prefrontal cortex. *Proc. Natl. Acad. Sci. U.S.A.* 114, 394–399. doi: 10.1073/pnas.1619449114

Paspalas, C. D., Wang, M., and Arnsten, A. F. T. (2013). Constellation of HCN channels and cAMP regulating proteins in dendritic spines of the primate prefrontal cortex: potential substrate for working memory deficits in schizophrenia. *Cereb. Cortex* 23, 1643–1654. doi: 10.1093/cercor/bhs152

Paxinos, G., and Watson, C. (2013). *The Rat Brain in Stereotaxic Coordinates*. Sydney, NSW: Academic Press.

Rosell, D. R., Zaluda, L. C., McClure, M. M., Perez-Rodriguez, M. M., Strike, K. S., Barch, D. M., et al. (2015). Effects of the D1 dopamine receptor agonist dihydrexidine (DAR-0100A) on working memory in schizotypal personality disorder. *Neuropsychopharmacology* 40, 446–453. doi: 10.1038/npp.2014.192

Singh, A., Peyrache, A., and Humphries, M. D. (2019). Medial prefrontal cortex population activity is plastic irrespective of learning. *J. Neurosci.* 39, 3470–3483. doi: 10.1523/JNEUROSCI.1370-17.2019

Sohur, U. S., Gray, D. L., Duvvuri, S., Zhang, Y., Thayer, K., and Feng, G. (2018). Phase 1 parkinson's disease studies show the dopamine D1/D5 agonist PF-06649751 is safe and well tolerated. *Neurol. Ther.* 7, 307–319. doi: 10.1007/s40120-018-0114-z

Spaak, E., Watanabe, K., Funahashi, S., and Stokes, M. G. (2017). Stable and dynamic coding for working memory in primate prefrontal cortex. *J. Neurosci.* 37, 6503–6516. doi: 10.1523/JNEUROSCI.3364-16.2017

Thorn, C. A., Atallah, H., Howe, M., and Graybiel, A. M. (2010). Differential dynamics of activity changes in dorsolateral and dorsomedial striatal loops during learning. *Neuron* 66, 781–795. doi: 10.1016/j.neuron.2010.04.036

Urban, J. D., Clarke, W. P., von Zastrow, M., Nichols, D. E., Kobilka, B., Weinstein, H., et al. (2007). Functional selectivity and classical concepts of quantitative pharmacology. *J. Pharmacol. Exp. Ther.* 320, 1–13. doi: 10.1124/jpet.106.104463

Urs, N. M., Bido, S., Peterson, S. M., Daigle, T. L., Bass, C. E., Gainetdinov, R. R., et al. (2015). Targeting beta-arrestin2 in the treatment of L-DOPA-induced dyskinesia in Parkinson's disease. *Proc. Natl. Acad. Sci. U.S.A.* 112, E2517–E2526. doi: 10.1073/pnas.1502740112

Urs, N. M., Daigle, T. L., and Caron, M. G. (2011). A dopamine D1 receptor-dependent beta-arrestin signaling complex potentially regulates morphine-induced psychomotor activation but not reward in mice. *Neuropsychopharmacology* 36, 551–558.

Vijayraghavan, S., Wang, M., Birnbaum, S. G., Williams, G. V., and Arnsten, A. F. (2007). Inverted-U dopamine D1 receptor actions on prefrontal neurons engaged in working memory. *Nat. Neurosci.* 10, 376–384. doi: 10.1038/nn1846

Wang, M., Datta, D., Enwright, J., Galvin, V., Yang, S. T., Paspalas, C., et al. (2019). A novel dopamine D1 receptor agonist excites delay-dependent working memory-related neuronal firing in primate dorsolateral prefrontal cortex. *Neuropharmacology* 150, 46–58. doi: 10.1016/j.neuropharm.2019.03.001

Yang, Y. (2021). Functional selectivity of dopamine D1 receptor signaling: retrospect and prospect. *Int. J. Mol. Sci.* 22:11914. doi: 10.3390/ijms222111914

Yang, Y., and Mailman, R. B. (2018). Strategic neuronal encoding in medial prefrontal cortex of spatial working memory in the T-maze. *Behav. Brain Res.* 343, 50–60. doi: 10.1016/j.bbr.2018.01.020

Yang, Y., Lee, S. M., Imamura, F., Gowda, K., Amin, S., and Mailman, R. B. (2021). D1 dopamine receptors intrinsic activity and functional selectivity affect working memory in prefrontal cortex. *Mol. Psychiatry* 26, 645–655.

Yang, S. T., Shi, Y., Wang, Q., Peng, J. Y., and Li, B. M. (2014). Neuronal representation of working memory in the medial prefrontal cortex of rats. *Mol. Brain* 7:61.

Zahrt, J., Taylor, J. R., Mathew, R. G., and Arnsten, A. F. (1997). Supranormal stimulation of D1 dopamine receptors in the rodent prefrontal cortex impairs spatial working memory performance. *J. Neurosci.* 17, 8528–8535.

Conflict of Interest: RM has interests in issued and pending patents related to dopamine D1 receptor mechanisms that constitute a conflict of interest for which there is University oversight.

The remaining authors declare that the research was conducted in the absence of any commercial or financial relationships that could be construed as a potential conflict of interest.

Publisher's Note: All claims expressed in this article are solely those of the authors and do not necessarily represent those of their affiliated organizations, or those of the publisher, the editors and the reviewers. Any product that may be evaluated in this article, or claim that may be made by its manufacturer, is not guaranteed or endorsed by the publisher.

frontiers | Frontiers in Pharmacology

MINI REVIEW
published: 17 June 2022
doi: 10.3389/fphar.2022.882158

Food for Thought: Leptin and Hippocampal Synaptic Function

*Jenni Harvey**

Division of Systems Medicine, Ninewells Hospital and Medical School, University of Dundee, Dundee, United Kingdom

It is well documented that the endocrine hormone, leptin controls energy homeostasis by providing key signals to specific hypothalamic nuclei. However, our knowledge of leptin's central actions has advanced considerably over the last 20 years, with the hippocampus now established as an important brain target for this hormone. Leptin receptors are highly localised to hippocampal synapses, and increasing evidence reveals that activation of synaptically located leptin receptors markedly impacts cognitive processes, and specifically hippocampal-dependent learning and memory. Here, we review the recent actions of leptin at hippocampal synapses and explore the consequences for brain health and disease.

Keywords: leptin, hippocampus (CA1), NMDA R, AMPA receptor, synaptic plasiticity

OPEN ACCESS

Edited by:
Divya Vohora,
Jamia Hamdard University, India

Reviewed by:
Victor Manuel Pulgar,
Wake Forest School of Medicine, United States
Hong Ni,
Children's Hospital of Soochow University, China
Toru Hosoi,
Sanyo-Onoda City University, Japan

***Correspondence:**
Jenni Harvey
j.z.harvey@dundee.ac.uk

Specialty section:
This article was submitted to Neuropharmacology, a section of the journal Frontiers in Pharmacology

Received: *23 February 2022*
Accepted: *02 June 2022*
Published: *17 June 2022*

Citation:
Harvey J (2022) Food for Thought: Leptin and Hippocampal Synaptic Function. Front. Pharmacol. 13:882158. doi: 10.3389/fphar.2022.882158

INTRODUCTION

A fundamental role of the adipocyte-derived hormone, leptin is to regulate energy balance by signalling the status of food stores to the hypothalamus. Leptin receptors (LepRs) are highly localised to specific hypothalamic nuclei, like the arcuate nucleus, that control energy homeostasis. When circulating leptin levels rise after eating, leptin binds to and activates arcuate nucleus LepRs which triggers a chain of events that culminates in feeling full (Friedman, 2019). However, the discovery that neuronal LepRs are not restricted to hypothalamic sites, fuelled speculation that the central functions of leptin were far more widespread. Studies using rodents with naturally occurring leptin or LepR gene mutations were pivotal in identifying a prime role for leptin in several extra-hypothalamic brain regions, including the hippocampus (Ahima et al., 1998; Ahima et al., 1999). Subsequent observations that leptin-insensitive rodents had significant impairments in hippocampal-dependent learning and memory processes suggested involvement of leptin in higher cognitive functions and raised the possibility that altering neuronal leptin responsiveness also influenced the functioning of hippocampal synapses (Li et al., 2002).

LEPTIN AND LEPRS

Leptin is the product of the obese (ob) gene and the circulating leptin levels are directly proportional to body adiposity (Campfield et al., 1995). Adipocytes are the main source of leptin, but other peripheral tissues and central neurons can also generate this hormone (Schwartz et al., 1996; Ur et al., 2002). Leptin reaches the brain via transport across the blood brain barrier and evokes its biological actions by binding to leptin receptors (LepRs). Six different LepR isoforms (LepRa-f) exist. Although leptin binds to all isoforms, LepRb which is the long form, is the only isoform capable of activating the full spectrum of LepR-driven signalling pathways (Chen et al., 1996). In contrast, the shorter isoforms (LepRa,c,d,f) are implicated in the transport of leptin into the brain, whereas LepRe, which lacks a transmembrane domain, acts as a carrier for leptin in the plasma.

LepRs are class I cytokine receptors that signal via recruitment of janus tyrosine kinases (JAKs), and specifically JAK2 (Ihle, 1995). LepR-dependent activation of JAK2 leads to phosphorylation of tyrosine residues located within the LepR C-terminal. This sequence of events triggers activation of various downstream signalling pathways, including signal transducers and activators of transcription (STAT3), phosphoinositide 3-kinase (PI3K) and mitogen-activated protein kinase (MAPK), with hippocampal LepR capable of activating all of these downstream signalling pathways (Irving and Harvey, 2021).

HIPPOCAMPAL EXPRESSION OF LEPRS

In the CNS, specific hypothalamic neurons within the arcuate nucleus and ventromedial hypothalamus, express the highest density of LepRs, which is consistent with these nuclei being prime sites for controlling energy balance (Schwartz et al., 1996; Elmquist et al., 1998). However, LepR-positive immunoreactivity and LepR mRNA has been verified in other brain regions, like the hippocampal formation, which are not directly involved in control of energy homeostasis (Mercer et al., 1996; Elmquist et al., 1998; Hakansson et al., 1998). Interestingly, hippocampal LepR expression is regulated by metabolic hormones, like melatonin (Ni et al., 2015). Evidence also suggests that leptin may indirectly modulate hippocampal neuron energy homeostasis via regulation of mitochondrial function (Jin et al., 2018; Li et al., 2018).

Several studies have probed the cellular localisation of LepR in hippocampal neurons and found evidence for synaptic expression of LepRs (Shanley et al., 2002; O'Malley et al., 2007). Dual labelling immunocytochemistry detected a high degree of co-localisation between LepR and GluN2A-containing NMDA receptors (NMDARs), indicating that LepRs are localised to excitatory synapses (O'Malley et al., 2007). Together these findings point to a possible modulatory role for leptin at hippocampal excitatory synapses.

LEPTIN MODULATES EXCITATORY SYNAPTIC TRANSMISSION AT HIPPOCAMPAL CA1 SYNAPSES

NMDARs have minimal involvement in basal glutamatergic synaptic transmission. But during periods of high frequency stimulation, synaptic activation of NMDARs occurs, leading to persistent changes in synaptic efficacy and this process is known as long-term potentiation (LTP; Bliss and Collingridge, 1993). It is widely accepted that NMDAR activation is necessary for activity-dependent LTP at hippocampal Schaffer-Collateral (SC)-CA1 synapses (Collingridge et al., 1983). However, activation of NMDARs is also pivotal for other forms of hippocampal synaptic plasticity, such as long-term depression (LTD), which is induced by periods of low frequency stimulation. Activity-dependent changes in synaptic efficacy at hippocampal synapses, are thought to be key cellular processes underlying learning and memory (Bliss and Collingridge, 1993).

It is known that modifying NMDAR function is a key way of altering efficacy at hippocampal synapses. Significant evidence indicates that leptin regulates excitatory synaptic transmission at SC-CA1 synapses; effects that are highly dependent on NMDARs. At postnatal days 11–18 (P11-18), a transient depression of SC-CA1 synaptic transmission is evoked in leptin-treated brain slices (Shanley et al., 2001; Moult et al., 2010). Leptin also reduces synaptic transmission at SC-CA1 synapses earlier in development (P5-8), but this is a persistent process (leptin-induced LTD), as synaptic transmission remains depressed on leptin washout. The ability of leptin to reduce SC-CA1 synaptic transmission at P5-8 and P11-18 is prevented by NMDAR antagonists, indicating a central role for NMDARs in the depressant actions of leptin (Moult and Harvey, 2011).

At adult SC-CA1 synapses, leptin has completely opposite actions as a long-term increase in synaptic transmission (leptin-induced LTP) is observed in adult slices (Moult et al., 2010; Moult and Harvey, 2011). But NMDAR activation is also a pre-requisite for leptin's effects in adult tissue, as leptin failed to influence synaptic transmission following antagonism of NMDARs. The effects of leptin were also absent when synaptic stimulation was paused, indicating involvement of synaptic NMDARs in leptin-induced LTP (Moult and Harvey, 2011). Earlier studies demonstrated that leptin potentiates NMDA-induced Ca2+ influx in hippocampal neurons and it facilitates pharmacologically isolated NMDA excitatory postsynaptic currents (EPSCN) in hippocampal slices (Shanley et al., 2001). Consequently, leptin is likely to drive enhancement of NMDAR function which in turn leads to long-lasting changes in excitatory synaptic strength.

Although NMDARs are required for the bi-directional effects of leptin at SC-CA1 synapses, detailed pharmacological analysis using subunit-specific NMDAR antagonists, uncovered that the molecular identity of NMDARs is pivotal for leptin's divergent effects at different developmental stages. Thus, the synaptic depression induced by leptin at P5-8 or P11-18 requires selective activation of GluN2B-containing NMDARs. By contrast, GluN2A subunits underlie leptin-induced LTP in adult as this process was blocked by specific GluN2A, but not GluN2B antagonists (Moult and Harvey, 2011). This NMDAR subunit dependence parallels the reported developmental switch in synaptic NMDAR composition and the age-related decline in relative contribution of GluN2B subunits to synaptic NMDARs at SC-CA1 synapses (Monyer et al., 1994; Rumbaugh and Vicini, 1999; Moult and Harvey, 2011). Distinct LepR-dependent signalling pathways are also a factor in leptin's bi-directional actions at SC-CA1 synapses, as PI3K mediates leptin-induced LTP in adult, whereas the leptin-driven reduction in synaptic transmission requires ERK-dependent signalling (Moult and Harvey, 2011).

Interestingly, LepR-driven enhancement of NMDAR function is implicated in leptin's ability to restrict food intake. In the nucleus of the solitary tract (NTS), leptin enhances NMDA synaptic currents, which increases NTS neuron sensitivity to vagal stimulation and culminates in reduced food intake (Neyens et al., 2020). Facilitation of NMDA responses is also crucial for peripheral actions of this hormone, as leptin regulates

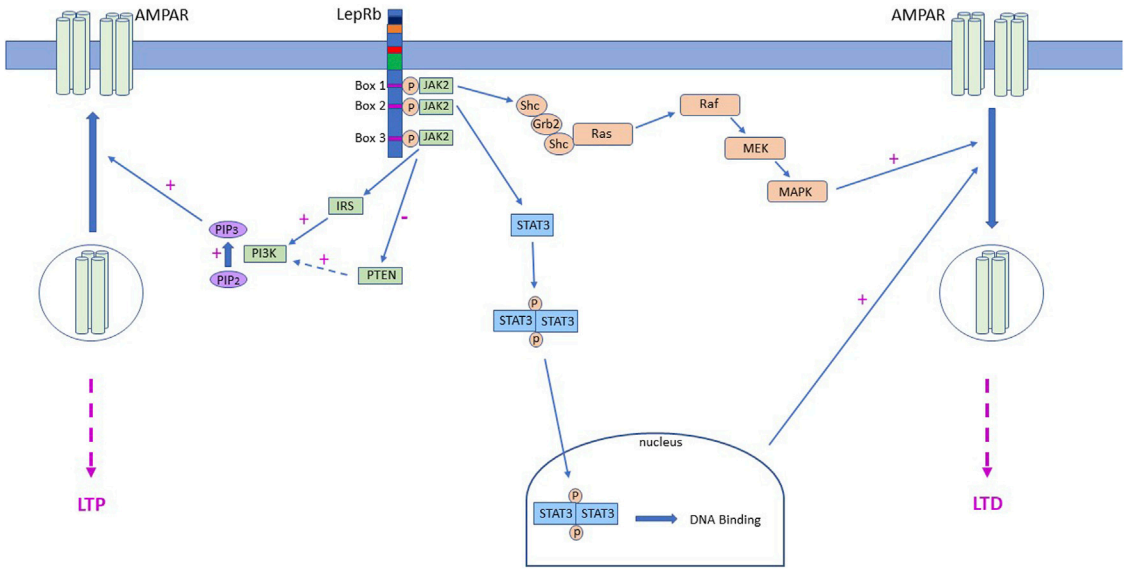

FIGURE 1 | LepR activation drives alterations in AMPA receptor trafficking via different signalling mechanisms. Schematic representation of the signalling cascades activated downstream of LepRs that contribute to movement of AMPA receptors (AMPAR) to and from hippocampal CA1 synapses. In juvenile tissue, LepR stimulation of Ras-RAF-MAPK (ERK) signalling and subsequent removal of AMPAR from synapses, leads to induction of Ltd. at SC-CA1 synapses. Leptin is also capable of stimulating PI3K activity which increases intracellular PIP3 levels and drives delivery of GluA2-lacking AMPA receptors into TA-CA1 synapses, resulting in induction of LTP. Conversely, in adult hippocampus, LepRb activation drives inhibition of PTEN, which in turn elevates PIP3 levels and insertion of GluA2-lacking AMPARs into SC-CA1 synapses. In contrast, at adult TA-CA1 synapses, activation of LepRb stimulates canonical JAK2-STAT3 signalling which drives removal of synaptic AMPARs and subsequent LTD.

pancreatic beta cell excitability by potentiating NMDA-dependent Ca2+ influx which triggers AMPK and trafficking of potassium channels to the membrane (Wu et al., 2017).

LEPTIN REGULATES GLUTAMATE RECEPTOR TRAFFICKING PROCESSES

Movement of AMPA receptors (AMPARs) into and out of synapses is key for cellular processes that modify excitatory synaptic strength, like LTP (Collingridge et al., 2004). However, NMDARs are also highly dynamic, with bi-directional changes in NMDAR movement linked to synaptic plasticity (Grosshans et al., 2002; Lau and Zuckin, 2007). Various neuromodulators, including leptin, can influence synaptic efficacy by modifying the mobility of glutamate receptors to and away from hippocampal synapses. Previous work uncovered that leptin facilitates NMDA-driven responses, as electrophysiological studies established that NMDAR synaptic currents are potentiated by leptin. Moreover, in primary hippocampal neurons treated with leptin, Ca2+ influx via NMDAR channels is amplified relative to control neurons (Shanley et al., 2001). However, studies in *Xenopus* oocytes revealed that leptin enhanced maximal NMDA-induced currents, in the absence of altered NMDAR channel kinetics, thereby signifying increased delivery of NMDARs to the membrane (Harvey et al., 2005). Leptin-driven NMDAR movement is implicated in the formation of new glutamatergic synapses, as hippocampal GluN2B surface expression is enhanced by leptin (Bland et al., 2020). In line with tyrosine phosphorylation mediating the anchoring of GluN2B subunits at synaptic sites (Vieira et al., 2020), tyrosine phosphorylation is also essential for leptin-driven movement of GluN2B subunits during synapse formation (Bland et al., 2020). Consequently, as facilitation of NMDA currents by leptin is blocked after tyrosine kinase inhibition (Harvey et al., 2005), phosphorylation of tyrosine residues may also be vital for NMDAR trafficking by leptin at later stages of postnatal development, although this remains to be explored.

Persistent changes in hippocampal synaptic strength involve delivery or removal of synaptic AMPARs (Collingridge et al., 2004; Herring and Nicoll, 2016), with a short-lasting shift in synaptic AMPAR subunit composition reported in some cases (Plant et al., 2006; Morita et al., 2013). Likewise, leptin-induced LTP at adult SC-CA1 synapses is accompanied by delivery of AMPARs to synapses. Insertion of GluA2-lacking AMPARs is specifically involved as synaptic AMPAR rectification is raised after leptin treatment and pharmacological block of GluA2-lacking AMPARs prevents leptin-induced LTP (Moult et al., 2010). Additional evidence from studies in primary neurons and brain slices supports these findings as leptin boosts GluA1 levels at the plasma membrane and at hippocampal synapses (Moult et al., 2010). Mechanistically movement of AMPARs by leptin involves a rise in intracellular PIP3 levels which is attributed to inhibition of the phosphatase, PTEN by leptin (**Figure 1**). Interestingly an increase in PIP3 levels also underlies leptin-dependent synaptic insertion of AMPAR and subsequent induction of LTP at juvenile TA-CA1 synapses,

however PI3K activation, not PTEN inhibition, drives this change in PIP3 levels (Luo et al., 2015).

REGULATION OF TEMPOROAMMONIC (TA)-CA1 SYNAPSES BY LEPTIN

Although the classical SC input to CA1 neurons is one of the most well-studied synaptic connections, direct innervation of CA1 pyramidal neurons via the TA input is also pivotal for hippocampal learning and memory (Vago et al., 2007). The TA pathway originates in entorhinal cortex layer III and extends to hippocampal stratum-moleculare where it forms synapses onto CA1 distal dendrites. Increasing evidence indicates that the two discrete inputs onto CA1 neurons have distinct functions, and that divergent mechanisms regulate SC-CA1 and TA-CA1 synapses. Thus, monoamines like dopamine depress excitatory TA-CA1 synapses but fail to affect SC-CA1 synapses (Otmakhova and Lisman 1999). Differential effects of other monoamines, including serotonin and noradrenaline, have been observed at the two CA1 synapses (Otmakhova et al., 2005). Electrophysiological studies indicate that leptin modifies TA-CA1 and SC-CA1 synaptic efficacy, but that it exhibits directly opposing actions at the two synapses. At juvenile TA-CA1 synapses leptin induces LTP, whereas a synaptic depression occurs at juvenile SC-CA1 synapses (Moult and Harvey, 2011; Luo et al., 2015). Interestingly, although GluN2B-containing NMDARs mediate the differential effects of leptin at these synapses (Moult and Harvey, 2011), distinct signalling pathways are involved as PI3K underlies leptin-induced TA-CA1 LTP, whereas ERK is implicated in the SC-CA1 synaptic depression induced by leptin. Similarly, opposing actions of leptin have been observed in adult hippocampus, despite GluN2A-containing NMDARs being required for leptin's effects at both CA1 synapses. Thus, leptin induces NMDA-dependent LTD at adult TA-CA1 synapses *via* a process requiring JAK-STAT3 signalling (McGregor et al., 2018). By contrast, inhibition of PTEN underlies leptin-induced LTP at adult SC-CA1 synapses (Moult et al., 2010; **Figure 1**). Interestingly, parallels exist between leptin-induced TA-CA1 LTD and activity-dependent SC-CA1 LTD as activation of JAK2-STAT3 signalling is required for both forms of synaptic plasticity (Nicolas et al., 2012; McGregor et al., 2018), however gene transcriptional changes are necessary for leptin-induced LTD but not for NMDA-LTD at SC-CA1 synapses.

REGULATION OF INHIBITORY GABAERGIC SYNAPSES BY LEPTIN

Several studies have ascertained that leptin also modifies central inhibitory synaptic connections. In the hypothalamus, leptin reduces GABAA-mediated inhibitory synaptic transmission onto proopiomelanocortin (POMC) neurons (Cowley et al., 2001; Munzberg et al., 2007; Vong et al., 2011), whereas increased GABAergic inhibitory tone is observed in leptin deficient ob/ob mice (Pinto et al., 2004). In rat insular cortex, leptin regulates pyramidal neuron excitability by facilitating GABA release (Murayama et al., 2019). In the developing hippocampus leptin promotes development of functional inhibitory networks as it enhances GABAergic synaptogenesis (Sahin et al., 2021) and controls chloride homeostasis by modifying KCC2 activity (Dumon et al., 2020). At later postnatal stages (P13-19), leptin enhances GABAA-mediated synaptic transmission onto CA1 pyramidal neurons *via* a PI3K-dependent mechanism (Solovyova et al., 2009). The ability of leptin to potentiate GABAergic synaptic transmission in developing neurons also requires PI3K signalling (Guimond et al., 2014). However, the signalling pathways activated downstream of PI3K, and mediate leptin's effects on GABAergic synaptic transmission during development and postnatally remain to be determined.

ALTERATIONS IN HIPPOCAMPAL SYNAPTIC RESPONSIVENESS TO LEPTIN

Dietary Changes

Accumulating evidence indicates that neuronal sensitivity to leptin is influenced by various factors. Diurnal changes in plasma leptin levels give rise to alterations in neuronal LepR expression, which in turn influences the magnitude of leptin responses (Lin and Huang, 1997; Baskin et al., 1998). Diets that are high in fats (so-called Western diets) can lead to an obese phenotype concomitant with development of resistance to insulin and leptin (Morrison et al., 2009). High fat diets (HFD) interfere with the neuronal actions of leptin, including its effects at hippocampal synapses. Thus, the ability of leptin to induce LTP at SC-CA1 synapses and to stimulate STAT3 signalling is absent in mice fed an HFD, compared to those on standard chow (Mainardi et al., 2017). Diet-induced obesity also triggers increased astrocytic expression of LepRs (Koga et al., 2014). As astrocytic LepRs help maintain glutamatergic synaptic transmission and synaptic plasticity at CA1 synapses (Naranjo et al., 2020), dietary driven changes in astrocytic LepR expression are likely to drive modifications in hippocampal synaptic efficacy.

Age-Related Alterations in Leptin Sensitivity

The ageing process is also coupled to altered neuronal sensitivity to leptin. Age-related variations in leptin-driven signalling occur in hypothalamic neurons (Scarpace et al., 2001), which may underlie the reduced effects of leptin on food intake in aged rats (Shek and Scarpace, 2000). Reduced brain uptake of leptin also manifests with increasing age, which is likely to impact overall sensitivity to leptin (Fernandez-Galaz et al., 2001). These age-related shifts in leptin sensitivity parallel the changes in body composition and energy homeostasis that occur during ageing. Indeed, elevations in body weight and adiposity occur as humans get older, with this increase in adiposity accompanied by increased circulating leptin levels which enhances the likelihood of developing leptin resistance (Petervari et al., 2014; Cunnane et al., 2020). Obesity-related leptin resistance influences overall brain health, as increasing evidence supports a link between obesity and neurodegenerative disease (see *Leptin*

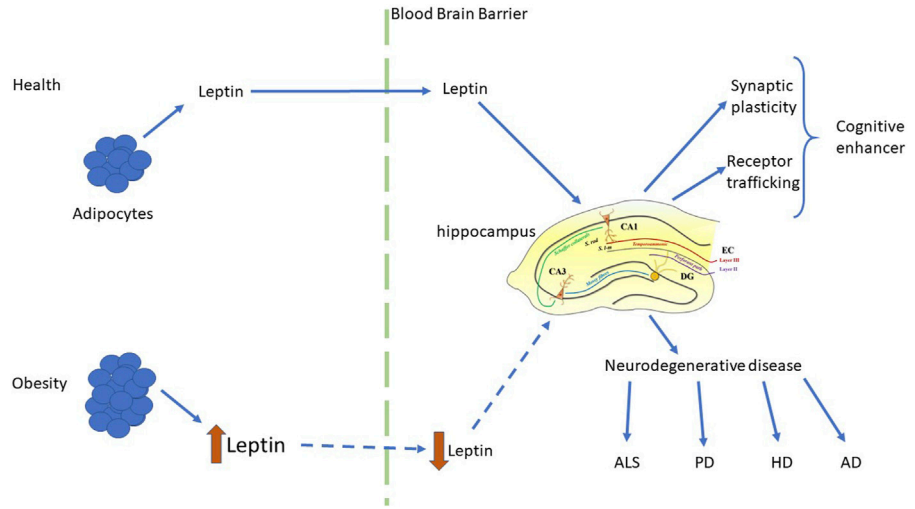

FIGURE 2 | Regulation of hippocampal function by leptin in health and disease. Schematic representation of the key synaptic effects of leptin and the functional consequences of leptin-driven alterations in hippocampal function. In health, physiological levels of leptin are released from adipocytes and readily cross the blood brain barrier to reach the brain. Within the hippocampus, leptin has pro-cognitive actions via its ability to rapidly modulate hippocampal synaptic plasticity and glutamate receptor trafficking. In contrast, in the obese state leptin levels are elevated, leading to development of leptin resistance, and reduced transport of leptin into the brain. This subsequently leads to dysfunctions in the ability of leptin to regulate hippocampal synaptic function, which is associated with an increased risk of neurodegenerative disorders, such as AD, HD, ALS and PD.

and Neurodegenerative Disorders Section). Moreover, midlife obesity is a significant risk factor for development of type II diabetes (T2D), and the link between T2D and increased AD risk is well established.

The reported alterations in leptin responsiveness linked to ageing are not restricted to metabolic tissues, as hippocampal leptin function also declines with age (Moult and Harvey, 2011; McGregor et al., 2018). Thus, electrophysiological analyses revealed that the magnitude of leptin-induced SC-CA1 LTP diminishes with age (Moult and Harvey, 2011). Interestingly, the ability of leptin to induce TA-CA1 LTD is completely absent in aged hippocampus (McGregor et al., 2018). Although age-related alterations in leptin potency could explain the lack of leptin effect, this is unlikely as leptin failed to induce TA-CA1 LTD over a wide concentration range. Moreover, delivery of a low frequency stimulation paradigm also failed to induce LTD, suggesting that TA-CA1 synapses have been modified with age, rendering them insensitive to LTD inducing patterns of synaptic activity (McGregor et al., 2017). Further studies are needed to fully assess the cellular changes responsible for the alterations in TA-CA1 synaptic responsiveness to leptin with age.

LEPTIN AND NEURODEGENERATIVE DISORDERS

Growing epidemiological evidence supports the notion that life-style choices and particularly those adopted in mid-life, influence neurodegenerative disease risk. Indeed, an elevated risk of Alzheimer's disease (AD) is connected to mid-life weight gain or obesity (Hassing et al., 2009; Xu, et al., 2011; Gustafson, et al., 2012). As feeding behaviour and thus body weight is controlled by leptin, this implies a prominent role for this hormone in overall AD risk. In support of this, abnormal leptin levels manifest in AD patients, whereas correlations between plasma leptin levels and disease risk have been described in prospective studies (Power et al., 2001; Lieb et al., 2009; Bonda et al., 2014). Abnormal leptin function occurs in various AD rodent models (Fewlass et al., 2004), indicating potential contribution of leptin dysfunction in both human and rodent forms of AD.

Obesity is associated with an increased likelihood of other neurodegenerative disorders including Huntington's disease (HD; Gaba et al., 2005; Procaccini et al., 2016), Parkinson's disease (PD; Abbott et al., 2002), multiple sclerosis (Munger et al., 2009) and amyotrophic lateral sclerosis (ALS; Paganoni et al., 2011). A significant fall in circulating leptin levels has been reported in PD and HD patients (Evidente et al., 2001), suggesting correlation between leptin dysfunction and disease pathogenesis. Consequently, it is feasible that boosting leptin levels may have therapeutic benefit in these CNS-driven diseases. Although there is as yet no direct clinical evidence to support leptin's efficacy in human neurodegenerative disorders, there is mounting evidence from pre-clinical studies that leptin has therapeutic potential as it has pro-cognitive and neuroprotective effects in cellular and rodent models of AD, PD and ALS (Greco et al., 2010; Doherty et al., 2013; Malekizadeh et al., 2017; Weng et al., 2007; Lim et al., 2014; **Figure 2**). It is also note-worthy that in addition to neurodegenerative disease, alterations in circulating leptin levels have been linked to other CNS disorders, such as childhood febrile seizures (Chen et al., 2020), suggesting that leptin's ability to regulate hippocampal synaptic function has implications not only for brain health during the aging process, but also in childhood.

CONCLUSION

There is now overwhelming evidence that the scope of leptin's central actions extends beyond the hypothalamus, with hippocampal synapses a prime target for leptin's regulatory actions. Leptin displays pro-cognitive actions as it modifies the efficacy of both SC-CA1 and TA-CA1 synaptic connections, which in turn impacts hippocampal-dependent memory. Leptin's synaptic effects are highly age-dependent, with the polarity of leptin action driven by the activation of subunit-specific NMDARs and specific signalling molecules. Hippocampal CA1 synapse sensitivity to leptin also declines during the ageing process, which coincides with a fall in the functionality of metabolic hormonal systems. Age-related alterations in leptin function have implications for brain health, and specifically are correlated with an increased risk of neurodegenerative disease. Consequently, boosting brain levels of leptin may have therapeutic benefits in human neurodegenerative disorders, although this remains to be demonstrated clinically.

AUTHOR CONTRIBUTIONS

JH wrote the review.

FUNDING

Jh is supported by funding from Alzheimer's Society United Kingdom (449 AS-PhD-18-007) and Medical Research Scotland (PHD-50034-2019).

REFERENCES

Abbott, R. D., Ross, G. W., White, L. R., Nelson, J. S., Masaki, K. H., Tanner, C. M., et al. (2002). Midlife Adiposity and the Future Risk of Parkinson's Disease. *Neurology* 59 (7), 1051–1057. doi:10.1212/wnl.59.7.1051

Ahima, R. S., Bjorbaek, C., Osei, S., and Flier, J. S. (1999). Regulation of Neuronal and Glial Proteins by Leptin: Implications for Brain Development. *Endocrinology* 140, 2755–2762. doi:10.1210/endo.140.6.6774

Ahima, R. S., Prabakaran, D., and Flier, J. S. (1998). Postnatal Leptin Surge and Regulation of Circadian Rhythm of Leptin by Feeding. Implications for Energy Homeostasis and Neuroendocrine Function. *J. Clin. Invest.* 101, 1020–1027. doi:10.1172/jci1176

Baskin, D. G., Seeley, R. J., Kuijper, J. L., Lok, S., Weigle, D. S., Erickson, J. C., et al. (1998). Increased Expression of mRNA for the Long Form of the Leptin Receptor in the Hypothalamus Is Associated with Leptin Hypersensitivity and Fasting. *Diabetes* 47, 538–543. doi:10.2337/diabetes.47.4.538

Bland, T., Zhu, M., Dillon, C., Sahin, G. S., Rodriguez-Llamas, J. L., Appleyard, S. M., et al. (2020). Leptin Controls Glutamatergic Synaptogenesis and NMDA-Receptor Trafficking via Fyn Kinase Regulation of NR2B. *Endocrinol* 161, bqz030.

Bliss, T. V. P., and Collingridge, G. L. (1993). A Synaptic Model of Memory: Long-Term Potentiation in the hippocampus. *Nature* 361, 31–39. doi:10.1038/361031a0

Bonda, D. J., Stone, J. G., Torres, S. L., Siedlak, S. L., Perry, G., Kryscio, R., et al. (2014). Dysregulation of Leptin Signaling in Alzheimer Disease: Evidence for Neuronal Leptin Resistance. *J. Neurochem.* 128, 162–172. doi:10.1111/jnc.12380

Campfield, L. A., Smith, F. J., Guisez, Y., Devos, R., and Burn, P. (1995). Recombinant Mouse OB Protein: Evidence for a Peripheral Signal Linking Adiposity and Central Neural Networks. *Science* 269, 546–549. doi:10.1126/science.7624778

Chen, H., Charlat, O., Tartaglia, L. A., Woolf, E. A., Weng, X., Ellis, S. J., et al. (1996). Evidence that the Diabetes Gene Encodes the Leptin Receptor: Identification of a Mutation in the Leptin Receptor Gene in Db/db Mice. *Cell* 84, 491–495. doi:10.1016/s0092-8674(00)81294-5

Chen, J.-r., Jin, M.-f., Tang, L., Liu, Y.-y., and Ni, H. (2020). Acute Phase Serum Leptin, Adiponectin, Interleukin-6, and Visfatin Are Altered in Chinese Children with Febrile Seizures: A Cross-Sectional Study. *Front. Endocrinol.(Lausanne)* 11, 531. doi:10.3389/fendo.2020.00531

Collingridge, G. L., Isaac, J. T., and Wang, Y. T. (2004). Receptor Trafficking and Synaptic Plasticity. *Nat. Rev. Neurosci.* 5, 952–962. doi:10.1038/nrn1556

Collingridge, G. L., Kehl, S. J., and McLennan, H. (1983). The Antagonism of Amino Acid-Induced Excitations of Rat Hippocampal CA1 Neurones *In Vitro*. *J. Physiol.* 334, 19–31. doi:10.1113/jphysiol.1983.sp014477

Cowley, M. A., Smart, J. L., Rubinstein, M., Cerdán, M. G., Diano, S., Horvath, T. L., et al. (2001). Leptin Activates Anorexigenic POMC Neurons through a Neural Network in the Arcuate Nucleus. *Nature* 411, 480–484. doi:10.1038/35078085

Cunnane, S. C., Trushina, E., Morland, C., Prigione, A., Casadesus, G., Andrews, Z. B., et al. (2020). Brain Energy Rescue: an Emerging Therapeutic Concept for Neurodegenerative Disorders of Ageing. *Nat. Rev. Drug Discov.* 19, 609–633. doi:10.1038/s41573-020-0072-x

Doherty, G. H., Beccano-Kelly, D., Yan, S. D., Gunn-Moore, F. J., and Harvey, J. (2013). Leptin Prevents Hippocampal Synaptic Disruption and Neuronal Cell Death Induced by Amyloid β. *Neurobiol. Aging* 34, 226–237. doi:10.1016/j.neurobiolaging.2012.08.003

Dumon, C., Belaidouni, Y., Diabira, D., Appleyard, S. M., Wayman, G. A., and Gaiarsa, J.-L. (2020). Leptin Down-Regulates KCC2 Activity and Controls Chloride Homeostasis in the Neonatal Rat hippocampus. *Mol. Brain* 13, 151. doi:10.1186/s13041-020-00689-z

Elmquist, J. K., Bjørbaek, C., Ahima, R. S., Flier, J. S., and Saper, C. B. (1998). Distributions of Leptin Receptor mRNA Isoforms in the Rat Brain. *J. Comp. Neurol.* 395, 535–547. doi:10.1002/(sici)1096-9861(19980615)395:4<535::aid-cne9>3.0.co;2-2

Evidente, V. G. H., Caviness, J. N., Adler, C. H., Gwinn-Hardy, K. A., and Pratley, R. E. (2001). Serum Leptin Concentrations and Satiety in Parkinson's Disease Patients with and without Weight Loss. *Mov. Disord.* 16, 924–927. doi:10.1002/mds.1165

Fernández-Galaz, C., Fernández-Agulló, T., Campoy, F., Arribas, C., Gallardo, N., Andrés, A., et al. (2001). Decreased Leptin Uptake in Hypothalamic Nuclei with Ageing in Wistar Rats. *J. Endocrinol.* 171, 23–32. doi:10.1677/joe.0.1710023

Fewlass, D. C., Noboa, K., Pi-Sunyer, F. X., Johnston, J. M., Yan, S. D., and Tezapsidis, N. (2004). Obesity-related leptin regulates Alzheimer's Abeta. *FASEB J.* 18, 1870–1878.

Friedman, J. M. (2019). Leptin and the Endocrine Control of Energy Balance. *Nat. Metab.* 1 (8), 754–764. doi:10.1038/s42255-019-0095-y

Gaba, A. M., Zhang, K., Marder, K., Moskowitz, C. B., Werner, P., and Boozer, C. N. (2005). Energy Balance in Early-Stage Huntington Disease. *Am. J. Clin. Nutr.* 81, 1335–1341. doi:10.1093/ajcn/81.6.1335

Greco, S. J., Bryan, K. J., Sarkar, S., Zhu, X., Smith, M. A., Ashford, J. W., et al. (2010). Leptin Reduces Pathology and Improves Memory in a Transgenic Mouse Model of Alzheimer's Disease. *J. Alzheimers Dis.* 19, 1155–1167. doi:10.3233/jad-2010-1308

Grosshans, D. R., Clayton, D. A., Coultrap, S. J., and Browning, M. D. (2002). LTP Leads to Rapid Surface Expression of NMDA but Not AMPA Receptors in Adult Rat CA1. *Nat. Neurosci.* 5, 27–33. doi:10.1038/nn779

Guimond, D., Diabira, D., Porcher, C., Bader, F., Ferrand, N., Zhu, M., et al. (2014). Leptin Potentiates GABAergic Synaptic Transmission in the Developing Rodent hippocampus. *Front. Cell. Neurosci.* 8, 235. doi:10.3389/fncel.2014.00235

Gustafson, D. R., Bäckman, K., Joas, E., Waern, M., Östling, S., Guo, X., et al. (2012). 37 Years of Body Mass Index and Dementia: Observations from the Prospective Population Study of Women in Gothenburg, Sweden. *J. Alzheimers Dis.* 28, 163–171. doi:10.3233/JAD-2011-110917

Håkansson, M. L., Brown, H., Ghilardi, N., Skoda, R. C., and Meister, B. (1998). Leptin Receptor Immunoreactivity in Chemically Defined Target Neurons of the Hypothalamus. *J. Neurosci.* 18, 559–572.

Harvey, J., Shanley, L. J., O'Malley, D., and Irving, A. J. (2005). Leptin: a Potential Cognitive Enhancer? *Biochem. Soc. Trans.* 33, 1029–1032. doi:10.1042/BST20051029

Hassing, L. B., Dahl, A. K., Thorvaldsson, V., Berg, S., Gatz, M., Pedersen, N. L., et al. (2009). Overweight in Midlife and Risk of Dementia: A 40-year Follow-Up Study. *Int. J. Obes. (Lond)* 33, 893–898. doi:10.1038/ijo.2009.104

Herring, B. E., and Nicoll, R. A. (2016). Long-Term Potentiation: From CaMKII to AMPA Receptor Trafficking. *Annu. Rev. Physiol.* 78, 351–365. doi:10.1146/annurev-physiol-021014-071753

Ihle, J. N. (1995). Cytokine Receptor Signalling. *Nature* 377, 591–594. doi:10.1038/377591a0

Irving, A., and Harvey, J. (2021). Regulation of Hippocampal Synaptic Function by the Metabolic Hormone Leptin: Implications for Health and Disease. *Prog. Lipid. Res.* 82, 101098. doi:10.1016/j.plipres.2021.101098

Jin, M. F., Ni, H., and Li, L. L. (2018). Leptin Maintained Zinc Homeostasis Against Glutamate-Induced Excitotoxicity by Preventing Mitophagy-Mediated Mitochondrial Activation in HT22 Hippocampal Neuronal Cells. *Front. Neurol.* 9, 322. doi:10.3389/fneur.2018.00322

Koga, S., Kojima, A., Kuwabara, S., and Yoshiyama, Y. (2014). Immunohistochemical Analysis of Tau Phosphorylation and Astroglial Activation with Enhanced Leptin Receptor Expression in Diet-Induced Obesity Mouse hippocampus. *Neurosci. Lett.* 571, 11–16. doi:10.1016/j.neulet.2014.04.028

Lau, C. G., and Zukin, R. S. (2007). NMDA Receptor Trafficking in Synaptic Plasticity and Neuropsychiatric Disorders. *Nat. Rev. Neurosci.* 8, 413–426. doi:10.1038/nrn2153

Li, L. L., Jin, M. F., and Ni, H. (2018). Zinc/CaMK II Associated-Mitophagy Signaling Contributed to Hippocampal Mossy Fiber Sprouting and Cognitive Deficits Following Neonatal Seizures and its Regulation by Chronic Leptin Treatment. *Front. Neurol.* 9, 802. doi:10.3389/fneur.2018.00802

Li, X. L., Aou, S., Oomura, Y., Hori, N., Fukunaga, K., and Hori, T. (2002). Impairment of Long-Term Potentiation and Spatial Memory in Leptin Receptor-Deficient Rodents. *Neuroscience* 113, 607–615. doi:10.1016/s0306-4522(02)00162-8

Lieb, W., Beiser, A. S., Vasan, R. S., Tan, Z. S., Au, R., Harris, T. B., et al. (2009). Association of Plasma Leptin Levels with Incident Alzheimer Disease and MRI Measures of Brain Aging. *JAMA* 302, 2565–2572. doi:10.1001/jama.2009.1836

Lim, M. A., Bence, K. K., Sandesara, I., Andreux, P., Auwerx, J., Ishibashi, J., et al. (2014). Genetically Altering Organismal Metabolism by Leptin-Deficiency Benefits a Mouse Model of Amyotrophic Lateral Sclerosis. *Hum. Mol. Genet.* 23, 4995–5008. doi:10.1093/hmg/ddu214

Lin, S., and Huang, X. F. (1997). Fasting Increases Leptin Receptor mRNA Expression in Lean but Not Obese (Ob/ob) Mouse Brain. *Neuroreport* 8, 3625–3629.

Luo, X., McGregor, G., Irving, A. J., and Harvey, J. (2015). Leptin Induces a Novel Form of NMDA Receptor-dependent LTP at Hippocampal temporoammonic-CA1 Synapses. *eNeuro* 2. doi:10.1523/ENEURO.0007-15.2015

Mainardi, M., Spinelli, M., Scala, F., Mattera, A., Fusco, S., D'Ascenzo, M., et al. (2017). Loss of Leptin-Induced Modulation of Hippocampal Synaptic Trasmission and Signal Transduction in High-Fat Diet-Fed Mice. *Front. Cell. Neurosci.* 11, 225. doi:10.3389/fncel.2017.00225

Malekizadeh, Y., Holiday, A., Redfearn, D., Ainge, J. A., Doherty, G., and Harvey, J. (2017). A Leptin Fragment Mirrors the Cognitive Enhancing and Neuroprotective Actions of Leptin. *Cereb. Cortex.* 27, 4769–4782. doi:10.1093/cercor/bhw272

McGregor, G., Clements, L., Farah, A., Irving, A. J., and Harvey, J. (2018). Age-dependent Regulation of Excitatory Synaptic Transmission at Hippocampal temporoammonic-CA1 Synapses by Leptin. *Neurobiol. Aging* 69, 76–93. doi:10.1016/j.neurobiolaging.2018.05.007

McGregor, G., Irving, A. J., and Harvey, J. (2017). Canonical JAK-STAT Signaling Is Pivotal for Long-term Depression at Adult Hippocampal temporoammonic-CA1 Synapses. *FASEB J.* 31, 3449–3466. doi:10.1096/fj.201601293rr

Mercer, J. G., Hoggard, N., Williams, L. M., Lawrence, C. B., Hannah, L. T., and Trayhurn, P. (1996). Localization of Leptin Receptor mRNA and the Long Form Splice Variant (Ob-Rb) in Mouse Hypothalamus and Adjacent Brain Regions by *In Situ* Hybridization. *FEBS Lett.* 387, 113–116. doi:10.1016/0014-5793(96)00473-5

Monyer, H., Burnashev, N., Laurie, D. J., Sakmann, B., and Seeburg, P. H. (1994). Developmental and Regional Expression in the Rat Brain and Functional Properties of Four NMDA Receptors. *Neuron* 12, 529–540. doi:10.1016/0896-6273(94)90210-0

Morita, D., Rah, J. C., and Isaac, J. T. (2013). Incorporation of Inwardly Rectifying AMPA Receptors at Silent Synapses during Hippocampal Long-Term Potentiation. *Philos. Trans. R. Soc. Lond. B Biol. Sci.* 369, 20130156. doi:10.1098/rstb.2013.0156

Morrison, C. D., Huypens, P., Stewart, L. K., and Gettys, T. W. (2009). Implications of Crosstalk between Leptin and Insulin Signaling during the Development of Diet-Induced Obesity. *Biochimica Biophysica Acta (BBA) - Mol. Basis Dis.* 1792, 409–416. doi:10.1016/j.bbadis.2008.09.005

Moult, P. R., Cross, A., Santos, S. D., Carvalho, A. L., Lindsay, Y., Connolly, C. N., et al. (2010). Leptin Regulates AMPA Receptor Trafficking via PTEN Inhibition. *J. Neurosci.* 30, 4088–4101. doi:10.1523/JNEUROSCI.3614-09.2010

Moult, P. R., and Harvey, J. (2011). NMDA Receptor Subunit Composition Determines the Polarity of Leptin-Induced Synaptic Plasticity. *Neuropharmacology* 61, 924–936. doi:10.1016/j.neuropharm.2011.06.021

Munger, K. L., Chitnis, T., and Ascherio, A. (2009). Body Size and Risk of MS in Two Cohorts of US Women. *Neurology* 73, 1543–1550. doi:10.1212/WNL.0b013e3181c0d6e0

Münzberg, H., Jobst, E. E., Bates, S. H., Jones, J., Villanueva, E., Leshan, R., et al. (2007). Appropriate Inhibition of Orexigenic Hypothalamic Arcuate Nucleus Neurons Independently of Leptin receptor/STAT3 Signaling. *J. Neurosci.* 27, 69–74. doi:10.1523/JNEUROSCI.3168-06.2007

Murayama, S., Yamamoto, K., Fujita, S., Takei, H., Inui, T., Ogiso, B., et al. (2019). Extracellular Glucose-dependent IPSC Enhancement by Leptin in Fast-Spiking to Pyramidal Neuron Connections via JAK2-PI3K Pathway in the Rat Insular Cortex. *Neuropharmacology* 149, 133–148. doi:10.1016/j.neuropharm.2019.02.021

Naranjo, V., Contreras, A., Merino, B., Plaza, A., Lorenzo, M. P., García-Cáceres, C., et al. (2020). Specific Deletion of the Astrocyte Leptin Receptor Induces Changes in Hippocampus Glutamate Metabolism, Synaptic Transmission and Plasticity. *Neuroscience* 447, 182–190. doi:10.1016/j.neuroscience.2019.10.005

Neyens, D., Zhao, H., Huston, N. J., Wayman, G. A., Ritter, R. C., and Appleyard, S. M. (2020). Leptin Sensitizes NTS Neurons to Vagal Input by Increasing Postsynaptic NMDA Receptor Currents. *J. Neurosci.* 40, 7054–7064. doi:10.1523/jneurosci.1865-19.2020

Ni, H., Sun, Q., Tian, T., Feng, X., and Sun, B.-L. (2015). Long-term Expression of Metabolism-Associated Genes in the Rat hippocampus Following Recurrent Neonatal Seizures and its Regulation by Melatonin. *Mol. Med. Rep.* 12, 2727–2734. doi:10.3892/mmr.2015.3691

Nicolas, C. S., Peineau, S., Amici, M., Csaba, Z., Fafouri, A., Javalet, C., et al. (2012). The JAK/STAT Pathway Is Involved in Synaptic Plasticity. *Neuron* 73, 374–390. doi:10.1016/j.neuron.2011.11.024

O'Malley, D., MacDonald, N., Mizielinska, S., Connolly, C. N., Irving, A. J., and Harvey, J. (2007). Leptin Promotes Rapid Dynamic Changes in Hippocampal Dendritic Morphology. *Mol. Cell. Neurosci.* 35, 559–572. doi:10.1016/j.mcn.2007.05.001

Otmakhova, N. A., Lewey, J., Asrican, B., and Lisman, J. E. (2005). Inhibition of Perforant Path Input to the CA1 Region by Serotonin and Noradrenaline. *J. Neurophysiology* 94, 1413–1422. doi:10.1152/jn.00217.2005

Otmakhova, N. A., and Lisman, J. E. (1999). Dopamine Selectively Inhibits the Direct Cortical Pathway to the CA1 Hippocampal Region. *J. Neurosci.* 19, 1437–1445. doi:10.1523/jneurosci.19-04-01437.1999

Paganoni, S., Deng, J., Jaffa, M., Cudkowicz, M. E., and Wills, A.-M. (2011). Body Mass Index, Not Dyslipidemia, Is an Independent Predictor of Survival in Amyotrophic Lateral Sclerosis. *Muscle Nerve* 44, 20–24. doi:10.1002/mus.22114

Pétervári, E., Rostás, I., Soós, S., Tenk, J., Mikó, A., Füredi, N., et al. (2014). Age versus Nutritional State in the Development of Central Leptin Resistance. *Peptides* 56, 59–67. doi:10.1016/j.peptides.2014.03.011

Pinto, S., Roseberry, A. G., Liu, H., Diano, S., Shanabrough, M., Cai, X., et al. (2004). Rapid Rewiring of Arcuate Nucleus Feeding Circuits by Leptin. *Science* 304, 110–115. doi:10.1126/science.1089459

Plant, K., Pelkey, K. A., Bortolotto, Z. A., Morita, D., Terashima, A., McBain, C. J., et al. (2006). Transient Incorporation of Native GluR2-Lacking AMPA Receptors during Hippocampal Long-Term Potentiation. *Nat. Neurosci.* 9, 602–604. doi:10.1038/nn1678

Power, D. A., Noel, J., Collins, R., and O'Neill, D. (2001). Circulating Leptin Levels and Weight Loss in Alzheimer's Disease Patients. *Dement. Geriatr. Cogn. Disord.* 12, 167–170. doi:10.1159/000051252

Procaccini, C., Santopaolo, M., Faicchia, D., Colamatteo, A., Formisano, L., de Candia, P., et al. (2016). Role of Metabolism in Neurodegenerative Disorders. *Metabolism* 65, 1376–1390. doi:10.1016/j.metabol.2016.05.018

Rumbaugh, G., and Vicini, S. (1999). Distinct Synaptic and Extrasynaptic NMDA Receptors in Developing Cerebellar Granule Neurons. *J. Neurosci.* 19, 10603–10610.

Sahin, G. S., Luis Rodriguez-Llamas, J., Dillon, C., Medina, I., Appleyard, S. M., Gaiarsa, J. L., et al. (2021). Leptin Increases GABAergic Synaptogenesis through the Rho Guanine Exchange Factor Beta-PIX in Developing Hippocampal Neurons. *Sci. Signal.* 14, eabe4111. doi:10.1126/scisignal.abe4111

Scarpace, P. J., Matheny, M., and Tümer, N. (2001). Hypothalamic Leptin Resistance Is Associated with Impaired Leptin Signal Transduction in Aged Obese Rats. *Neuroscience* 104, 1111–1117. doi:10.1016/s0306-4522(01)00142-7

Schwartz, M. W., Seeley, R. J., Campfield, L. A., Burn, P., and Baskin, D. G. (1996). Identification of Targets of Leptin Action in Rat Hypothalamus. *J. Clin. Invest.* 98 (5), 1101–1106. doi:10.1172/jci118891

Shanley, L. J., Irving, A. J., and Harvey, J. (2001). Leptin Enhances NMDA Receptor Function and Modulates Hippocampal Synaptic Plasticity. *J. Neurosci.* 21, RC186. doi:10.1523/jneurosci.21-24-j0001.2001

Shanley, L. J., O'Malley, D., Irving, A. J., Ashford, M. L., and Harvey, J. (2002). Leptin Inhibits Epileptiform-like Activity in Rat Hippocampal Neurones via PI 3-Kinase-Driven Activation of BK Channels. *J. Physiol.* 545, 933–944. doi:10.1113/jphysiol.2002.029488

Shek, E. W., and Scarpace, P. J. (2000). Resistance to the Anorexic and Thermogenic Effects of Centrally Administrated Leptin in Obese Aged Rats. *Regul. Pept.* 92, 65–71. doi:10.1016/s0167-0115(00)00151-8

Solovyova, N., Moult, P. R., Milojkovic, B., Lambert, J. J., and Harvey, J. (2009). Bidirectional Modulation of Fast Inhibitory Synaptic Transmission by Leptin. *J. Neurochem.* 108 (1), 190–201. doi:10.1111/j.1471-4159.2008.05751.x

Ur, E., Wilkinson, D. A., Morash, B. A., and Wilkinson, M. (2002). Leptin Immunoreactivity Is Localized to Neurons in Rat Brain. *Neuroendocrinology* 75 (4), 264–272. doi:10.1159/000054718

Vago, D. R., Bevan, A., and Kesner, R. P. (2007). The Role of the Direct Perforant Path Input to the CA1 Subregion of the Dorsal hippocampus in Memory Retention and Retrieval. *Hippocampus* 17, 977–987. doi:10.1002/hipo.20329

Vieira, M., Yong, X. L. H., Roche, K. W., and Anggono, V. (2020). Regulation of NMDA Glutamate Receptor Functions by the GluN2 Subunits. *J. Neurochem.* 154 (2), 121–143. doi:10.1111/jnc.14970

Vong, L., Ye, C., Yang, Z., Choi, B., Chua, S., Jr, and Lowell, B. B. (2011). Leptin Action on GABAergic Neurons Prevents Obesity and Reduces Inhibitory Tone to POMC Neurons. *Neuron* 71 (1), 142–154. doi:10.1016/j.neuron.2011.05.028

Weng, Z., Signore, A. P., Gao, Y., Wang, S., Zhang, F., Hastings, T., et al. (2007). Leptin Protects against 6-Hydroxydopamine-Induced Dopaminergic Cell Death via Mitogen-Activated Protein Kinase Signaling. *J. Biol. Chem.* 282, 34479–34491. doi:10.1074/jbc.M705426200

Wu, Y., Fortin, D. A., Cochrane, V. A., Chen, P.-C., and Shyng, S.-L. (2017). NMDA Receptors Mediate Leptin Signaling and Regulate Potassium Channel Trafficking in Pancreatic β-cells. *J. Biol. Chem.* 292 (37), 15512–15524. doi:10.1074/jbc.m117.802249

Xu, W. L., Atti, A. R., Gatz, M., Pedersen, N. L., Johansson, B., and Fratiglioni, L. (2011). Midlife Overweight and Obesity Increase Late-Life Dementia Risk: A Population-Based Twin Study. *Neurology* 76, 1568–1574. doi:10.1212/WNL.0b013e3182190d09

Conflict of Interest: The author declares that the research was conducted in the absence of any commercial or financial relationships that could be construed as a potential conflict of interest.

Publisher's Note: All claims expressed in this article are solely those of the authors and do not necessarily represent those of their affiliated organizations, or those of the publisher, the editors and the reviewers. Any product that may be evaluated in this article, or claim that may be made by its manufacturer, is not guaranteed or endorsed by the publisher.

frontiers | Frontiers in Pharmacology

MINI REVIEW
published: 11 July 2022
doi: 10.3389/fphar.2022.898797

Nitric Oxide Involvement in Cardiovascular Dysfunctions of Parkinson Disease

Marli Cardoso Martins-Pinge[1], Lorena de Jager[1], Blenda Hyedra de Campos[1], Lorena Oliveira Bezerra[1], Pamela Giovana Turini[1] and Phileno Pinge-Filho[2]*

[1]Departamento de Ciências Fisiológicas, Universidade Estadual de Londrina—UEL, Londrina, Brazil, [2]Departamento de Ciências Patológicas, Universidade Estadual de Londrina- UEL, Londrina, Brazil

Parkinson's disease (PD) is characterized by the loss of dopaminergic neurons in the substantia nigra, causing motor changes. In addition to motor symptoms, non-motor dysfunctions such as psychological, sensory and autonomic disorders are recorded. Manifestations related to the autonomic nervous system include the cardiovascular system, as postural hypotension, postprandial hypotension, and low blood pressure. One of the mediators involved is the nitric oxide (NO). In addition to the known roles such as vasodilator, neuromodulator, NO acts as an important mediator of the immune response, increasing the inflammatory response provoked by PD in central nervous system. The use of non-specific NOS inhibitors attenuated the neurodegenerative response in animal models of PD. However, the mechanisms by which NO contributes to neurodegeneration are still not well understood. The literature suggest that the contribution of NO occurs through its interaction with superoxides, products of oxidative stress, and blocking of the mitochondrial respiratory chain, resulting in neuronal death. Most studies involving Parkinsonism models have evaluated brain NO concentrations, with little data available on its peripheral action. Considering that studies that evaluated the involvement of NO in the neurodegeneration in PD, through NOS inhibitors administration, showed neuroprotection in rats, it has prompted new studies to assess the participation of NOS isoforms in cardiovascular changes induced by parkinsonism, and thus to envision new targets for the treatment of cardiovascular disorders in PD. The aim of this study was to conduct a literature review to assess available information on the involvement of nitric oxide (NO) in cardiovascular aspects of PD.

Keywords: arterial pressure, heart rate, hypotension, 6-OHDA, NO-synthase, parkinsonism

OPEN ACCESS

Edited by:
Nidhi Agarwal,
Jamia Hamdard University, India

Reviewed by:
José Ronaldo dos Santos,
Federal University of Sergipe, Brazil

****Correspondence:***
Marli Cardoso Martins-Pinge
martinspinge@uel.br

Specialty section:
This article was submitted to Neuropharmacology, a section of the journal Frontiers in Pharmacology

Received: *17 March 2022*
Accepted: *20 June 2022*
Published: *11 July 2022*

Citation:
Martins-Pinge MC, de Jager L, de Campos BH, Bezerra LO, Turini PG and Pinge-Filho P (2022) Nitric Oxide Involvement in Cardiovascular Dysfunctions of Parkinson Disease. Front. Pharmacol. 13:898797. doi: 10.3389/fphar.2022.898797

INTRODUCTION

Parkinson's disease (PD) is the second most common neurodegenerative disease and affects approximately 1% of the world population aged over 65 years (Lau and Breteler, 2006). It is characterized by the degeneration of dopaminergic neurons in the substantia nigra pars compacta (SNpc) and formation of α-synuclein aggregates, called Lewy bodies. When the neurodegenerative process reduces dopamine levels by about 60%, motor symptoms such as bradykinesia, rigidity and tremor at rest are manifested, mainly (Dauer and Przedborski, 2003). PD also has non-motor

symptoms present in the most basal stages of the disease, such as sensory, neuropsychiatric and autonomic disorders, known as dysautonomias (Sian et al., 1999; Rodriguez-Oroz et al., 2009; Schapira et al., 2017)

The worldwide occurrence of Parkinson's Disease (PD) is estimated between 5 and 35 new cases per 100 thousand inhabitants. The age of onset is usually around 50 years of age, with a higher incidence after the sixth decade of life (Simon et al., 2020). There is a higher prevalence in males, with 134 cases in men and 41 in women per 100,000 inhabitants, aged between 50 and 59 years (Pringsheim et al., 2014). There is also evidence that PD is more prevalent in postmenopausal women compared to premenopausal women of similar age (Ragonese et al., 2006).

With its idiopathic etiology, it is believed that genetic issues are linked to the existence of genes that favor the development of the disease, but acting indirectly. Environmental factors are linked to PD patients who live in rural areas, use well water and are more exposed to pesticides and herbicides (Teive, 2005). Regarding the contribution of brain aging, it would be related to the prevalence of age, associated with progressive neuronal loss (Pereira and Garrett, 2010).

The cardinal signs of PD are: bradykinesia and oligokinesis, observed by slowness and reduction of movements in quantity and amplitude; generalized stiffness; resting tremor and postural instability (Sung and Nicholas, 2013). As the disease progresses, other motor symptoms can be identified, such as reduced facial expression; micrography; disorders in oral communication and swallowing, difficulty in gait, which include freezing, difficulty in changing direction and in overcoming obstacles; postural changes, with a tendency to bend the limbs and respiratory changes, especially due to the decrease in chest expansion (Peterson and Horak, 2016). Motor characteristics of the extrapyramidal region of PD emerge when 30%–50% of the dopamine-producing neurons in the substantia nigra are lost (Fazio et al., 2018). Motor impairment becomes bilateral three to 5 years after the initial diagnosis (Scorza et al., 2001).

Some non-motor symptoms may precede motor dysfunction by several years, such as: neuropsychiatric disorders, sleep disorders, olfactory deficit, anxiety and depression and dysautonomias (Schapira and Tolosa, 2010), but in general, these symptoms occur at any stage of PD, and may vary according to each patient (Jain and Goldstein, 2012).

The autonomic nervous system (ANS), responsible for controlling physiological adjustment parameters, seems to be altered in PD inducing dysautonomias (Azevedo and Cardoso, 2009; Sharabi et al., 2021). A subset of these symptoms are associated with altered function of the ANS, where orthostatic hypotension, hyperhidrosis and gastrointestinal dysfunction are common manifestations in PD that can affect the quality of life of patients and can have an impact even more than the motor symptoms (Teive, 2006). Among the cardiovascular alterations are the orthostatic arterial hypotension (OH), postprandial arterial hypotension, alteration of arterial pressure (BP) variability and, possibly, fatigue and intolerance to physical exercise (Nicaretta et al., 2011; Jain and Goldstein, 2012; Schapira et al., 2017). Those symptoms are quite relevant and impact on the patient's clinical condition (Sian et al., 1999; Rodriguez-Oroz et al., 2009; Schapira et al., 2017; Balestrino and Schapira, 2020). However, little is know about the origins of those alterations.

Nitric oxide (NO) is a small and highly diffuse molecule that, despite having a half-life of only a few seconds, has an ambiguous action as an important physiological mediator, acting as a vasodilator and immune response mediator, and cytotoxic mediator, exacerbating the inflammatory response caused by PD (Doherty, 2011; Rochette et al., 2013). Considering the involvement of this mediator in the central alterations evaluated in animal models of parkinsonism, the question of its possible involvement in the cardiovascular dysfunctions of PD arises, since NO is a modulator of several neurotransmitter systems, such as dopaminergic, cholinergic and adrenergic (Paredes-Rodriguez et al., 2020). Studies in this direction have been initiated and may provide greater support for the use of new therapies.

ANIMAL MODELS OF PARKINSONISM

The study of Parkinson's disease (PD) is possible through the induction of the disease in animal models, such as rats and mice. To simulate the main characteristics, pharmacological models such as reserpine and haloperidol, and neurotoxic models such as 6-hydroxydopamine (6-OHDA), 1-methyl-4-phenyl-1,2,3,6-tetrahydropyridine (MPTP), rotenone, paraquat, lipopolysaccharide (LPS) and methamphetamine are utilized (Blum et al., 2001). Neurotoxic models damage the nigrostriatal pathway by infusing neurotoxins into different areas unilaterally or bilaterally in the substantia nigra pars compacta (SNpc), medial forebrain bundle or striatum. 6-OHDA and MPTP are the most used experimental models, since their induction causes the degeneration of 60%–70% of the nigrostriatal pathway, which corresponds to the onset of motor symptoms. Due to the complexity of PD, there is no experimental model that presents all the characteristics of the disease (Duty and Jenner, 2011; Jackson-Lewis et al., 2012).

6-OHDA is unable to cross the blood-brain barrier, so it is administered directly into the SNpc or striatum *via* stereotaxic surgery. The neurotoxin binds to dopamine transporters and is carried to dopaminergic neurons, accumulating in the cytosol and causing the formation of reactive oxygen species that lead to neuronal death. Additionally, 6-OHDA can accumulate in the mitochondria, where it binds to complex I of the electron transport chain and inhibits flow (Blandini et al., 2008).

CARDIOVASCULAR AND AUTONOMIC DYSFUNCTION AND PARKINSON'S DISEASE

Cardiovascular alterations such as orthostatic hypotension, heart rate variability, modifications in cardiogram parameters and baroreflex dysfunction can appear in both the early and late stages of PD, worsening as the disease progresses. Cardiovascular abnormalities can also appear as a side effect of PD treatment by

L-DOPA leading to a decrease in blood pressure aggravating the orthostatic hypotension. This side effect limits the therapeutic use of L-DOPA in geriatric patients with PD and can contribute to the number of hospital admissions (Cuenca–Bermejo et al., 2021). It is estimated that 80% of PD patients have heart rate and blood pressure abnormalities (Gibbons et al., 2017). Orthostatic hypotension affects 40% of PD patients and causes dizziness and syncope, increasing the risk of falls and injuries. These changes seem to be due to noradrenergic cardiac denervation, extracardiac noradrenergic denervation and baroreflex insufficiency (Jain and Goldstein, 2012; Paredes-Rodriguez et al., 2020). Changes in HR appear to be related to dysfunctional parasympathetic responses, while the inability to regulate BP is related to the loss of sympathetic regulation (Jain and Goldstein, 2012).

Heart rate variability assesses the modulation of the autonomic nervous system on the cardiovascular system and works as an indicator of health (Vanderlei et al., 2009). Patients with PD have a reduction in heart rate variability (HRV) and lower LF values than patients in the control group (Solla et al., 2015; Salsone et al., 2016; Strano et al., 2016). Sorensen and colleagues observed attenuated sympathetic activity in patients with PD, with a reduction in the components related to the sympathetic system in HRV (Sorensen et al., 2013). Evidence also shows loss of sympathetic noradrenergic nerves in the heart and kidneys of patients with PD (Goldstein, 2007).

In experimental models, male rats with bilateral induction of the neurotoxin 6-hydroxydopamine (6-OHDA) directly in the SNpc leads to a decrease in baseline parameters of mean arterial pressure (MAP) and heart rate (HR), which are accompanied by a reduction in modulation systolic blood pressure (Ariza et al., 2015b). Baroreflex and chemoreflex responses are altered in these animals (Ariza et al., 2015a). Bilateral injection also caused a drop in the night/day cycle change of heart rate and weakened phenylephrine-induced bradycardia, suggesting a drop in heart rate (Metzger and Emborg, 2019). Furthermore, rats with 6-OHDA parkinsonism show a decreased response to alpha-adrenergic blocker, suggesting an impaired sympathetic vascular synaptic transmission (Ariza et al., 2015b). Bilateral 6-OHDA animals and Prolopa control animals presented a lower cardiovascular compensation during head up tilt, suggesting a possible autonomic impairment in parkinsonism induced by 6-OHDA (Silva et al., 2015). Also, in the 6-OHDA injury model, lower baroreflex sensitivity and decreased number of cardiovascular neurons in the brainstem were observed (Falquetto et al., 2017). Recent literature has described altered central and peripheral mechanisms affecting the feedback-controlled loops that comprise the reflex arc in patients with PD and animal models (Sabino-Carvalho et al., 2021).

In the MPTP model, in mice, attenuation of baroreflex sensitivity was observed, associated with loss of TH + neurons and decrease of catecholamines in the brainstem. There was an increase in HR and a decrease in HRV power. Regarding the frequency domains, an increase in sympathetic tone and a decrease in parasympathetic tone were observed (Liu et al., 2020).

NITRIC OXIDE AND PARKINSON'S DISEASE

NO is synthesized by nitric oxide synthase (NOS) through the oxidation of L-Arginine. The enzyme is found into constitutive NOS (cNOS), whose activation depends on calcium, and inducible NOS (iNOS), dependent on cytokines. cNOS is expressed at basal levels and has two isoforms: endothelial NOS (eNOS) and neuronal NOS (nNOS). Among the functions of eNOS are vasodilation, inhibition of platelet adhesion and aggregation in blood vessels, inhibition of vascular inflammation and leukocyte adhesion, while nNOS regulates synaptic transmission in the central nervous system (CNS) and is present in smooth muscles promoting vasoregulation. The expression of iNOS occurs specially under inflammatory conditions through immunological or microbial stimuli (Förstermann and Sessa, 2012).

Post mortem analyses, clinical findings and experimental models of parkinsonism suggest the involvement of NO in the neurodegeneration observed in PD. Barthwal et al. (2001) demonstrated that the use of a non-specific inhibitor for NO (Nw-nitro-arginine-methyl-ester or L-NAME) results in a decrease in the neurodegenerative response after 6-OHDA injury in rats (Barthwal et al., 2001). In the MPTP model, inhibitors of nNOS—7-Nitroindazole (7-NI) and of iNOS—S-methylisothiourea (SMT) were effective in protecting against the neurotoxic effects of the lesion, suggesting the participation of NO in PD (Schulz et al., 1995; Di Monte et al., 1996; Aras et al., 2014). The administration of GW274150 [(2-((1-iminoethyl)amino)ethyl]-L-homocysteine - selective iNOS inhibitor) after unilateral 6-OHDA injury significantly attenuated the loss of DA in the striatum of Sprague-Dawley rats (Broom et al., 2011). Furthermore, the increased degeneration of dopaminergic neurons in 6-OHDA-injured rats leads to a decrease in the concentration of nNOS in the substantia nigra of these animals (Czarnecka et al., 2013), while MPTP injury in mice results in an increase in iNOS (Liberatore et al., 1999). Literature showed differences in the effects of MPTP toxicity between males and females, with males having a faster decrease in DA and later, females having better recovery from this decrease. Furthermore, males were the first to show increased expression of iNOS and nNOS in the striatum (Joniec et al., 2009)

Another factor that suggests the involvement of NOS is the correlation between alterations in the genes responsible for iNOS and nNOS and the risk of developing PD (Levecque et al., 2003). Regarding peripheral NO, Çubukçu et al. (2016) demonstrate a decrease in plasma NO concentration, without a decrease in NOS activity in patients with PD. Thus, evidence indicates that NOS appear to participate in the neurodegeneration of dopaminergic neurons in animal models of PD. Therefore, the use of NOS inhibitors in the treatment of PD has been discussed (Broom et al., 2011).

The mechanisms by which NO contributes to neurodegeneration are not well understood. It is known that the induction of PD is related to increased oxidative stress in

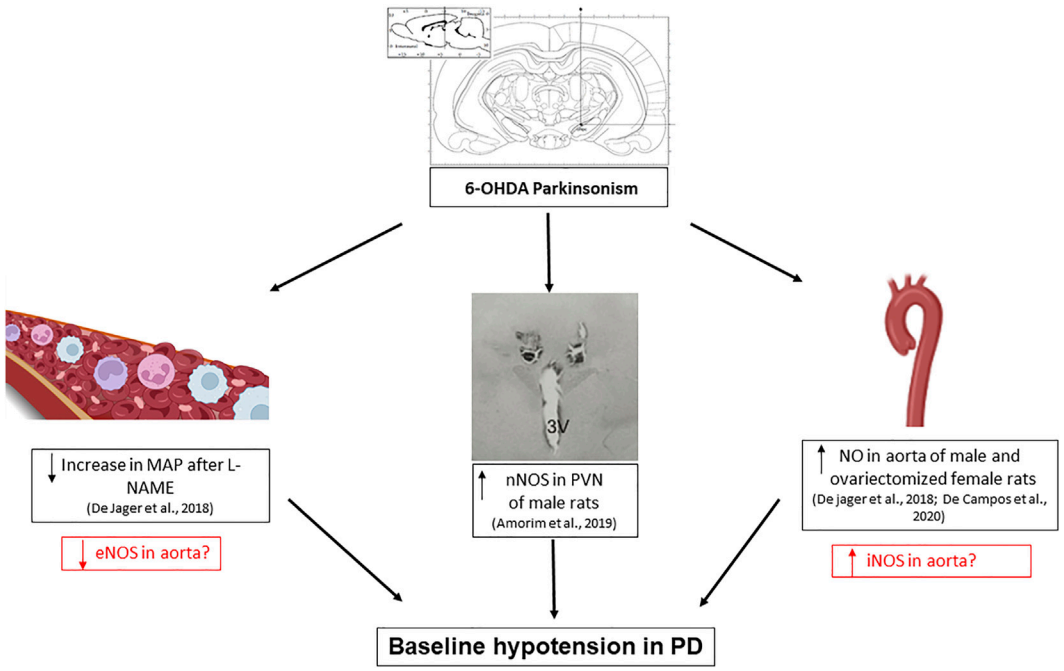

FIGURE 1 | Scheme of changes involving nitric oxide alterations found in the cardiovascular system of rats induced to Parkinsonism using the bilateral model of substantia nigra pars compacta lesion with 6-hydroxydopamine (6-OHDA). The increased production of nitrite in the aorta of male and ovariectomized female rats, associated with an increase in nNOS activity in the region of the paraventricular nucleus of the hypothalamus (PVN), and a smaller increase in mean arterial pressure (MAP) after intravenous administration of L-NAME, suggests the involvement of the 3 isoforms of NO-synthase (NOS) in blood pressure dysfunction in PD. The boxes in red are questions and possible hypotheses. The central illustrations were taken from the cited articles by Ariza et al., 2015b and Turossi Amorim et al., 2019. The lateral illustrations were taken from BioRender.

the brain, which leads to damage to the neurons of the substantia nigra (Dias et al., 2013). Studies suggest that the combination of NO with superoxides formed through the process of oxidative stress results in the formation of peroxynitrites (ONOO-), a molecule that is highly harmful to nervous tissue. In addition, NO has a high affinity for the heme group present in oxygen-carrying proteins, causing a delay in the functioning of the mitochondrial respiratory chain and consequently neuronal death (McDonald and Murad, 1996; Przedborski et al., 1996). Oxidative stress, in turn, decreases the availability of NO in endothelial cells and the central nervous system (Tieu et al., 2003). NO appears to be also involved in the dopamine metabolism by a common toxic pathway that involves mitochondrial compromise, nitroxidative stress and GSH depletion and that may be operating and contributing to the neurodegeneration observed in this disease (Nunes and Laranjinha, 2021).

NITRIC OXIDE IN CARDIOVASCULAR DYSFUNCTION IN PARKINSON'S DISEASE

Peripherally, NO acts as a potent vasodilator to increase blood flow, and it synthesis and bioavailability by the vascular endothelium contributes to greater vasodilation for adaptation in different conditions by the cardiovascular system (Green et al., 2004; McAllister and Laughlin, 2006; Di Francescomarino et al., 2009). Changes in its production can hamper hemodynamic responses and compromise cardiovascular health.

To date, few studies have evaluated NO in the cardiovascular system of animals with parkinsonism de Jager et al. (2018) observed differences in tissue concentrations of nitrite in sedentary animals or animals submitted to physical training before 6-OHDA injury, with NO being increased in the aorta of 6-OHDA animals compared to their controls. However, inhibition of NOS by L-NAME administration promoted a smaller increase in MAP in 6-OHDA animals, suggesting that eNOS nitrergic tonus is lower in animals injured by 6-OHDA than in Sham animals (de Jager et al., 2018). In this sense, it is possible that different isoforms are participating in these responses. Ongoing studies assess which isoform may be involved in vascular alterations in 6-OHDA animals and may contribute to explain the basal hypotension and sympathetic decrease in male rats.

Data from our group using female rats observed that adult females do not present the cardiovascular dysfunction observed by males, who have hypotension compared to their control group. However, when the females are submitted to ovariectomy they show basal hypotension, and a higher concentration of nitrite in the

aorta, suggesting a role for NO associated with ovarian hormones at the vascular level (de Campos et al., 2020). Our group has studied the possible mechanisms of gender involvement in the cardiovascular dysfunctions of PD, including redox balance.

Regarding the central control of the cardiovascular system, it was observed that nNOS is increased in the paraventricular nucleus of the hypothalamus, an area of cardiovascular control, leading to an increase in GABAergic tone on cardiovascular function and contributing to the lower basal BP values in male 6-OHDA injured rats (Turossi Amorim et al., 2019). By this way, the decreased baseline blood pressure in animals with Parkinsonism by 6-OHDA may be due to a central effect mediated by the NO in the PVN. However, we do not rule out the hypothesis of peripheral mechanisms participating in these cardiovascular dysfunctions (**Figure 1**). The study of these mechanisms is important to focus on future therapeutic targets for patients with PD.

CONCLUSION

The findings so far regarding the participation of NO in the cardiovascular dysfunctions in PD show that hypothalamic nuclei that participate in tonic autonomic and cardiovascular control seem to be a target for NO alterations. In addition, still initial data have suggested the participation of NO peripherally (blood vessels), which brings us perspectives about possible new treatments for the cardiovascular dysfunctions in PD, especially related to hypotension.

AUTHOR CONTRIBUTIONS

Conception and design: MM-P. Drafting of the manuscript: MM-P, LJ, BC, LB, PT, and PP-F. Final revision: MM-P, LJ, BC, LB, PT, and PP-F. All authors read and approved the final version of the manuscript.

ACKNOWLEDGMENTS

We thank Superintendência de Ciência, Tecnologia e Ensino Superior (SETI), Fundação Araucária (FA), Universidade Estadual de Londrina (PROPPG), and Programa de Pós-graduação em Patologia Experimental, for assistance in paying the publication fee for the journal.

REFERENCES

Aras, S., Tanriover, G., Aslan, M., Yargicoglu, P., and Agar, A. (2014). The Role of Nitric Oxide on Visual-Evoked Potentials in MPTP-Induced Parkinsonism in Mice. *Neurochem. Int.* 72 (1), 48–57. doi:10.1016/j.neuint.2014.04.014

Ariza, D., Lopes, F. N. C., Crestani, C. C., and Martins-Pinge, M. C. (2015a). Chemoreflex and Baroreflex Alterations in Parkinsonism Induced by 6-OHDA in Unanesthetized Rats. *Neurosci. Lett.* 607, 77–82. doi:10.1016/j.neulet.2015.09.024

Ariza, D., Sisdeli, L., Crestani, C. C., Fazan, R., and Martins-Pinge, M. C. (2015b). Dysautonomias in Parkinson's Disease: Cardiovascular Changes and Autonomic Modulation in Conscious Rats after Infusion of Bilateral 6-OHDA in Substantia Nigra. *Am. J. Physiol. Heart Circ. Physiol.* 308 (3), H250–H257. doi:10.1152/ajpheart.00406.2014

Azevedo, L. L. D., and Cardoso, F. (2009). Ação da levodopa e sua influência na voz e na fala de indivíduos com doença de Parkinson The action of levodopa and its influence on voice and speech of patients. *Rev. Soc. Bras. Fonoaudiol.* 14 (8), 136–141. doi:10.1590/s1516-80342009000100021

Balestrino, R., and Schapira, A. H. V. (2020). Parkinson Disease. *Eur. J. Neurol.* 27 (1), 27–42. doi:10.1111/ene.14108

Barthwal, M. K., Srivastava, N., and Dikshit, M. (2001). Role of Nitric Oxide in a Progressive Neurodegeneration Model of Parkinson's Disease in the Rat. *Redox Rep.* 6 (5), 297–302. doi:10.1179/135100001101536436

Blandini, F., Armentero, M. T., and Martignoni, E. (2008). The 6-hydroxydopamine Model: News from the Past. *Park. Relat. Disord.* 14 (Suppl. 2), S124–S129. doi:10.1016/j.parkreldis.2008.04.015

Blum, D., Torch, S., Lambeng, N., Nissou, M., Benabid, A. L., Sadoul, R., et al. (2001). Molecular Pathways Involved in the Neurotoxicity of 6-OHDA, Dopamine and MPTP: Contribution to the Apoptotic Theory in Parkinson's Disease. *Prog. Neurobiol.* 65 (2), 135–172. doi:10.1016/S0301-0082(01)00003-X

Broom, L., Marinova-Mutafchieva, L., Sadeghian, M., Davis, J. B., Medhurst, A. D., and Dexter, D. T. (2011). Neuroprotection by the Selective iNOS Inhibitor GW274150 in a Model of Parkinson Disease. *Free Radic. Biol. Med.* 50 (5), 633–640. doi:10.1016/j.freeradbiomed.2010.12.026

Çubukçu, H. C., Yurtdaş, M., Durak, Z. E., Aytaç, B., Güneş, H. N., Çokal, B. G., et al. (2016). Oxidative and Nitrosative Stress in Serum of Patients with Parkinson's Disease. *Neurol. Sci.* 37 (11), 1793–1798. doi:10.1007/s10072-016-2663-1

Cuenca-Bermejo, L., Almela, P., Navarro-Zaragoza, J., Fernández Villalba, E., González-Cuello, A. M., Laorden, M. L., et al. (2021). Cardiac Changes in Parkinson's Disease: Lessons from Clinical and Experimental Evidence. *Int. J. Mol. Sci.* 22 (24), 13488. doi:10.3390/ijms222413488

Czarnecka, A., Lenda, T., Domin, H., Konieczny, J., Smiałowska, M., and Lorenc-Koci, E. (2013). Alterations in the Expression of nNOS in the Substantia Nigra and Subthalamic Nucleus of 6-OHDA-Lesioned Rats: The Effects of Chronic Treatment with L-DOPA and the Nitric Oxide Donor, Molsidomine. *Brain Res.* 1541, 92–105. doi:10.1016/j.brainres.2013.10.011

Dauer, W., and Przedborski, S. (2003). Parkinson's Disease: Mechanisms and Models. *Neuron* 39 (6), 889–909. doi:10.1016/S0896-6273(03)00568-3

de Campos, B. H., de Jager, L., Reginato, G. S., Pereira, R. S., Crestani, C. C., Pinge-Filho, P., et al. (2020). Cardiovascular Evaluation of Female Rats with 6-OHDA-Induced Parkinsonism: Possible Protection by Ovarian Hormones and Participation of Nitric Oxide. *Life Sci.* 259, 118259. doi:10.1016/j.lfs.2020.118259

de Jager, L., Amorim, E. D. T., Lucchetti, B. F. C., Lopes, F. N. C., Crestani, C. C., Pinge-Filho, P., et al. (2018). Nitric Oxide Alterations in Cardiovascular System of Rats with Parkinsonism Induced by 6-OHDA and Submitted to Previous Exercise. *Life Sci.* 204, 78–86. doi:10.1016/j.lfs.2018.05.017‘

de Lau, L. M., and Breteler, M. M. (2006). Epidemiology of Parkinson's Disease. *Lancet Neurology* 5, 525–535. doi:10.1016/S1474-4422(06)70471-9

Di Francescomarino, S., Sciartilli, A., Di Valerio, V., Di Baldassarre, A., and Gallina, S. (2009). The Effect of Physical Exercise on Endothelial Function. *Sports Med.* 39 (10), 797–812. doi:10.2165/11317750-000000000-00000

Di Monte, D. A., Royland, J. E., Jakowec, M. W., and Langston, J. W. (1996). Role of Nitric Oxide in Methamphetamine Neurotoxicity: Protection by 7-nitroindazole, an Inhibitor of Neuronal Nitric Oxide Synthase. *J. Neurochem.* 67 (6), 2443–2450. doi:10.1046/j.1471-4159.1996.67062443.x

Dias, V., Junn, E., and Mouradian, M. M. (2013). The Role of Oxidative Stress in Parkinson's Disease. *J. Park. Dis.* 3 (4), 461–491. doi:10.3233/JPD-130230

Doherty, G. H. (2011). Nitric Oxide in Neurodegeneration: Potential Benefits of Non-steroidal Anti-inflammatories. *Neurosci. Bull.* 27 (6), 366–382. doi:10.1007/s12264-011-1530-6

Duty, S., and Jenner, P. (2011). Animal Models of Parkinson's Disease: a Source of Novel Treatments and Clues to the Cause of the Disease. *Br. J. Pharmacol.* 164 (4), 1357–1391. doi:10.1111/j.1476-5381.2011.01426.x

Falquetto, B., Tuppy, M., Potje, S. R., Moreira, T. S., Antoniali, C., and Takakura, A. C. (2017). Cardiovascular Dysfunction Associated with Neurodegeneration in an Experimental Model of Parkinson's Disease. *Brain Res.* 1657, 156–166. doi:10.1016/j.brainres.2016.12.008

Fazio, P., Svenningsson, P., Cselényi, Z., Halldin, C., Farde, L., and Varrone, A. (2018). Nigrostriatal Dopamine Transporter Availability in Early Parkinson's Disease. *Mov. Disord.* 33 (4), 592–599. doi:10.1002/mds.27316

Forstermann, U., and Sessa, W. C. (2012). Nitric Oxide Synthases: Regulation and Function. *Eur. Heart J.* 33 (7), 829–837. doi:10.1093/eurheartj/ehr304

Gibbons, C. H., Simon, D. K., Huang, M., Tilley, B., Aminoff, M. J., Bainbridge, J. L., et al. (2017). Autonomic and Electrocardiographic Findings in Parkinson's Disease. *Aut. Neurosci.* 205, 93–98. doi:10.1016/j.autneu.2017.04.002. Autonomic

Goldstein, D. S. (2007). Cardiac Denervation in Patients with Parkinson Disease. *Clevel. Clin. J. Med.* 74 (Suppl. 1), S91. doi:10.3949/ccjm.74.Suppl_1.S91

Green, D. J., Maiorana, A., O'Driscoll, G., and Taylor, R. (2004). Effect of Exercise Training on Endothelium-Derived Nitric Oxide Function in Humans. *J. Physiol.* 561 (1), 1–25. doi:10.1113/jphysiol.2004.068197

Jackson-Lewis, V., Blesa, J., and Przedborski, S. (2012). Animal Models of Parkinson's Disease. *Park. Relat. Disord.* 18 (Suppl. 1), S183–S185. doi:10.1016/S1353-8020(11)70057-8

Jain, S., and Goldstein, D. S. (2012). Cardiovascular Dysautonomia in Parkinson Disease: From Pathophysiology to Pathogenesis. *Neurobiol. Dis.* 46, 572–580. doi:10.1016/j.nbd.2011.10.025

Joniec, I., Ciesielska, A., Kurkowska-Jastrzebska, I., Przybylkowski, A., Czlonkowska, A., and Czlonkowski, A. (2009). Age- and Sex-Differences in the Nitric Oxide Synthase Expression and Dopamine Concentration in the Murine Model of Parkinson's Disease Induced by 1-Methyl-4-Phenyl-1,2,3,6-Tetrahydropyridine. *Brain Res.* 1261, 7–19. doi:10.1016/j.brainres.2008.12.081

Levecque, C., Elbaz, A., Clavel, J., Richard, F., Vidal, J. S., Amouyel, P., et al. (2003). Association between Parkinson's Disease and Polymorphisms in the nNOS and iNOS Genes in a Community-Based Case-Control Study. *Hum. Mol. Genet.* 12 (1), 79–86. doi:10.1093/hmg/ddg009

Liberatore, G. T., Jackson-Lewis, V., Vukosavic, S., Mandir, A. S., Vila, M., McAuliffe, W. G., et al. (1999). Inducible Nitric Oxide Synthase Stimulates Dopaminergic Neurodegeneration in the MPTP Model of Parkinson Disease. *Nat. Med.* 5 (12), 1403–1409. doi:10.1038/70978

Liu, X., Wei, B., Bi, Q., Sun, Q., Li, L., He, J., et al. (2020). MPTP-induced Impairment of Cardiovascular Function. *Neurotox. Res.* 38 (1), 27–37. doi:10.1007/s12640-020-00182-4

McAllister, R. M., and Laughlin, M. H. (2006). Vascular Nitric Oxide: Effects of Physical Activity, Importance for Health. *Essays Biochem.* 42, 119–131. doi:10.1042/bse0420119

McDonald, L. J., and Murad, F. (1996). Nitric Oxide and Cyclic GMP Signaling. *Proc. Soc. Exp. Biol. Med.* 211 (1), 1–6. doi:10.1177/153537020623100901103181/00379727-211-43950a

Metzger, J. M., and Emborg, M. E. (2019). Autonomic Dysfunction in Parkinson Disease and Animal Models. *Clin. Auton. Res.* 29 (4), 397–414. doi:10.1007/s10286-018-00584-7

Nicaretta, D. H., Rosso, A. L., and Mattos, J. P. D. (2011). Disautonomia na Doença de Parkinson, Revisão da literatura. *Rev. Bras. Neurol.* 47 (4), 25–29.

Nunes, C., and Laranjinha, J. (2021). Nitric Oxide and Dopamine Metabolism Converge via Mitochondrial Dysfunction in the Mechanisms of Neurodegeneration in Parkinson's Disease. *Arch. Biochem. Biophys.* 704, 108877. doi:10.1016/j.abb.2021.108877

Paredes-Rodriguez, E., Vegas-Suarez, S., Morera-Herreras, T., De Deurwaerdere, P., and Miguelez, C. (2020). The Noradrenergic System in Parkinson's Disease. *Front. Pharmacol.* 11, 435. doi:10.3389/fphar.2020.00435

Pereira, D., and Garrett, C. (2010). Fatores de risco na doença de Parkinson. *Acta Med. Port.* 23 (1), 15–24.

Peterson, D. S., and Horak, F. B. (2016). Neural Control of Walking in People with Parkinsonism. *Physiol. (Bethesda)* 31 (2), 95–107. doi:10.1152/physiol.00034.2015

Pringsheim, T., Jette, N., Frolkis, A., and Steeves, T. D. (2014). The Prevalence of Parkinson's Disease: a Systematic Review and Meta-Analysis. *Mov. Disord.* 29 (13), 1583–1590. doi:10.1002/mds.25945

Przedborski, S., Jackson-Lewis, V., Yokoyama, R., Shibata, T., Dawson, V. L., and Dawson, T. M. (1996). Role of Neuronal Nitric Oxide in 1-Methyl-4-Phenyl-1,2,3,6-Tetrahydropyridine (MPTP)-induced Dopaminergic Neurotoxicity. *Proc. Natl. Acad. Sci. U. S. A.* 93 (10), 4565–4571. doi:10.1073/pnas.93.10.4565

Ragonese, P., D'Amelio, M., Callari, G., Salemi, G., Morgante, L., and Savettieri, G. (2006). Age at Menopause Predicts Age at Onset of Parkinson's Disease. *Mov. Disord.* 21 (12), 2211–2214. doi:10.1002/mds.21127

Rochette, L., Lorin, J., Zeller, M., Guilland, J. C., Lorgis, L., Cottin, Y., et al. (2013). Nitric Oxide Synthase Inhibition and Oxidative Stress in Cardiovascular Diseases: Possible Therapeutic Targets? *Pharmacol. Ther.* 140 (3), 239–257. doi:10.1016/j.pharmthera.2013.07.004

Rodriguez-Oroz, M. C., Jahanshahi, M., Krack, P., Litvan, I., Macias, R., Bezard, E., et al. (2009). Initial Clinical Manifestations of Parkinson's Disease: Features and Pathophysiological Mechanisms. *Lancet Neurol.* 8 (12), 1128–1139. doi:10.1016/S1474-4422(09)70293-5

Sabino-Carvalho, J. L., Falquetto, B., Takakura, A. C., and Vianna, L. C. (2021). Baroreflex Dysfunction in Parkinson's Disease: Integration of Central and Peripheral Mechanisms. *J. Neurophysiol.* 125 (4), 1425–1439. doi:10.1152/jn.00548.2020

Salsone, M., Nistico', R., Vescio, B., Novellino, F., Morelli, M., Lupo, A., et al. (2016). Heart Rate Variability in Patients with Essential Tremor: A Cross Sectional Study. *Park. Relat. Disord.* 33, 134–137. doi:10.1016/j.parkreldis.2016.09.027

Schapira, A. H., and Tolosa, E. (2010). Molecular and Clinical Prodrome of Parkinson Disease: Implications for Treatment. *Nat. Rev. Neurol.* 6 (6), 309–317. doi:10.1038/nrneurol.2010.52

Schapira, A. H. V., Chaudhuri, K. R., and Jenner, P. (2017). Non-motor Features of Parkinson Disease. *Nat. Rev. Neurosci.* 18 (7), 435–450. doi:10.1038/nrn.2017.62

Schulz, J. B., Matthews, R. T., Muqit, M. M., Browne, S. E., and Beal, M. F. (1995). Inhibition of Neuronal Nitric Oxide Synthase by 7-Nitroindazole Protects against MPTP-Induced Neurotoxicity in Mice. *J. Neurochem.* 64 (2), 936–939. doi:10.1046/j.1471-4159.1995.64020936.x

Scorza, F. A., Henriques, L. D., and Albuquerque, M. (2001). Doença de Parkinson: tratamento medicamentoso e seu impacto na reabilitação de seus portadores. *Mundo Saúde* 25 (4), 365–370.

Sharabi, Y., Vatine, G. D., and Ashkenazi, A. (2021). Parkinson's Disease outside the Brain: Targeting the Autonomic Nervous System. *Lancet Neurol.* 20 (10), 868–876. doi:10.1016/S1474-4422(21)00219-2

Sian, J., Gerlach, M., Youdim, M. B., and Riederer, P. (1999). Parkinson's Disease: a Major Hypokinetic Basal Ganglia Disorder. *J. Neural Transm. (Vienna)* 106 (5–6), 443–476. doi:10.1007/s007020050171

Silva, A. S., Ariza, D., Dias, D. P., Crestani, C. C., and Martins-Pinge, M. C. (2015). Cardiovascular and Autonomic Alterations in Rats with Parkinsonism Induced by 6-OHDA and Treated with L-DOPA. *Life Sci.* 127, 82–89. doi:10.1016/j.lfs.2015.01.032

Simon, D. K., Tanner, C. M., and Brundin, P. (2020). Parkinson Disease Epidemiology, Pathology, Genetics, and Pathophysiology. *Clin. Geriatr. Med.* 36 (1), 1–12. doi:10.1016/j.cger.2019.08.002

Solla, P., Cadeddu, C., Cannas, A., Deidda, M., Mura, N., Mercuro, G., et al. (2015). Heart Rate Variability Shows Different Cardiovascular Modulation in Parkinson's Disease Patients with Tremor Dominant Subtype Compared to Those with Akinetic Rigid Dominant Subtype. *J. Neural Transm. (Vienna)* 122 (10), 1441–1446. doi:10.1007/s00702-015-1393-5

Sorensen, G. L., Mehlsen, J., and Jennum, P. (2013). Reduced Sympathetic Activity in Idiopathic Rapid-Eye-Movement Sleep Behavior Disorder and Parkinson's Disease. *Auton. Neurosci.* 179 (1–2), 138–141. doi:10.1016/j.autneu.2013.08.067

Strano, S., Fanciulli, A., Rizzo, M., Marinelli, P., Palange, P., Tiple, D., et al. (2016). Cardiovascular Dysfunction in Untreated Parkinson's Disease: A Multi-Modality Assessment. *J. Neurol. Sci.* 370, 251–255. doi:10.1016/j.jns.2016.09.036

Sung, V. W., and Nicholas, A. P. (2013). Nonmotor Symptoms in Parkinson's Disease: Expanding the View of Parkinson's Disease beyond a Pure Motor, Pure Dopaminergic problemNeurologic Clinics. *Neurol. Clin.* 31, S1–S16. doi:10.1016/j.ncl.2013.04.013

Teive, H. A. G. (2005). Etiopatogenia da doença de Parkinson. *Rev. Neurocienc.* 13, 201–214.

Teive, H. A. G. (2006). "Neuroproteção: fatos, mitos e quimeras," in *Teive HAG. Doença de Parkinson: estratégias atuais de tratamento*. Editors L. A. F. Andrade, R. E. Barbosa, and F. Cardoso (São Paulo: Segmento Farma), 17–35.

Tieu, K., Ischiropoulos, H., and Przedborski, S. (2003). Nitric Oxide and Reactive Oxygen Species in Parkinson's Disease. *IUBMB Life* 55 (6), 329–335. doi:10.1080/1521654032000114320

Turossi Amorim, E. D., de Jager, L., Martins, A. B., Rodrigues, A. T., Cruz Lucchetti, B. F., Ariza, D., et al. (2019). Glutamate and GABA Neurotransmission Are Increased in Paraventricular Nucleus of Hypothalamus in Rats Induced to 6-OHDA Parkinsonism: Involvement of nNOS. *Acta Physiol. (Oxf)* 226 (3), e13264–16. doi:10.1111/apha.13264

Vanderlei, L. C., Pastre, C. M., Hoshi, R. A., Carvalho, T. D., and Godoy, M. F. (2009). Basic Notions of Heart Rate Variability and its Clinical Applicability. *Rev. Bras. Cir. Cardiovasc* 24 (2), 205–217. doi:10.1590/S0102-76382009000200018

Conflict of Interest: The authors declare that the research was conducted in the absence of any commercial or financial relationships that could be construed as a potential conflict of interest.

Publisher's Note: All claims expressed in this article are solely those of the authors and do not necessarily represent those of their affiliated organizations, or those of the publisher, the editors and the reviewers. Any product that may be evaluated in this article, or claim that may be made by its manufacturer, is not guaranteed or endorsed by the publisher.

frontiers | Frontiers in Pharmacology

ORIGINAL RESEARCH
published: 12 July 2022
doi: 10.3389/fphar.2022.924955

The Antioxidant N-Acetyl-L-Cysteine Restores the Behavioral Deficits in a Neurodevelopmental Model of Schizophrenia Through a Mechanism That Involves Nitric Oxide

*Ana Lopes-Rocha†, Thiago Ohno Bezerra†, Roberta Zanotto, Inda Lages Nascimento, Angela Rodrigues and Cristiane Salum**

Núcleo Interdisciplinar em Neurociência Aplicada, Centro de Matemática, Computação e Cognição, Universidade Federal do ABC, São Bernardo do Campo, Brazil

OPEN ACCESS

Edited by:
Nidhi Agarwal,
Jamia Hamdard University, India

Reviewed by:
José Ronaldo dos Santos,
Federal University of Sergipe, Brazil
Claudia Bregonzio,
CCT CONICET Córdoba, Argentina

***Correspondence:**
Cristiane Salum
cristiane.salum@ufabc.edu.br

†*These authors share first authorship*

Specialty section:
This article was submitted to Neuropharmacology, a section of the journal Frontiers in Pharmacology

Received: *20 April 2022*
Accepted: *25 May 2022*
Published: *12 July 2022*

Citation:
Lopes-Rocha A, Bezerra TO, Zanotto R, Lages Nascimento I, Rodrigues A and Salum C (2022) The Antioxidant N-Acetyl-L-Cysteine Restores the Behavioral Deficits in a Neurodevelopmental Model of Schizophrenia Through a Mechanism That Involves Nitric Oxide. Front. Pharmacol. 13:924955. doi: 10.3389/fphar.2022.924955

The disruption of neurodevelopment is a hypothesis for the emergence of schizophrenia. Some evidence supports the hypothesis that a redox imbalance could account for the developmental impairments associated with schizophrenia. Additionally, there is a deficit in glutathione (GSH), a main antioxidant, in this disorder. The injection of metilazoximetanol acetate (MAM) on the 17th day of gestation in Wistar rats recapitulates the neurodevelopmental and oxidative stress hypothesis of schizophrenia. The offspring of rats exposed to MAM treatment present in early adulthood behavioral and neurochemical deficits consistent with those seen in schizophrenia. The present study investigated if the acute and chronic (250 mg/kg) treatment during adulthood with N-acetyl-L-cysteine (NAC), a GSH precursor, can revert the behavioral deficits [hyperlocomotion, prepulse inhibition (PPI), and social interaction (SI)] in MAM rats and if the NAC-chronic-effects could be canceled by L-arginine (250 mg/kg, i.p, for 5 days), nitric oxide precursor. Analyses of markers involved in the inflammatory response, such as astrocytes (glial fibrillary acid protein, GFAP) and microglia (binding adapter molecule 1, Iba1), and parvalbumin (PV) positive GABAergic, were conducted in the prefrontal cortex [PFC, medial orbital cortex (MO) and prelimbic cortex (PrL)] and dorsal and ventral hippocampus [CA1, CA2, CA3, and dentate gyrus (DG)] in rats under chronic treatment with NAC. MAM rats showed decreased time of SI and increased locomotion, and both acute and chronic NAC treatments were able to recover these behavioral deficits. L-arginine blocked NAC behavioral effects. MAM rats presented increases in GFAP density at PFC and Iba1 at PFC and CA1. NAC increased the density of Iba1 cells at PFC and of PV cells at MO and CA1 of the ventral hippocampus. The results indicate that NAC recovered the behavioral deficits observed in MAM rats through a mechanism involving nitric oxide. Our data suggest an ongoing inflammatory process in MAM rats and support a potential antipsychotic effect of NAC.

Keywords: schizophrenia, N-acetyl-L-cysteine, MAM model, neuroinflammation, oxidative stress, nitric oxide, GFAP, Iba

1 INTRODUCTION

Schizophrenia affects around 0.3% of the world population (Charlson et al., 2018) and is characterized by hallucination, delusion, social anhedonia, and cognitive deficits (Kahn et al., 2015). Some studies point to a developmental origin of schizophrenia, showing that problems during the gestation involving neuroinflammation and oxidative stress can increase the risk of developing this disorder (Stilo and Murray, 2019; Ermakov et al., 2021). Patients with schizophrenia show a reduction in blood and anterior cingulate cortex concentration of glutathione (GSH), one of the main antioxidants of the brain (Tsugawa et al., 2019). Accordingly, treatment with N-acetyl-L-cysteine (NAC), a precursor of GSH, has shown improvement in schizophrenia symptoms (Cho et al., 2019).

The increased oxidative stress and brain inflammatory response can cause functional alteration in brain circuits in schizophrenia (Dwir et al., 2020). The subclass of GABAergic interneurons that express parvalbumin (PV) is altered in schizophrenia, with post-mortem studies showing a reduction in tissue in the prefrontal cortex (PFC) and hippocampus (Beasley and Reynolds, 1997; Zhang and Reynolds, 2002) and hypermethylation of PV promoter gene in the hippocampus (Fachim et al., 2018), when compared to control subjects. The reduction of PV positive interneurons was associated with the increased activity in the ventral hippocampus detected in patients with this disorder (McHugo et al., 2019), possibly leading to the symptoms of schizophrenia (Grace and Gomes, 2019). Some studies with the animal models of schizophrenia showed that the increased oxidative stress could be a causing factor to the reductions in the PV positive interneurons. Indeed, the animal model with knockout for the glutamate–cysteine ligase regulatory subunit gene (GCLM), an enzyme involved in GSH synthesis, showed behavioral impairments and reduction of PV interneurons in the PFC and hippocampus (Kulak et al., 2012; Dwir et al., 2021).

It is important to note that glial cells, such as astrocytes and microglia, can modulate and mediate the oxidative stress and inflammatory responses in the brain (Giovannoni and Quintana, 2020). A study with post-mortem tissue of patients with schizophrenia found an association between increased GFAP (glial fibrillary acidic protein, an astrocyte marker) protein and mRNA with neuroinflammation (Catts et al., 2014). Some animal models of schizophrenia also presented increased GFAP positive astrocytes in the frontal cortex and hippocampus (Kim et al., 2018). Since astrocytes modulate the inflammatory response in the brain (Giovannoni and Quintana, 2020) and the microglia mediates that process, these cells could be involved in the oxidative stress and neuroinflammation in schizophrenia. A study of patients with schizophrenia found an increased density of cells expressing the ionized calcium-binding adapter molecule 1, a microglia marker (Iba1), and positive cells in the post-mortem brain in the frontal, cingulate, and temporal cortex when compared to control subjects (Gober et al., 2022).

The methylazoxymethanol (MAM) model of schizophrenia in rats recapitulates several hallmarks of schizophrenia. Pregnant rats received an injection of MAM at the 17° day of gestation, temporarily interrupting the neurodevelopment of the offspring (Grace and Gomes, 2019). Among the various behavioral deficits observed in rats whose mothers received MAM, hyperlocomotion induced by a psychotomimetic agent, deficits in social interaction (SI) and in prepulse inhibition (PPI) tests are observed in their adult life (Moore et al., 2006; Perez et al., 2019a). Those rats also showed a reduction in the PV positive interneurons density in the ventral hippocampus and PFC (Penschuck et al., 2006; Du and Grace, 2016; Perez et al., 2019b), increased ventral tegmental area activity, oxidative stress, and neuroinflammatory markers (Zhu et al., 2021). Interestingly, the treatment with NAC during the prepubertal stage of development prevented the increased activity of the ventral tegmental area in MAM rats (Zhu et al., 2021).

However, it is not clear if the treatment with NAC during adulthood could also recover the behavioral and cellular alterations detected in the MAM model of schizophrenia. Hence, the objective of the present study was to evaluate the acute and chronic treatments with NAC over the hyperlocomotion, SI, and PPI tests of adult MAM rats. As we found a recovery of the MAM impaired behaviors with NAC treatments, we then investigated if the NAC mechanism of action involved nitric oxide. Additionally, we evaluated the effects of MAM and/or NAC chronic treatment on the density of PV positive interneurons, GFAP positive astrocytes, and Iba1 positive microglia in the hippocampus and PFC after chronic NAC treatment.

2 MATERIALS AND METHODS

2.1 Animals

Wistar rats (University of São Paulo, Institute of Biomedical Science, Brazil), with approximately 85 days and weighing about 300 g, were subjected to the mating procedure: female (N = 16) rats in the proestrus or estrus phase were maintained with one sexually experienced male (N = 8). Pregnancy was verified by vaginal smear and sperm detection. These females were housed in at most two per cage. All the rats were housed in cages of polypropylene walls (40.0 cm × 33.0 cm × 18.0 cm), with 3.0 cm of sawdust and controlled condition of temperature (23.0 ± 1.0°C) and light (12/12 h light/dark cycle, beginning at 7 a.m.). The rats had food and water ad libitum. All the experiments were performed in the laboratories of the Interdisciplinary Nucleus of Applied Neuroscience at the Federal University of ABC (UFABC), São Bernardo do Campo, Brazil and the procedures had the ethical approval of the Ethics Committee of UFABC (CEUA/UFABC, protocol 007/2014 and 8946130619/2019). All behavioral tests were conducted in rats at postnatal days (PN) 90 or 91. After completion of behavioral experiments, each rat was euthanized with an injection of urethane (Sigma, 3 mg/kg, i.p.).

2.2 Drugs

Antimitotic acetate of metilazoximetanol (MAM, Midwest Research Institute, Kansas City, United States) was dissolved in saline (0.9%) and administered i.p. at a dose of 25 mg/kg and 1 ml/kg (Lodge et al., 2009). NAC (Sigma-Aldrich, United States

), an antioxidant precursor of GSH, was dissolved in saline and NaOH was used to set pH at 6.0 (Fukami et al., 2004; Khan et al., 2004). NAC was administered i.p. at the doses of 150, 250, and 500 mg/kg at the volume of 1 ml/kg (Dean et al., 2011; Möller et al., 2013). L-arginine (Sigma-Aldrich, United States), a nitric oxide precursor, was dissolved in saline and administered i.p. at a dose of 250 mg/kg at 1 ml/kg (Johansson et al., 1997).

2.3 Experimental Design

2.3.1 MAM Treatment

At the 17° gestational day (GD17), pregnant rats received either an injection of MAM (25 mg/kg, i.p) or saline above the midline, to avoid reaching gestational sacs, and they were placed individually in separate cages. After birth (between GD21 to GD23) and weaning period (PN21), male offsprings were separated from their mothers and housed, with four rats per cage. In experiment 1, male offsprings received one single injection of either NAC or saline at PN90, and in experiment 2, male offsprings received 15 days of treatment with NAC or saline, starting at PN75. In experiment 2, male offsprings also received a sub-chronic treatment of L-arginine or saline for 5 days, starting at PN85.

2.3.2 Experiment 1—Acute Effect of NAC in Male Rats of the MAM Model

At PN90, adult MAM and saline rats (N = 36) were subdivided into four subgroups each, which then received either an injection of saline or NAC (150, 250, or 500 mg/kg and volume of 1 ml/kg, i.p.), one hour before the PPI test. Following that test, the rats were subjected to SI and then to hyperlocomotion tests.

2.3.3 Experiment 2—Chronic Effect of NAC (250 mg/kg) and/or L-Arginine in the Rats of MAM Model

From PN75 to PN90, adult MAM and saline rats (n = 44) were divided into two subgroups each, which then received a daily injection of NAC (250 mg/kg, at 1 ml/kg, i.p.) or saline for 15 days. From the PN85th day of life, these rats were subdivided again into two groups receiving daily injections of L-arginine (250 mg/kg, at 1 ml/kg, i.p.) or saline for 5 days. One day after the last injection of both treatments (PN91), they were subjected to SI and hyperlocomotion tests.

2.4 Behavioral Tests

2.4.1 Prepulse Inhibition of Startle

The tests were conducted in a sound-attenuating startle box chamber (Insight Equipamentos, Brazil) of plywood (64.0 cm × 60.0 cm × 40.0 cm) ventilated by a fan at the top of the chamber. In the center, there was a wire-mesh stabilimeter cage (16.5 cm × 5.1 cm × 7.6 cm) suspended within a PVC frame (25.0 cm × 9.0 cm × 9.0 cm) and attached to the response platform by four thumbscrews. The floor of the cage consisted of six stainless steel bars with a 3.0 mm diameter spaced 1.5 mm apart. The startle reaction of the rats generated a pressure on the response platform and analog signals were amplified, digitalized, and analyzed by a software of the startle measure system. Two loudspeakers located 10 cm above the floor on each side of the acoustic chamber presented all sound stimuli. Calibration procedures were conducted daily before the experiments to ensure equal sensitivity of the response platform over the test period.

At least 2 days prior to the experiments, all rats were subjected to the PPI test described in the following section for the matching procedure. This process ensures a homogeneous animal distribution by baseline PPI among treatment groups and provides greater data reliability.

Each rat was placed in a startle chamber with background noise of 57 dB. The PPI session began with the presentation of 10 pulses (white noise, 120 dB, 40 ms) to determine the baseline startle and produce startle habituation. In sequence, 72 trials were divided into pseudorandom presentations of eight different types of stimuli: pulse (P), prepulse (PP, 20 ms pure tone at the frequency of 3,000 Hz and intensities of 69, 73, and 81 dB), pulse preceded by prepulse (PP + P, with an interstimulus interval of 100 ms), and no stimuli (background noise, 57 dB). The average intertrial interval was 20 s during the habituation block and 30 s during the rest of the session.

2.4.2 Social Interaction in the Open Field

The open field consisted of a cylindrical arena of transparent acrylic 50.0 cm (height) × 60.0 cm (diameter) with a wooden base (100.0 cm × 80.0 cm) painted in matte black. After the PPI test, each rat was placed in the open field for exploration and habituation for 5 min. Following that, each rat was placed in the open field containing an unfamiliar male rat under the same treatment, for the SI test. The rats were positioned at opposite sides of the open field. All behaviors performed for 10 min were recorded by a camera positioned above the equipment and connected to a computer with an EthoVision System (Noldus, Netherlands). The behaviors analyzed were divided into active interaction (sniffing, following, anal/genital inspection, and mounting) and passive interaction (when the rat was allowed to get closer), and the total time of interaction was evaluated.

2.4.3 Hyperlocomotion Induced by Psychostimulant

After the SI test, each rat received a subcutaneous injection of saline or the NMDA receptor antagonist MK-801 (0.05 mg/kg, Sigma-Aldrich, United States), 40 min before the test. Each rat was placed individually in the open field to explore it for 30 min. During the entire test, a low light was used to illuminate the room. The trial was recorded, and the total distance traveled (cm) was analyzed by EthoVision (Noldus, Netherlands). In experiment 2, all animals received MK-801 injection before hyperlocomotion test.

2.5 Immunohistochemistry

After the behavioral tests, all the rats were euthanized with urethane (1,500 mg/kg, i.p.) and perfused transcardially with saline (200 ml) and paraformaldehyde (200 ml, 4% w/v). The rats were decapitated and their brains were removed, postfixed for 2 h (4% w/v), and cryoprotected in sucrose for 42 h (30% w/v in 0.1 M phosphate buffer). The brain slices of the rats under chronic treatment with NAC were made in a cryostat (Leica, Germany), comprising coronal sections with 40 μm taken from the hippocampus (bregma: −4.56 to −6.12 mm)

and PFC (bregma: 3.72–5.16 mm). The sections were first rinsed (3 × 5 min) in phosphate buffer (PBS) + 0.15% TritonX-100 (pH 7.4, washing buffer) and incubated in sodium citrate buffer (pH 6.0, 1 × 5 min). Next, they were incubated a second time with a sodium citrate buffer at heating temperature (60°C, 1 × 30 min). After that, the slices were pre-incubated with hydrogen peroxide 1% in 0.1 PBS (1 × 30 min) to block endogenous peroxidase. The slices were then rinsed again in the washing buffer (3 × 5 min) and incubated in 2% bovine serum albumin + 5% normal goat serum for GFAP and Iba1 or 5% normal horse serum for PV prepared in the washing buffer (1 × 60 min). The slices were incubated overnight with primary polyclonal antibodies for GFAP (rabbit, 1:1,000, Z0334, Dako, Denmark), PV (mice, 1:1,000, P227, Sigma-RBI, EUA), or Iba1 (rabbit, 1:500, Thermo Fisher Scientific, PA5-27436, United States). Subsequently, the slices were rinsed again in the washing buffer (3 × 5 min) and incubated in goat anti-rabbit (1:400, ThermoFisher Scientific, EUA, for GFAP and IBA1) or horse anti-mouse (1:400, Vector Laboratories, for PV) biotinylated secondary antibodies (1 × 60 min). Once removed, the slices were successively washed with a washing buffer (3 × 5 min) and then with the biotin–avidin-peroxidase complex (1:300, Vectastain ABC Kit, Vector Laboratories, EUA; 1 × 120 min). Immunoreactions were revealed using 3,3'-diaminobenzidine + hydrogen peroxide 0.02% (DAB, Sigma Aldrich, EUA) in saline tris (hydroxymethyl) aminomethane 0.1 M (TBS). All reactions were conducted at 21°C under agitation. The slices were observed under an optical microscope (Leica, D5500M, Germany) with the amplification of 5×. The structures evaluated were: CA1, CA2, CA3, dentate gyrus (DG), and ventral subiculum (Sub) from the dorsal or ventral hippocampus and medial orbital cortex (MO) and prelimbic cortex (PrL) from PFC (Paxinos and Watson, 2006). The total density in each region was calculated by taking the sum of all the positive cells in each region divided by the entire area. The density of all positive immunoreactive cells for PV, GFAP, and Iba1 in each area was obtained using ImageJ.

2.6 Statistical Analysis

In experiment 1, statistical analysis was developed with factors: treatment 1: MAM × saline, treatment 2: NAC1 (150 mg/kg), NAC2 (250 mg/kg), and NAC3 (500 mg/kg) × saline, and treatment 3: MK-801 × saline. In experiment 2, factors are: treatment 1: MAM × saline, treatment 2: NAC × saline, and treatment 3: L-arginine × saline.

The total distance traveled (cm) for each rat in the hyperlocomotion test was analyzed for both experiments by a three-way ANOVA considering treatment 1, treatment 2, and treatment 3 as between subjects' factors. In the SI test, total (active plus passive) interaction time was analyzed by a two-way ANOVA in experiment 1, with treatment 1 and treatment 2 as between subjects' factors, and three-way ANOVA in experiment 2, with treatment 1, treatment 2, and treatment 3 as between subjects' factors.

On the PPI test, mean ASR to pulse-alone (P) and prepulse-pulse (PP + P) trials were calculated for each subject. The %PPI (percentage of ASR to PP + P related to P) was calculated by.

$$\%PPI = 100 - \left[100 \times \left(\frac{PP + P}{P}\right)\right].$$

The %PPI was analyzed by a repeated measure ANOVA with stimulus intensity (69, 73, and 81 dB) as within subjects' factor, and treatment 1 and treatment 2 as between subjects' factors. Similarly, an analysis was made of the ASR with the stimulus as a within subjects' factor (P, PP69 + P, PP73 + P, and PP81 + P).

For immunohistochemistry results, the statistical analysis was carried out with a two-way ANOVA and treatment 1 and treatment 2 as between subjects' factors.

Statistical analyses were performed using the statistical package SPSS (version 20, IBM), and considered statistically significant differences at $p < 0.05$. When necessary, there was *post hoc* analysis with multiple comparisons using the Duncan test to explore interactions that might reveal significant differences between specific groups.

3 RESULTS

3.1 Experiment 1—NAC Acute Effect in Male Rats of MAM Model

3.1.1 Hyperlocomotion Induced by the NMDA Antagonist

A three-way ANOVA revealed significant main effects for treatment 1 (MAM or saline) [$F(1, 98) = 22.179$; $p < 0.01$], treatment 2 (150 mg NAC, NAC 250 mg, 500 mg or NAC saline) [$F(3, 98) = 6.934$; $p < 0.01$], and treatment 3 (MK or saline) [$F(1, 98) = 55.415$; $p < 0.01$], and interactions between treatment 1 × treatment 2 [$F(3, 98) = 8.774$; $p < 0.01$] and treatment 1 × treatment 3 [$F(1, 98) = 4.875$; $p < 0.05$]. The *post hoc* Duncan analysis showed that the group treated with MAM/Sal/MK differed significantly from the MAM/Sal/Sal group ($p < 0.05$), while the group Sal/Sal/MK did not differ from the Sal/Sal/Sal group (**Figure 1**). MAM rats presented hyperresponsiveness to the sub-dose of the MK-801, which was significantly reduced by the treatment with NAC at all doses. This was not observed in the saline animals. MAM rats also showed significantly increased locomotion, compared to the control group, and the doses of 250 and 500 mg of NAC were able to reduce this effect ($p < 0.05$). Although MK801 did not cause a significant increase in locomotion of the control group, when it was administered with NAC at the dose of 150 mg, there was an unexpected significant increase in locomotion, compared to control ($p < 0.05$, Duncan).

3.1.2 Social Interaction

The two-way ANOVA for time spent in SI behaviors showed the main effects of treatment 1 (MAM × Sal) [$F(1, 62) = 3.775$; $p = 0.05$] and treatment 2 (NAC × Sal) [$F(4, 62) = 17.362$; $p < 0.01$], and interaction between treatment 1 × treatment 2 [$F(2, 62) = 5.199$, $p < 0.05$] (**Figure 2**). The *post hoc* analysis of Duncan revealed that MAM rats showed significantly reduced social

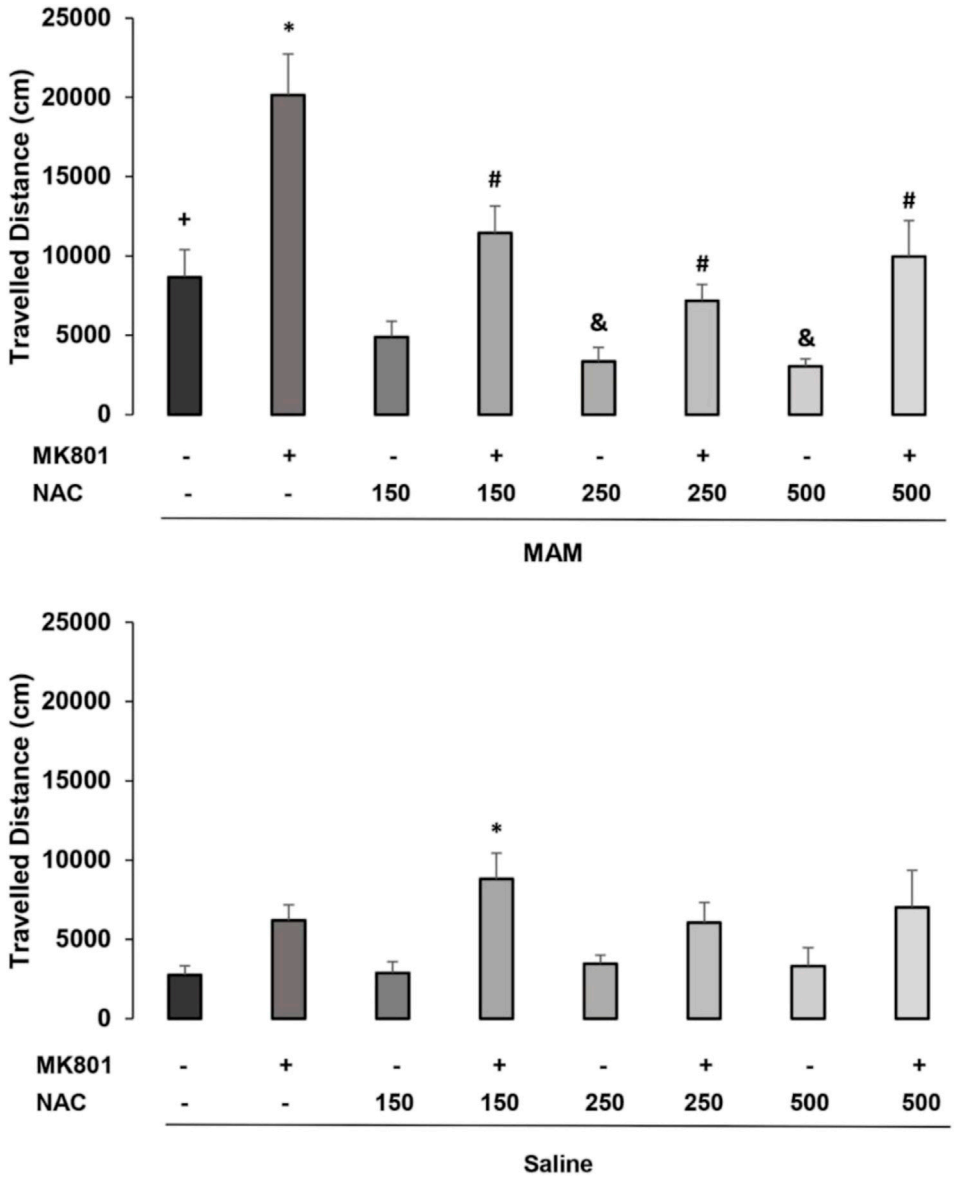

FIGURE 1 | Effect of acute NAC treatment (150 , 250, and 500 mg/kg) in the MAM model on the distance (cm) traveled at the open field (mean ± SE). Adult male offspring of MAM- or saline (Sal)-treated rats received at adulthood a single NAC (or saline) injection (1 h before) and an injection of MK801 (0.05 mg/kg) or saline, 40 min before testing. * indicates significant difference from the Sal/Sal/MK group. # indicates significant difference from group MAM/Sal/MK. + indicates significant difference from the group Sal/Sal/Sal and & indicates significant difference compared to the MAM/Sal/Sal group (Duncan, $p < 0.05$).

interaction time, compared to saline rats, and NAC treatment at the dose of 250 mg/kg was able to raise this behavior in MAM rats ($p < 0.05$). The dose of 150 mg/kg of NAC did not affect the behavior of MAM rats, but decreased the time of SI behavior in saline rats, while the other two doses did not change these behaviors in the control group.

3.1.3 Prepulse Inhibition

A three-way repeated measures ANOVA, with treatment 1 and treatment 2 as between subjects factors and intensity (of prepulse, 69, 73, and 81 dB) as within subjects for %PPI showed the significant main effects of treatment 1 (MAM × Sal) [$F(1,121) = 5.136$; $p < 0.05$] and of intensity [$F(2, 242) = 10.776$; $p < 0.001$]. The Duncan *post hoc* test showed a statistically significant effect of treatment 1 on the intensity of 69 dB ($p < 0.05$) and marginal effects with the intensities of 73 dB ($p = 0.071$) and 81 dB ($p = 0.063$) (**Figure 3**).

3.1.4 Acoustic Startle Response

The three-way repeated measures ANOVA, with treatment 1 and treatment 2 as between subjects factor and intensity (pulse of

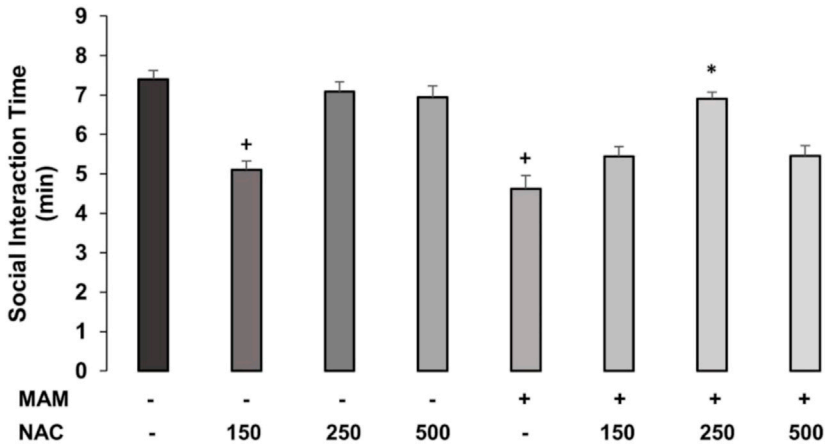

FIGURE 2 | Time (min) spent (mean ± SE) on active and passive social interaction behaviors in MAM rats treated with NAC (150 mg, 250 mg, and 500 mg/kg). Adult male offspring of MAM- or Sal-treated rats received a single NAC (or saline) injection at one of the doses and were placed in the open field with another unfamiliar rat, under the same treatment, for 10 min. + indicates significant difference compared to the Sal/Sal group. * indicates a significant difference related to the MAM-saline group (Duncan, $p < 0.05$).

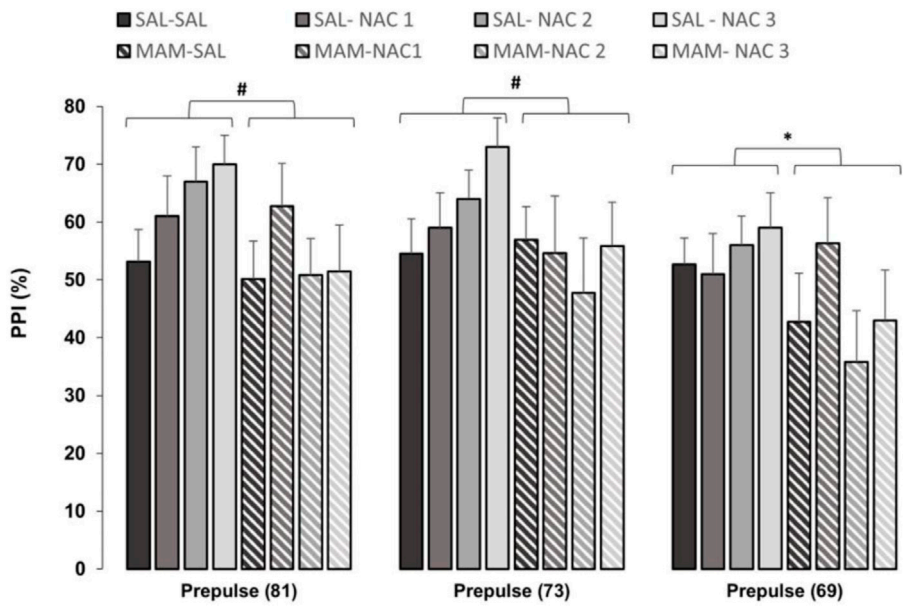

FIGURE 3 | Effect of NAC1, NAC2, or NAC3 (150, 250, and 500 mg/kg, respectively) on the MAM model at %PPI (mean ± SE). Adult male offspring of MAM- or Sal-treated rats received a single injection of NAC1, NAC2, or NAC3 and were placed at the chamber for a PPI session, consisting on presentation of 10 pulses (P, 120 dB), then 72 trials divided into: P, prepulse (PP of 69, 73, and 81 dB), P preceded by PP (interstimulus interval of 100 ms), and no stimuli (background noise, 57 dB). * Indicates significant difference between MAM and Sal groups (Duncan, $p < 0.05$). # Indicates marginal differences between MAM and Sal groups (Duncan, prepulse (81): $p = 0.063$; prepulse (73): $p = 0.071$).

120 dB and prepulses of 69, 73, and 81 dB) as within subjects, for ASR to stimuli revealed the main effects of treatment 1 (MAM × saline) [F (1, 121) = 16.803; $p < 0.001$] and stimulus [F (3, 363) = 129.590; $p < 0.001$]. The Duncan *post hoc* test showed that MAM rats had an ASR significantly higher than that of the saline group to all stimuli intensity ($p < 0.05$), except for PP73 ($p = 0.081$) (**Figure 4**). The NAC (250 mg/kg) reduced the responses to the pulse ($p < 0.05$) in the MAM/NAC2 group compared to the MAM/SAL group. The analysis also revealed that NAC did not cause any significant change in the ASR in saline groups.

3.2 Experiment 2—Effect of Chronic Treatment With NAC (250 mg/kg) and/or L-Arginine in MAM Rats

3.2.1 Social Interaction

The three-way ANOVA for time of SI revealed the main effects of treatment 1 (MAM × Sal) [F (1, 36) = 22.559; $p < 0.01$], treatment 2 (NAC × Sal) [F (1, 36) = 5,271; $p < 0.05$], and treatment 3 (L-arginine × Sal) [F (1, 36) = 20.409; $p < 0.01$]. There were also statistically significant interactions between treatment 1 ×

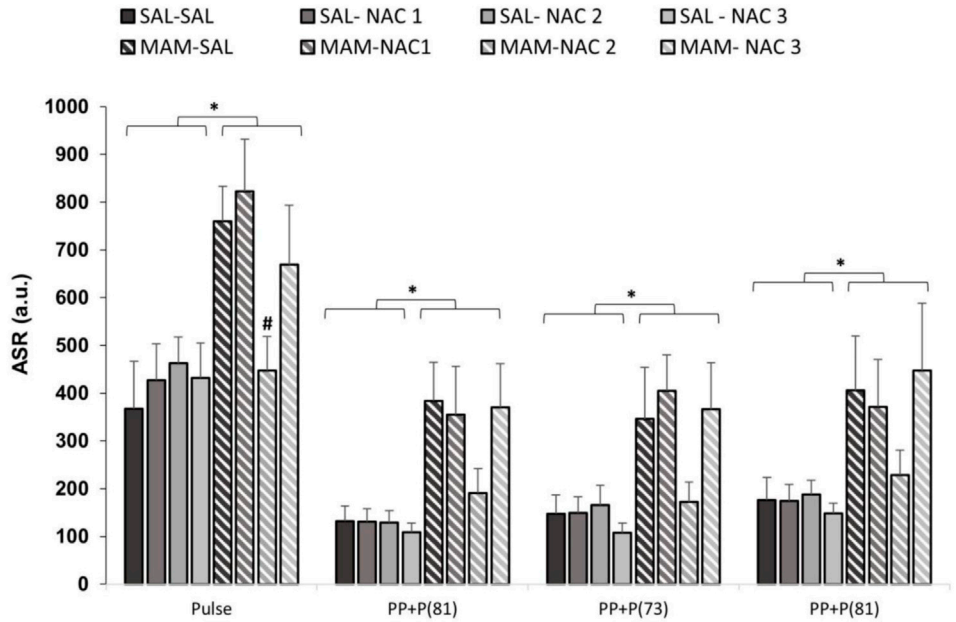

FIGURE 4 | Effect of NAC1, NAC2, or NAC3 (150, 250, and 500 mg/kg, respectively) on the MAM model at the acoustic startle response (ASR) (mean ± SE) to the stimulus. Adult male offspring of MAM- or saline- (Sal) treated rats received a single NAC1, NAC2, or NAC3 injection and were placed at the chamber for a PPI session, consisting on presentation of 10 pulses (P, 120 dB), then 72 trials divided into: P, prepulse (PP of 69, 73 and 81 dB), P preceded by PP (interstimulus interval of 100 ms) and no stimuli (background noise, 57 dB). * indicates significant difference when compared to SAL groups. # indicates significant difference when compared to the MAM/Sal group (Duncan, $p < 0.05$).

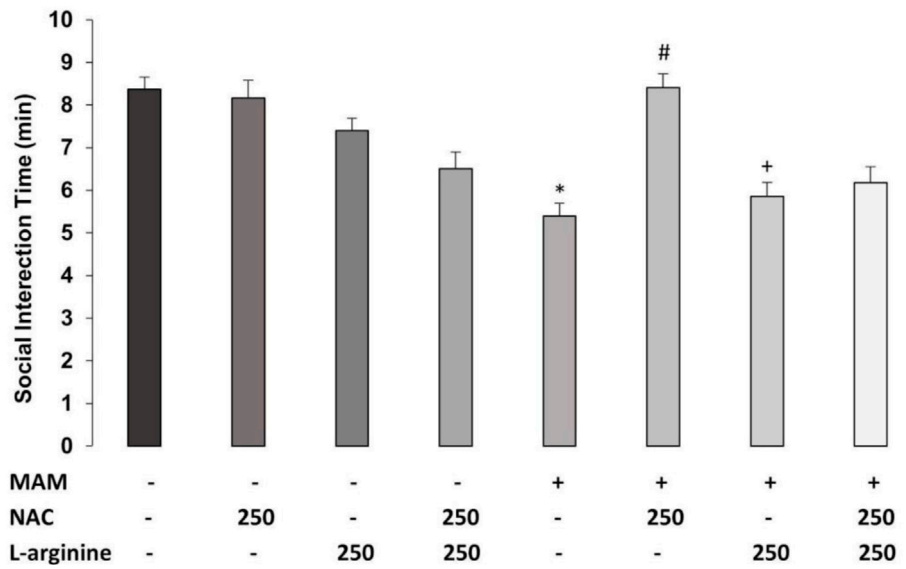

FIGURE 5 | Effect of chronic treatment (15 days) with NAC (250 mg/kg) and/or L-arginine (5 days) (250 mg/kg) on the time (min) of social interaction (SI) behaviors (mean ± SE) on the MAM model. Adult male offspring of MAM- or saline (Sal)-treated rats, chronically treated with NAC or Sal and/or sub-chronically with L-arginine or Sal, were placed in an open field with an unfamiliar male rat under the same treatment, for 10 min * indicates significant difference compared to the Sal/Sal/Sal group. # indicates significant difference from the MAM/Sal/Sal group. + indicates significant difference from MAM/NAC/Sal (Duncan, $p < 0.05$).

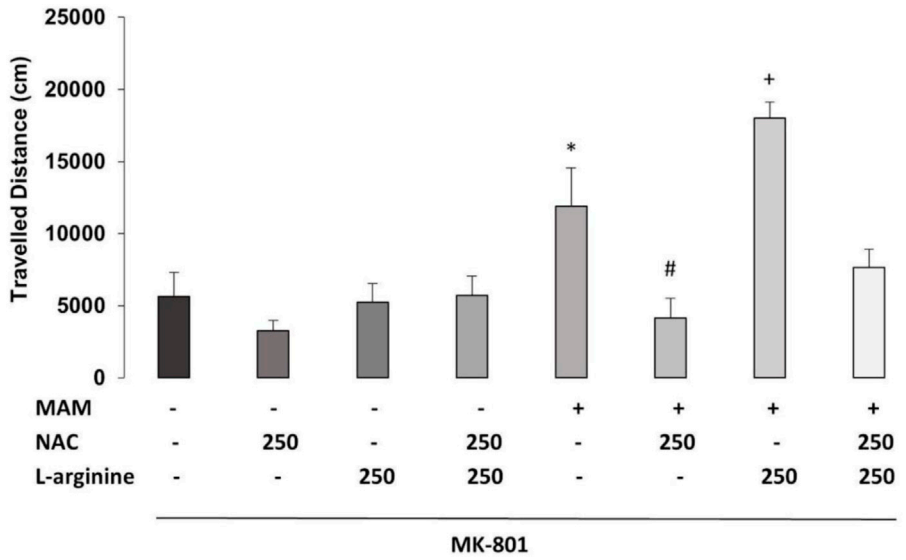

FIGURE 6 | Effect of chronic treatment (15 days) with NAC (250 mg/kg) and/or L-arginine (5 days) (250 mg/kg) on the traveled distance (cm) at the arena (30 min) (mean ± SE) on the MAM model. Adult male offspring of MAM- or saline (Sal)-treated rats, chronically treated with NAC or Sal and/or sub-chronically with L-arginine or Sal, received an MK801 (0.05 mg/kg) injection 40 min before they were placed on the center of an open field, for 30 min exploration. * indicates significant difference compared to the group Sal/Sal/Sal. # indicates significant difference compared to the MAM/Sal/Sal group. + indicates a significant difference compared to all other groups (Duncan, $p < 0.05$).

treatment 2 [F (1, 36) = 20.918; $p < 0.01$] and treatment 2 × treatment 3 [F (1, 36) = 12.241; $p < 0.01$]. The Duncan *post hoc* test revealed that MAM treatment caused a reduction on SI time, compared to Sal rats ($p < 0.05$) (**Figure 5**). Chronic treatment with NAC (250 mg/kg) increased the time of SI in MAM rats ($p < 0.05$). However, the sub-chronic treatment with L-arginine reduced the SI time on MAM rats treated with NAC ($p < 0.05$), showing that the NO precursor was able to block the effect of NAC in MAM rats.

3.2.2 Hyperlocomotion Induced by the NMDA Antagonist

The three-way ANOVA found statistically significant main effects of treatment 1 (MAM × Sal) [F (1, 36) = 26.913; $p < 0.01$], treatment 2 (NAC × Sal) [F (1, 36) = 22.481; $p < 0.01$], and treatment 3 (L-arginine × Sal) [F (1, 36) = 7.682, $p < 0.05$]. There was a statistically significant interaction between treatment 1 × treatment 2 [F (1, 36) = 14.868; $p < 0.01$] (**Figure 6**). Duncan's *post hoc* analysis revealed that MAM rats showed a higher locomotor activity, compared to saline rats, all under the treatment with a sub-dose of MK-801 ($p < 0.05$). This hyperresponse to MK-801 in MAM rats was significantly enhanced by the sub-chronic treatment with L-arginine ($p < 0.05$). The chronic treatment with NAC (250 mg/kg) was able to prevent the increase of locomotor activity caused by MK-801 in MAM rats. However, the NAC effect was partially blocked by L-arginine treatment in MAM rats ($p < 0.05$) (**Figure 6**).

3.2.3 Immunohistochemistry for Detection of PV

The two-way ANOVA test revealed no effect for treatment 1 on the PV positive interneuron density in any subregion of the PFC, dorsal, and ventral hippocampus (**Figures 7**, **8**; **Supplementary Table 1**). However, a main effect for treatment 2 was observed in MO [F (1, 15) = 5.92; $p < 0.05$] and CA1 [F (1, 15) = 7.037; $p < 0.05$] of the ventral hippocampus and a marginally significant difference in the ventral subiculum [F (1, 15) = 4.117, $p = 0.063$], indicating an increase in the PV positive interneuron density in rats treated with NAC compared to controls, but no effect in any subregion of the dorsal hippocampus.

3.2.4 Immunohistochemistry for Detection of GFAP

A two-way ANOVA test showed the main effect for treatment 1 on PrL [F (1, 15) = 7.1; $p < 0.05$], on MO [F (1, 15) = 5.773; $p < 0.05$] and total PFC [F (1, 15) = 10.14; $p < 0.05$], with an increase in the GFAP positive cell density in MAM-treated groups, compared to controls (**Figures 7**, **8**; **Supplementary Table 2**). However, there was no effect of treatment 1 on dorsal CA1 ($p = 0.143$) and CA2 ($p = 0.096$), and ventral hippocampus [CA1 ($p = 0.737$), CA3 ($p = 0.092$), DG ($p = 0.627$), and total ($p = 0.503$)], only marginal effects in dorsal CA3 ($p = 0.073$) and DG ($p = 0.068$). There was no effect of treatment 2 in any subregion of PFC [PrL ($p = 0.549$), MO ($p = 0.838$), and total PFC ($p = 0.726$)], dorsal hippocampus [CA1 ($p = 0.140$), CA2 ($p = 0.244$), CA3 ($p = 0.350$), and DG ($p = 0.154$)], and ventral hippocampus [CA1 ($p = 0.503$), CA3 ($p = 0.535$), DG ($p = 0.323$), and total ($p = 0.746$)].

3.2.5 Immunohistochemistry for Detection of Iba1

A two-way ANOVA test indicated the main effect of treatment 1 on PrL [F (1,15) = 6.814; $p < 0.05$], MO [F (1, 15) = 5.267; $p < 0.05$], total PFC [F (1, 15) = 4.795; $p < 0.05$], on the total dorsal hippocampus [F (1, 15) = 5.036; $p < 0.05$], dorsal CA1 [F (1, 15) =

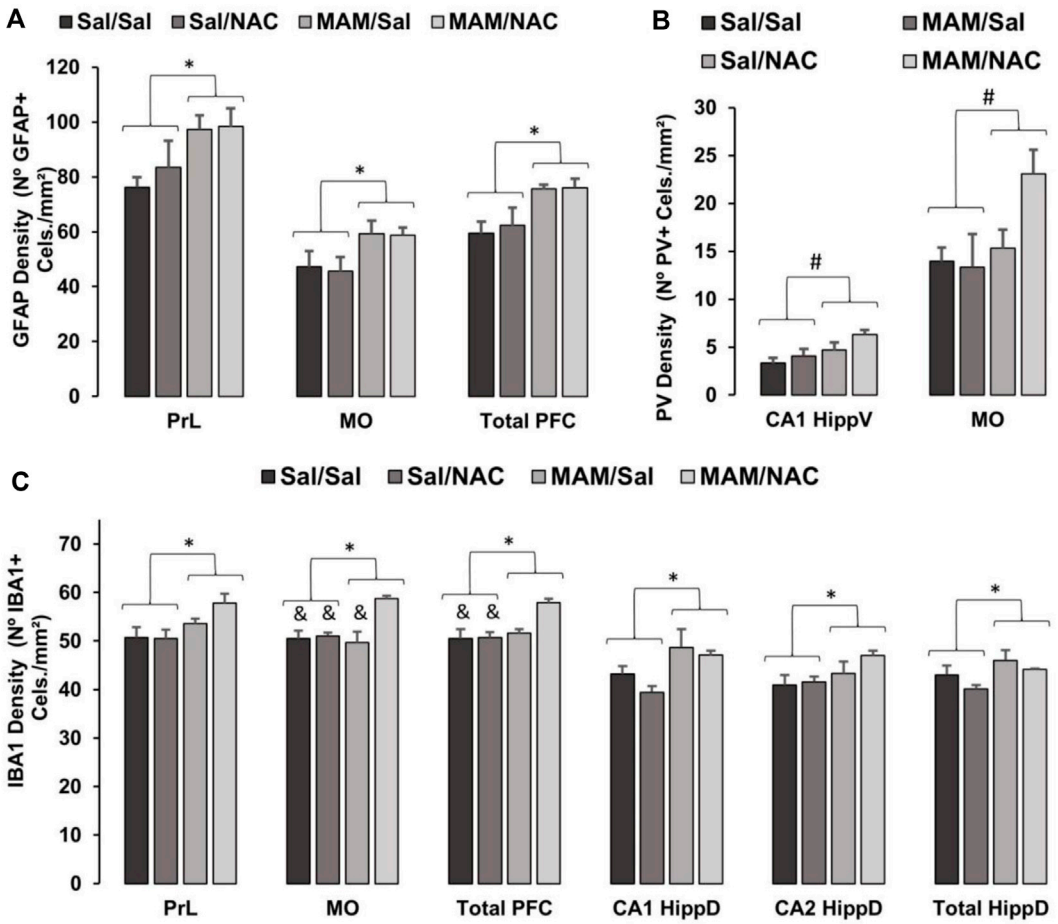

FIGURE 7 | Effect of MAM and chronic treatment (15 days) with NAC (250 mg/kg) in GFAP positive astrocytes, PV positive interneurons and Iba1 positive microglia density (mean ± SE). DAB immunohistochemistry was performed to assess **(A)** GFAP, **(B)** PV, and **(C)** Iba1 in PFC and hippocampus of male offspring of MAM- or saline (SAL)-treated animals, subjected to chronic treatment with NAC or saline (Sal). The cell density was given by the sum of all cells divided by the total area in each region of interest, both data obtained by manual analysis using ImageJ software. **(A)** * indicates a significant difference compared to the SAL group in the prelimbic cortex (PrL), medial orbital cortex (MO), and total prefrontal cortex (PFC). **(B)** # indicates a significant difference for the NAC-treated group in MO and total PFC. **(C)** * indicates a significant difference compared to the SAL group in PrL, MO, total PFC, dorsal hippocampus (HippD), and its subregions CA1 and CA2. & indicates a significant difference compared to the MAM/NAC group (Duncan, $p < 005$).

10.315; $p < 0.05$], and dorsal CA2 [F (1, 15) = 4.523; $p = 0.05$]. In these regions, there was an increase in the density of Iba1 positive cells of MAM rats, compared to control rats (**Figures 7**, **8**; **Supplementary Table 3**). This effect was not observed in dorsal CA3 ($p = 0.585$) or in any subregion of the ventral hippocampus [CA1 ($p = 0.802$), CA3 ($p = 0.941$), DG ($p = 0.488$), and total ($p = 0.384$)].

The analysis also showed the main effect of treatment 2 on MO [F (1, 15) = 10.563; $p < 0.05$] and total PFC [F (1, 15) = 4.795; $p < 0.05$], with an increase in Iba1 positive microglia density in NAC-treated groups (**Figures 7**, **8**; **Supplementary Table 3**). However, no difference was found in the PrL [F (1, 15) = 1.074; $p = 0.317$], in any subregion of the dorsal hippocampus [CA1 ($p = 0.216$), CA2 ($p = 0.260$), CA3 ($p = 0.128$), DG ($p = 0.257$), and total ($p = 0.149$)] or ventral hippocampus [CA1 ($p = 0.139$), CA3 ($p = 0.095$), DG ($p = 0.178$), and total ($p = 0.152$)].

There was also an interaction between treatment 1 × treatment 2 on MO [F (1, 15) = 8, 14; $p < 0.05$]. The Duncan *post hoc* test revealed a higher Iba1 positive cell density in MAM/NAC compared to Sal/Sal in MO ($p < 0.05$) and PFC ($p < 0.05$), compared to Sal/NAC in MO ($p < 0.05$) and PFC ($p < 0.05$) and compared to MAM/Sal in MO ($p < 0.05$).

4 DISCUSSION

To the best of our knowledge, the present study showed for the first time the effectiveness of the treatment with NAC during adulthood in restoring behavioral deficits in MAM rats. Both acute and chronic treatments with NAC were able to restore the deficit in the SI test, reduce both spontaneous and MK-801-induced hyperlocomotion, and reduce the increase in the ASR of most of the stimuli on the PPI test, in male offspring of rats

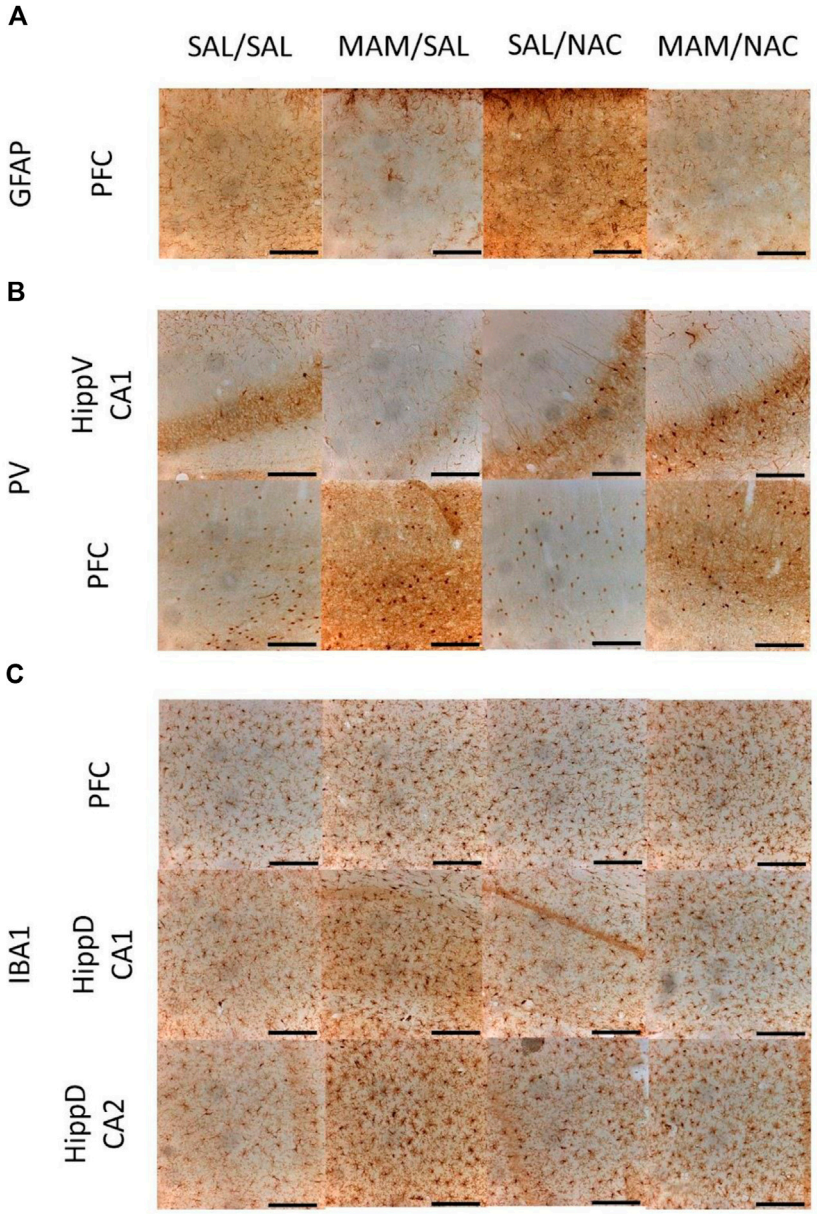

FIGURE 8 | Immunohistochemistry for GFAP positive astrocytes, PV positive interneurons, and Iba1 positive microglia from the male offspring of MAM- or saline (SAL)- treated rats, under chronic treatment (15 days) with NAC (250 mg/kg) or saline (Sal). Representative photos obtained using an optical microscope with the 10× amplification of DAB immunostaining in 40 µm thickness slices show **(A)** increased expression of GFAP in the prefrontal cortex (PFC) of MAM rats, **(B)** increased expression of PV in PFC and CA1 from the ventral hippocampus (HippV) of rats treated with NAC, and **(C)** increased expression of Iba1 in PFC and in CA1 and CA2 of the dorsal hippocampus (HippD) in MAM rats (Duncan, $p < 0.05$). Scale bars represent 200 µm.

treated with MAM. Additionally, sub-chronic treatment with the precursor of NO, L-arginine, prevented the NAC effect in recovering SI behaviors and in reducing the hyperlocomotion in these rats. Moreover, L-arginine potentiated hyperlocomotion caused by MK-801 in MAM rats, suggesting that NO mediates these behavioral changes, and the observed effects of NAC may involve its ability to act as an NO scavenger.

The deficits observed in MAM rats on the SI test are in accordance with previous findings with the MAM model (Flagstad et al., 2004; Le Pen et al., 2006; Hazane et al., 2009) and other animal models, such as the neonatal lesion in the ventral hippocampus (Genis-Mendoza et al., 2014) and the administration of the ammonitic epidermal growth factor (EGF) cytokine (Sotoyama et al., 2021). Our findings support the potential of the MAM animal model in mimicking negative symptoms observed in patients with schizophrenia (Wierońska et al., 2015; Potasiewicz et al., 2020).

The increased spontaneous (Le Pen et al., 2006; Ratajczak et al., 2015) or MK-801-induced hyperlocomotion tests (Le Pen et al., 2006; Pen et al., 2011) in our results also corroborate previous data using the MAM model (Lodge and Grace, 2012), and other animal models of schizophrenia, such as the neonatal lesion of the ventral hippocampus (Genis-Mendoza et al., 2014) and the spontaneously hypertensive rats (Almeida et al., 2014). Given that MK-801 causes the hypoactivation of NMDA receptors preferably in GABAergic interneurons (Thomases et al., 2013), it is conceivable that the spontaneous hyperlocomotion observed in MAM rats is due to both dopaminergic hyperactivity and glutamatergic hyperactivity (Hradetzky et al., 2012; Gomes et al., 2015a).

In contrast to some studies (Le Pen et al., 2006; Moore et al., 2006), we did not detect %PPI deficits in MAM rats. The lack of significant deficits in %PPI in MAM rats is related to a MAM effect of increasing all stimuli's ASR, both to pulse and to prepulse + pulse. It is important to consider differently from these prior studies, which used white noise for the background, pulse, and for the three prepulses (Le Pen et al., 2006), we used pure tone for the prepulse stimuli and a higher prepulse intensity (Ewing and Grace, 2013; Wang et al., 2015). The use of higher intensity of prepulses, such as those used in the present study, did not demonstrate significant deficits in this test, but low intensity prepulses appear to be less discriminated by MAM rats, leading to deficits in PPI, as MAM rats appear to be able to discriminate between different sound intensities but fail to evoke gradual potential in response to different intensities of sound (Ewing and Grace, 2013).

Both acute and chronic treatments with NAC in adult rats were able to reduce hyperlocomotion caused by the NMDA antagonist and the deficit in SI in the MAM model. The treatment with NAC in juvenile animals or during adolescence had already been shown to be effective in other animal models of schizophrenia, such as the neonatal ventral hippocampus lesion (Cabungcal et al., 2014), the acute phencyclidine administration (Baker et al., 2008), knockout mice for GCLM (Otte et al., 2011), and the social isolation rearing model (Möller et al., 2013). Our data show that treatment with NAC in adulthood was also able to significantly improve behavioral deficits.

In the acute experiment, NAC at the dose of 250 mg/kg was able to revert the deficit in SI. For spontaneous locomotion, NAC, at doses of 250 mg/kg and 500 mg/kg, was able to revert the increased locomotor activity in the MAM group, and for hyperlocomotion induced by MK-801, all the three doses of NAC were able to revert the increased locomotion. The dose of 250 mg/kg was the most effective in reducing hyperlocomotion in MAM rats. The lower and higher doses (150 mg/kg and 500 mg/kg, respectively) of NAC were unable to reverse the deficit in SI and to reduce responsiveness to the NMDA antagonist. The lower dose of 150 mg/kg of NAC impaired these behaviors in the control groups. Thus, NAC treatment with the intermediate dose of 250 mg/kg was more effective in reversing deficits in the MAM model than with doses of 150 mg/kg and 500 mg/kg, showing a dose-dependent effect and a trend to an inverted "U" shaped dose-response curve.

The co-treatment with L-arginine (a precursor of NO) prevented the positive effect of NAC on SI and hyperlocomotion, indicating an involvement of the nitrergic system in the NAC mechanism of action. In previous studies, we showed that NAC could abolish the dopamine release and reuptake in the mesencephalic neuron culture induced by NO donors (Salum et al., 2008; Salum et al., 2016). Thus, it is possible that NAC prevents the increased dopaminergic activity in the ventral tegmental area and the dopaminergic induced hyperlocomotion in MAM rats (Hradetzky et al., 2012; Gomes et al., 2015b). Interestingly, the treatment with NG-nitro-L-arginine methyl, a NO synthase inhibitor, also prevented the hyperlocomotion and deficits in PPI caused by phencyclidine administration (Fejgin et al., 2008). Similarly, the treatment with NAC prevented the loss of PV positive interneurons and perineuronal net in the mice with the impaired GSH synthesis model of schizophrenia (Dwir et al., 2021). It is important to note that GSH can reduce the concentration of NO (Berk et al., 2013). We have observed that the acute treatment with the NO synthase inhibitor, L-NOARG, was able to significantly reduce MAM behavior deficits on %PPI and SI (under submission). The present results corroborate our previous data and reinforce that the NAC mechanism of action involves NO.

To further understand the mechanisms behind MAM and NAC treatments, immunohistochemistry was performed to investigate a possible involvement of neuroinflammation and oxidative stress in the MAM rats' deficits. Our immunohistochemistry results for the animals subjected to chronic treatment with NAC, which did not receive L-arginine, showed indications of the ongoing inflammatory process. Those tests showed an increase in the density of GFAP cells in total PFC in MAM-treated groups, but no changes were observed in the dorsal and ventral hippocampus. No significant effects due to NAC were observed in the GFAP expression in any region. Furthermore, the Iba1 positive cell density was increased in all PFC subregions, total dorsal hippocampus, dorsal CA1, and CA2 of MAM rats. Unexpectedly, NAC increased the Iba1 cell density in MO and total PFC, in both SAL and MAM groups, compared to the rats treated with saline, but did not affect either dorsal or ventral hippocampus. The PV interneurons density was higher in MO and in CA1 of the ventral hippocampus of NAC-treated groups, but MAM treatment did not affect the PV expression in any region analyzed.

Dwir et al. (2020) showed that oxidative stress and neuroinflammation are connected by the activity of the redox-sensitive matrix metalloproteinase 9. In that study, they showed that the activity of metalloproteinase 9 enhanced the neuroinflammation in the GCLM knockout mice, connecting oxidative stress with neuroinflammatory processes. In the present study, there was a slight increase in Iba1 cell density of the hippocampus and PFC and in GFAP cell density of PFC from MAM rats. These alterations are indicatives of an ongoing inflammatory process in MAM rats. In the animal model of chronic treatment with MK-801 during 28 days beginning at PN42, an increase in the GFAP expression was observed, a decrease in resting microglia and an increase in activated

microglia in medial PFC was also observed (Gomes et al., 2015b). However, another study with the same animal model showed a decrease in the GFAP marker on the PFC (Rahati et al., 2016). In the neonatal model of polyl:C, an increase in microglial activation was also observed in the PFC, hippocampus, and striatum from adolescence to adulthood (Ribeiro et al., 2013).

The present study did not consider the morphology of astrocytes and microglia, that is, the GFAP and Iba1 positive cells were not separated according to the characteristics of pro-inflammatory or anti-inflammatory processes. Considering that an increase in the expression of those protein markers is associated with both inflammatory responses (Howes and McCutcheon, 2017), it is not possible to determine whether the increases in microglia and astrocyte cell markers are related to pro- or anti-inflammatory mechanisms. Our results suggest that the effect of MAM can lead to a pro-inflammatory activation of microglia and astrocytes. On the other hand, the effect of NAC would lead to an anti-inflammatory activation in microglial cells. Further studies are necessary to uncover that question through the quantification of different inflammatory factors secreted by each cell in both inflammatory states.

The reduction of PV cells has previously been reported in the MAM model, specifically in the medial PFC and ventral subiculum of the hippocampus (Lodge and Grace, 2008) and this has been related to altered PFC and hippocampal during cognitive tasks, such as latent inhibition or PPI. Several studies with the MAM model presented contradictory results. Although some studies showed a decrease in PV expression in PFC (Lodge et al., 2009; Gastambide et al., 2012), in the ventral hippocampus (Lodge et al., 2009; Du and Grace, 2016) and dorsal hippocampus (Penschuck et al., 2006), others reported no changes in PV cells in the PFC (Penschuck et al., 2006) and dorsal hippocampus (Lodge et al., 2009). These different results could be related to the age of the animals when the cells were analyzed, as different results are found according to the age of the animal. In the MAM model, no difference was found in the PV cell density in PFC after 90 days of life (Penschuck et al., 2006), but a reduction was found in the 84 days studies in the medial PFC and ventral subiculum of the hippocampus of MAM-treated rats (Lodge et al., 2009). Although the age appears to be important, the number of cells expressing PV may not be correlated to the level of the PV protein and mRNA, as presented in a recent study where MAM failed to change the number of cells, but decreased levels of the PV protein in adulthood (Maćkowiak et al., 2019). The present samples were collected from animals at 90–91 days of life and did not show reduction in the PV positive cell density in MAM rats.

It is possible that a delayed maturation of the PV positive cells or a reduction in the expression of PV could also alter the function of PFC and hippocampus. Indeed, some studies with the knockdown of PV in rats produced similar behavioral deficits to those observed in the MAM model (Boley et al., 2014; Perez et al., 2019a). Therefore, NAC could also prevent a delayed maturation of perineuronal net and PV positive interneurons. It is interesting to note that the treatment with NAC before weaning was able to revert the increased dopaminergic activity in the ventral tegmental area and recover the loss of PV interneurons and the perineuronal net in the thalamic reticular nucleus in MAM rats (Zhu et al., 2021). Since the oxidative stress prevents the maturations of the perineuronal net and, consequently, the PV cells, NAC could act by preventing and recovering that delayed maturation. In fact, a study using mice with impaired synthesis of GSH revealed the ability of NAC in preventing the delay in the maturation of PV interneurons (Cabungcal et al., 2013). Consistently with this hypothesis, the treatment with NAC increased the density of PV interneuron in both PFC and hippocampus in the present study. Here, NAC was administered in adult rats from 75 to 90 days of life, indicating that NAC could increase PV interneurons even in adulthood.

The lack of effect of NAC treatment for glial cells suggests that its mechanism of action may not occur in the neuroinflammation promoted by MAM, but by reducing the oxidative stress and stimulating the maturations of PV interneurons. We, therefore, hypothesize that, in order to reverse the effects on GFAP and Iba1 cells, NAC treatment should be administered during the juvenile phase of these animals.

5 CONCLUSION

vOur results show that the antioxidant NAC was effective in recovering the behavioral deficits observed in MAM rats. Immunohistochemistry results suggest an ongoing inflammatory process in MAM rats. Additionally, our data give support to a potential antipsychotic effect of the antioxidant NAC. Although recovering the behavioral deficits, there was no effect on the inflammatory markers detected in MAM rats, suggesting that this may only be achieved with an early age antioxidant treatment. The present study corroborates previous findings suggesting that oxidative stress may have an important contribution for the schizophrenia symptomatology and support oxidative stress as a potential target for treatment.

DATA AVAILABILITY STATEMENT

The raw data supporting the conclusion of this article will be made available by the authors, without undue reservation.

ETHICS STATEMENT

The animal study was reviewed and approved by the Ethics Committee of UFABC (CEUA/UFABC, protocol 007/2014 and 8946130619/2019).

AUTHOR CONTRIBUTIONS

We declare the following contribution roles: CS conceived the idea. CS and ILN developed the methodological and analytical strategies. ILN and AR developed the animal experiments and their data analysis. AL-R, TOB, and RZ developed the histochemical experiments and their data analysis. AL-R and

TOB drafted the manuscript. CS reviewed the manuscript. All authors critically reviewed and approved the final manuscript.

FUNDING

CS – received grants from Foundation of Support for Research of the State of São Paulo (FAPESP) #2011/09548-3 and National Council for Scientific and Technological Development (CNPq) #476162/2011-4. AL-R – received a scientific initiation scholarship #2018/22079-1 from Foundation of Support for Research of the State of São Paulo (FAPESP). TOB – received a scientific initiation scholarship #2018/22142-5 from Foundation of Support for Research of the State of São Paulo (FAPESP). ILN – received master scholarship from Federal University of ABC (UFABC).

ACKNOWLEDGMENTS

CS, AL-R and TOB acknowledge Foundation of Support for Research of the State of São Paulo (FAPESP) for the financial support. CS acknowledge National Council for Scientific and Technological Development (CNPq) for the financial support. ILN acknowledge Federal University of ABC (UFABC) for the financial support. All authors acknowledge UFABC for providing laboratories and animal facility to develop this work.

SUPPLEMENTARY MATERIAL

The Supplementary Material for this article can be found online at: https://www.frontiersin.org/articles/10.3389/fphar.2022.924955/full#supplementary-material

REFERENCES

Almeida, V., Peres, F. F., Levin, R., Suiama, M. A., Calzavara, M. B., Zuardi, A. W., et al. (2014). Effects of Cannabinoid and Vanilloid Drugs on Positive and Negative-like Symptoms on an Animal Model of Schizophrenia: the SHR Strain. *Schizophr. Res.* 153 (1-3), 150–159. doi:10.1016/j.schres.2014.01.039

Baker, D. A., Madayag, A., Kristiansen, L. V., Meador-Woodruff, J. H., Haroutunian, V., and Raju, I. (2008). Contribution of Cystine-Glutamate Antiporters to the Psychotomimetic Effects of Phencyclidine. *Neuropsychopharmacology* 33 (7), 1760–1772. doi:10.1038/sj.npp.1301532

Beasley, C. L., and Reynolds, G. P. (1997). Parvalbumin-immunoreactive Neurons Are Reduced in the Prefrontal Cortex of Schizophrenics. *Schizophr. Res.* 24 (3), 349–355. doi:10.1016/S0920-9964(96)00122-3

Berk, M., Malhi, G. S., Gray, L. J., and Dean, O. M. (2013). The Promise of N-Acetylcysteine in Neuropsychiatry. *Trends Pharmacol. Sci.* 34 (3), 167–177. doi:10.1016/j.tips.2013.01.001

Boley, A. M., Perez, S. M., and Lodge, D. J. (2014). A Fundamental Role for Hippocampal Parvalbumin in the Dopamine Hyperfunction Associated with Schizophrenia. *Schizophr. Res.* 157 (1-3), 238–243. doi:10.1016/j.schres.2014.05.005

Cabungcal, J. H., Counotte, D. S., Lewis, E., Tejeda, H. A., Piantadosi, P., Pollock, C., et al. (2014). Juvenile Antioxidant Treatment Prevents Adult Deficits in a Developmental Model of Schizophrenia. *Neuron* 83 (5), 1073–1084. doi:10.1016/j.neuron.2014.07.028

Cabungcal, J. H., Steullet, P., Kraftsik, R., Cuenod, M., and Do, K. Q. (2013). Early-life Insults Impair Parvalbumin Interneurons via Oxidative Stress: Reversal by N-Acetylcysteine. *Biol. Psychiatry* 73 (6), 574–582. doi:10.1016/j.biopsych.2012.09.020

Catts, V. S., Wong, J., Fillman, S. G., Fung, S. J., and Shannon Weickert, C. (2014). Increased Expression of Astrocyte Markers in Schizophrenia: Association with Neuroinflammation. *Aust. N. Z. J. Psychiatry* 48 (8), 722–734. doi:10.1177/0004867414531078

Charlson, F. J., Ferrari, A. J., Santomauro, D. F., Diminic, S., Stockings, E., Scott, J. G., et al. (2018). Global Epidemiology and Burden of Schizophrenia: Findings from the Global Burden of Disease Study 2016. *Schizophr. Bull.* 44 (6), 1195–1203. doi:10.1093/schbul/sby058

Cho, M., Lee, T. Y., Kwak, Y. B., Yoon, Y. B., Kim, M., and Kwon, J. S. (2019). Adjunctive Use of Anti-inflammatory Drugs for Schizophrenia: a Meta-Analytic Investigation of Randomized Controlled Trials. *Aust. N. Z. J. Psychiatry* 53 (8), 742–759. doi:10.1177/0004867419835028

Dean, O., Giorlando, F., and Berk, M. (2011). N-acetylcysteine in Psychiatry: Current Therapeutic Evidence and Potential Mechanisms of Action. *J. Psychiatry Neurosci.* 36 (2), 78–86. doi:10.1503/jpn.100057

Du, Y., and Grace, A. A. (2016). Loss of Parvalbumin in the hippocampus of MAM Schizophrenia Model Rats Is Attenuated by Peripubertal Diazepam. *Int. J. Neuropsychopharmacol.* 19 (11), pyw065. doi:10.1093/ijnp/pyw065

Dwir, D., Cabungcal, J. H., Xin, L., Giangreco, B., Parietti, E., Cleusix, M., et al. (2021). Timely N-Acetyl-Cysteine and Environmental Enrichment Rescue Oxidative Stress-Induced Parvalbumin Interneuron Impairments via MMP9/RAGE Pathway: a Translational Approach for Early Intervention in Psychosis. *Schizophr. Bull.* 47 (6), 1782–1794. doi:10.1093/schbul/sbab066

Dwir, D., Giangreco, B., Xin, L., Tenenbaum, L., Cabungcal, J. H., Steullet, P., et al. (2020). Correction: MMP9/RAGE Pathway Overactivation Mediates Redox Dysregulation and Neuroinflammation, Leading to Inhibitory/excitatory Imbalance: a Reverse Translation Study in Schizophrenia Patients. *Mol. Psychiatry* 25 (11), 3105–2904. doi:10.1038/s41380-020-0716-6

Ermakov, E. A., Dmitrieva, E. M., Parshukova, D. A., Kazantseva, D. V., Vasilieva, A. R., and Smirnova, L. P. (2021). Oxidative Stress-Related Mechanisms in Schizophrenia Pathogenesis and New Treatment Perspectives. *Oxidative Med. Cell. Longev.* 2021, 1–37. doi:10.1155/2021/8881770

Ewing, S. G., and Grace, A. A. (2013). Evidence for Impaired Sound Intensity Processing During Prepulse Inhibition of the Startle Response in a Rodent Developmental Disruption Model of Schizophrenia. *J. Psychiatr. Res.* 47, 1630–1635. doi:10.1016/j.jpsychires.2013.07.012

Fachim, H. A., Srisawat, U., Dalton, C. F., and Reynolds, G. P. (2018). Parvalbumin Promoter Hypermethylation in Postmortem Brain in Schizophrenia. *Epigenomics* 10 (5), 519–524. doi:10.2217/epi-2017-0159

Fejgin, K., Pålsson, E., Wass, C., Svensson, L., and Klamer, D. (2008). Nitric Oxide Signaling in the Medial Prefrontal Cortex Is Involved in the Biochemical and Behavioral Effects of Phencyclidine. *Neuropsychopharmacology* 33 (8), 1874–1883. doi:10.1038/sj.npp.1301587

Flagstad, P., Mørk, A., Glenthøj, B. Y., Van Beek, J., Michael-Titus, A. T., and Didriksen, M. (2004). Disruption of Neurogenesis on Gestational Day 17 in the Rat Causes Behavioral Changes Relevant to Positive and Negative Schizophrenia Symptoms and Alters Amphetamine-Induced Dopamine Release in Nucleus Accumbens. *Neuropsychopharmacology* 29 (11), 2052–2064. doi:10.1038/sj.npp.1300516

Fukami, G., Hashimoto, K., Koike, K., Okamura, N., Shimizu, E., and Iyo, M. (2004). Effect of Antioxidant N-Acetyl-L-Cysteine on Behavioral Changes and Neurotoxicity in Rats after Administration of Methamphetamine. *Brain Res.* 1016 (1), 90–95. doi:10.1016/j.brainres.2004.04.072

Gastambide, F., Cotel, M. C., Gilmour, G., O'neill, M. J., Robbins, T. W., and Tricklebank, M. D. (2012). Selective Remediation of Reversal Learning Deficits in the Neurodevelopmental MAM Model of Schizophrenia by a Novel mGlu5 Positive Allosteric Modulator. *Neuropsychopharmacology* 37 (4), 1057–1066. doi:10.1038/npp.2011.298

Genis-Mendoza, A. D., Beltrán-Villalobos, I., and Nicolini-Sánchez, H. (2014). Behavioral Assessment of the "Schizophrenia-like" Phenotype in an Animal Model of Neonatal Lesion in the Ventral hippocampus (NLVH) of Young and Adult Rats. *Gac. Med. Mex.* 150 (5), 420–431.

Giovannoni, F., and Quintana, F. J. (2020). The Role of Astrocytes in CNS Inflammation. *Trends Immunol.* 41 (9), 805–819. doi:10.1016/j.it.2020.07.007

Gober, R., Ardalan, M., Shiadeh, S. M. J., Duque, L., Garamszegi, S. P., Ascona, M., et al. (2022). Microglia Activation in Postmortem Brains with Schizophrenia

Demonstrates Distinct Morphological Changes between Brain Regions. *Brain Pathol.* 32 (1), e13003. doi:10.1111/bpa.13003

Gomes, F. V., Guimarães, F. S., and Grace, A. A. (2015a). Effects of Pubertal Cannabinoid Administration on Attentional Set-Shifting and Dopaminergic Hyper-Responsivity in a Developmental Disruption Model of Schizophrenia. *Int. J. Neuropsychopharmacol.* 18 (2), pyu018. doi:10.1093/ijnp/pyu018

Gomes, F. V., Llorente, R., Del Bel, E. A., Viveros, M. P., López-Gallardo, M., and Guimarães, F. S. (2015b). Decreased Glial Reactivity Could Be Involved in the Antipsychotic-like Effect of Cannabidiol. *Schizophr. Res.* 164 (1-3), 155–163. doi:10.1016/j.schres.2015.01.015

Grace, A. A., and Gomes, F. V. (2019). The Circuitry of Dopamine System Regulation and its Disruption in Schizophrenia: Insights into Treatment and Prevention. *Schizophr. Bull.* 45 (1), 148–157. doi:10.1093/schbul/sbx199

Hazane, F., Krebs, M. O., Jay, T. M., and Le Pen, G. (2009). Behavioral Perturbations after Prenatal Neurogenesis Disturbance in Female Rat. *Neurotox. Res.* 15 (4), 311–320. doi:10.1007/s12640-009-9035-z

Howes, O. D., and McCutcheon, R. (2017). Inflammation and the Neural Diathesis-Stress Hypothesis of Schizophrenia: a Reconceptualization. *Transl. Psychiatry* 7 (2), e1024. doi:10.1038/tp.2016.278

Hradetzky, E., Sanderson, T. M., Tsang, T. M., Sherwood, J. L., Fitzjohn, S. M., Lakics, V., et al. (2012). The Methylazoxymethanol Acetate (MAM-E17) Rat Model: Molecular and Functional Effects in the hippocampus. *Neuropsychopharmacology* 37 (2), 364–377. doi:10.1038/npp.2011.219

Johansson, C., Jackson, D. M., and Svensson, L. (1997). Nitric Oxide Synthase Inhibition Blocks Phencyclidine-Induced Behavioural Effects on Prepulse Inhibition and Locomotor Activity in the Rat. *Psychopharmacol. Berl.* 131 (2), 167–173. doi:10.1007/s002130050280

Kahn, R. S., Sommer, I. E., MurrayMeyer-Lindenberg, R. M. A., Meyer-Lindenberg, A., Weinberger, D. R., Cannon, T. D., et al. (2015). Schizophrenia. *Nat. Rev. Dis. Prim.* 1 (1), 15067. doi:10.1038/nrdp.2015.67

Khan, M., Sekhon, B., Jatana, M., Giri, S., Gilg, A. G., Sekhon, C., et al. (2004). Administration of N-Acetylcysteine after Focal Cerebral Ischemia Protects Brain and Reduces Inflammation in a Rat Model of Experimental Stroke. *J. Neurosci. Res.* 76 (4), 519–527. doi:10.1002/jnr.20087

Kim, R., Healey, K. L., Sepulveda-Orengo, M. T., and Reissner, K. J. (2018). Astroglial Correlates of Neuropsychiatric Disease: from Astrocytopathy to Astrogliosis. *Prog. Neuropsychopharmacol. Biol. Psychiatry* 87, 126–146. doi:10.1016/j.pnpbp.2017.10.002

Kulak, A., Cuenod, M., and Do, K. Q. (2012). Behavioral Phenotyping of Glutathione-Deficient Mice: Relevance to Schizophrenia and Bipolar Disorder. *Behav. Brain Res.* 226 (2), 563–570. doi:10.1016/j.bbr.2011.10.020

Le Pen, G., Gourevitch, R., Hazane, F., Hoareau, C., Jay, T. M., and Krebs, M. O. (2006). Peri-pubertal Maturation after Developmental Disturbance: a Model for Psychosis Onset in the Rat. *Neuroscience* 143 (2), 395–405. doi:10.1016/j.neuroscience.2006.08.004

Le Pen, G., Jay, T. M., and Krebs, M. O. (2011). Effect of Antipsychotics on Spontaneous Hyperactivity and Hypersensitivity to MK-801-Induced Hyperactivity in Rats Prenatally Exposed to Methylazoxymethanol. *J. Psychopharmacol.* 25 (6), 822–835. doi:10.1177/0269881110387839

Lodge, D. J., Behrens, M. M., and Grace, A. A. (2009). A Loss of Parvalbumin-Containing Interneurons Is Associated with Diminished Oscillatory Activity in an Animal Model of Schizophrenia. *J. Neurosci.* 29 (8), 2344–2354. doi:10.1523/JNEUROSCI.5419-08.2009

Lodge, D. J., and Grace, A. A. (2012). Gestational Methylazoxymethanol Acetate Administration Alters Proteomic and Metabolomic Markers of Hippocampal Glutamatergic Transmission. *Neuropsychopharmacology* 37 (2), 319–320. doi:10.1038/npp.2011.255

Lodge, D. J., and Grace, A. A. (2008). Hippocampal Dysfunction and Disruption of Dopamine System Regulation in an Animal Model of Schizophrenia. *Neurotox. Res.* 14 (2), 97–104. doi:10.1007/BF03033801

Maćkowiak, M., Latusz, J., Głowacka, U., Bator, E., and Bilecki, W. (2019). Adolescent Social Isolation Affects Parvalbumin Expression in the Medial Prefrontal Cortex in the MAM-E17 Model of Schizophrenia. *Metab. Brain Dis.* 34 (1), 341–352. doi:10.1007/s11011-018-0359-3

McHugo, M., Talati, P., Armstrong, K., Vandekar, S. N., Blackford, J. U., Woodward, N. D., et al. (2019). Hyperactivity and Reduced Activation of Anterior hippocampus in Early Psychosis. *Am. J. Psychiatry* 176 (12), 1030–1038. doi:10.1176/appi.ajp.2019.19020151

Möller, M., Du Preez, J. L., Viljoen, F. P., Berk, M., Emsley, R., and Harvey, B. H. (2013). Social Isolation Rearing Induces Mitochondrial, Immunological, Neurochemical and Behavioural Deficits in Rats, and Is Reversed by Clozapine or N-Acetyl Cysteine. *Brain Behav. Immun.* 30, 156–167. doi:10.1016/j.bbi.2012.12.011

Moore, H., Jentsch, J. D., Ghajarnia, M., Geyer, M. A., and Grace, A. A. (2006). A Neurobehavioral Systems Analysis of Adult Rats Exposed to Methylazoxymethanol Acetate on E17: Implications for the Neuropathology of Schizophrenia. *Biol. Psychiatry* 60 (3), 253–264. doi:10.1016/j.biopsych.2006.01.003

Otte, D. M., Sommersberg, B., Kudin, A., Guerrero, C., Albayram, O., Filiou, M. D., et al. (2011). N-acetyl Cysteine Treatment Rescues Cognitive Deficits Induced by Mitochondrial Dysfunction in G72/G30 Transgenic Mice. *Neuropsychopharmacology* 36 (11), 2233–2243. doi:10.1038/npp.2011.109

Paxinos, G., and Watson, C. (2006). *The Rat Brain in Stereotaxic Coordinates: Hard Cover Edition*. Elsevier.

Penschuck, S., Flagstad, P., Didriksen, M., Leist, M., and Michael-Titus, A. T. (2006). Decrease in Parvalbumin-Expressing Neurons in the hippocampus and Increased Phencyclidine-Induced Locomotor Activity in the Rat Methylazoxymethanol (MAM) Model of Schizophrenia. *Eur. J. Neurosci.* 23 (1), 279–284. doi:10.1111/j.1460-9568.2005.04536.x

Perez, S. M., Boley, A., and Lodge, D. J. (2019a). Region Specific Knockdown of Parvalbumin or Somatostatin Produces Neuronal and Behavioral Deficits Consistent with Those Observed in Schizophrenia. *Transl. Psychiatry* 9, 264. doi:10.1038/s41398-019-0603-6

Perez, S. M., Donegan, J. J., and Lodge, D. J. (2019b). Effect of Estrous Cycle on Schizophrenia-like Behaviors in MAM Exposed Rats. *Behav. Brain Res.* 362, 258–265. doi:10.1016/j.bbr.2019.01.031

Potasiewicz, A., Holuj, M., Litwa, E., Gzielo, K., Socha, L., Popik, P., et al. (2020). Social Dysfunction in the Neurodevelopmental Model of Schizophrenia in Male and Female Rats: Behavioural and Biochemical Studies. *Neuropharmacology* 170, 108040. doi:10.1016/j.neuropharm.2020.108040

Rahati, M., Nozari, M., Eslami, H., Shabani, M., and Basiri, M. (2016). Effects of Enriched Environment on Alterations in the Prefrontal Cortex GFAP- and S100B-Immunopositive Astrocytes and Behavioral Deficits in MK-801-Treated Rats. *Neuroscience* 326, 105–116. doi:10.1016/j.neuroscience.2016.03.065

Ratajczak, P., Kus, K., Murawiecka, P., Słodzińska, I., Giermaziak, W., and Nowakowska, E. (2015). Biochemical and Cognitive Impairments Observed in Animal Models of Schizophrenia Induced by Prenatal Stress Paradigm or Methylazoxymethanol Acetate Administration. *Acta Neurobiol. Exp. (Wars)* 75 (3), 314–325.

Ribeiro, B. M., do Carmo, M. R., Freire, R. S., Rocha, N. F., Borella, V. C., de Menezes, A. T., et al. (2013). Evidences for a Progressive Microglial Activation and Increase in iNOS Expression in Rats Submitted to a Neurodevelopmental Model of Schizophrenia: Reversal by Clozapine. *Schizophr. Res.* 151 (1-3), 12–19. doi:10.1016/j.schres.2013.10.040

Salum, C., Raisman-Vozari, R., Michel, P. P., Gomes, M. Z., Mitkovski, M., Ferrario, J. E., et al. (2008). Modulation of Dopamine Uptake by Nitric Oxide in Cultured Mesencephalic Neurons. *Brain Res.* 1198, 27–33. doi:10.1016/j.brainres.2007.12.054

Salum, C., Schmidt, F., Michel, P. P., Del-Bel, E., and Raisman-Vozari, R. (2016). Signaling Mechanisms in the Nitric Oxide Donor- and Amphetamine-Induced Dopamine Release in Mesencephalic Primary Cultured Neurons. *Neurotox. Res.* 29 (1), 92–104. doi:10.1007/s12640-015-9562-8

Sotoyama, H., Namba, H., Kobayashi, Y., Hasegawa, T., Watanabe, D., Nakatsukasa, E., et al. (2021). Resting-state Dopaminergic Cell Firing in the Ventral Tegmental Area Negatively Regulates Affiliative Social Interactions in a Developmental Animal Model of Schizophrenia. *Transl. Psychiatry* 11, 236. doi:10.1038/s41398-021-01346-2

Stilo, S. A., and Murray, R. M. (2019). Non-genetic Factors in Schizophrenia. *Curr. Psychiatry Rep.* 21 (10), 100–110. doi:10.1007/s11920-019-1091-3

Thomases, D. R., Cass, D. K., and Tseng, K. Y. (2013). Periadolescent Exposure to the NMDA Receptor Antagonist MK-801 Impairs the Functional Maturation of Local GABAergic Circuits in the Adult Prefrontal Cortex. *J. Neurosci.* 33 (1), 26–34. doi:10.1523/JNEUROSCI.4147-12.2013

Tsugawa, S., Noda, Y., Tarumi, R., Mimura, Y., Yoshida, K., Iwata, Y., et al. (2019). Glutathione Levels and Activities of Glutathione Metabolism Enzymes in

Patients with Schizophrenia: A Systematic Review and Meta-Analysis. *J. Psychopharmacol.* 33 (10), 1199–1214. doi:10.1177/0269881119845820

Wang, J., Li, G., Xu, Y., and Zhang, W.-N. (2015). Hyperactivity and Disruption of Prepulse Inhibition Induced by NMDA Infusion of the Rat Ventral Hippocampus: Comparison of Uni- and Bilateral Stimulation.. *Neurosci. Lett.* 594, 150–154. doi:10.1016/j.neulet.2015.03.066

Wierońska, J. M., Sławińska, A., Łasoń-Tyburkiewicz, M., Gruca, P., Papp, M., Zorn, S. H., et al. (2015). The Antipsychotic-like Effects in Rodents of the Positive Allosteric Modulator Lu AF21934 Involve 5-HT1A Receptor Signaling: Mechanistic Studies. *Psychopharmacol. Berl.* 232 (1), 259–273. doi:10.1007/s00213-014-3657-4

Zhang, Z. J., and Reynolds, G. P. (2002). A Selective Decrease in the Relative Density of Parvalbumin-Immunoreactive Neurons in the hippocampus in Schizophrenia. *Schizophr. Res.* 55 (1-2), 1–10. doi:10.1016/S0920-9964(01)00188-8

Zhu, X., Cabungcal, J.-H., Cuenod, M., Uliana, D. L., Do, K. Q., and Grace, A. A. (2021). Thalamic Reticular Nucleus Impairments and Abnormal Prefrontal Control of Dopamine System in a Developmental Model of Schizophrenia: Prevention by N-Acetylcysteine. *Mol. Psychiatry* 26, 7679–7689. doi:10.1038/s41380-021-01198-8

Conflict of Interest: The authors declare that the research was conducted in the absence of any commercial or financial relationships that could be construed as a potential conflict of interest.

Publisher's Note: All claims expressed in this article are solely those of the authors and do not necessarily represent those of their affiliated organizations, or those of the publisher, the editors, and the reviewers. Any product that may be evaluated in this article, or claim that may be made by its manufacturer, is not guaranteed or endorsed by the publisher.

frontiers | Frontiers in Pharmacology

TYPE Mini Review
PUBLISHED 09 August 2022
DOI 10.3389/fphar.2022.900610

OPEN ACCESS

EDITED BY
Nejat Duzgunes,
University of the Pacific, United States

REVIEWED BY
Mario Ariatti,
University of KwaZulu-Natal, South Africa

*CORRESPONDENCE
Vasiliki Mahairaki,
vmachai1@jhmi.edu

†These authors share last authorship

SPECIALTY SECTION
This article was submitted to Neuropharmacology, a section of the journal Frontiers in Pharmacology

RECEIVED 20 March 2022
ACCEPTED 13 July 2022
PUBLISHED 09 August 2022

CITATION
Tsakiri M, Zivko C, Demetzos C and Mahairaki V (2022), Lipid-based nanoparticles and RNA as innovative neuro-therapeutics. *Front. Pharmacol.* 13:900610. doi: 10.3389/fphar.2022.900610

Lipid-based nanoparticles and RNA as innovative neuro-therapeutics

Maria Tsakiri[1], Cristina Zivko[2,3], Costas Demetzos[1†] and Vasiliki Mahairaki[2,3*†]

[1]Section of Pharmaceutical Technology, Department of Pharmacy, School of Health Sciences, National and Kapodistrian University of Athens, Athens, Greece, [2]Department of Genetic Medicine, Johns Hopkins School of Medicine, Baltimore, MD, United States, [3]The Richman Family Precision Medicine Center of Excellence in Alzheimer's Disease, Johns Hopkins Medicine, Baltimore, MD, United States

RNA-delivery is a promising tool to develop therapies for difficult to treat diseases such as neurological disorders, by silencing pathological genes or expressing therapeutic proteins. However, in many cases RNA delivery requires a vesicle that could effectively protect the molecule from bio-degradation, bypass barriers i.e., the blood brain barrier, transfer it to a targeted tissue and efficiently release the RNA inside the cells. Many vesicles such as viral vectors, and polymeric nanoparticles have been mentioned in literature. In this review, we focus in the discussion of lipid-based advanced RNA-delivery platforms. Liposomes and lipoplexes, solid lipid nanoparticles and lipid nanoparticles are the main categories of lipidic platforms for RNA-delivery to the central nervous systems (CNS). A variety of surface particles' modifications and routes of administration have been studied to target CNS providing encouraging results *in vivo*. It is concluded that lipid-based nanoplatforms will play a key role in the development of RNA neuro-therapies.

KEYWORDS

lipid nanoparticles, liposomes, lipoplexes, solid lipid nanoparticles, gene delivery, RNA, central nervous system

Introduction

Approximately 50 years ago, the first conversation of whether gene therapy could be the solution for the treatment of serious diseases such as cancer or genetic disorders began (Friedmann and Roblin, 1972). Since then, the science of gene therapy has flourished. However, currently, only a few products based on *in vivo* or *ex vivo* gene therapy have been approved by the US Food and Drug Administration (FDA) and the European Medicines Agency (EMA) as serious limitations have not yet been overcome. Indeed, the first gene therapy clinical trials resulted in serious adverse effects or even deaths that lead the US National Institute of Health (NIH) to suspend the trials in pre-clinical stages (Orkin and Motulsky, 1996).

Although today many of the early shortcomings of this technology such as off-target effects, vector safety, or inefficient administration have been solved, there still remain

some unsolved questions. Especially in the case of *in vivo* gene therapy, nucleic acid should bypass the immune system and biodegradation processes of the human organism, reach the target tissue, and even cross cell or nucleus membranes. Thus, the accomplishment of the therapeutic genetic modifications requires that the nucleic acid will remain effective till the time of its expression by the target cells. For this purpose, the use of a vector is very common. The vector is responsible for the delivery of the nucleic acid to the target, avoiding its degradation and systematic adverse effects. The majority of vectors are viral vectors such as adenoviruses (Zhu et al., 2020; Voysey et al., 2021; Watanabe et al., 2021), retroviruses (Rastegar et al., 2009), lentiviruses (Maude et al., 2014; Sessa et al., 2016) or adeno-associated viruses (Wuh-Liang et al., 2012; Keiser et al., 2016; Mendell et al., 2017; Wang et al., 2018). Currently, many scientific groups propose generally safe viral vectors as efficient gene delivery platforms (Walther and Stein, 2000; Bulcha et al., 2021; Selvaraj et al., 2021).

Nevertheless, other alternatives to the viral vectors have also been developed and studied over a period of approximately 40 years (Patil et al., 2019; Faneca, 2021). Indeed, the first medicinal product that used a lipid nanoplatform (LNP) for the delivery of a siRNA molecule has been approved by FDA and EMA in 2018 by the trade name Patisiran or Onppatro respectively for the treatment of hereditary transthyretin-mediated amyloidosis (hATTR amyloidosis) in adult patients with stage 1 or stage 2 polyneuropathy (DeWeerdt, 2019). Today, this technology has been used for the development of mRNA COVID-19 vaccines (Tsakiri et al., 2021), while a few other similar platforms are in clinical trials (Damase et al., 2021).

Diseases of the central nervous system (CNS) such as tumors or neurodegenerative pathologies, have high mortality rates as there are no medicinal products to cure them (Liang et al., 2021). For example, approximately 6.2 million American citizens aged ≥65 years were estimated to suffer from Alzheimer's disease (AD) while 121,499 deaths from the same pathology were reported in 2019 (Wiley, 2021). Centers for disease control and prevention (CDC) mention that by 2050 13.8 million US. adults aged ≥65 years are expected to suffer from AD (Taylor et al., 2017). Notably, these numbers refer to only one degenerative disease. Moreover, in many of these conditions such as AD, the only available treatment options are symptomatic and do not address the underlying cause of the disease (Breijyeh and Karaman, 2020). Thus, gene therapy for the treatment of CNS diseases holds the potential to bring promising results.

Although many approaches to deliver RNA molecules that do not contain viral vectors exist such as chemically modified antisense oligonucleotides (ASO), N-acetylgalactosamine (GalNAc) ligand-modified short interfering RNA (siRNA) conjugates (Kulkarni et al., 2021) or polymeric delivery platforms (Wahane et al., 2020) the role of non-viral, lipid vectors in the development of advanced therapeutic medicinal products for gene therapy is of great importance. In addition to protecting the nucleic acid from degradation, these platforms can be engineered to target the brain and ensure intracellular release through endosomal escape mechanisms in some cases. In this mini-review, we will discuss the approaches that are utilized for the development of lipid gene delivery nanoplatforms that target CNS and the perspectives of this technology in the treatment of brain diseases.

Lipid-based nanoparticles

Lipid-based nanoparticles are the most well-studied non-viral platforms for the delivery of RNA molecules (Zhao and Huang, 2014; Meng et al., 2017). This broad category includes liposomes, lipoplexes, lipid nanoparticles and solid lipid nanoparticles, as presented in Figure 1. By virtue of their biochemical composition, lipidic nanoparticles provide bio-mimicking and bio-degradable platforms. As a result of their lipophilicity, they can penetrate more easily the BBB while the inclusion of cationic lipids stabilize the negatively charged RNA molecules via electrostatic interactions.

Liposomes and lipoplexes

Liposomes are self-assembled pseudospherical vesicles in which the lipid bilayers surround the aqueous core. Liposomes have been widely and for a long time used as drug delivery systems for the treatment of a plethora of diseases. Indeed, more than 15 liposomal drugs are currently on the market (Large et al., 2021). However, their application in encapsulating nucleic acids is in the pre-clinical or early clinical phase.

Liposomes can be categorized by their size, charge, key surface molecules or surface modifications to modulate circulation time and avoid detection and elimination by the immune system. The development of liposomes for gene therapy often involves the use of cationic lipids which interact electrostatically with the negatively charged genetic material (Mishra et al., 2022). The complexation of nucleic acids with cationic lipids leads to the formation of the lipoplexes in which nucleic acids are either on the external surface of the structure or in the internal cavity (Pereira et al., 2021). The most commonly used cationic lipids are 2,3-Dioleoyloxy-propyl)-trimethylammonium-chloride (DOTAP) (Lechanteur et al., 2018; Hattori et al., 2019), di-O-octadecenyl-3-trimethylammonium propane (DOTMA) and dimethyldioctadecylammonium bromide DDA (Putzke et al., 2020).

Concerning the central nervous system, certain liposomes/lipoplexes experiments have proved efficacious. Recently, Bender and others developed DOTAP:Cholesterol 1:1 liposomes that were incubated with small interfering RNA (siRNA) that

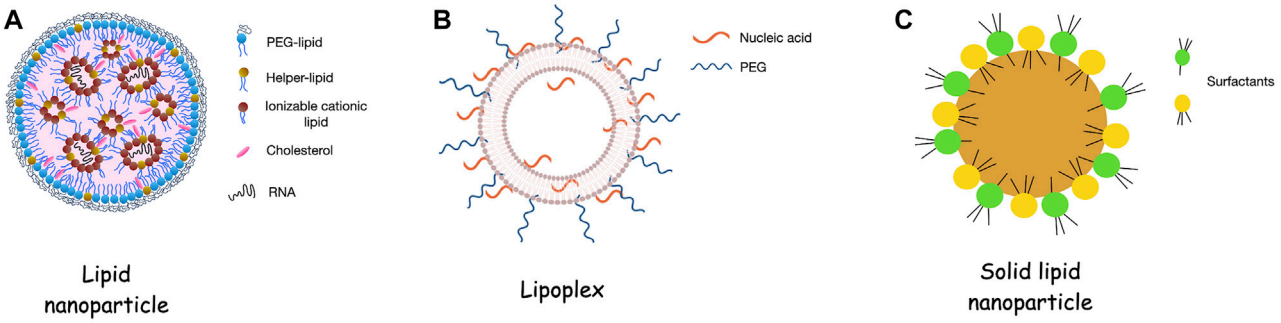

FIGURE 1
Consistency of lipidic nanoparticles for RNA delivery. **(A)**. Lipid nanoparticles (LNPs) contain an ionizable cationic lipid that allows the encapsulation of the RNA molecules into the internal aqueous cavities of the platform. Addition of PEG-lipid, helper lipid and cholesterol contribute in physicochemical and biological stability of the LNPs. **(B)**. Lipoplexes are liposomes that contain cationic lipids and are conjugated with nucleic acids i.e., RNA. IN this case the nucleic acids are mainly in the external surface of the systems leading which indicates that the RNA is more exposed to the environment than in the case of the LNPs. **(C)**. Solid lipid nanoparticles are formed by the lipid core of solid lipids and the amphiphilic surfactants that decorate the surface of the particles. Figure 1B adapted from Pereira et al. (2021).

decrease the amount of neuronal cellular prion protein (PrP^c) and rabies virus glycoprotein fragment (RVG-9r). As it is presented in the literature, RVG selectively interacts with the nicotinic achetilocholine receptor on the surface of the neuronal cells while the addition of a positively charged arginine residue at the carboxyl terminus of RVG (9r modification) allows the electrostatic interaction of the modified peptide and the siRNA chains (Kumar et al., 2007). Indeed, their formulations can effectively bypass the BBB and prolong the lifetime of prion-infected mice. The targeting to the brain cells was successful due to the RVG-9r protein while the therapeutic effect suggests that the siRNA successfully knockdown the PrP^c expression (Zabel, 2013; Bender et al., 2016, 2019). Since many neurodegenerative diseases such as Alzheimer's, Parkinson's or Huntington's pathology, belong to the category of prion diseases, those results could bring great promise for their treatment. In another study, DOTAP: Cholesterol siRNA-liposomes associated with transferrin that were topically administrated in mouse brain proved to have high efficiency in downregulation of pathological genes while having limited toxicity (Cardoso et al., 2008). Finally, Yuan et al. show that siRNA (siGOLPH3) loaded cationic liposomes incorporated with angiopep2GOLPH3 ligand for LRP-1 receptor that is expressed in human BBB and glioma cells, protein provide could result in a potential treatment of glioma (Yuan et al., 2018).

Furthermore, different routes of administration can improve the brain delivery efficiency of liposomes. Dhaliwal et al. chose to administer their mRNA lipoplexes intranasally. The liposomes were loaded with the mRNA, labeled with GFP-mRNA or luciferase-mRNA to evaluate the transfection efficiency of the formulations (Dhaliwal et al., 2020). The results proved that the expression of the mRNA was higher when the liposomal vesicles were utilized to vehiculate the mRNA than when the mRNA was administered in naked form. In comparison with the administration of the naked mRNA. Interestingly, Hu and others showed that intranasal administration of core-cell lipoplexes could effectively transfer the siRNA (Hu et al., 2022).

Lipid nanoparticles

Disadvantages associated with the use of cationic lipids in liposomes and lipoplexes such as rapid clearance from the reticuloendothelial system (RES) due to opsonization and activation of the complement system and toxicity issues connected with cell apoptotic mechanisms, enhanced reactive oxygen species (ROS) levels, have prompted the development of the ionizable cationic lipids and the lipid nanoparticles (LNPs) (Filion and Phillips, 1997; Knudsen et al., 2015; Cui et al., 2018; Liu et al., 2020; Kulkarni et al., 2021). Cationic lipids that are positively charged at about pH 4, but that are electroneutral at physiological pH are key components of LNPs (Tenchov et al., 2021). Consequently, they provide a safer solution as advanced delivery platforms. Their safety is well-established due to the recent approval and massive administration of Pfizer/BioNTech and Moderna mRNA vaccines (Polack et al., 2020; Baden et al., 2021). However, only a few studies evaluate the safety and efficiency of LNP-RNA platforms intended for therapy in the CNS. To the best of our knowledge, the first research article to address this particular question was published in 2013. In this study, Rugta et al. provide evidence that when their siRNA-LNPs were administrated within mice cortex or via intracerebroventricular injection a good rate of uptake by neuronal cells and reduction of associated protein levels was observed. Furthermore, no toxicity to neurons was observed (Rungta et al., 2013). More recently, two separate research

groups from Israel and Denmark have studied the potential role of RNA interference-LNPs in the treatment of glioma. The former, developed Dlin-MC3-DMA, DSPC, Chol, DMG-PEG, and DSPE-PEG LNPs decorated with hyaluronan, which is a CD44 ligand (Cohen et al., 2015). The latter, chose a more complex formulation that externally has a slight negative charge due to a PEGylated cleavable lipopeptide. Metalloproteinases present in the tumor microenvironment are responsible for the cleavage of the PEGylated lipoprotein leading to positively charged LNPs that subsequently endocytosed. Thus, intracellular release of the siRNA is achieved (Bruun et al., 2015). Both groups resulted in good toxicological results and a high knockdown percentage of the targeted mRNA after *in vitro* experiments and topical administration in mice. Tanaka et al. developed LNPs that contained SS-cleavable proton-activated lipid-like materials as the ionizable elements. These synthetic lipids provide a neutral charge of the platform at physiological pH values while they are protonated at the low endosomal pH. Similarly with the work of Bruun et al. (2015), such a phenomenon leads to the protection of the RNA molecule when administrated *in vivo* and the intracellular release of this sensitive bio-molecule (Tanaka et al., 2018). Finally, Khare et al., recently showed that LNPs with $C_{12\text{-}200}$ lipidoid, which is a syntetic lipid-like molecule that displays tertiary amines in the headgroups, could provide a safer approach for RNA delivery into the neurons than other platforms that contain lipofectamine [mixture of 2,3-dioleoyloxy-N- [2 (sperminecarboxamido)ethyl]-N,N-dimethyl-1-propaniminium trifluoroacetate (DOSPA) and 1,2-Dioleoyl-sn-glycerophosphoethanolamine (DOPE)]. The platform offers favourable loading capacity, displays efficient cellular uptake and low *in vitro* cytotoxicity in human cortical cell lines (Khare et al., 2021).

Solid lipid nanoparticles

Solid lipid nanoparticles (SLNs) are another category of lipidic nanoparticles. They from liposomes in that SLNs do not have an aqueous central cavity but a solid lipid:surfactant one (Scioli Montoto et al., 2020). Depending on their composition, size and charge SLNs present unique physicochemical properties (Naseri et al., 2015).

Concerning their role in the protection and delivery of nucleic acids, SLNs have not been widely studied, maybe due to their morphological characteristics. Since nucleic acids are hydrophilic molecules, their interaction with the SLN could take place only on the surface of the delivery platforms electrostatically. However, electrostatic interactions are not particularly stable and could easily break under environmental pressure (Wojnarowska et al., 2018). Nevertheless, an interesting study was performed by Rassu et al. They stabilized BACE-1 siRNA negatively charged molecules, that could have a valuable role in the treatment of Alzheimer's disease, with RVG-9R, which was positively charged. Afterward, the siRNA-RVG-9R complex solution was mixed with triglycerides, poly (vinyl alcohol) and chitosan for the formation of a double emulsion that contains the SLNs. The chitosan coated SNPs presented higher *in vitro* mucoadhesiveness and permeability properties than the non-coated SNPs (Rassu et al., 2017). Another study utilized two different siRNA molecules that knockdown the human c-Met, which is found in glioma to deliver them by SLN. The siRNA molecules were first conjugated with polyethylene glycol (PEG) via a disulfide bond. The SLN-siRNA-PEG formulations displayed accumulation in the brain tumor, no systemic toxicity as well as suppression of the tumor growth after intravenous administration in the glioblastoma xenograft tumor model (Jin et al., 2011).

Discussion

Today, the treatment of brain malignancies such as glioblastoma or neurodegenerative diseases still remains an elusive (Mullard, 2021; Sun and Roy, 2021). Gene therapy is a promising approach to developing new medicinal products for a plethora of different diseases (Sudhakar and Richardson, 2019; Parambi et al., 2022). For instance, the small interfering RNAs can downregulate the expression of pathological proteins that are present in diseases. Such pharmacological action is not possible with other therapeutic approaches (i.e., by small drugs or proteins). Viral vectors have been the gold standard of brain gene delivery in the past years as they can easily pass the BBB, they are taken up by the brain cells and transfer their genes into the cell nucleus (Lundstrom, 2018). Although the viruses that are utilized are either attenuated or non-replicating, concerns about the safety of these vectors exist in terms of immunogenicity and mutagenicity.

The BBB remains one of the main obstacles for the lipidic delivery systems. Three pathways responsible for the lipidic vesicles by-pass through the BBB are mentioned in the literature: 1) adsorptive-mediated transcytosis (AMT), 2) receptor-mediated transcytosis (RMT), and 3) carrier-mediated transcytosis (CMT) (Juhairiyah and de Lange, 2021). Concerning AMT, cationic vesicles interact electrostatically with the endothelial cells of the BBB. However, the cationic charge leads to toxicity effects and fast inactivation of the particles via opsonization processes. The decoration of the lipidic nanoparticles with accessory molecules such as peptides or antibodies is a common procedure. Transferrin (Kong et al., 2020), glucose or mannose and their derivatives (Qu et al., 2014; Arora et al., 2020), vitamin C (Peng et al., 2018) and glutathione

(Salem et al., 2015; Trapani et al., 2021) are some of these accessory molecules. Another effective way to avoid the BBB via non-invasive administration is the nose-to-brain pathway. Although the exact mechanism of action of nose-to-brain delivery is not clear, transfer through olfactory nerves or trigeminal nerves seems to be the most common way after intranasal administration. For the former, the nanoparticles paracellularly pass through the gaps of olfactory cells, finally reaching the subarachnoid space (Crowe et al., 2018). Indeed, Godfrey and others found that their intranasally administrated nanoplatforms were located in the olfactory bulb only 5 min after the administration (Godfrey et al., 2018). On the other hand, the transport through the trigeminal nerves seems to be less common but possible both by intra- or extra-cellular routes (Cunha et al., 2017; Bourganis et al., 2018). However, some consideration still exists of whether today, nose-to-brain administration of nanovesicles increase the effectiveness of active molecules (Feng et al., 2018).

The majority of recent and current studies related to the delivery of small molecules or bio-molecules in the CNS with the aid of nanotechnology have focused *on* liposomal nanovesicles. However, other platforms, such as LNPs may be better choices for the transport of genetic material in the brain due to the better encapsulation of a sensitive RNA cargo. For instance, although many of the studies mentioned above indicate that LNPs containing RNA molecules could play an important role in the treatment of CNS diseases, all of them used a patient unfriendly route of administration and more work is necessary for the development of platforms that are not only safe and efficacious but also not demanding for the patient. Moreover, *in vivo* toxicity studies after repeated administration is necessary to verify the safety of the platform as in many cases the therapeutic regimen would entail multiple, rather than single, dose protocol. Nevertheless, lipidic nanoparticles that carry RNAs hold great promise as advanced therapeutic medicinal products that could provide effective results in the treatment of neurodegenerative disorders, such as Alzheimer's disease, or brain tumors like glioblastoma.

Author contributions

Data acquisition (literature review) and conceptualization, MT, CD, and VM; Critical revisions, CZ and VM All authors have read and agreed to the published version of the manuscript.

Funding

The Richman Family Precision Medicine Center of Excellence in Alzheimer's Disease, Johns Hopkins Medicine and Johns Hopkins Bayview Medical Center, Baltimore, MD, United States.

Conflict of interest

The authors declare that the research was conducted in the absence of any commercial or financial relationships that could be construed as a potential conflict of interest.

Publisher's note

All claims expressed in this article are solely those of the authors and do not necessarily represent those of their affiliated organizations, or those of the publisher, the editors and the reviewers. Any product that may be evaluated in this article, or claim that may be made by its manufacturer, is not guaranteed or endorsed by the publisher.

References

Arora, S., Sharma, D., and Singh, J. (2020). GLUT-1: an effective target to deliver brain-derived neurotrophic factor gene across the blood brain barrier. *ACS Chem. Neurosci.* 11, 1620–1633. doi:10.1021/acschemneuro.0c00076

Baden, L. R., El Sahly, H. M., Essink, B., Kotloff, K., Frey, S., Novak, R., et al. (2021). Efficacy and safety of the mRNA-1273 SARS-CoV-2 vaccine. *N. Engl. J. Med.* 384, 403–416. doi:10.1056/NEJMoa2035389

Bender, H., Noyes, N., Annis, J. L., Hitpas, A., Mollnow, L., Croak, K., et al. (2019). PrPC knockdown by liposome-siRNA-peptide complexes (LSPCs) prolongs survival and normal behavior of prion-infected mice immunotolerant to treatment. *PLoS One* 14, e0219995. doi:10.1371/journal.pone.0219995

Bender, H. R., Kane, S., and Zabel, M. D. (2016). Delivery of therapeutic siRNA to the CNS using cationic and anionic liposomes. *J. Vis. Exp.*, 54106. doi:10.3791/54106

Bourganis, V., Kammona, O., Alexopoulos, A., and Kiparissides, C. (2018). Recent advances in carrier mediated nose-to-brain delivery of pharmaceutics. *Eur. J. Pharm. Biopharm.* 128, 337–362. doi:10.1016/j.ejpb.2018.05.009

Breijyeh, Z., and Karaman, R. (2020). Comprehensive review on Alzheimer's disease: Causes and treatment. *Molecules* 25, 5789. doi:10.3390/molecules25245789

Bruun, J., Larsen, T. B., Jølck, R. I., Eliasen, R., Holm, R., Gjetting, T., et al. (2015). Investigation of enzyme-sensitive lipid nanoparticles for delivery of siRNA to blood–brain barrier and glioma cells. *Int. J. Nanomedicine* 10, 5995–6008. doi:10.2147/IJN.S87334

Bulcha, J. T., Wang, Y., Ma, H., Tai, P. W. L., and Gao, G. (2021). Viral vector platforms within the gene therapy landscape. *Signal Transduct. Target. Ther.* 6, 53. doi:10.1038/s41392-021-00487-6

Cardoso, A. L. C., Simões, S., de Almeida, L. P., Plesnila, N., Pedroso de Lima, M. C., Wagner, E., et al. (2008). Tf-lipoplexes for neuronal siRNA delivery: a promising system to mediate gene silencing in the CNS. *J. Control. Release* 132, 113–123. doi:10.1016/j.jconrel.2008.08.014

Cohen, Z. R., Ramishetti, S., Peshes-Yaloz, N., Goldsmith, M., Wohl, A., Zibly, Z., et al. (2015). Localized RNAi therapeutics of chemoresistant grade IV glioma using hyaluronan-grafted lipid-based nanoparticles. *ACS Nano* 9, 1581–1591. doi:10.1021/nn506248s

Crowe, T. P., Greenlee, M. H. W., Kanthasamy, A. G., and Hsu, W. H. (2018). Mechanism of intranasal drug delivery directly to the brain. *Life Sci.* 195, 44–52. doi:10.1016/j.lfs.2017.12.025

Cui, S., Wang, Y., Gong, Y., Lin, X., Zhao, Y., Zhi, D., et al. (2018). Correlation of the cytotoxic effects of cationic lipids with their headgroups. *Toxicol. Res.* 7, 473–479. doi:10.1039/C8TX00005K

Cunha, S., Almeida, H., Amaral, M. H., Lobo, J. M. S., and Silva, A. C. (2017). Intranasal lipid nanoparticles for the treatment of neurodegenerative diseases. *Curr. Pharm. Des.* 23, 6553–6562. doi:10.2174/1381612824666171128105305

Damase, T. R., Sukhovershin, R., Boada, C., Taraballi, F., Pettigrew, R. I., Cooke, J. P., et al. (2021). The limitless future of RNA therapeutics. *Front. Bioeng. Biotechnol.* 9, 628137. doi:10.3389/fbioe.2021.628137

DeWeerdt, S. (2019). RNA therapies explained. *Nature* 574, S2–S3. doi:10.1038/d41586-019-03068-4

Dhaliwal, H. K., Fan, Y., Kim, J., and Amiji, M. M. (2020). Intranasal delivery and transfection of mRNA therapeutics in the brain using cationic liposomes. *Mol. Pharm.* 17, 1996–2005. doi:10.1021/acs.molpharmaceut.0c00170

Faneca, H. (2021). Non-viral gene delivery systems. *Pharmaceutics* 13, 446. doi:10.3390/pharmaceutics13040446

Feng, Y., He, H., Li, F., Lu, Y., Qi, J., Wu, W., et al. (2018). An update on the role of nanovehicles in nose-to-brain drug delivery. *Drug Discov. Today* 23, 1079–1088. doi:10.1016/j.drudis.2018.01.005

Filion, M. C., and Phillips, N. C. (1997). Toxicity and immunomodulatory activity of liposomal vectors formulated with cationic lipids toward immune effector cells. *Biochim. Biophys. Acta* 1329, 345–356. doi:10.1016/s0005-2736(97)00126-0

Friedmann, T., and Roblin, R. (1972). Gene therapy for human genetic disease? *Science* 175, 949–955. doi:10.1126/science.175.4025.949

Godfrey, L., Iannitelli, A., Garrett, N. L., Moger, J., Imbert, I., King, T., et al. (2018). Nanoparticulate peptide delivery exclusively to the brain produces tolerance free analgesia. *J. Control. Release* 270, 135–144. doi:10.1016/j.jconrel.2017.11.041

Hattori, Y., Nakamura, M., Takeuchi, N., Tamaki, K., Shimizu, S., Yoshiike, Y., et al. (2019). Effect of cationic lipid in cationic liposomes on siRNA delivery into the lung by intravenous injection of cationic lipoplex. *J. Drug Target.* 27, 217–227. doi:10.1080/1061186X.2018.1502775

Hu, Y., Jiang, K., Wang, D., Yao, S., Lu, L., Wang, H., et al. (2022). Core-shell lipoplexes inducing active macropinocytosis promote intranasal delivery of c-Myc siRNA for treatment of glioblastoma. *Acta Biomater.* 138, 478–490. doi:10.1016/j.actbio.2021.10.042

Jin, J., Bae, K. H., Yang, H., Lee, S. J., Kim, H., Kim, Y., et al. (2011). *In vivo* specific delivery of c-met siRNA to glioblastoma using cationic solid lipid nanoparticles. *Bioconjug. Chem.* 22, 2568–2572. doi:10.1021/bc200406n

Juhairiyah, F., and de Lange, E. C. M. (2021). Understanding drug delivery to the brain using liposome-based strategies: Studies that provide mechanistic insights are essential. *AAPS J.* 23, 114. doi:10.1208/s12248-021-00648-z

Keiser, M. S., Monteys, A. M., Corbau, R., Gonzalez-Alegre, P., and Davidson, B. L. (2016). RNAi prevents and reverses phenotypes induced by mutant human ataxin-1. *Ann. Neurol.* 80, 754–765. doi:10.1002/ana.24789

Khare, P., Dave, K. M., Kamte, Y. S., Manoharan, M. A., O'Donnell, L. A., Manickam, D. S., et al. (2021). Development of lipidoid nanoparticles for siRNA delivery to neural cells. *AAPS J.* 24, 8. doi:10.1208/s12248-021-00653-2

Knudsen, K. B., Northeved, H., Ek, P. K., Permin, A., Gjetting, T., Andresen, T. L., et al. (2015). *In vivo* toxicity of cationic micelles and liposomes. *Nanomedicine* 11, 467–477. doi:10.1016/j.nano.2014.08.004

Kong, L., Li, X., Ni, Y., Xiao, H., Yao, Y., Wang, Y., et al. (2020). Transferrin-modified osthole PEGylated liposomes travel the blood-brain barrier and mitigate alzheimer's disease-related pathology in APP/PS-1 mice. *Int. J. Nanomedicine* 15, 2841–2858. doi:10.2147/IJN.S239608

Kulkarni, J. A., Witzigmann, D., Thomson, S. B., Chen, S., Leavitt, B. R., Cullis, P. R., et al. (2021). The current landscape of nucleic acid therapeutics. *Nat. Nanotechnol.* 16, 630–643. doi:10.1038/s41565-021-00898-0

Kumar, P., Wu, H., McBride, J. L., Jung, K.-E., Hee Kim, M., Davidson, B. L., et al. (2007). Transvascular delivery of small interfering RNA to the central nervous system. *Nature* 448, 39–43. doi:10.1038/nature05901

Large, D. E., Abdelmessih, R. G., Fink, E. A., and Auguste, D. T. (2021). Liposome composition in drug delivery design, synthesis, characterization, and clinical application. *Adv. Drug Deliv. Rev.* 176, 113851. doi:10.1016/j.addr.2021.113851

Lechanteur, A., Sanna, V., Duchemin, A., Evrard, B., Mottet, D., Piel, G., et al. (2018). Cationic liposomes carrying siRNA: Impact of lipid composition on physicochemical properties, cytotoxicity and endosomal escape. *Nanomaterials* 8, 270. doi:10.3390/nano8050270

Liang, C.-S., Li, D.-J., Yang, F.-C., Tseng, P.-T., Carvalho, A. F., Stubbs, B., et al. (2021). Mortality rates in Alzheimer's disease and non-alzheimer's dementias: a systematic review and meta-analysis. *Lancet Healthy Longev.* 2, e479–e488. doi:10.1016/S2666-7568(21)00140-9

Liu, C., Zhang, L., Zhu, W., Guo, R., Sun, H., Chen, X., et al. (2020). Barriers and strategies of cationic liposomes for cancer gene therapy. *Mol. Ther. Methods Clin. Dev.* 18, 751–764. doi:10.1016/j.omtm.2020.07.015

Lundstrom, K. (2018). Viral vectors in gene therapy. *Diseases* 6, E42. doi:10.3390/diseases6020042

Maude, S. L., Frey, N., Shaw, P. A., Aplenc, R., Barrett, D. M., Bunin, N. J., et al. (2014). Chimeric antigen receptor T cells for sustained remissions in leukemia. *N. Engl. J. Med.* 371, 1507–1517. doi:10.1056/NEJMoa1407222

Mendell, J. R., Al-Zaidy, S., Shell, R., Arnold, W. D., Rodino-Klapac, L. R., Prior, T. W., et al. (2017). Single-dose gene-replacement therapy for spinal muscular atrophy. *N. Engl. J. Med.* 377, 1713–1722. doi:10.1056/NEJMoa1706198

Meng, Z., O'Keeffe-Ahern, J., Lyu, J., Pierucci, L., Zhou, D., Wang, W., et al. (2017). A new developing class of gene delivery: messenger RNA-based therapeutics. *Biomater. Sci.* 5, 2381–2392. doi:10.1039/c7bm00712d

Mishra, N., Ashique, S., Garg, A., Rai, V. K., Dua, K., Goyal, A., et al. (2022). Role of siRNA-based nanocarriers for the treatment of neurodegenerative diseases. *Drug Discov. Today* 27, 1431–1440. doi:10.1016/j.drudis.2022.01.003

Mullard, A. (2021). More Alzheimer's drugs head for FDA review: What scientists are watching. *Nature* 599, 544–545. doi:10.1038/d41586-021-03410-9

Naseri, N., Valizadeh, H., and Zakeri-Milani, P. (2015). Solid lipid nanoparticles and nanostructured lipid carriers: structure, preparation and application. *Adv. Pharm. Bull.* 5, 305–313. doi:10.15171/apb.2015.043

Orkin, S. H., and Motulsky, A. G. (1996). Report and recommendations of the panel to assess the NIH investment in research on gene therapy. *Bull. Med. Ethics* 116, 10

Parambi, D. G. T., Alharbi, K. S., Kumar, R., Harilal, S., Batiha, G. E.-S., Cruz-Martins, N., et al. (2022). Gene therapy approach with an emphasis on growth factors: theoretical and clinical outcomes in neurodegenerative diseases. *Mol. Neurobiol.* 59, 191–233. doi:10.1007/s12035-021-02555-y

Patil, S., Gao, Y.-G., Lin, X., Li, Y., Dang, K., Tian, Y., et al. (2019). The development of functional non-viral vectors for gene delivery. *Int. J. Mol. Sci.* 20, 5491. doi:10.3390/ijms20215491

Peng, Y., Zhao, Y., Chen, Y., Yang, Z., Zhang, L., Xiao, W., et al. (2018). Dual-targeting for brain-specific liposomes drug delivery system: synthesis and preliminary evaluation. *Bioorg. Med. Chem.* 26, 4677–4686. doi:10.1016/j.bmc.2018.08.006

Pereira, S., Santos, R. S., Moreira, L., Guimarães, N., Gomes, M., Zhang, H., et al. (2021). Lipoplexes to deliver oligonucleotides in gram-positive and gram-negative bacteria: towards treatment of blood infections. *Pharmaceutics* 13, 989. doi:10.3390/pharmaceutics13070989

Polack, F. P., Thomas, S. J., Kitchin, N., Absalon, J., Gurtman, A., Lockhart, S., et al. (2020). Safety and efficacy of the BNT162b2 mRNA covid-19 vaccine. *N. Engl. J. Med.* 383, 2603–2615. doi:10.1056/NEJMoa2034577

Putzke, S., Feldhues, E., Heep, I., Ilg, T., and Lamprecht, A. (2020). Cationic lipid/pDNA complex formation as potential generic method to generate specific IRF pathway stimulators. *Eur. J. Pharm. Biopharm.* 155, 112–121. doi:10.1016/j.ejpb.2020.08.010

Qu, B., Li, X., Guan, M., Li, X., Hai, L., Wu, Y., et al. (2014). Design, synthesis and biological evaluation of multivalent glucosides with high affinity as ligands for brain targeting liposomes. *Eur. J. Med. Chem.* 72, 110–118. doi:10.1016/j.ejmech.2013.10.007

Rastegar, M., Hotta, A., Pasceri, P., Makarem, M., Cheung, A. Y. L., Elliott, S., et al. (2009). MECP2 isoform-specific vectors with regulated expression for rett syndrome gene therapy. *PLoS One* 4, e6810. doi:10.1371/journal.pone.0006810

Rassu, G., Soddu, E., Posadino, A. M., Pintus, G., Sarmento, B., Giunchedi, P., et al. (2017). Nose-to-brain delivery of BACE1 siRNA loaded in solid lipid nanoparticles for Alzheimer's therapy. *Colloids Surf. B Biointerfaces* 152, 296–301. doi:10.1016/j.colsurfb.2017.01.031

Rungta, R. L., Choi, H. B., Lin, P. J., Ko, R. W., Ashby, D., Nair, J., et al. (2013). Lipid nanoparticle delivery of siRNA to silence neuronal gene expression in the brain. *Mol. Ther. Nucleic Acids* 2, e136. doi:10.1038/mtna.2013.65

Salem, H. F., Ahmed, S. M., Hassaballah, A. E., and Omar, M. M. (2015). Targeting brain cells with glutathione-modulated nanoliposomes: *In vitro* and *in vivo* study. *Drug Des. devel. Ther.* 9, 3705–3727. doi:10.2147/DDDT.S85302

Scioli Montoto, S., Muraca, G., and Ruiz, M. E. (2020). Solid lipid nanoparticles for drug delivery: pharmacological and biopharmaceutical aspects. *Front. Mol. Biosci.* 7, 587997. doi:10.3389/fmolb.2020.587997

Selvaraj, N., Wang, C.-K., Bowser, B., Broadt, T., Shaban, S., Burns, J., et al. (2021). Detailed protocol for the novel and scalable viral vector upstream process for AAV

gene therapy manufacturing. *Hum. Gene Ther.* 32, 850–861. doi:10.1089/hum.2020.054

Sessa, M., Lorioli, L., Fumagalli, F., Acquati, S., Redaelli, D., Baldoli, C., et al. (2016). Lentiviral haemopoietic stem-cell gene therapy in early-onset metachromatic leukodystrophy: an ad-hoc analysis of a non-randomised, open-label, phase 1/2 trial. *Lancet* 388, 476–487. doi:10.1016/S0140-6736(16)30374-9

Sudhakar, V., and Richardson, R. M. (2019). Gene therapy for neurodegenerative diseases. *Neurotherapeutics* 16, 166–175. doi:10.1007/s13311-018-00694-0

Sun, J., and Roy, S. (2021). Gene-based therapies for neurodegenerative diseases. *Nat. Neurosci.* 24, 297–311. doi:10.1038/s41593-020-00778-1

Tanaka, H., Nakatani, T., Furihata, T., Tange, K., Nakai, Y., Yoshioka, H., et al. (2018). *In vivo* introduction of mRNA encapsulated in lipid nanoparticles to brain neuronal cells and astrocytes via intracerebroventricular administration. *Mol. Pharm.* 15, 2060–2067. doi:10.1021/acs.molpharmaceut.7b01084

Taylor, C. A., Greenlund, S. F., McGuire, L. C., Lu, H., and Croft, J. B. (2017). Deaths from Alzheimer's disease—United States, 1999–2014. *MMWR. Morb. Mortal. Wkly. Rep.* 66, 521–526. doi:10.15585/mmwr.mm6620a1

Tenchov, R., Bird, R., Curtze, A. E., and Zhou, Q. (2021). Lipid Nanoparticles─From liposomes to mRNA vaccine delivery, a landscape of research diversity and advancement. *ACS Nano* 15, 16982–17015. doi:10.1021/acsnano.1c04996

Trapani, A., De Giglio, E., Cometa, S., Bonifacio, M. A., Dazzi, L., Di Gioia, S., et al. (2021). Dopamine-loaded lipid based nanocarriers for intranasal administration of the neurotransmitter: a comparative study. *Eur. J. Pharm. Biopharm.* 167, 189–200. doi:10.1016/j.ejpb.2021.07.015

Tsakiri, M., Naziris, N., and Demetzos, C. (2021). Innovative vaccine platforms against infectious diseases: under the scope of the COVID-19 pandemic. *Int. J. Pharm.* 610, 121212. doi:10.1016/j.ijpharm.2021.121212

Voysey, M., Clemens, S. A. C., Madhi, S. A., Weckx, L. Y., Folegatti, P. M., Aley, P. K., et al. (2021). Safety and efficacy of the ChAdOx1 nCoV-19 vaccine (AZD1222) against SARS-CoV-2: an interim analysis of four randomised controlled trials in Brazil, South Africa, and the UK. *Lancet* 397, 99–111. doi:10.1016/S0140-6736(20)32661-1

Wahane, A., Waghmode, A., Kapphahn, A., Dhuri, K., Gupta, A., Bahal, R., et al. (2020). Role of lipid-based and polymer-based non-viral vectors in nucleic acid delivery for next-generation gene therapy. *Molecules* 25, 2866. doi:10.3390/molecules25122866

Walther, W., and Stein, U. (2000). Viral vectors for gene transfer: a review of their use in the treatment of human diseases. *Drugs* 60, 249–271. doi:10.2165/00003495-200060020-00002

Wang, L., Chen, S.-R., Ma, H., Chen, H., Hittelman, W. N., Pan, H.-L., et al. (2018). Regulating nociceptive transmission by VGluT2-expressing spinal dorsal horn neurons. *J. Neurochem.* 147, 526–540. doi:10.1111/jnc.14588

Watanabe, M., Nishikawaji, Y., Kawakami, H., and Kosai, K.-I. (2021). Adenovirus biology, recombinant adenovirus, and adenovirus usage in gene therapy. *Viruses* 13, 2502. doi:10.3390/v13122502

Wiley, J. (2021). Alzheimer's disease facts and figures. *Alzheimers Dement.* 17, 327–406. doi:10.1002/alz.12328

Wojnarowska, Z., Smolka, W., Zotova, J., Knapik-Kowalczuk, J., Sherif, A., Tajber, L., et al. (2018). The effect of electrostatic interactions on the formation of pharmaceutical eutectics. *Phys. Chem. Chem. Phys.* 20, 27361–27367. doi:10.1039/C8CP05905E

Wuh-Liang, H., Shin-ichi, M., Sheng-Hong, T., Kai-Yuan, T., Ni-Chung, L., Yin-Hsiu, C., et al. (2012). Gene therapy for aromatic l-amino acid decarboxylase deficiency. *Sci. Transl. Med.* 4, 134ra61. doi:10.1126/scitranslmed.3003640

Yuan, Z., Zhao, L., Zhang, Y., Li, S., Pan, B., Hua, L., et al. (2018). Inhibition of glioma growth by a GOLPH3 siRNA-loaded cationic liposomes. *J. Neurooncol.* 140, 249–260. doi:10.1007/s11060-018-2966-6

Zabel, M. D. (2013). Lipopeptide delivery of siRNA to the central nervous system. *Methods Mol. Biol.* 948, 251–262. doi:10.1007/978-1-62703-140-0_17

Zhao, Y., and Huang, L. (2014). "Chapter two - lipid nanoparticles for gene delivery," in *Nonviral vectors for gene therapy*. Editors L. Huang, D. Liu, and G. Wagner (Academic Press), 13–36. doi:10.1016/B978-0-12-800148-6.00002-X

Zhu, F.-C., Guan, X.-H., Li, Y.-H., Huang, J.-Y., Jiang, T., Hou, L.-H., et al. (2020). Immunogenicity and safety of a recombinant adenovirus type-5-vectored COVID-19 vaccine in healthy adults aged 18 years or older: a randomised, double-blind, placebo-controlled, phase 2 trial. *Lancet* 396, 479–488. doi:10.1016/S0140-6736(20)31605-6

frontiers | Frontiers in Neuroscience

TYPE Original Research
PUBLISHED 26 August 2022
DOI 10.3389/fnins.2022.923957

OPEN ACCESS

EDITED BY
Divya Vohora,
Jamia Hamdard University, India

REVIEWED BY
Andrew Arrant,
University of Alabama at Birmingham, United States
Adriano Targa,
Instituto de Salud Carlos III (ISCIII), Spain

*CORRESPONDENCE
Regina H. Silva
reginahsilva@gmail.com

SPECIALTY SECTION
This article was submitted to Neuropharmacology, a section of the journal Frontiers in Neuroscience

RECEIVED 20 April 2022
ACCEPTED 04 August 2022
PUBLISHED 26 August 2022

CITATION
Cunha DMG, Becegato M, Meurer YSR, Lima AC, Gonçalves N, Bioni VS, Engi SA, Bianchi PC, Cruz FC, Santos JR and Silva RH (2022) Neuroinflammation in early, late and recovery stages in a progressive parkinsonism model in rats. *Front. Neurosci.* 16:923957. doi: 10.3389/fnins.2022.923957

Neuroinflammation in early, late and recovery stages in a progressive parkinsonism model in rats

Debora M. G. Cunha[1], Marcela Becegato[1], Ywlliane S. R. Meurer[1], Alvaro C. Lima[1], Narriman Gonçalves[1], Vinícius S. Bioni[1], Sheila A. Engi[1], Paula C. Bianchi[1], Fabio C. Cruz[1], Jose R. Santos[2] and Regina H. Silva[1]*

[1]Behavioral Neuroscience Laboratory, Department of Pharmacology, Universidade Federal de São Paulo, São Paulo, Brazil, [2]Behavioral and Evolutionary Neurobiology Laboratory, Department of Bioscience, Universidade Federal do Sergipe, Itabaiana, Brazil

Parkinson's disease (PD) is characterized by motor and non-motor signs, which are accompanied by progressive degeneration of dopaminergic neurons in the substantia nigra. Although the exact causes are unknown, evidence links this neuronal loss with neuroinflammation and oxidative stress. Repeated treatment with a low dose of reserpine—inhibitor of VMAT2—has been proposed as a progressive pharmacological model of PD. The aim of this study was to investigate whether this model replicates the neuroinflammation characteristic of this disease. Six-month-old Wistar rats received repeated subcutaneous injections of reserpine (0.1 mg/kg) or vehicle on alternate days. Animals were euthanized after 5, 10, or 15 injections, or 20 days after the 15th injection. Catalepsy tests (motor assessment) were conducted across treatment. Brains were collected at the end of each treatment period for immunohistochemical and RT-PCR analyzes. Reserpine induced a significant progressive increase in catalepsy duration. We also found decreased immunostaining for tyrosine hydroxylase (TH) in the substantia nigra *pars compacta* (SNpc) and increased GFAP + cells in the SNpc and dorsal striatum after 10 and 15 reserpine injections. Phenotyping microglial M1 and M2 markers showed increased number of CD11b + cells and percentage of CD11b + /iNOS + cells in reserpine-treated animals after 15 injections, which is compatible with tissue damage and production of cytotoxic factors. In addition, increased CD11b + /ArgI + cells were found 20 days after the last reserpine injection, together with an increment in IL-10 gene expression in the dorsal striatum, which is indicative of tissue repair or regeneration. Reserpine also induced increases in striatal interleukin TNF-alpha mRNA levels in early stages. In view of these results, we conclude that reserpine-induced progressive parkinsonism model leads to neuroinflammation in regions involved in the pathophysiology of PD, which is reversed 20 days

after the last injection. These findings reveal that withdrawal period, together with the shift of microglial phenotypes from the pro-inflammatory to the anti-inflammatory stage, may be important for the study of the mechanisms involved in reversing this condition, with potential clinical applicability.

KEYWORDS

microglia phenotypes, reserpine, rats, tyrosine hydroxylase, interleukins, catalepsy

Introduction

Neurodegenerative diseases are characterized by the loss of neuronal populations due to metabolic and toxic changes (Dugger and Dickson, 2017). These alterations lead to crucial events that precede neurodegenerative processes such as oxidative stress and neuroinflammation. Investigating these events is of paramount importance for understanding the pathophysiology of these diseases and identifying promising therapeutic targets.

With the increase in life span, the incidence of aging-related diseases becomes higher. For example, according to an epidemiological study carried out in 2017, Parkinson's Disease (PD) affects 1–2 people per 1,000 in the general population, reaching 1% in the population over 60 years old (Tysnes and Storstein, 2017). The pathophysiology of PD consists of neurodegeneration of the substantia nigra pars compacta (SNpc), affecting the dopaminergic neurons that send their projections to the dorsal striatum (Tan et al., 2020). Dopamine depletion in the striatum leads to the known motor symptoms of the disease.

Numerous studies with *postmortem*, *in vitro* and non-human animals approaches have shown that neuroinflammation is an important pathway in the PD pathogenesis, and that this process involves both innate and adaptive immunity mechanisms (Thakur and Nehru, 2014; Gelders et al., 2018; Grozdanov and Danzer, 2018). McGeer et al. (1988) were the first to report microgliosis in the brains of PD patients. Subsequently, increases in the gene expression of TNFα and other pro-inflammatory cytokines were found in the brain and cerebrospinal fluid of patients, which led to the "inflammatory hypothesis of neurodegeneration" (Mogi et al., 1994a,b, 1995).

Glial cells play a key role in neuroinflammatory processes. Microglial cells correspond to 10–15% of the central nervous system cells (Mittelbronn et al., 2001) and are resident macrophages from precursor cells of the red marrow. However, unlike peripheral macrophages, these cells cannot be excessively stimulated because they can promote harmful consequences to the neuronal tissue, including death of dopaminergic neurons (Reale et al., 2009).

Among the factors involved in this process, there is the polarization of microglia in M1 or M2 phenotypes in response to a harmful stimulus. M1 is characterized by the production of pro-inflammatory mediators such as interleukins IL1β, IL-6, IL-12, IL-17, IL-18, IL-23, tumor necrosis factor α (TNF-α) and interferon y (INF-y) (Benarroch, 2013; Nakagawa and Chiba, 2015). Nitric oxide induced synthase (iNOS) is one of the membrane markers for this phenotype (Franco and Fernández-Suárez, 2015). M2 phenotype plays a role in immunoregulation, repair and resolution of the inflammatory process, and produces a range of anti-inflammatory mediators such as cytokines IL-4 and IL-10. This phenotype expresses membrane receptors such as protein Arginase I (Arg I); Ym1 (chitinase-like protein), Fizz1 and PPAR (activated peroxisome proliferation receptor) (Subramaniam and Federoff, 2017).

Among the pharmacological animal models used to study PD are those induced by neurotoxins (such as 6-OHDA and MPTP) and by reserpine, an inhibitor of the vesicular transport of monoamines (Leão et al., 2015). In the past, reserpine was used in high doses ranging from 1 to 10 mg/kg, which rapidly induced severe motor impairments (Baskin and Salamone, 1993; Salamone and Baskin, 1996). More recent studies have proposed the repeated administration of 0.1 mg/kg of this drug, which leads to the gradual appearance of motor signs in rats or mice, similar to the condition in humans (Fernandes et al., 2012; Santos et al., 2013; Peres et al., 2016; Campêlo et al., 2017; Leão et al., 2017; Lins et al., 2018; Beserra-Filho et al., 2019; Bispo et al., 2019; Rahman et al., 2020). Furthermore, Santos et al. (2013) demonstrated that animals that received repeated reserpine at low dosages also had cognitive deficits compatible with the non-motor sings of PD. In addition, this protocol also induces reduction in the tyrosine hydroxylase (TH) labeling, increase in lipid peroxidation and increased alpha-synuclein levels in the nigro-striatal dopaminergic pathway (Fernandes et al., 2012; Santos et al., 2013; Leão et al., 2017), which are important factors related to PD pathophysiology. However, neuroinflammation processes possibly related to the alterations induced by this protocol have not been investigated yet.

The aim of this study is to investigate whether the low-dose repeated reserpine model of parkinsonism induces neuroinflammation. Specifically, considering the dopaminergic

pathway involved in PD, we investigated immunostaining for astrocytes and microglia markers, the polarization of activated microglia in the M1 (pro-inflammatory) and M2 (anti-inflammatory) microglial phenotypes, and cytokines expression.

Materials and methods

Subjects and general procedures

Six-month-old male Wistar rats (n = 80) from the Central Bioterium of the Federal University of São Paulo (CEDEME/UNIFESP) were used. All animals were housed under controlled temperature (22–23°C) and lighting (12 h light/12 h dark, with the lights on at 7:30 a.m.) and food and water were provided *ad libidum* throughout the experiment. This project was approved by the local Research Ethics Committee (CEUA N 2790010416) and all procedures were in accordance with the Brazilian law for the use of animals in scientific research (law no. 11794).

Subcutaneous administrations of reserpine or vehicle were performed according to the following experimental groups: animals that received 5 (Res or Veh 5); 10 (Res or Veh 10) or 15 (Res or Veh 15) injections and animals that after the 15th injection remained untreated for 20 days (W/D 20 days) for subsequent euthanasia. Before the beginning of the experimental procedures, the animals were handled for 20 min/day, for 5 consecutive days. Between the experimental sessions, the apparatuses were cleaned with a 5% alcohol solution.

Drug

Reserpine (Sigma Chemical Co., St. Louis, MO) was dissolved in 100 μL of glacial acetic acid and diluted in distilled water. The control solution contained the same amount of acetic acid and distilled water as the reserpine solution. Vehicle or 0.1 mg/kg reserpine were injected subcutaneously (SC) every other day.

Experimental design

Animals were randomly distributed in the above-mentioned groups. Injections were administered every other day, and the behavioral evaluations were conducted as shown in **Figure 1**.

Briefly, the catalepsy test was performed every other day before the next injection. Euthanasia was performed on the 10th, 20th, 30th, and 50th days of the protocol, according to the experimental group. Rats were either transcardially perfused (brains collected for immunohistochemistry) or euthanized by decapitation (striatum dissected and immediately frozen in liquid nitrogen for quantitative PCR) (qPCR).

Catalepsy test

Each animal was placed with the forepaws resting on a horizontal bar (positioned 9 cm from the surface in which the hind paws were supported). The duration the animal remained in an immobile posture, keeping both forepaws on the bar, was quantified by direct observation up to a maximum of 180 s. This procedure was repeated 3 times on each test day, and the average of the 3 attempts for each animal was considered for analysis.

Immunohistochemistry

After completion of each treatment duration, the animals were euthanized with an intraperitoneal injection of sodium thiopental (40 mg/kg) and transcardially perfused with 200 mL of phosphate-buffered saline (PBS), pH = 7.4, containing 500 IU of heparin (Roche, Brazil), followed by 300 mL 4.0% paraformaldehyde in 0.1 M phosphate buffer, pH 7.4. Brains were removed and post fixed in the same 4.0% paraformaldehyde solution for 4 h and subsequently transferred to a 30% sucrose solution in 0.1 M PBS, pH 7.4. Brains were serially cut in the coronal plane into 50-μm thick sections with a cryostat (Leica, Germany). The sections were placed sequentially and stored in antifreeze solution. Free-floating sections were washed 4 times (5 min each) in 0.1 M phosphate buffer, pH = 7.4, and incubated for 20 min in a 0.1 M phosphate buffer solution with hydrogen peroxide. After this period, the sections were incubated with a blocker (bovine albumin 2%, Triton X-100 0.3%) for 15 min. Afterward, sections were incubated for 18 h with one of the primary antibodies—anti-TH (Millipore, Billerica, MA, United States, 1: 5,000); anti-GFAP (Millipore, Billerica, MA, United States, 1: 1,000); anti-IBA 1 (Millipore, Billerica, MA, United States, 1: 500). After 18 h, the sections were incubated with a specific secondary antibody for each primary antibody (Vector Labs, 1: 1,000). The sections were again incubated in the avidin-biotin complex (ABC Kit, Vector Labs, United States) for 2 h and then incubated in a 0.05% solution of 3.3′ diaminobenzidine (DAB) (Sigma Company, United States) for 2 min. Subsequently, we added 100 μL of hydrogen peroxide for the deposition of the chromogen. After reaching an adequate level of color, the sections were submitted to a battery of dehydration, and mounted on slides and cover slipped with Entellan (Merck, Darmstadt, Germany).

Photomicrographs of the brain structures of interest—striatum and substantia nigra—were taken using an Olympus Microscope, BX-41, with CCD (Nikon, DXM-1200) camera

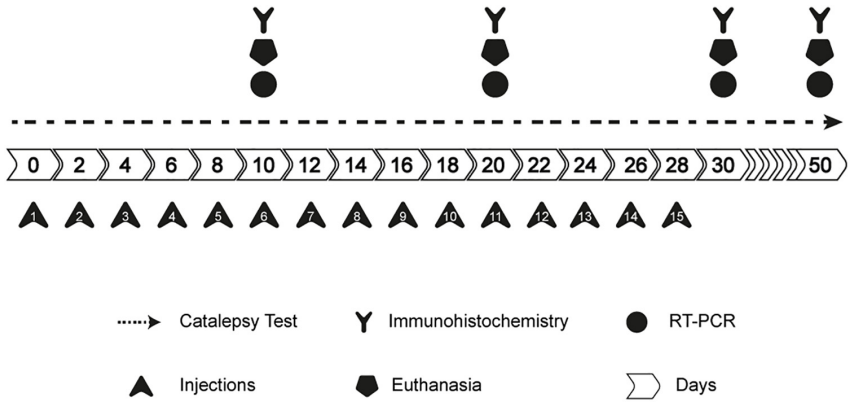

FIGURE 1
Experimental design.

attached. For each animal, 4 sections of each area were selected (one at the rostral level, two at the medium level, and one at the caudal level). The location of the region was determined based on the Paxinos and Watson rat brain atlas (2009). We delineated SNpc or Dorsal Striatum in ImageJ software and performed manual counting of the marked cells for the whole extension within each section for the analysis of TH immunostaining. Relative optical density (ROI) was used to analyze GFAP and IBA 1 markers. Values were expressed relative to Veh 5 injections group (Santos et al., 2013; Leão et al., 2017).

Immunofluorescence

After perfusion and post fixation (as described above), brain sections were washed 4 times (5 min) in 0.1 M phosphate buffer, pH = 7.4, and antigenic recovery was performed with 0.01 molar sodium citrate (pH 8.0) in a water bath at 70°C for 20 min. Subsequently, the sections remained at room temperature submerged in the citrate for 20 min. The material was washed 4 times and incubated in phosphate buffer, hydrogen peroxide and 10% methanol, remaining in agitation for 20 min. Sections were again washed and then incubated in 1% Tween 20 (Sigma) together with 1% Bovine Serum Albumin (BSA—Merck) and the primary antibodies, namely anti-CD11b (OX42—CBL1512—1: 400); anti-iNOS (AB5382- 1: 600) and anti-ArginaseI (ArgI—PA5-32267—1: 250) remaining in slow agitation for 42 h. Afterward, the cuts were washed and incubated with respective secondary antibody (Alexa Fluor® 568 and 488—1:500) for 2 h. 1 μL of DAPI (Thermo Fisher Scientific, Waltham, MA, United States) was added during the washing procedure for 5 min and then the sessions were mounted on slides and cover slipped with Vectashield (Vector Laboratories, Newark, CA, United States). Illustrative images were treated for background subtraction using the open bioimage informatics platform Icy (de Chaumont et al., 2012).

Gene expression of pro-inflammatory cytokines (TNF-α, IL-10, and IL-1β)

The quantification of pro-inflammatory cytokines in the striatum was carried out using RT-PCR. We investigated the expression of TNF-α, IL-10, and IL-1β genes. Total RNA extraction from the samples was carried out using the total RNA purification kit (Cellco Biotec) and subsequently the RNA quantification was performed in the SPECTROstar® Nano (BMG LabTech). The complementary DNA (cDNA) was synthesized from 0.5 μg total RNA using SuperScript™ III First-Strand Synthesis System kit (Invitrogen Life Technologies) according to the manufacturer's specifications.

Each 15 μL RT-PCR reaction was performed with 2.0 μL cDNA as a template, using the TaqMan® Fast Advanced Master Mix (Applied Biosystems, Thermo Fisher Scientific, Waltham, MA, United States). The RT-PCR assays were performed in duplicates on the Applied Biosystem 7500 Real-Time PCR System using TaqMan probes for TNF-α (Rn00562055_m1); IL-10 (Rn01483988_g1) and IL-1β (Rn00676333_g1). Pde10A (Rn00673152_m1) was used as the endogenous control gene. The samples were subjected to the followed PCR protocol template: 50°C for 2 min, 95°C for 10 min, then 40 cycles with denaturation at 95°C for 15 s and annealing and extension at 60°C for 1 min. Data were collected using 7500 Fast SDS Software version 1.5.1 (Applied Biosystems). Calculations of relative expression from Ct (threshold cycle) data were performed using the formula ΔCt = Ct (target gene) – Ct (Pde10A).

Statistical analysis

All data were checked for normality using the Kolmogorov-Smirnov test. Subsequently, data were analyzed by the two-way

ANOVA. Analyses *a posteriori* were performed using the Sidak's test or Bonferroni's test (catalepsy behavior). The results were considered statistically significant at $p < 0.05$. Effect size tests (partial η^2) were applied to significant results of the immunofluorescence analysis. IBM-SPSS Statistics, version 22.0 and GraphPad Prism 8.0 softwares were used to perform the analyses.

Results

Behavioral analysis

Bar catalepsy

Two-way ANOVA with repeated measures for catalepsy duration considering only the groups that went through the whole protocol revealed effects of treatment [$F = (1, 425) = 1174.1$; $p = 0.0001$]; time [$F = (24, 425) = 3.591$; $p = 0.0001$] and interaction between time and treatment [$F = (24, 425) = 2.989$; $p = 0.0001$]. *Post hoc* analysis with Bonferroni's test revealed that reserpine-treated group had increase catalepsy duration compared to vehicle from the 10th injection until the 40th day of the protocol (Figure 2). In addition, the mean catalepsy duration in all observations was compared among groups. Two-way ANOVA revealed effects of treatment [$F = (1, 70) = 30.60$; $p < 0.0001$], number of injections [$F = (3, 70) = 6.596$; $p = 0.0005$] and interaction between treatment and number of injections [$F = (3, 70) = 6.246$; $p < 0.0008$]. Sidak's *post hoc* revealed that Reserpine 15 injections group had increase catalepsy duration compared to all vehicles and all other reserpine-treated groups, as demonstrated in Table 1.

TABLE 1 Effects of repeated administration of 0.1 mg/kg reserpine (Res) or vehicle (Veh) on catalepsy test ($n = 9–10$).

Injections	Treatment	Mean catalepsy duration(s)
5 injections	Veh	01.51 ± 0.44
	Res	02.73 ± 0.75
10 injections	Veh	02.20 ± 0.38
	Res	10.72 ± 1.35
15 injections	Veh	02.12 ± 0.52
	Res	33.30 ± 8.28*
W/D 20 days	Veh	01.17 ± 0.28
	Res	16.53 ± 5.17

Data are expressed as mean ± SEM. *p < 0.05 compared to all other groups (two-way ANOVA followed by Sidak's test).

Neurochemical analysis

Immunohistochemistry for tyrosine hydroxylase

Two-way ANOVA for TH immunostaining in SNpc revealed effects of treatment [$F = (1, 28) = 51.21$; $p < 0.0001$]. Sidak's test revealed reduced number of TH + cells in the SNpc region in Res10 ($p = 0.013$) and Res 15 ($p = 0.003$) compared to their respective controls. Res10 injections also differed from the Veh 5 injections ($p = 0.018$) and Veh W/D 20 ($p < 0.001$), as shown in Figure 3. Figure 3C displays representative photomicrographs of TH immunostaining.

Immunohistochemistry for GFAP

In the dorsal striatum, two-way ANOVA revealed effects of treatment [$F = (1, 23) = 18.92$; $p < 0.0002$] and number of

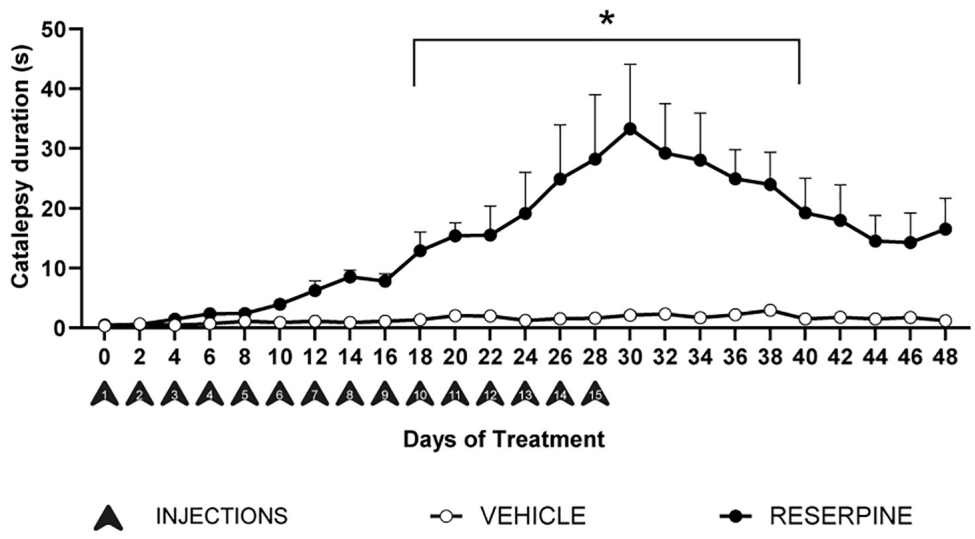

FIGURE 2
Effects of repeated administration of 0.1 mg/kg reserpine on catalepsy behavior ($n = 9–10$). Data are shown as mean + SEM.; *$p < 0.05$ comparing Reserpine and Vehicle groups (Two-way ANOVA with repeated measures followed by Bonferroni's test).

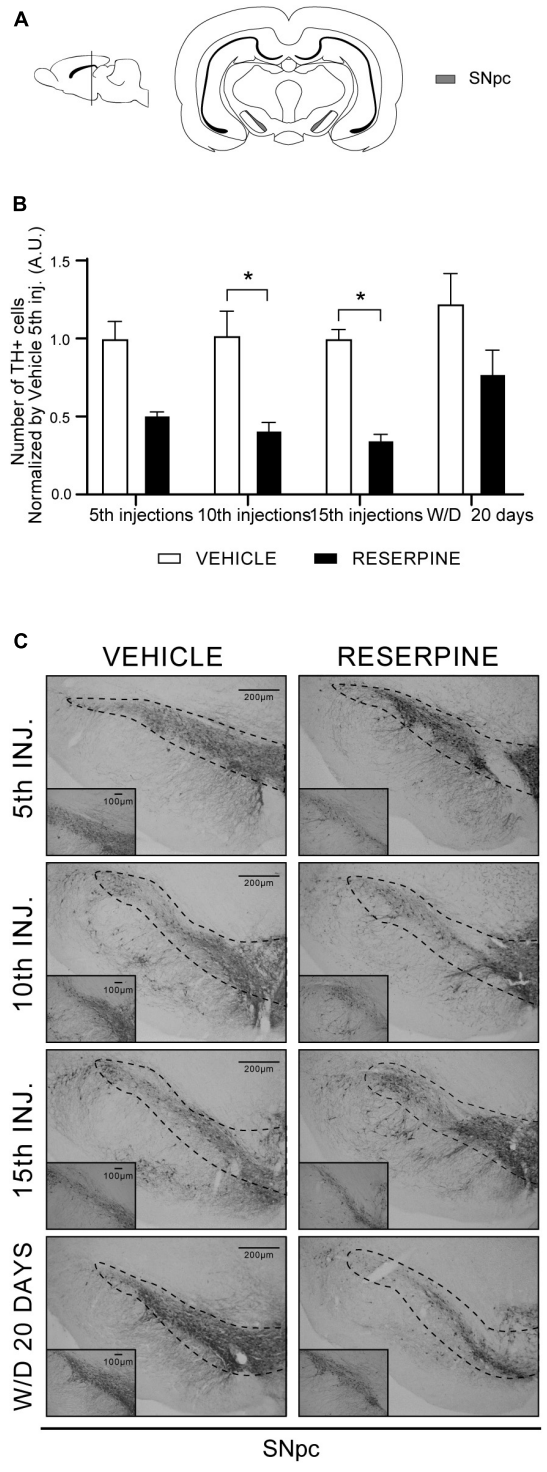

FIGURE 3
Coronal slice scheme of SNpc **(A)** effects of repeated administration of 0.1 mg/kg reserpine (n = 5) on number of TH + cells in the SNpc **(B)** and representative photomicrographs of TH immunostaining in SNpc coronal sections **(C)**. Data are shown as mean + SEM., *$p < 0.05$ comparing Reserpine and Vehicle groups (ANOVA followed by Sidak's test). Scale bar in SNpc: 200 μm and magnification 4x in overview images and scale bar of 100 μm further magnified insets (10x).

injections [F = (3, 23) = 10.07; $p < 0.0002$], as well as in the interaction between number of injections and treatment [F = (3, 23) = 6.622; $p < 0.0022$]. Sidak's *post hoc* showed that there was a significant increase of ROI in Res15 compared of all reserpine and vehicle groups (Figures 4A,B,E).

Two-way ANOVA analysis for data of the SNpc revealed effects of number of injections [F = (3, 23) = 3.459; p = 0.0329], treatment [F = (1, 23) = 81.30; $p < 0.0001$] and interaction between these factors [F = (3, 23) = 3.170; p = 0.0435]. Sidak's *post hoc* showed an increase of ROI in the SNpc after 10 (p = 0.0022) and 15 (p = 0.0002) injections of reserpine and in the 20th day after withdrawal (p = 0.0029) compared to their respective controls. In addition, Res10 group had higher ROI value compared to the Res5 group (p = 0.0300) (Figures 4C–E).

Immunohistochemistry for IBA 1

In the dorsal striatum, two-way ANOVA revealed effect of treatment [$F(1, 21) = 104.1$; $p < 0.0001$]. The Sidak's test revealed increased of ROI in all reserpine groups compared with Veh5. Furthermore, Sidak's test revealed increased of ROI of Res W/D 20 days injections compared with Veh W/D 20 days injections (p = 0.0001), as shown in Figures 5A,B,E.

In the SNpc, two-way ANOVA for IBA I immunostaining revealed effects of number of injections [$F(2, 21)$ = 8.012, p = 0.0026], treatment [$F(1, 21)$ = 14.57, p = 0.0010], as well as of the interaction between number of injections and treatment [F = (2, 21) = 7.223; $p < 0.0041$]. *A posteriori* analysis using the Sidak's test showed increased of ROI in the Res10 compared to all reserpine and vehicle groups, as shown in Figures 5C,D.

Immunofluorescence for CD11b/iNOS (microglia M1 phenotype)

In the dorsal striatum two-way ANOVA showed effects of number of injections [$F(2, 12)$ = 4.973 p = 0.026], treatment [$F(1, 12)$ = 21.91, p = 0.0005] and interaction between the factors [$F(2, 12)$ = 4.086, p = 0.044]. In Sidak's *post hoc* Res5 injections and ResW/D 20 days presented higher number of CD11b + cells when compared to their respective vehicles, as shown in Figure 6A. The Res15 injections group (p = 0.0076) showed a higher percentage of CD11b + /iNOS + cells in relation to vehicles. The effect size test indicated a large effect of treatment (η^2 = 0.54) (Figures 7A,B,E).

Two-way ANOVA for SNpc data showed treatment effect [$F(1, 12)$ = 33.01, $p < 0.0001$]. In Sidak's *post hoc* we found increased number of microglia CD11b + cells in Res15 injections (p = 0.041) and Res W/D 20 days (p = 0.002) groups compared to Veh 5 (Figure 6B). The Res W/D 20 days injections also had a higher number of CD11b + cells compared to the Veh W/D 20 days (p = 0.004) as shown in Figure 6B. Furthermore, Res15 injections group had a higher percentage of CD11b + /iNOS + cells (p = 0.033) when compared to the Veh 5

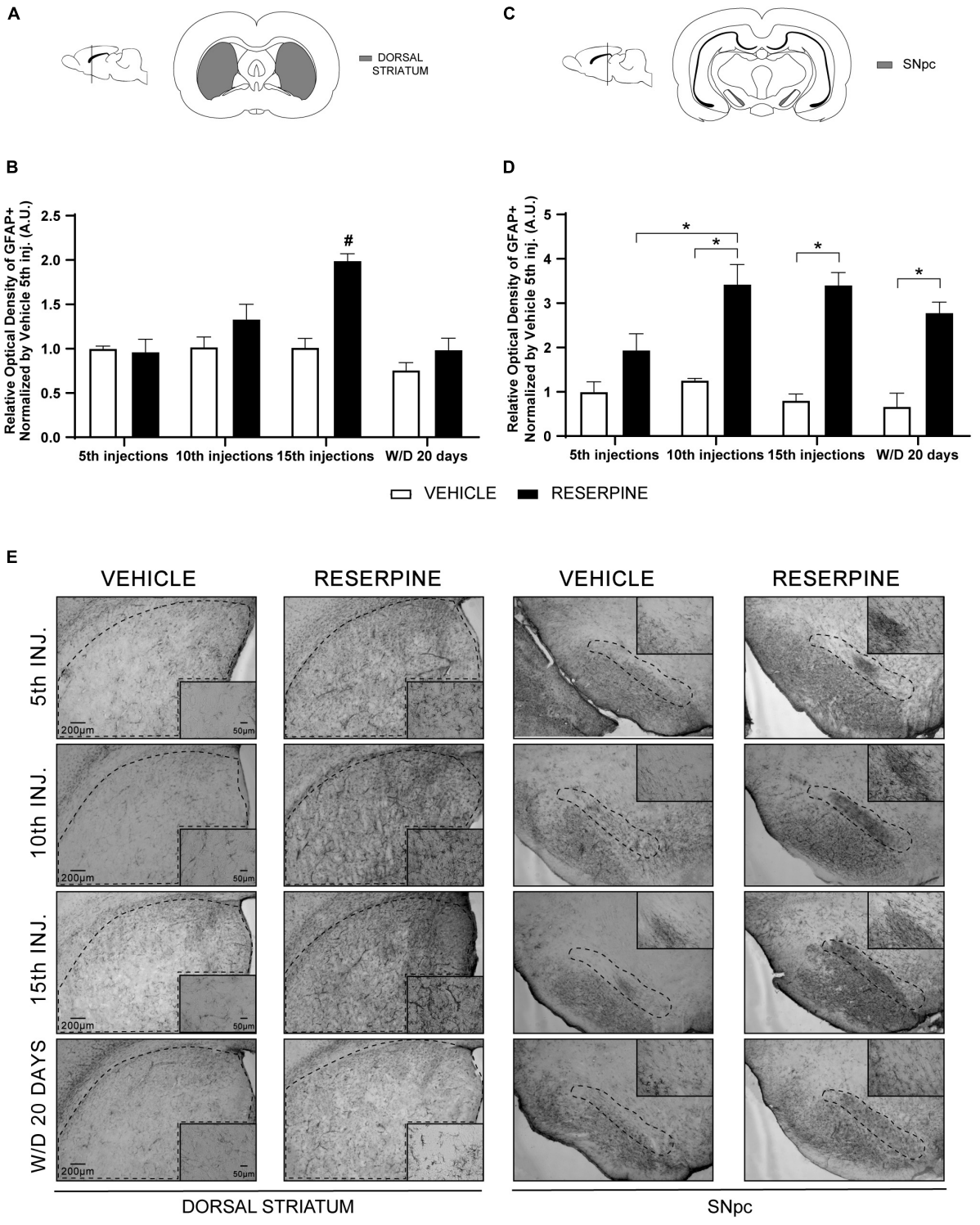

FIGURE 4
Coronal slice scheme of Dorsal Striatum **(A)** and SNpc **(C)**; effects of repeated administration of 0.1 mg/kg reserpine (n = 5) on relative optical density (ROI) of GFAP staining in Dorsal Striatum **(B)** and SNpc **(D)**; and representative photomicrographs of GFAP immunostaining in coronal sections **(E)**. Data are shown as mean + SEM. #$p < 0.05$ comparing Res15 with all Reserpine and Vehicle groups; *$p < 0.05$ comparing Reserpine and Vehicle groups (ANOVA followed by Sidak's test). Scale bar 200 µm and magnification 4x in overview images and scale bar of 50 µm further magnified insets (20x).

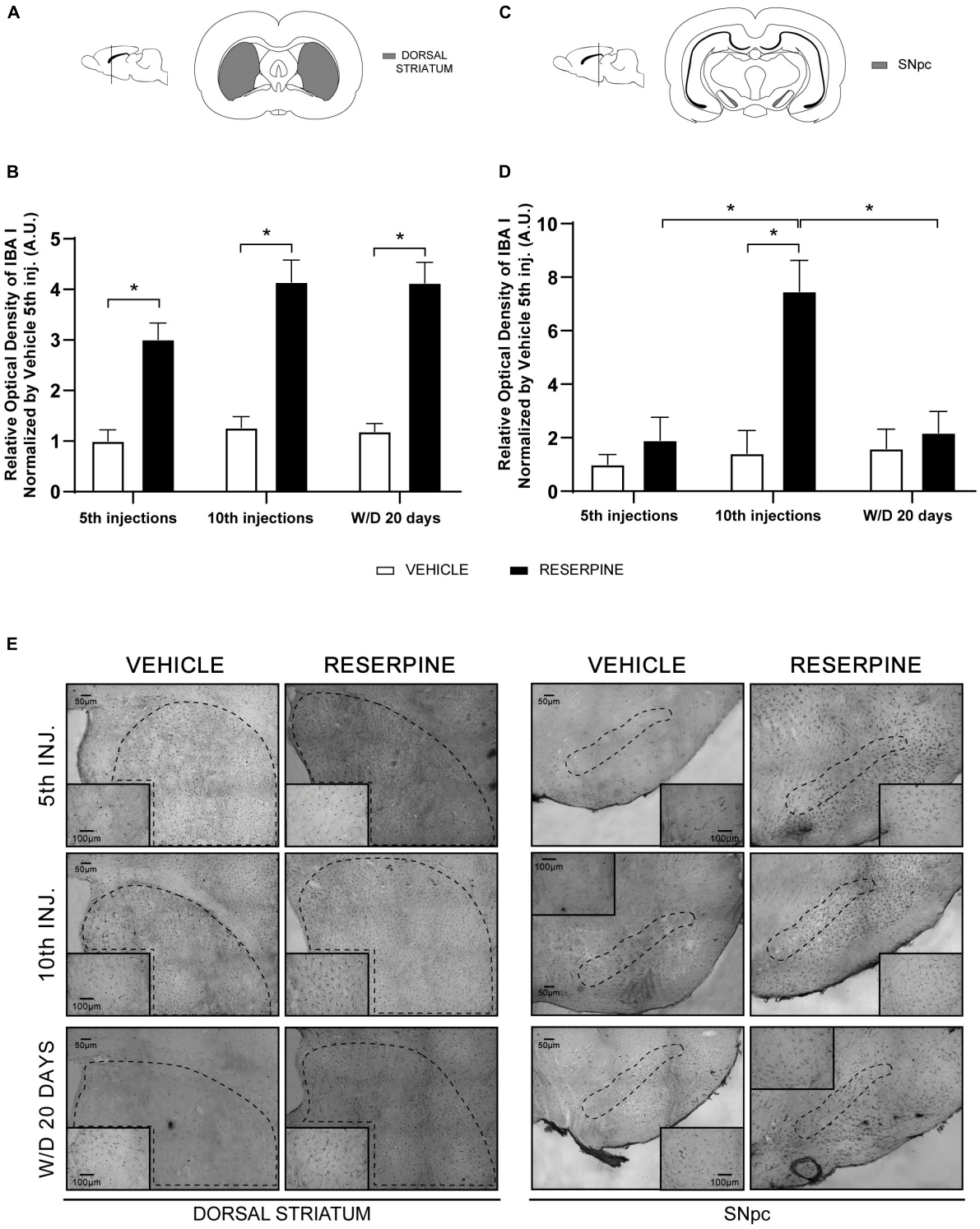

FIGURE 5
Coronal slice scheme of Dorsal Striatum **(A)** and SNpc **(C)**; effects of repeated administration of 0.1 mg/kg reserpine (n = 5) on relative optical density (ROI) for IBA 1 staining in Dorsal Striatum **(B)** and SNpc **(D)**; and representative photomicrographs in coronal sections **(E)**. Data are shown as mean + SEM, *$p < 0.05$ comparing Reserpine and Vehicle groups (ANOVA followed by Sidak's test). SNpc: scale bar 200 μm; magnification 4x in overview images and scale bar of 100 μm further magnified insets (10x). Dorsal Striatum: scale bar 300 μm; magnification 2x in overview images and scale bar of 200 μm further magnified insets (4x).

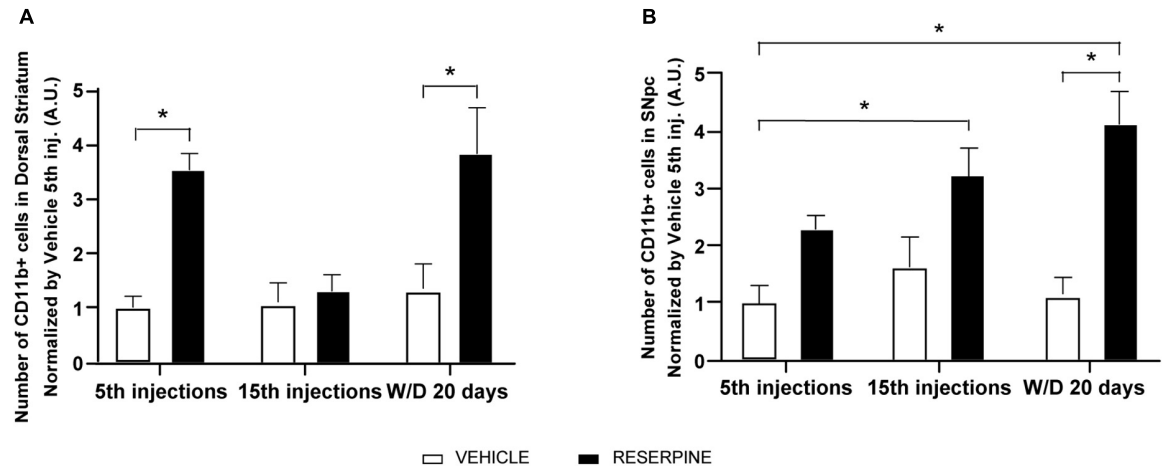

FIGURE 6
Effects of repeated administration of 0.1 mg/kg reserpine (n = 3) on number of CD11b + cells in Dorsal Striatum **(A)** e SNpc **(B)**. Data are shown as mean + SEM, *p < 0.05 comparing Reserpine and Vehicle groups (ANOVA followed by Sidak's test).

injections in the Sidak's test. The effect size test indicated a large effect of treatment (η^2 = 0.46) (**Figures 7C–E**).

Immunofluorescence CD11b/ArgI (microglia M2 phenotype)

In the dorsal striatum, we also obtained an effect of treatment [F(1.12) = 13.87; p = 0.002] and an increase in the number of CD11b + /ArgI + cells in ResW/D 20 days group when compared to the respective control group (p = 0.035). The effect size test indicated a large effect of treatment (η^2 = 0.71) (**Figure 8B**). **Figure 8D** shows the percentage of CD11b + /ArgI + cells in SNpc. Two-way ANOVA revealed effect of treatment [F(1.12) = 29.67; p < 0.0001] and interaction between factors [F(2.12) = 8.906; p = 0.004]. *A posteriori* analysis using Sidak's test revealed an increase in CD11b + /ArgI + cells in ResW/D 20 days group when compared to their respective control (p = 0.017). The effect size test indicated a large effect of treatment (η^2 = 0.54).

RT-PCR gene expression of pro-inflammatory cytokines TNF-α, IL-10, and IL-1β

Two-way ANOVA for TNF-α gene expression showed effect of treatment [F = (1, 48) = 6.713; p = 0.012]. Sidak's *post hoc* revealed an increase in TNF-α gene expression in the Res10 group in relation to Veh10 injections (p = 0.042), as shown in **Figure 9A**. Two-way ANOVA for the IL-1β gene showed a marginal effect of the treatment [F(1, 52) = 3.835; p = 0.055) (**Figure 9B**). Two-way ANOVA for IL-10 revealed effect of treatment [F(1, 32) = 5.264; p = 0.028] and Sidak's test showed increase gene expression of IL10 in ResW/D 20 days group when compared to the respective control group (p = 0.025], as shown in **Figure 9C**.

Discussion

The animal model of PD proposed by Fernandes et al. (2012) is induced by repeated administrations of a low dose (0.1 mg/kg) of reserpine. This protocol induces progressive motor changes (catalepsy, decreased spontaneous motor activity and oral dyskinesia), in addition to non-motor signs and neuronal changes compatible with the pathophysiology of PD in both rats (Fernandes et al., 2012; Santos et al., 2013; Sarmento-Silva, 2015; Brandão et al., 2017; Leão et al., 2017; Lins et al., 2017) and mice (Campêlo et al., 2017; Beserra-Filho et al., 2019). Recent adaptations of this protocol have also shown the applicability of reserpine in the study of several aspects of parkinsonism (Pereira et al., 2020; Rahman et al., 2020). In this study, we sought to extend the validation of this protocol, by verifying if neuroinflammation is induced concomitantly to the other alterations related to PD pathophysiology seen in previous studies (decreased dopaminergic markers, increased alpha-synuclein and oxidative stress). Our results reproduced the motor impairment evaluated by the catalepsy test. We demonstrated a progressive increase in the duration of catalepsy, which was statistically significant from the 10th reserpine injection until 12 days after the 15th injection (**Figure 2**), as well as an increase in the duration of catalepsy in Res 15 injections group compared with all other groups (**Table 1**). This outcome reinforces that this model mimics the progressiveness of motor decrement and corroborates the results by Santos et al. (2013). However, in that study, only 10 reserpine injections were applied, and 20 days after the 10th injection the duration of catalepsy returned to control levels. Herein, although there was a decline in the duration of catalepsy after the last injection, the difference between the groups remained, showing that the increase in the number of injections precluded the reversion

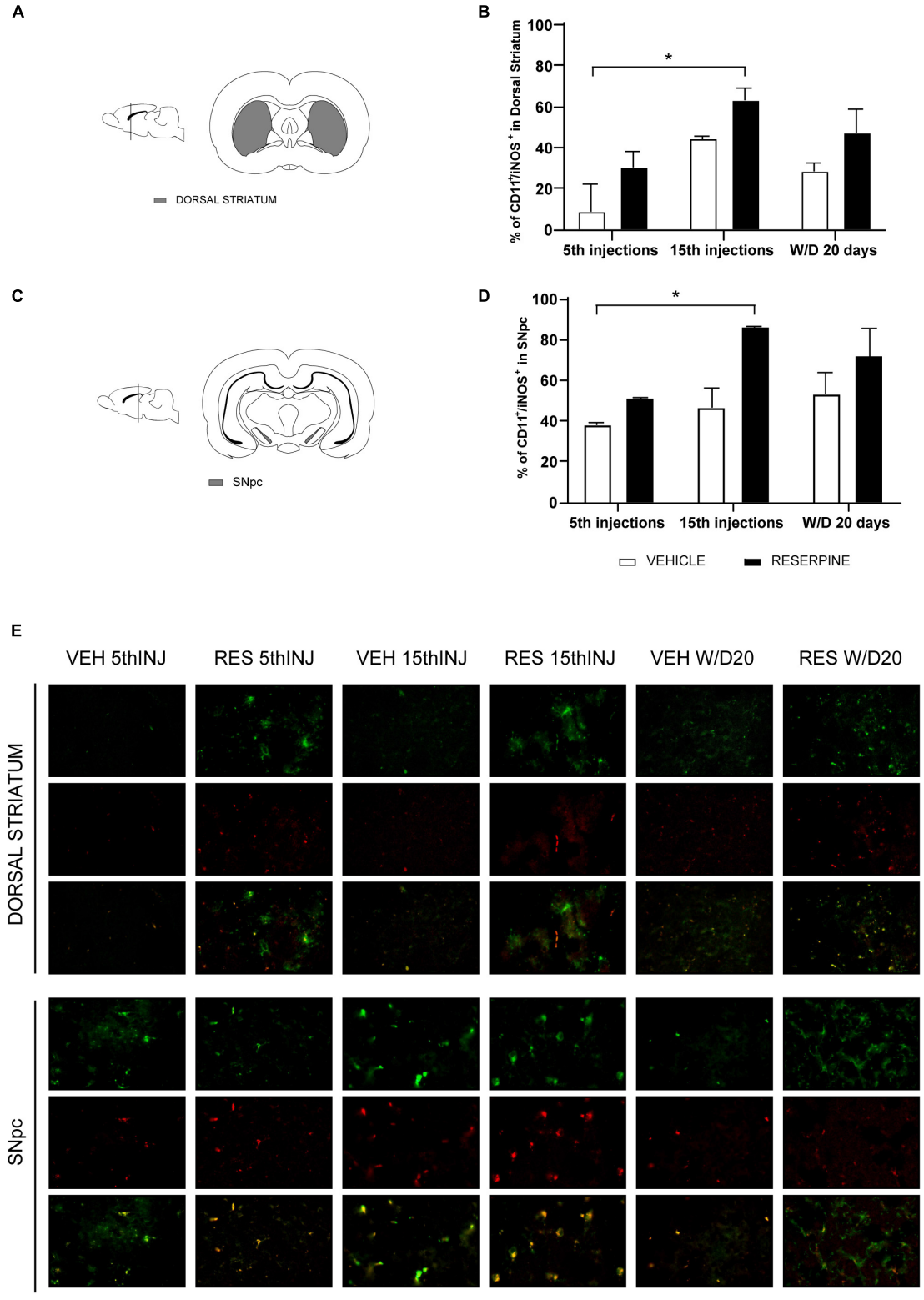

FIGURE 7
Coronal slice scheme of Dorsal Striatum **(A)** and SNpc **(C)**; effects of repeated administration of 0.1 mg/kg reserpine (n = 3) on immunofluorescence with double labeling for CD11b (green) and iNOS (red) expressed by percentage of CD11 + /iNOS + cells in Dorsal Striatum **(B)** and SNpc **(D)**; and representative photomicrographs of immunofluorescence in SNpc coronal sections and Dorsal Striatum **(E)**. Data are shown as mean + SEM, *$p < 0.05$ comparing Reserpine and Vehicle groups (ANOVA followed by Sidak's test). Magnification 40x.

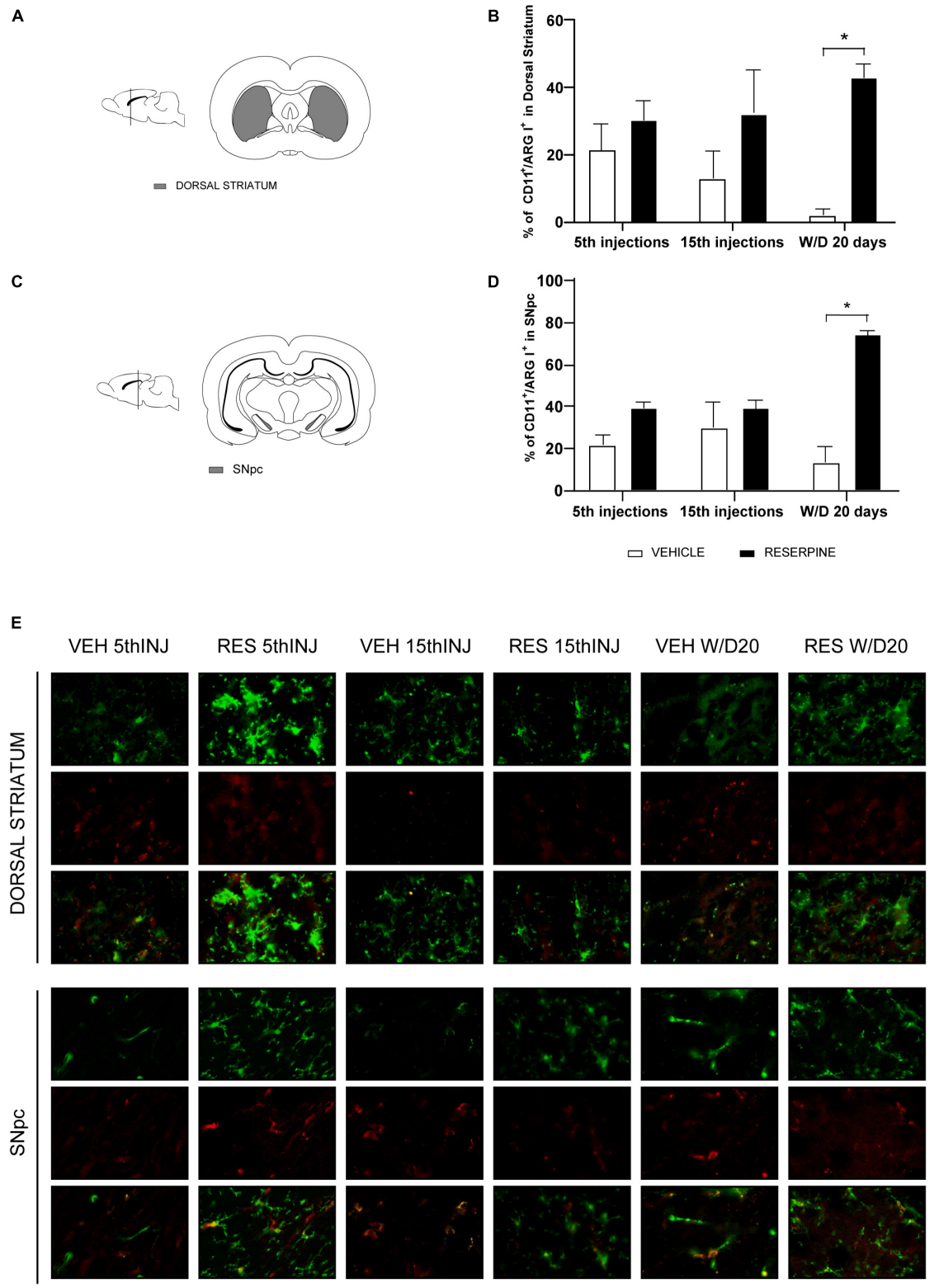

FIGURE 8
Coronal slice scheme of Dorsal Striatum **(A)** and SNpc **(C)**; effects of repeated administration of 0.1 mg/kg reserpine (n = 3) on immunofluorescence with double labeling for CD11b (green) and ArgI (red) expressed by percentage of CD11 + /ArgI + cells in Dorsal Striatum **(B)** and SNpc **(D)**; and representative photomicrographs of immunofluorescence in SNpc coronal sections and Dorsal Striatum **(E)**. Data are shown as mean + SEM, *$p < 0.05$ comparing Reserpine and Vehicle groups (ANOVA followed by Sidak's test). Magnification 40x.

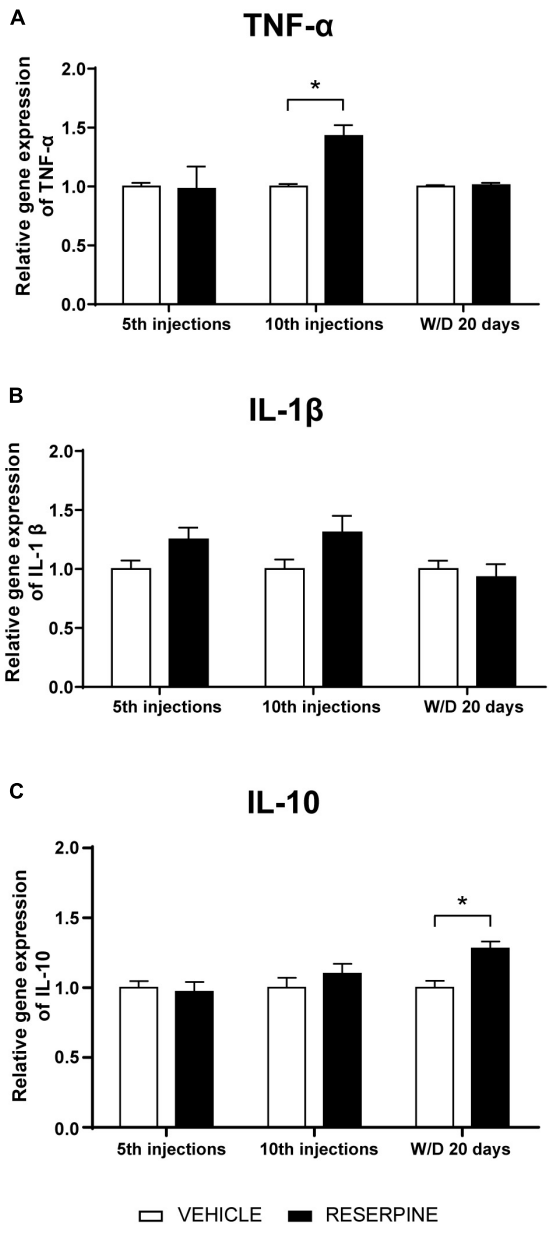

FIGURE 9
Effects of repeated administration of 0.1 mg/kg reserpine (n = 6–8) on gene expression of the cytokines TNF-α **(A)**, IL-1β **(B)**, and IL-10 **(C)** in the dorsal striatum of rats submitted to 5 and 10 injections of reserpine or vehicle and 20 days after the last injection. Data are shown as mean + SEM, *$p < 0.05$ comparing Reserpine and Vehicle groups (ANOVA followed by Sidak's test).

of the motor deficits after treatment interruption. It should be noted that 20 days after the last injection, the increase in catalepsy that is still present (although not statistically significant in the last measures) is hardly due to the acute dopamine depletion caused by each injection of reserpine.

Furthermore, **Figure 3** shows a decrease in TH + cells in the SNpc after the 10th and 15th injections, with a partial recovery in withdrawal. This partial recovery corresponds to the reduction in the catalepsy curve in the withdrawal period. These results have also been obtained by other studies with the reserpine model, although there were small differences in protocol and dosage (Santos et al., 2013; de Freitas et al., 2016; Leão et al., 2017). To date, there is no evidence of dopaminergic neuronal death induced by this low-dose reserpine treatment *in vivo*. However, different protocols of reserpine administration induce neuronal effects related to neurodegeneration, such as oxidative stress, α-synuclein and morphology alterations (Abílio et al., 2004; Fernandes et al., 2012; Lee et al., 2015; Reckziegel et al., 2016; Leão et al., 2017). In addition, the neonatal administration of a high dose of reserpine induced neuronal loss and alpha-synuclein brain inclusions (van Onselen and Downing, 2021). Importantly, the irreversibility of neuronal impairment in conventional toxin models has also been questioned. For example, a study showed partial recovery over time after infusion of 6-OHDA (Deumens et al., 2002). In this way, the reversibility of dopaminergic dysfunction after a damaging intervention could be an interesting phenomenon to study potential therapeutic targets.

The above observations support that this protocol of repeated low-dose reserpine administration, despite probably not irreversible, induces long-term changes related to PD. As discussed below, the present study showed that parameters related to neuroinflammation, an important feature of PD pathophysiology, are altered after repeated reserpine treatment.

Increased number of astrocytes in the SNpc and striatum has long been evidenced in PD (Sheng et al., 1993; Hirsch and Hunot, 2009). These cells are over activated by microglia and produce growth factors that enable neuroprotection, and they also participate in the oxidative stress process (Niranjan et al., 2012). In line with these findings, we demonstrated an increase in GFAP + immunoreactive cells in Res10, 15 and ResW/D 20 days in SNpc and in Res15 injections in the dorsal striatum (**Figure 4**). This result indicates that even 20 days after the end of reserpine administration, inflammation remains in the SNpc, but not in the dorsal striatum, which corroborates both the long-term neuronal changes induced by the treatment and the partial recovery after withdrawal discussed above.

Microglial cells participate in a key pathway of neuroinflammation in neurodegenerative diseases, especially PD (Zhao et al., 2015), and are found in larger quantities in the SNpc compared to other brain areas, even in the healthy brain (Kim et al., 2000). Moreover, this cell type can alternate between neurotoxic and neurotrophic actions, mediating the production of pro or anti-inflammatory cytokines and molecules related to reactive oxygen species (ROS), leading to neuronal death (Trudler et al., 2014). Here, we showed that low-dose repeated reserpine increased immunohistochemical staining of the microglia marker ionized calcium binding adapter molecule 1 (IBA-1), which persisted at least 20 days after treatment

withdrawal, in line with other long-term alterations mentioned above (**Figure 5**).

We also investigated the profile of microglia phenotypes in the different phases of the experimental design. We performed double labeling for activated microglia M1 phenotype using the microglia markers CD11b and iNOS and M2 phenotype using CD11b and ArgI markers, according to previous studies (Zhao et al., 2015; He et al., 2016). We demonstrated an increase in CD11b + microglia in the SNpc of Res15 and ResW/D 20 animals, and in the dorsal striatum in Res5 and ResW/D 20 groups (**Figure 6**). However, the highest percentage of M1 microglia (CD11b + /iNOS +) was found in the Res15 group for both areas (**Figure 7**). This reinforces that the period corresponding to 15 reserpine injections shows an established inflammatory process that progressively increased from the beginning of treatment. On the other hand, the results of the CD11b + /ArgI + analysis demonstrated that M2 microglia is significantly higher in SNpc and dorsal striatum only in Res W/D 20 rats (**Figure 8**). These results are consistent with features of the neuroinflammatory process. Indeed, an insult/injury promotes tissue damage leading to the production of cytotoxic factors such as iNOS, characterizing the M1 (cytotoxic) phenotype (Chhor et al., 2013). The same cell turns to an M2- repair/regenerative phenotype over time (Chhor et al., 2013; Tang and Le, 2016). ArgI catalytic activity produces molecules that repair extracellular matrix and mitochondrial function (Chhor et al., 2013). However, the hypothesis that there is a shift from M1 to M2 microglial phenotype across reserpine treatment and recovery should be considered with caution. Indeed, there are some limitations regarding these analyses. First, due to technical issues, the sample sizes of the immunofluorescence assays are small (although effect size tests indicated large effects for all significant differences). Second, additional M1 and M2 markers would add strong evidence of this claim and should be included in future studies.

Nevertheless, corroborating our observations, an increase in CD11b + /iNOS + microglia was shown in an MPTP model of PD. Rodents submitted to the MPTP model were treated with fasudil, which limits axonal growth, leading to axonal degeneration. As a result, fasudil induces polarization to M2 microglia as well as suppression of inflammatory responses (IL-1β; TNF-α and NF- κB-p65) (Zhao et al., 2015). 6-OHDA led to polarization toward the M1 state in BV2 microglia with increased IL6, IL-1β, TNF-α, and suppressed M2 phenotype (Zhang et al., 2017).

It should be noted that microglial activation is closely associated with aggregated misfolded proteins such as α-synuclein (Rojanathammanee et al., 2011; Tang and Le, 2016). Aggregated α-synuclein released into the extracellular space from dead dopaminergic neurons leads to an increase in reactive oxygen species (ROS) and cytokines (Zhang et al., 2005; Lee et al., 2010). A previous study of our group showed an increase in immunostaining for α-synuclein in the substantia nigra of rats that received 15 injections of 0.1 mg/kg of reserpine (Leão et al., 2017). Herein, we investigated α-synuclein staining after 5 and 10 reserpine injections and in the withdrawal period (see **Supplementary material**). The results showed an increase in α-synuclein labeling in groups treated with 5 and 10 injections in the SNpc and dorsal striatum when compared to the Veh 5 group. Additionally, in the striatum, the Res W/D 20 days group also had a higher ROI compared to the Veh5 injections. It is possible that the increased TNF-α gene expression in the dorsal striatum after 10 injections found here was related to the α-synuclein peak identified in this same period (**Supplementary Figure 1**).

We also investigated the gene expression of pro-inflammatory cytokines (TNF-α and IL-1β), which can be produced by both astrocytes and activated microglia in addition to damaged neurons. An increase in TNF-α gene expression was observed after the 10th reserpine injection (**Figure 9A**). This –result corroborates the fact that this cytokine is usually produced in the early phase of inflammation (Frankola et al., 2011). As described above, with the progression of the neuroinflammatory process, there was subsequent M1 microglial activation (observed in the group that received 15 injections). In the reserpine group, IL-1β did not differ from the control group in the *post hoc* analysis, but there was a marginal effect of the treatment in the two-way ANOVA test (**Figure 9B**).

Increased proinflammatory cytokines have been reported after treatment with 1 mg/kg reserpine. In that study (Arora and Chopra, 2013), three consecutive days of reserpine administration induced an increase in TNF-α and IL-1β levels in the cerebral cortex and hippocampus. Here, we did not observe changes in the IL-1β gene expression, as mentioned above. However, regarding reserpine effects on neuroinflammation parameters, the present results are unprecedented in the literature due to the analysis of microglia polarization, astrocyte evaluation and the protocol used (low dose, various treatment durations and long-term consequences in the withdrawal period).

We also investigated the gene expression of cytokine IL-10, an anti-inflammatory molecule that acts in periods of tissue repairment. IL-10 gene expression was increased during the withdrawal period (**Figure 9C**), in accordance with M2 microglia activation in the same period. These data indicate a possible process of CNS restoration following the reserpine-induced inflammatory process. IL-10 has been shown to induce M2 phenotype of microglia or promote the switch from the M1 to M2. Also, this cytokine can suppress iNOS expression by inhibiting NFkB. Interestingly, IL-10 and vitamin D have been tested in pre-clinical trials as possible candidates for a more effective treatment in PD, by reducing the neuroinflammation (Schwenkgrub et al., 2013).

Finally, it is important to mention that due to technical constraints, it was not possible to evaluate all groups in immunofluorescence and in the gene expression assays.

TABLE 2 Summary of the results.

Parameter	Figure	5 Res	10 Res	15 Res	W/D 20 days
Catalepsy duration	2	ns	↑	↑	ns
Tyrosine Hydroxylase/SNpc (IH)	3	ns	↑	↑	ns
GFAP/DS (IH)	4	ns	ns	↑	ns
GFAP/SNpc (IH)	4	ns	↑	↑	↑
IBA 1/DS (IH)	5	↑	↑	ni	↑
IBA 1/SNpc (IH)	5	ns	↑	ni	ns
CD11b/DS (IH)	6	↑	ni	ns	↑
CD11b/SNpc (IH)	6	↑	ni	↑	↑
CD11b + iNOS/DS (IF)	7	ns	ni	↑	ns
CD11b + iNOS/SNpc (IF)	7	ns	ni	↑	ns
CD11b + Arg I/DS (IF)	8	ns	ni	ns	↑
CD11b + Arg I/SNpc (IF)	8	ns	ni	ns	↑
TNF-α/DS (RTPCR)	9	ns	↑	ni	ns
IL-1β/DS (RTPCR)	9	ns	ns	ni	ns
IL-10/DS (RTPCR)	9	ns	ns	ni	↑
α-synuclein/DS (IH)	Suppl.	↑	↑	ni	↑
α-synuclein/SNpc (IH)	Suppl.	↑	↑	ni	ns

Outcomes after 5, 10, or 15 injections of reserpine (Res) or after 20 days of treatment withdrawal (W/D 20 days) compared to vehicle-treated groups.↑, increase; ↓, decrease; ns, no significant effect; ni, not included in the analysis; DS, dorsal striatum; SNpc, substantia nigra pars compacta; IH, immunohistochemistry assay; IF, immunofluorescence assay.

In this respect, although the completion of experimental groups in all analyses would be ideal, the lack of some time points does not seem to hinder the general interpretation of the findings. Indeed, as illustrated in Table 2, the peak of the neuronal alteration indicative of neuroinflammation and dopaminergic deficits occur between the 10th and 15th injections, with some of them starting to appear after the 5th injection, even before the emergence of the motor deficit. Overall, these alterations had partial or total recovery 20 days after withdrawal, concomitant to increased anti-inflammatory indicatives. Thus, our results showed that reserpine-induced PD model leads to neuroinflammation, which reinforces the etiological validation of this model and provides tools for the study of this important process in neurodegenerative diseases.

Data availability statement

The raw data supporting the conclusions of this article will be made available by the authors, without undue reservation.

Ethics statement

The animal study was reviewed and approved by the Comissão de ética no uso de animais—Universidade Federal de São Paulo.

Author contributions

DC and RS designed the study. DC coordinated and performed the experiments, conducted statistical analysis, and wrote the manuscript. MB, YM, AL, NG, VB, and JS participated in the data collection. SE, PB, and FC coordinated and participated in RT-PCR procedures. VB and JS participated in Figures design. JS and YM contributed to technical standardizations and theoretical discussions. RS coordinated the study and revised the final version. All authors contributed to the article and approved the submitted version.

Funding

This study was financed in part by the Coordenação de Aperfeiçoamento de Pessoal de Nível Superior—Brasil (CAPES, Finance Code 001) and the Fundação de Amparo à Pesquisa do Estado de São Paulo (FAPESP, grants 2015/03354-3, 2017/26253-3, and 2019/02821-8). RS and JS were recipients of research fellowships from Conselho Nacional de Desenvolvimento Científico e Tecnológico (CNPq, grants 313631/2021-2 and 308837/2020-7).

Acknowledgments

We would like to thank Claudenice Moreira dos Santos for capable technical assistance.

Conflict of interest

The authors declare that the research was conducted in the absence of any commercial or financial relationships that could be construed as a potential conflict of interest.

Publisher's note

All claims expressed in this article are solely those of the authors and do not necessarily represent those of their affiliated organizations, or those of the publisher, the editors and the reviewers. Any product that may be evaluated in this article, or claim that may be made by its manufacturer, is not guaranteed or endorsed by the publisher.

Supplementary material

The Supplementary Material for this article can be found online at: https://www.frontiersin.org/articles/10.3389/fnins.2022.923957/full#supplementary-material

References

Abílio, V. C., Silva, R. H., Carvalho, R. C., Grassl, C., Calzavara, M. B., Registro, S., et al. (2004). Important role of striatal catalase in aging- and reserpine-induced oral dyskinesia. *Neuropharmacology* 47, 263–272. doi: 10.1016/j.neuropharm.2004.04.003

Arora, V., and Chopra, K. (2013). Possible involvement of oxido-nitrosative stress induced neuro-inflammatory cascade and monoaminergic pathway: Underpinning the correlation between nociceptive and depressive behaviour in a rodent model. *J. Affect. Disord.* 151, 1041–1052. doi: 10.1016/j.jad.2013.08.032

Baskin, P., and Salamone, J. (1993). Vacuous jaw movements in rats induced by acute reserpine administration: Interactions with different doses of apomorphine. *Pharmacol. Biochem. Behav.* 46, 793–797. doi: 10.1016/0091-3057(93)90203-6

Benarroch, E. E. (2013). Microglia: Multiple roles in surveillance, circuit shaping, and response to injury. *Neurology* 81, 1079–1088. doi: 10.1212/WNL.0b013e3182a4a577

Beserra-Filho, J. I. A., de Macêdo, A. M., Leão, A. H., Bispo, J. M. M., Santos, J. R., de Oliveira-Melo, A. J., et al. (2019). Eplingiella fruticosa leaf essential oil complexed with β-cyclodextrin produces a superior neuroprotective and behavioral profile in a mice model of Parkinson's disease. *Food Chem. Toxicol.* 124, 17–29. doi: 10.1016/j.fct.2018.11.056

Bispo, J. M. M., Melo, J. E. C., Gois, A. M., Leal, P. C., Lins, L. C. R. F., Souza, M. F., et al. (2019). Sex differences in the progressive model of parkinsonism induced by reserpine in rats. *Behav. Brain Res.* 363, 23–29. doi: 10.1016/j.bbr.2019.01.041

Brandão, L. E. M., Nôga, D. A. M. F., Dierschnabel, A. L., Campêlo, C. L. D. C., Meurer, Y. D. S. R., Lima, R. H., et al. (2017). *Passiflora cincinnata* extract delays the development of motor signs and prevents dopaminergic loss in a mice model of Parkinson's disease. *Evid. Based Complement. Altern. Med.* 2017, 14–16. doi: 10.1155/2017/8429290

Campêlo, C. L. C., Santos, J. R., Silva, A. F., Dierschnabel, A. L., Pontes, A., Cavalcante, J. S., et al. (2017). Exposure to an enriched environment facilitates motor recovery and prevents short-term memory impairment and reduction of striatal BDNF in a progressive pharmacological model of Parkinsonism in mice. *Behav. Brain Res.* 328, 138–148. doi: 10.1016/j.bbr.2017.04.028

Chhor, V., le Charpentier, T., Lebon, S., Oré, M. V., Celador, I. L., Josserand, J., et al. (2013). Characterization of phenotype markers and neuronotoxic potential of polarised primary microglia in vitro. *Brain Behav. Immun.* 32, 70–85. doi: 10.1016/j.bbi.2013.02.005

de Chaumont, F., Dallongeville, S., Chenouard, N., Hervé, N., Pop, S., Provoost, T., et al. (2012). Icy: An open bioimage informatics platform for extended reproducible research. *Nat. Methods* 9, 690–696. doi: 10.1038/nmeth.2075

de Freitas, C. M., Busanello, A., Schaffer, L. F., Peroza, L. R., Krum, B. N., Leal, C. Q., et al. (2016). Behavioral and neurochemical effects induced by reserpine in mice. *Psychopharmacology (Berl.).* 233, 457–467. doi: 10.1007/s00213-015-4118-4

Deumens, R., Blokland, A., and Prickaerts, J. (2002). Modeling Parkinson's disease in rats: An evaluation of 6-OHDA lesions of the nigrostriatal pathway. *Exp. Neurol.* 175, 303–317. doi: 10.1006/exnr.2002.7891

Dugger, B. N., and Dickson, D. W. (2017). Pathology of neurodegenerative diseases. *Cold Spring Harb. Perspect. Biol.* 9:a028035. doi: 10.1101/cshperspect.a028035

Fernandes, V. S., Santos, J. R., Leão, A. H. F. F., Medeiros, A. M., Melo, T. G., Izídio, G. S., et al. (2012). Repeated treatment with a low dose of reserpine as a progressive model of Parkinson's disease. *Behav. Brain Res.* 231, 154–163. doi: 10.1016/j.bbr.2012.03.008

Franco, R., and Fernández-Suárez, D. (2015). Alternatively activated microglia and macrophages in the central nervous system. *Prog. Neurobiol.* 131, 65–86. doi: 10.1016/j.pneurobio.2015.05.003

Frankola, K. A., Greig, N. H., Luo, W., and Tweedie, D. (2011). Targeting TNF-alpha to elucidate and ameliorate neuroinflammation in neurodegenerative diseases. *CNS Neurol. Disord. Drug Targets* 10, 391–403. doi: 10.2174/187152711794653751

Gelders, G., Baekelandt, V., and van der Perren, A. (2018). Linking neuroinflammation and neurodegeneration in Parkinson's disease. *J. Immunol. Res.* 2018, 1–12. doi: 10.1155/2018/4784268

Grozdanov, V., and Danzer, K. M. (2018). Release and uptake of pathologic alpha-synuclein. *Cell Tissue Res.* 373, 175–182. doi: 10.1007/s00441-017-2775-9

He, Q., Li, Y. H., Guo, S. S., Wang, Y., Lin, W., Zhang, Q., et al. (2016). Inhibition of Rho-kinase by Fasudil protects dopamine neurons and attenuates inflammatory response in an intranasal lipopolysaccharide-mediated Parkinson's model. *Eur. J. Neurosci.* 43, 41–52. doi: 10.1111/ejn.13132

Hirsch, E. C., and Hunot, S. (2009). Neuroinflammation in Parkinson's disease: A target for neuroprotection? *Lancet Neurol.* 8, 382–397. doi: 10.1016/S1474-4422(09)70062-6

Kim, W. G., Mohney, R. P., Wilson, B., Jeohn, G. H., Liu, B., and Hong, J. S. (2000). Regional difference in susceptibility to lipopolysaccharide-induced neurotoxicity in the rat brain: Role of microglia. *J. Neurosci.* 20, 6309–6316. doi: 10.1523/jneurosci.20-16-06309.2000

Leão, A. H. F. F., Meurer, Y. S. R., da Silva, A. F., Medeiros, A. M., Campêlo, C. L. C., Abílio, V. C., et al. (2017). Spontaneously hypertensive rats (SHR) are resistant to a reserpine-induced progressive model of Parkinson's disease: Differences in motor behavior, tyrosine hydroxylase and α-synuclein expression. *Front. Aging Neurosci.* 9:78. doi: 10.3389/fnagi.2017.00078

Leão, A. H. F. F., Sarmento-Silva, A. J., Santos, J. R., Ribeiro, A. M., and Silva, R. H. (2015). Molecular, neurochemical, and behavioral hallmarks of reserpine as a model for Parkinson's disease: New perspectives to a long-standing model. *Brain Pathol.* 25, 377–390. doi: 10.1111/bpa.12253

Lee, E.-J., Woo, M.-S., Moon, P.-G., Baek, M.-C., Choi, I.-Y., Kim, W.-K., et al. (2010). α-Synuclein activates microglia by inducing the expressions of matrix metalloproteinases and the subsequent activation of protease-activated receptor-1. *J. Immunol.* 185, 615–623. doi: 10.4049/jimmunol.0903480

Lee, K. I., Kim, M. J., Koh, H., Lee, J. I., Namkoong, S., Oh, W. K., et al. (2015). The anti-hypertensive drug reserpine induces neuronal cell death through inhibition of autophagic flux. *Biochem. Biophys. Res. Commun.* 462, 402–408. doi: 10.1016/j.bbrc.2015.04.145

Lins, L. C. R. F., Souza, M. F., Bispo, J. M. M., Gois, A. M., Melo, T. C. S., Andrade, R. A. S., et al. (2018). Carvacrol prevents impairments in motor and neurochemical parameters in a model of progressive Parkinsonism induced by reserpine. *Brain Res. Bull.* 139, 9–15. doi: 10.1016/j.brainresbull.2018.01.017

Lins, L., Souza, M., Cintra, R., Medeiros, K., Macêdo-Lima, M., Moraes, S. Z. C., et al. (2017). Attenuation of motor deficits by hydroethanolic extract of *Poincianella pyramidalis* in a Parkinson's disease model. *Bol. Latin. Am. Del Caribe De Plant. Med. Aromatic.* 16, 150–161.

McGeer, P. L., Itagaki, S., Boyes, B. E., and McGeer, E. G. (1988). Reactive microglia are positive for HLA-DR in the: Substantia nigra of Parkinson's and Alzheimer's disease brains. *Neurology* 38, 1285–1285. doi: 10.1212/wnl.38.8.1285

Mittelbronn, M., Dietz, K., Schluesener, H. J., and Meyermann, R. (2001). Local distribution of microglia in the normal adult human central nervous system differs by up to one order of magnitude. *Acta Neuropathol.* 101, 249–255. doi: 10.1007/s004010000284

Mogi, M., Harada, M., Kondo, T., Narabayashi, H., Riederer, P., and Nagatsu, T. (1995). Transforming growth factor-β1 levels are elevated in the striatum and in ventricular cerebrospinal fluid in Parkinson's disease. *Neurosci. Lett.* 193, 129–132. doi: 10.1016/0304-3940(95)11686-Q

Mogi, M., Harada, M., Riederer, P., Narabayashi, H., Fujita, K., and Nagatsu, T. (1994a). Tumor necrosis factor-α (TNF-α) increases both in the brain and in the cerebrospinal fluid from Parkinsonian patients. *Neurosci. Lett.* 165, 208–210. doi: 10.1016/0304-3940(94)90746-3

Mogi, M., Mogi, M., Harada, M., Harada, M., Kondo, T., Kondo, T., et al. (1994b). Interleukin-1 beta, interleukin-6, epidermal growth factor and transforming growth factor-alpha are elevated in the brain from parkinsonian patients. *Neurosci. Lett.* 180, 147–150. doi: 10.1016/0304-3940(94)90508-8

Nakagawa, Y., and Chiba, K. (2015). Diversity and plasticity of microglial cells in psychiatric and neurological disorders. *Pharmacol. Ther.* 154, 21–35. doi: 10.1016/j.pharmthera.2015.06.010

Niranjan, R., Rajasekar, N., Nath, C., and Shukla, R. (2012). The effect of guggulipid and nimesulide on MPTP-induced mediators of neuroinflammation in rat astrocytoma cells, C6. *Chem. Biol. Interact.* 200, 73–83. doi: 10.1016/j.cbi.2012.08.008

Pereira, A. G., Poli, A., Matheus, F. C., de Bortoli da Silva, L., Fadanni, G. P., Izídio, G. S., et al. (2020). Temporal development of neurochemical and cognitive impairments following reserpine administration in rats. *Behav. Brain Res.* 383:112517. doi: 10.1016/j.bbr.2020.112517

Peres, F. F., Levin, R., Almeida, V., Zuardi, A. W., Hallak, J. E., Crippa, J. A., et al. (2016). Cannabidiol, among other cannabinoid drugs, modulates prepulse inhibition of startle in the SHR animal model: Implications for schizophrenia pharmacotherapy. *Front. Pharmacol.* 7:303. doi: 10.3389/fphar.2016.00303

Rahman, M. M., Chakraborti, R. R., Potol, M. A., Abir, A. H., Sharmin, O., Alam, M., et al. (2020). Epalrestat improves motor symptoms by reducing oxidative stress and inflammation in the reserpine induced mouse model of Parkinson's disease. *Anim. Models Exp. Med.* 3, 9–21. doi: 10.1002/ame2.12097

Reale, M., Iarlori, C., Thomas, A., Gambi, D., Perfetti, B., di Nicola, M., et al. (2009). Peripheral cytokines profile in Parkinson's disease. *Brain Behav. Immun.* 23, 55–63. doi: 10.1016/j.bbi.2008.07.003

Reckziegel, P., Chen, P., Caito, S., Gubert, P., Soares, F. A. A., Fachinetto, R., et al. (2016). Extracellular dopamine and alterations on dopamine transporter are related to reserpine toxicity in *Caenorhabditis elegans*. *Arch. Toxicol.* 90, 633–645. doi: 10.1007/s00204-015-1451-7

Rojanathammanee, L., Murphy, E. J., and Combs, C. K. (2011). Expression of mutant alpha-synuclein modulates microglial phenotype in vitro. *J. Neuroinflamm.* 8, 1–12. doi: 10.1186/1742-2094-8-44

Salamone, J., and Baskin, P. (1996). Vacuous jaw movements induced by acute reserpine and low-dose apomorphine: Possible model of Parkinsonian tremor. *Pharmacol. Biochem. Behav.* 53, 179–183. doi: 10.1016/0091-3057(95)00164-6

Santos, J. R., Cunha, J. A. S., Dierschnabel, A. L., Campêlo, C. L., Leão, A. H., Silva, A. F., et al. (2013). Cognitive, motor and tyrosine hydroxylase temporal impairment in a model of Parkinsonism induced by reserpine. *Behav. Brain Res.* 253, 68–77. doi: 10.1016/j.bbr.2013.06.031

Sarmento-Silva, A. J. (2015). Alpha-tocopherol counteracts cognitive and motor deficits induced by repeated treatment with reserpine. *Biochem. Pharmacol. Open Access* 4, 2167–2501. doi: 10.4172/2167-0501.1000153

Schwenkgrub, J., Joniec-Maciejak, I., Sznejder-Pachołek, A., Wawer, A., Ciesielska, A., Bankiewicz, K., et al. (2013). Effect of human interleukin-10 on the expression of nitric oxide synthases in the MPTP-based model of Parkinson's disease. *Pharmacol. Rep.* 65, 44–49. doi: 10.1016/S1734-1140(13)70962-9

Sheng, J. G., Shirabe, S., Nishiyama, N., and Schwartz, J. P. (1993). Alterations in striatal glial fibrillary acidic protein expression in response to 6-hydroxydopamine-induced denervation. *Exp. Brain Res.* 95, 450–456. doi: 10.1007/BF00227138

Subramaniam, S. R., and Federoff, H. J. (2017). Targeting microglial activation states as a therapeutic avenue in Parkinson's disease. *Front. Aging Neurosci.* 9:176. doi: 10.3389/fnagi.2017.00176

Tan, E. K., Chao, Y. X., West, A., Chan, L. L., Poewe, W., and Jankovic, J. (2020). Parkinson disease and the immune system — associations, mechanisms and therapeutics. *Nat. Rev. Neurol.* 16, 303–318. doi: 10.1038/s41582-020-0344-4

Tang, Y., and Le, W. (2016). Differential roles of M1 and M2 microglia in neurodegenerative diseases. *Mol. Neurobiol.* 53, 1181–1194. doi: 10.1007/s12035-014-9070-5

Thakur, P., and Nehru, B. (2014). Inhibition of neuroinflammation and mitochondrial dysfunctions by carbenoxolone in the rotenone model of Parkinson's disease. *Mol. Neurobiol.* 51, 209–219. doi: 10.1007/s12035-014-8769-7

Trudler, D., Weinreb, O., Mandel, S. A., Youdim, M. B. H., and Frenkel, D. (2014). DJ-1 deficiency triggers microglia sensitivity to dopamine toward a pro-inflammatory phenotype that is attenuated by rasagiline. *J. Neurochem.* 129, 434–447. doi: 10.1111/jnc.12633

Tysnes, O. B., and Storstein, A. (2017). Epidemiology of Parkinson's disease. *J. Neural Trans.* 124, 901–905. doi: 10.1007/s00702-017-1686-y

van Onselen, R., and Downing, T. G. (2021). Neonatal reserpine administration produces widespread neuronal losses and α-synuclein inclusions in a rat model. *Neurotox. Res.* 39, 1762–1770. doi: 10.1007/s12640-021-00434-x

Zhang, P., Li, Y., Han, X., Xing, Q., and Zhao, L. (2017). Dexmedetomidine regulates 6-hydroxydopamine-induced microglial polarization. *Neurochem. Res.* 42, 1524–1532. doi: 10.1007/s11064-017-2209-9

Zhang, W., Wang, T., Pei, Z., Miller, D. S., Wu, X., Block, M. L., et al. (2005). Aggregated α−synuclein activates microglia: A process leading to disease progression in Parkinson's disease. *FASEB J.* 19, 533–542. doi: 10.1096/fj.04-2751com

Zhao, Y. F., Zhang, Q., Xi, J. Y., Li, Y. H., Ma, C. G., and Xiao, B. G. (2015). Multitarget intervention of Fasudil in the neuroprotection of dopaminergic neurons in MPTP-mouse model of Parkinson's disease. *J. Neurol. Sci.* 353, 28–37. doi: 10.1016/j.jns.2015.03.022

frontiers | Frontiers in Neuroscience

TYPE Original Research
PUBLISHED 10 November 2022
DOI 10.3389/fnins.2022.948517

OPEN ACCESS

EDITED BY
Nidhi Agarwal,
Jamia Hamdard University, India

REVIEWED BY
Taito Matsuda,
Kyushu University, Japan
Yusuke Kishi,
The University of Tokyo, Japan
Seiji Hitoshi,
Shiga University of Medical Science, Japan

*CORRESPONDENCE
Misuzu Hashimoto
hashimoto.misuzu.b9@f.gifu-u.ac.jp

SPECIALTY SECTION
This article was submitted to Neuropharmacology, a section of the journal Frontiers in Neuroscience

RECEIVED 19 May 2022
ACCEPTED 17 October 2022
PUBLISHED 10 November 2022

CITATION
Hashimoto M, Takeichi K, Murata K, Kozakai A, Yagi A, Ishikawa K, Suzuki-Nakagawa C, Kasuya Y, Fukamizu A and Nakagawa T (2022) Regulation of neural stem cell proliferation and survival by protein arginine methyltransferase 1. *Front. Neurosci.* 16:948517. doi: 10.3389/fnins.2022.948517

Regulation of neural stem cell proliferation and survival by protein arginine methyltransferase 1

Misuzu Hashimoto[1]*, Kaho Takeichi[1], Kazuya Murata[2], Aoi Kozakai[1], Atsushi Yagi[1], Kohei Ishikawa[1], Chiharu Suzuki-Nakagawa[1], Yoshitoshi Kasuya[3], Akiyoshi Fukamizu[4,5,6] and Tsutomu Nakagawa[1]

[1]Laboratory of Biological Chemistry, Faculty of Applied Biological Sciences, Gifu University, Gifu, Japan, [2]Laboratory Animal Resource Center in Transborder Medical Research Center, Faculty of Medicine, University of Tsukuba, Tsukuba, Japan, [3]Department of Biochemistry and Molecular Pharmacology, Graduate School of Medicine, Chiba University, Chiba, Japan, [4]Life Science Center for Survival Dynamics, Tsukuba Advanced Research Alliance, University of Tsukuba, Tsukuba, Japan, [5]World Premier International Research Center Initiative, International Institute for Integrative Sleep Medicine, University of Tsukuba, Tsukuba, Japan, [6]AMED-CREST, Japan Agency for Medical Research and Development, Tokyo, Japan

Protein arginine methyltransferase 1 (PRMT1), a major type I arginine methyltransferase in mammals, methylates histone and non-histone proteins to regulate various cellular functions, such as transcription, DNA damage response, and signal transduction. PRMT1 is highly expressed in neural stem cells (NSCs) and embryonic brains, suggesting that PRMT1 is essential for early brain development. Although our previous reports have shown that PRMT1 positively regulates oligodendrocyte development, it has not been studied whether PRMT1 regulates NSC proliferation and its survival during development. To examine the role of PRMT1 in NSC activity, we cultured NSCs prepared from embryonic mouse forebrains deficient in PRMT1 specific for NSCs and performed neurosphere assays. We found that the primary neurospheres of PRMT1-deficient NSCs were small and the number of spheres was decreased, compared to those of control NSCs. Primary neurospheres deficient in PRMT1 expressed an increased level of cleaved caspase-3, suggesting that PRMT1 deficiency-induced apoptosis. Furthermore, p53 protein was significantly accumulated in PRMT1-deficient NSCs. In parallel, p53-responsive pro-apoptotic genes including *Pmaip1* and *Perp* were upregulated in PRMT1-deficient NSCs. p53-target p21 mRNA and its protein levels were shown to be upregulated in PRMT1-deficient NSCs. Moreover, the 5-bromo-2′-deoxyuridine (BrdU) incorporation assay showed that the loss of PRMT1 led to cell cycle defects in the embryonic NSCs. In contrast to the above *in vitro* observations, NSCs normally proliferated and survived in the fetal brains of NSC-specific PRMT1-deficient mice.

We also found that *Lama1*, which encodes the laminin subunit α1, was significantly upregulated in the embryonic brains of PRMT1-deficient mice. These data implicate that extracellular factors provided by neighboring cells in the microenvironment gave a trophic support to NSCs in the PRMT1-deficient brain and recovered NSC activity to maintain brain homeostasis. Our study implies that PRMT1 plays a cell-autonomous role in the survival and proliferation of embryonic NSCs.

KEYWORDS

PRMT1, neural stem cell, apoptosis, development, p53

Introduction

Mammalian brain tissues are originally derived from neural stem cells (NSCs) proliferation and differentiation (Ohtsuka and Kageyama, 2019). During brain development, NSCs self-renew and expand to populate the central nervous system (CNS) (Ohtsuka and Kageyama, 2019). After proliferation, they differentiate into neurons, oligodendrocytes, and astrocytes to make a complex cell network and perform high-order functions in the brain (Ohtsuka and Kageyama, 2019). A small number of NSCs are also distributed in adult brains and are suggested to be important for neuronal regeneration (Bond et al., 2015). However, it is still unclear how NSCs proliferate before differentiating into functional cells. Recent studies attempt to use NSCs for stem cell therapy for various complications such as spinal cord injury (Yousefifard et al., 2016; Marsh and Blurton-Jones, 2017; Kitagawa et al., 2022). Therefore, understanding the molecular control on how NSC proliferation and viability are regulated is an important topic.

Protein arginine methylation is one of the major post-translational modifications mediated by a PRMT family (Bedford and Clarke, 2009; Blanc and Richard, 2017). The substrates of protein arginine methyltransferases (PRMTs) vary from histone and non-histone proteins, and their methylation controls cell survival, transcriptional regulation, and signal transduction (Bedford and Clarke, 2009). Type I PRMTs including PRMT1, 2, 3, 6, 8, CARM1, and METTL23 are responsible for the monomethylation and asymmetric dimethylation of arginine. On the other hand, type II PRMTs such as PRMT5 and 9 regulate monomethylation followed by symmetric dimethylation of arginine. PRMT7 is a type III PRMT that catalyzes only monomethylation. Among type I PRMTs, PRMT1 is known to perform 75% of type I activity in mammalian cells (Tang et al., 2000).

We have previously demonstrated that PRMT1 is essential for postnatal brain development, since *Prmt1*$^{flox/flox}$*;Nes-Cre* neural stem cell-specific protein arginine methyltransferase 1 knockout (CKO) mice exhibit severe hypomyelination as well as astroglial and microglial activations (Hashimoto et al., 2016, 2021b). Furthermore, CKO mice had deregulation of neuronal glycan expression (Hashimoto et al., 2020). These studies showed that PRMT1 is important for various regulatory systems of neuronal and glial development in the CNS (Hashimoto et al., 2021a). A previous study on the role of PRMT1 in embryonic NSCs has shown that *Prmt1* knockdown in NSCs suppressed differentiation to an astrocyte lineage (Honda et al., 2017). Similarly, a recent report showed that *Prmt1* knockdown in primitive NSCs derived from mouse embryonic stem cells spontaneously expressed neuronal proteins such as NeuroD1, indicating that PRMT1 is essential for the maintenance of neural stemness (Chen et al., 2021). Although PRMT1 shows significantly higher expression in NSCs than differentiated neurons or astrocytes (Honda et al., 2017), a knockout study to identify the role of PRMT1 in embryonic NSCs proliferation and stemness is lacking. Moreover, it is necessary to evaluate PRMT1 deletion in NSCs in *in vivo* settings.

Here, to clarify the importance of PRMT1 in the proliferation and stemness of NSCs, we examined NSCs derived from Nestin-Cre mediated *Prmt1*-deficient mouse embryo (*Prmt1*$^{flox/flox}$*;Nes-Cre*) both *in vivo* and *in vitro*. We found that NSCs in PRMT1-deficient embryonic brains proliferated normally *in vivo*. However, PRMT1-deficient NSCs showed reduced neurosphere formation and limited survival *in vitro*. NSCs cultured under hypoxic conditions modestly improved neurosphere formation but were PRMT1 independent. PRMT1 deficiency upregulated the accumulation of p21 and p53, which would be the main cause of the reduced proliferation and apoptosis in PRMT1-deficient NSCs.

Abbreviations: BrdU, 5-bromo-2′-deoxyuridine; CKO, neural stem cell-specific protein arginine methyltransferase 1 knockout; CNS, central nervous system; E, embryonic day; NSC, neural stem cell; OPCs, oligodendrocyte precursor cells; PRMT1, protein arginine methyltransferase 1; qRT-PCR, quantitative reverse transcription polymerase chain reaction.

Materials and methods

Animals

Nestin-Cre mediated *Prmt1*-deficient mice (*Prmt1*$^{flox/flox}$;*Nes-Cre*) (C57BL/6 background) were generated as previously described (Hashimoto et al., 2016). *Prmt1*$^{flox/flox}$;*Nes-Cre* mice are the CKO group and *Prmt1*$^{flox/flox}$ or *Prmt1*$^{flox/wt}$ mice are used as the control group throughout the study. On the following day of mating, the presence of a vaginal plug in the female mouse is defined as embryonic day 1 (E1). All animal experiments were carried out in accordance with and approved by the Institutional Animal Experiment Committee of Gifu University.

RNA extraction and quantitative reverse transcription polymerase chain reaction

Total RNA was extracted from the forebrain of E14 mice and NSCs using ISOGEN II (Nippon Gene, Ltd., Tokyo, Japan #311-07361) and Ethachinmate (Nippon Gene, #312-01791). Total RNA was reverse-transcribed with ReverTra Ace qPCR RT Master Mix with gDNA Remover (Toyobo Co., Ltd., Osaka, Japan #FSQ-301). The relative gene expression level was determined by SYBR Green-based quantitative reverse transcription polymerase chain reaction (RT-PCR) (Bio-Rad Laboratories, Hercules, CA, USA #CFB3120EDU). The expression levels of the target genes were corrected for those of glyceraldehyde-3-phosphate dehydrogenase (*Gapdh*) and β-*Actin* expression levels using the *ddCt* method. The primer sequences are listed in **Supplementary Table 1**.

In vivo 5-bromo-2′-deoxyuridine labeling and immunohistochemistry

Pregnant females at E14 were injected intraperitoneally with 5-bromo-2′-deoxyuridine (BrdU) (100 mg/kg body weight; Sigma-Aldrich, St. Louis, MO, USA #B5002). After 1 h, the females were sacrificed by cervical dislocation and the embryos were harvested. The embryonic heads were removed, fixed with 4% paraformaldehyde (PFA) overnight, and embedded in an O.C.T. compound (Tissue-Tek, Torrance, CA, USA #4583). Of note, 10-μm cryosections were performed heat-induced epitope retrieval with citrate buffer (pH 6.0). In case of BrdU staining, the sections were further incubated with 2N HCl. Sections were stained with primary antibodies after blocking with a 10% donkey serum donor herd (Millipore, Burlington, MA, USA #S30) in PBS or 10% normal goat serum (Sigma-Aldrich #G6767 and Jackson Immuno Research, West Grove, PA, USA #005-000-121) in PBS. The following antibodies and reagents were used: anti-Sox2 (Santa Cruz, Dallas, TX, USA #sc17320; 1:200), anti-BrdU (Novus Biologicals, Centennial, CO, USA NB500-169; 1:500), anti-TBR2 (Abcam, Cambridge, UK #ab23345; 1:100), anti-Ki67 (Thermo Fisher Scientific, Waltham, MA, USA #14-5698-82; 1:50), goat anti-rat IgG (H + L) cross-absorbed secondary antibody, Alexa Fluor 568 (Thermo Fisher Scientific #A-11077; 1:1,000), biotinylated rabbit anti-goat IgG antibody (H + L) (Vector, Newark, CA, USA #BA-5000; 1:200), biotinylated goat anti-rabbit IgG antibody (H + L) (Vector #BA-1000; 1:200), and Alexa Fluor 488-conjugated Streptavidin (Jackson Immuno Research, West Grove, PA, USA #016-540-084; 1:1,000). Cell nuclei were stained with Hoechst 33342 (Nacalai Tesque, Inc., Kyoto, Japan #04915-81 and FUJIFILM Wako Pure Chemical Corporation, Osaka, Japan #346-07951; 0.5 μg/ml). Fluorescence images were obtained with a fluorescence microscope (BIOREVO BZ-X710 and BZ-X810, Keyence, Osaka, Japan). Cell counting was performed using three to five mice per genotype and the same size areas were applied to manual cell counting using the ImageJ software. The area for cell counting is shown in **Figure 1B**. Each staining was performed in two sections from each animal and cell counting was performed using one of the two sections. The average count from both cortical sides was used for the graph and statistical analysis shown in **Figure 1C**.

Isolation, culture, and treatments of neural stem cells

Neurosphere culture was performed referring to previously published protocol with some modifications (Hirabayashi et al., 2009). In detail, the forebrain regions of E14 mice were dissociated into single-cell suspensions with Neural Tissue Dissociation Kit (P) (Miltenyi Biotech, Gladbach, Germany #130-092-628). The cell suspension was passed through a 40-μm cell strainer (Corning, NY, USA #431750). Cells from individual embryos, 2 × 10^6 cells/uncoated T25 flask, were cultured in 5 ml of proliferation media consisting of DMEM/Ham's F-12 (FUJIFILM Wako Pure Chemical Corporation, #042-30555) with insulin, recombinant human (5 μg/ml; SAFC Biosciences, Lenexa, KS, USA #91077C), transferrin (Apo), from human blood (100 μg/ml; FUJIFILM Wako Pure Chemical Corporation, #205-18121), progesterone (6.4 ng/ml; Sigma-Aldrich, #P8783), Putrescine dihydrochloride (16 μg/ml; Sigma-Aldrich, #P5780) and sodium selenite (26 ng/ml; Sigma-Aldrich, #S5261), B27 supplement (Thermo Fisher Scientific, Waltham, MA, USA #17504-044), penicillin-streptomycin mixed solution (Nacalai Tesque, #26253-84), bFGF (25 ng/ml; PeproTech, Cranbury, NJ, USA #450-33), and EGF (25 ng/ml; Thermo Fisher Scientific, #PMG8041). Heparin is not added to the neurosphere culture. For cell proliferation, bFGF and EGF were added every 3 or 4 days. Cells were incubated at 37°C in 5% CO_2 and 21% O_2 for normoxic culture. For hypoxic culture, cells

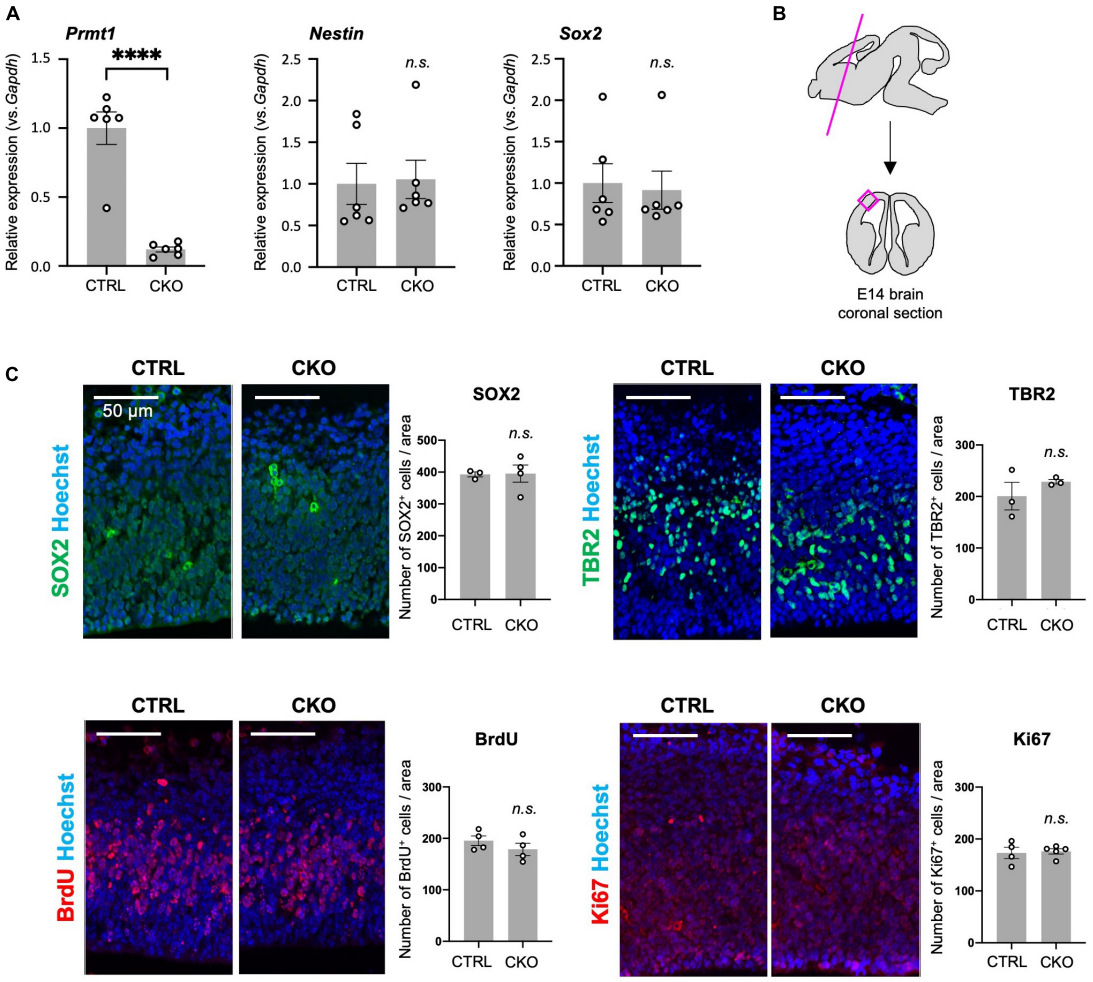

FIGURE 1
Protein arginine methyltransferase 1 (PRMT1)-deficient neural stem cells (NSCs) show substantial proliferation in the fetal cortices. **(A)** Relative expression of *Prmt1*, *Nestin*, and *Sox2* normalized to glyceraldehyde-3-phosphate dehydrogenase (*Gapdh)* in the forebrains of control (CTRL, *Prmt1*$^{flox/flox}$) and neural stem cell-specific protein arginine methyltransferase 1 knockout (CKO) (*Prmt1*$^{flox/flox}$;*Nes-Cre*) mice at embryonic day 14 (E14) analyzed by quantitative reverse transcription polymerase chain reaction (qRT-PCR). Data are shown as mean ± SEM (n = 6 animals) and were analyzed by a two-tailed Student's t-test. ****$p < 0.0001$. **(B)** Schematic illustration of the E14 brain area for histological analyses. The magenta line is the plane for the sections and the areas for the observation and signal quantifications in panel **(C)** are indicated as a magenta square. The average cell count from both left and right cerebral cortices from a single section was used for cell count comparison in panel **(C)**. **(C)** Representative images of immunohistochemistry for SOX2, TBR2, 5-bromo-2′-deoxyuridine (BrdU), and Ki67 with Hoechst nuclear staining of control (CTRL) and CKO cerebral cortices at E14. The quantification data are shown as mean ± SEM (n = 3–5 animals). Scale bars, 50 μm.

were maintained in 2.5% O_2 using Anaero Pack (Mitsubishi Gas Chemical, Tokyo, Japan #A-07). Primary neurosphere diameter was measured on day 5 *in vitro* using the ImageJ software. More than 100 spheres in three to six images obtained from one to two flasks were measured in each condition.

In vitro 5-bromo-2′-deoxyuridine labeling and immunocytochemistry

The primary spheres were dissociated and cells were seeded on poly-D-lysine-coated coverslips in 24-well plates. After 2 days, cells were labeled BrdU (10 μM; Sigma-Aldrich, #B5002) for 6 h, fixed with 4% PFA, treated with 2N HCl, and blocked with 10% goat serum donor herd (Sigma-Aldrich, #G6767) in 0.1% TritonX-100/PBS for 1 h. Primary antibodies were applied overnight at 4°C followed by secondary antibodies for 1 h at room temperature. The following antibodies were used: anti-BrdU (Novus Biologicals, NB500-169; 1:200), anti-cleaved caspase-3 (Asp175) (Cell Signaling Technology, Danvers, MA, USA #9661; 1:400), goat anti-rat IgG (H + L) cross-absorbed secondary antibody, Alexa Fluor 568 (Thermo Fisher Scientific, #A-11077: 1:1,000), Alexa Fluor 488-affinipure donkey anti-rabbit IgG (H + L) (Jackson Immuno Research,

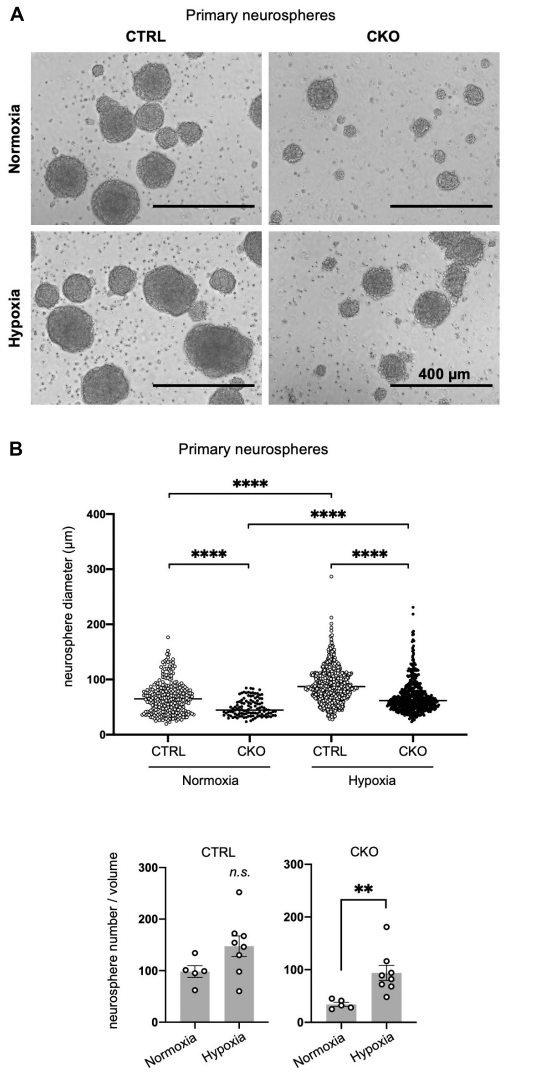

FIGURE 2
Decreased sphere formation of protein arginine methyltransferase 1 (PRMT1)-deficient neural stem cells (NSCs). **(A)** Representative phase contrast images of primary neurospheres. NSCs were obtained from E14 forebrains from control (CTRL, *Prmt1*$^{flox/flox}$ and *Prmt1*$^{flox/wt}$) and neural stem cell-specific protein arginine methyltransferase 1 knockout (CKO) (*Prmt1*$^{flox/flox}$;*Nes-Cre*) mice and were cultured for 5 days *in vitro* to obtain neurospheres. Cell culture was performed under normoxia (21% O_2) in upper panels and hypoxia (2.5% O_2) in lower panels. Scale bars, 400 μm. **(B)** Neurosphere diameter (upper panel) and neurosphere number (lower panel) were measured on day 5 *in vitro* under normoxia and hypoxia. Neurosphere diameter data ($n > 100$) are shown as mean ± SEM and were analyzed by the Kruskal–Wallis test followed by Dunn's multiple comparisons test. ****$p < 0.0001$. Sphere number data ($n > 5$) are shown as mean ± SEM and were analyzed by a two-tailed Student's *t*-test. **$p < 0.01$.

#016-540-084; 1:1,000). Cell nuclei were stained with Hoechst 33342. Fluorescence images were obtained with a fluorescence microscope (BIOREVO BZ-X710 and BZ-X810, Keyence). BrdU$^+$ cell and cleaved caspase-3$^+$ cells were counted using eight independent fields of 40× objectives per each group and were applied to manual cell counting using the ImageJ software.

Western blot analysis

The NSCs were homogenized by sonication in ice-cold TNE buffer (20 mM Tris–HCl pH 7.5, 150 mM NaCl, 1 mM EDTA) with 0.2% Nonidet P-40 and protease inhibitor mixture (Nacalai Tesque, #25955-11). Protein concentrations were determined by Bradford assays with XL-Bradford (APRO Life Science Institute, Tokushima, Japan #KY-1030). Proteins were separated by 8% SDS-PAGE and blotted onto polyvinylidene fluoride (PVDF) membranes (Millipore, #IPVH00010). The membranes were blocked with 3% skim milk in TBS containing 0.1% of Tween-20 (TBS-T), and incubated with primary antibody and then with HRP-conjugated secondary antibodies which were diluted with 1 and 0.5% skim milk in TBS-T. The following primary antibodies were used: anti-asymmetric dimethyl arginine, Asym26 (Epicypher, Durham, NC, USA #13-0011; 1:500), anti-p53 (1C12) (Cell Signaling Technology, #2524; 1:1,000), anti-phospho-p53 (FP3.2) (Santa Cruz Biotechnology, #sc-51690; 1:200), anti-p21 (EPR18021) (Abcam, Cambridge, UK #ab188224; 1:1,000), anti-H2AX (Sigma-Aldrich, #07-627; 1:1,000), anti-phospho-H2AX (Ser139) (Sigma-Aldrich, #05-636; 1:500), anti-PRMT1 (Millipore, #07-404; 1:1,000), and anti-Hsp70 (Bio-Legend, San Diego, CA, USA #648001; 1:500). Visualization was performed by chemiluminescent detection using ImmunoStar Zeta (FUJIFILM Wako Pure Chemical Corporation, #295-72404) or Immobilon ECL Ultra Western HRP Substrate (Millipore, WBULS0100). Immunoreactive images were captured by LAS-3000 (Fujifilm, Tokyo, Japan).

Statistical analysis

Results are shown as mean ± SEM. Normality assessment was not applied to all data. Data were analyzed using a two-tailed Student's *t*-test for comparisons of two groups. Neurosphere diameter data (**Figure 2B**, upper panel) was analyzed using the Kruskal–Wallis test followed by Dunn's multiple comparison test. Significance was considered at $p < 0.05$. Statistical analysis was performed using Prism 8 for macOS [Version 8.4.3 (471)].

Results

Normal neural stem cell proliferation in *Prmt1*$^{flox/flox}$;*Nes-Cre* embryonic brains

Although PRMT1 has been shown to be essential for neurons and glial cells (Hashimoto et al., 2016, 2021a), it

was unclear whether these origins, Nestin$^+$ NSCs, normally survive and proliferate after PRMT1 deficiency in the embryonic brain. Therefore, we measured the mRNA expression of NSC-specific genes by qRT-PCR. *Prmt1* was shown to be markedly downregulated in CKO forebrains compared to control tissues (**Figure 1A**). Both *Nestin* and *Sox2*, well-characterized NSC markers, were expressed at normal levels in CKO tissues, suggesting that a proper NSC population is maintained in the CKO forebrains (**Figure 1A**). We further verified by immunostaining that SOX2-positive cells were distributed in the cerebral cortices in both control and CKO (**Figure 1C**). To investigate the cell proliferation rate in the embryonic cerebral cortices, we performed BrdU assays at E14. At 1 h after BrdU injection into the pregnant dams, the number of proliferating cells incorporated with BrdU was the same between control and CKO in the cerebral cortices at E14 (**Figure 1C**). In consistent with this, the number of Ki67-positive proliferating cells was not affected in CKO (**Figure 1C**). We also found that the number of TBR2-positive intermediate progenitor cells, which is another proliferating cell type besides NSC, was comparable between CKO and control (**Figure 1C**). Taken together, these data suggest that the PRMT1-deficient NSC population, proliferation rate, and distribution are normal in embryonic cerebral cortices at E14.

Decreased proliferation and survival of protein arginine methyltransferase 1-deficient neural stem cells cultured as neurospheres under different oxygen concentrations

In our Nestin-Cre-driven PRMT1 knockout mice, PRMT1 is depleted not only in NSCs but also in all types of cells differentiated from NSCs. Thus, it is difficult to discriminate the role of PRMT1 in NSCs from some secondary effects on NSCs from surrounding cells in *in vivo* settings. To simply characterize the role of PRMT1 in NSC proliferation, we cultured NSCs derived from mouse forebrains and evaluated their proliferation by neurosphere-forming assays. To our surprise, PRMT1-deficient NSCs did not form many primary neurospheres on day 5 *in vitro* (**Figure 2A**). Furthermore, neurosphere diameter, which is an indicator of NSC proliferation, was significantly decreased in the CKO normoxia culture condition (**Figure 2B**, upper panel). These results are different from our observation that NSCs showed normal proliferation *in vivo* (**Figure 1C**).

In the embryonic brain, NSCs are considered to be in an environment with relatively low oxygen availability (Mohyeldin et al., 2010). Additionally, oxygen tension in the embryonic brain has been shown to be low by using a hypoxyprobe, pimonidazole (Mutoh et al., 2012), suggesting that lower oxygen concentrations would be more physiological. Therefore, we next tried the same neurosphere assay under hypoxic conditions (2.5% O_2). Compared to atmospheric oxygen concentration (21% O_2), NSCs appeared to survive and increased better in hypoxic culture in both control and CKO (**Figures 2A,B**, lower panel), although the diameter of the neurosphere was still significantly lower in PRMT1-CKO than in control groups even in hypoxia (**Figure 2B**, upper panel). It has been suggested that Wnt/β-catenin signaling positively regulates NSC proliferation under hypoxia (Braunschweig et al., 2015). Since both control and CKO NSCs responded to decreased oxygen concentration and increased cell proliferation, it is suggested that growth control signaling was upregulated in a PRMT1-independent manner. Therefore, the following experiments were performed only under normoxic conditions. Since we could not obtain enough secondary neurospheres suitable for the following biochemical assays in case of CKO, we decided to perform the following assays using primary neurospheres.

Reduced proliferation and viability of protein arginine methyltransferase 1-deficient neural stem cells

To investigate the mechanism by which PRMT1 deficiency deregulates cell proliferation, we first performed BrdU incorporation assays with dissociated primary neurospheres. At 6 h after BrdU treatment, compared to control cells, CKO NSCs exhibited a decrease in BrdU-positive cells under normoxia, suggesting that cell cycle progression was affected by PRMT1 deficiency in NSCs (**Figures 3A,B**). Furthermore, we have found that the number of cleaved caspase-3 positive cells was significantly increased in CKO NSCs (**Figures 3A,B**). From these data, it was shown that the loss of PRMT1 in NSCs provoked both cell cycle deregulation and apoptosis.

Decreased proliferation of NSCs commonly suggests its increased tendency to spontaneous differentiation (Braunschweig et al., 2015). To test this, we measured the expression of stemness marker mRNA (*Sox2, Nestin*) and differentiation markers (*Olig2, Nkx2.2, Cnp, Slc1a3* (encoding GLAST/EAAT1), *S100b*, and *Tubb3*) by qRT-PCR. *Olig2* and *Nkx2.2* are essential genes for oligodendrogenesis (Qi et al., 2001; Takebayashi et al., 2002). *Cnp* encodes 2′,3′-cyclic nucleotide-3′-phosphodiesterase and is known to be abundantly expressed in oligodendrocyte lineage cells (Yu et al., 1994). *Slc1a3* is an astrocyte-specific glutamate transporter and shows early expression in immature astrocytes (Molofsky et al., 2012). Since *Slc1a3* is also suggested to be expressed in oligodendrocyte precursors (Molofsky et al., 2012), we also tested another astrocytic gene called *S100b* (Molofsky et al., 2012). *Tubb3* encodes βIII-tubulin and is highly expressed in differentiated neurons. As a result, most of these genes were expressed at the same level between the control and CKO (**Figure 3C**). It is noteworthy that *Nkx2.2* and *Cnp* were downregulated in CKO (**Figure 3C**), which may explain

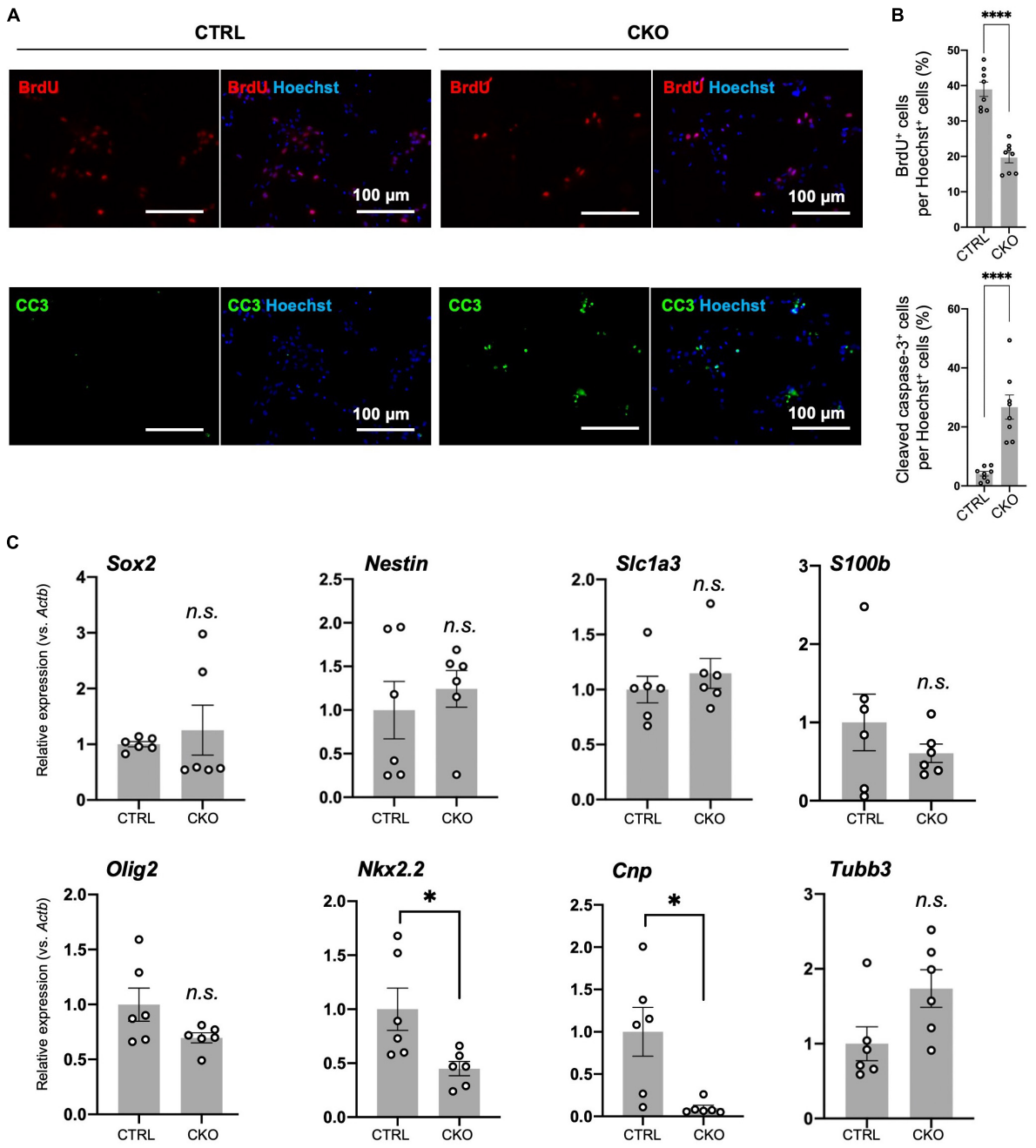

FIGURE 3
Protein arginine methyltransferase 1 (PRMT1)-deficient neural stem cells (NSCs) have reduced proliferation and viability in culture, but their differentiation potential has not changed. **(A)** Representative images of immunocytochemistry for 5-bromo-2′-deoxyuridine (BrdU) (top), cleaved caspase-3 (CC3) (bottom). Each image is merged with Hoechst nuclear staining (right side of each panel). Day 2 NSCs obtained after dissociation of the primary neurosphere were treated with BrdU for 6 h of incorporation and were used for the staining. Scale bars, 100 μm. **(B)** The quantification data of BrdU- or cleaved caspase-3-positive cells are shown as mean ± SEM (n = 8 fields from two independent cultures) and were analyzed by a two-tailed Student's t-test. ****$p < 0.0001$. **(C)** Relative expression of *Sox2*, *Nestin*, *Slc1a3* (encoding GLAST), *S100b*, *Olig2*, *Nkx2.2*, *Cnp*, and *Tubb* normalized to *Actb* in primary neurosphere at culture day 6 analyzed by quantitative reverse transcription polymerase chain reaction (qRT-PCR). Data are shown as mean ± SEM (n = 6) and were analyzed by a two-tailed Student's t-test. *$p < 0.05$.

the decreased potential for oligodendrocyte differentiation resulting in hypomyelination due to PRMT1 deficiency (Hashimoto et al., 2016). These results suggest that PRMT1 deficiency does not largely influence the stemness of NSCs, but rather severely affects the proliferation and survival of NSCs.

Cell cycle arrest, p53 accumulation, and apoptosis in protein arginine methyltransferase 1-deficient neural stem cells

Loss of PRMT1 in NSCs induced dramatic suppression of asymmetric dimethyl arginine of proteins (**Figure 4A**), suggesting that PRMT1 is the major enzyme for this modification in embryonic NSCs. Next, we focused on how this change affected elevated apoptosis and decreased proliferation in PRMT1-deficient NSCs. p53, a well-known tumor suppressor transcription factor, responds to various stresses and regulates both cell cycle repression and apoptosis in cancer and non-cancer cell types (Polager and Ginsberg, 2009). p53 is constantly degraded by mouse double minute 2 homolog (MDM2)-mediated proteasome pathways, while it accumulates under stresses (Polager and Ginsberg, 2009). To assess the accumulation of p53, we checked the level of p53 protein using protein extracts from primary neurospheres of CKO mice. We found that p53 levels were upregulated in the CKO neurospheres compared to the control (**Figure 4B**). On the other hand, the level of *Trp53* mRNA, which encodes p53, was unchanged in CKO NSCs (**Figure 4C**). These results suggest that the p53 protein was accumulated in PRMT1-deficient NSCs.

Furthermore, by Western blotting, we showed that p21, a cyclin-dependent kinase (CDK) inhibitor, was significantly increased in CKO NSCs (**Figure 4B**). Concomitantly, the level of *p21* mRNA increased in CKO NSCs (**Figure 4C**). p21 is one of the major p53 target genes and controls cell cycle arrest (Polager and Ginsberg, 2009). Taken together, our data suggest that p53 accumulation induced p21 transcription and led to the growth arrest of PRMT1-deficient NSCs.

In CKO NSCs, apoptosis was significantly induced (**Figures 3A,B**). The Bcl-2 family proteins play a crucial role in the induction or repression of apoptosis (Gross and Katz, 2017). Among pro-apoptotic members of the Bcl-2 family, we found that *Pmaip1*, encoding NOXA, was markedly upregulated in CKO NSCs (**Figure 4C**). Other pro-apoptotic Bcl-2 families such as *Bbc3* (encoding PUMA) and *Bax* did not show such a difference. However, in case of *Bax*, it is of note that CKO NSCs showed a higher trend than control NSCs (**Figure 4C**). Furthermore, *Perp*, one of the target genes for p53 and known as an apoptosis mediator (Attardi et al., 2000; Marques et al., 2005), increased significantly in CKO NSCs compared to the control group (**Figure 4C**).

Since DNA damage is one of the main stressors that induce p53 accumulation, we also tested whether DNA damage is a trigger for the upregulation of p53 in CKO NSCs. The phosphorylated histone H2AX (γH2AX) is a useful marker of DNA damage (Mah et al., 2010). Western blot analyses showed that γH2AX levels did not increase in CKO NSCs (**Figure 4B**), suggesting that DNA damage would not be the reason for the accumulation of p53 in PRMT1-deficient NSCs.

Taken together, after PRMT1 depletion in NSC, p21 showed a striking accumulation that caused cell cycle arrest. In parallel, p53 was accumulated followed by the induction of apoptosis mediators, including *Pmaip1* and *Perp*. Although p21 is generally known to suppress apoptosis and contribute to cellular repair, our data imply that the p53-mediated pro-apoptotic signals exceeded this effect in the case of PRMT1-deficient NSCs.

Potential extracellular factors that support neural stem cell proliferation and survival in protein arginine methyltransferase 1-deficient brains

We have previously demonstrated increased astrocytes and microglia as well as upregulated inflammatory responses in neonatal brain cortices of CKO mice (Hashimoto et al., 2021b). Therefore, we ask whether the cellular and molecular changes in the brain provided an ideal microenvironment for the survival of NSCs in PRMT1 deficiency. Indeed, many extracellular factors are known to contribute to the survival, attachment, and proliferation of NSCs (Kazanis and ffrench-Constant, 2011). Thus, we performed qRT-PCR of PRMT1-deficient brains at E14, when the normal distribution of NSC was confirmed (**Figure 1C**). A major extracellular matrix protein, laminin, has been reported to provide signaling cues for NSC adhesion and proliferation (Li et al., 2014; Kim et al., 2021). Laminin is a heterotrimeric protein, and astrocytes express laminins-111 (α1β1γ1) and -211 (α2β1γ1) (Yao et al., 2014). While α2 subunit (*Lama2*) was normal, the α1 subunit (*Lama1*) was significantly highly expressed in the brain cortices of CKO (**Figure 5**), indicating that laminin is one of the potential factors for the survival and proliferation of CKO NSCs. Among the main CNS cytokines, IL-6 secreted by astrocytes is known to stimulate NSC proliferation (Wang et al., 2011). LIF is also known to stimulate the formation of neurospheres of adult NSCs (Bauer, 2009). However, *Il-6* and *Lif* did not show a significant difference in the embryonic PRMT1-CKO brains (**Figure 5**). Taken together, our data indicate a potential contribution of the extracellular matrix to the survival/proliferation of PRMT1-deficient NSCs in the brain microenvironment.

Discussion

Effects of protein arginine methyltransferase 1 loss in neural stem cells *in vivo* and *in vitro*

In this study, we have shown that cultured PRMT1-deficient NSCs derived from E14 mouse forebrains showed deregulated

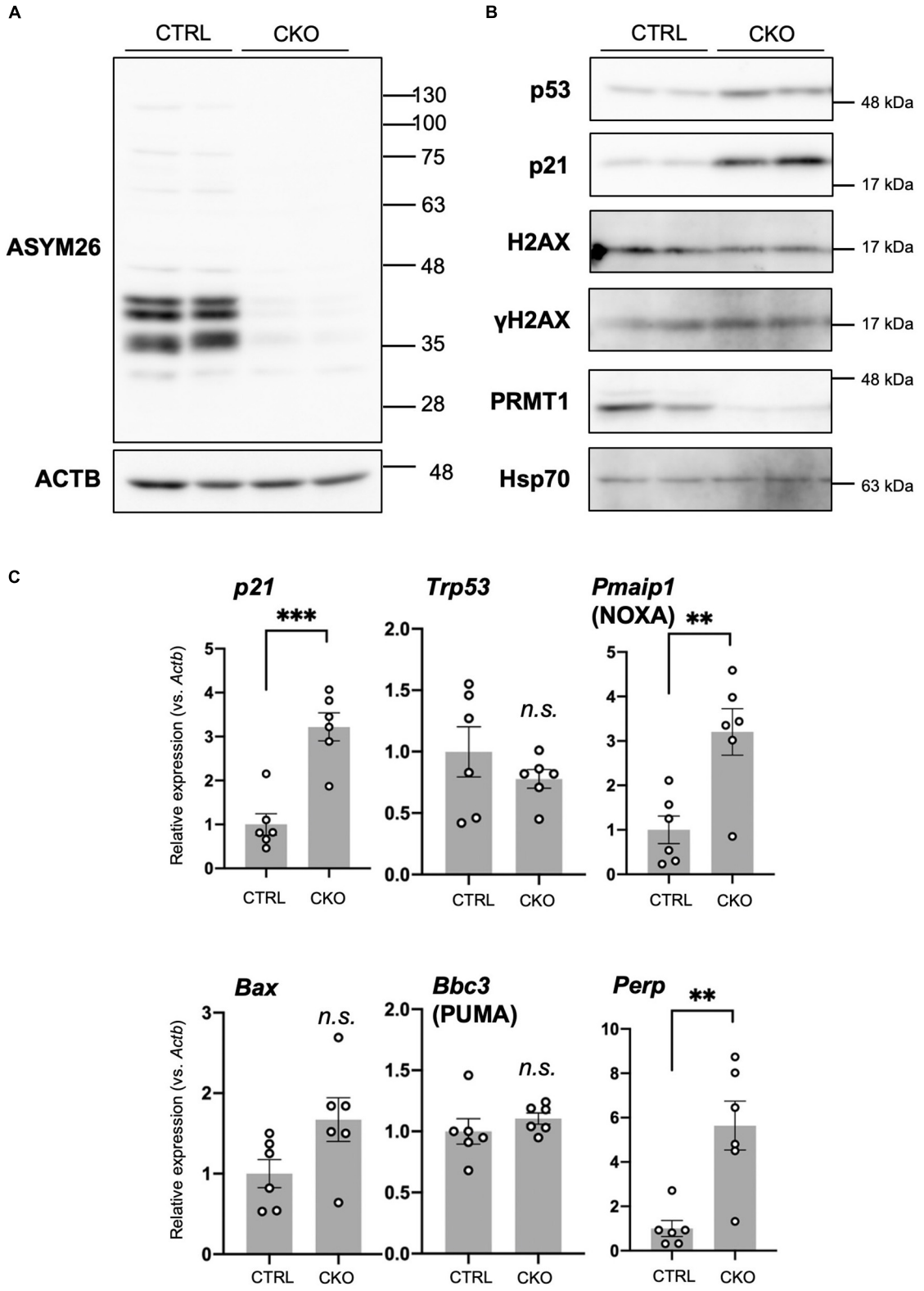

FIGURE 4
Cell cycle arrest, p53 accumulation, and apoptosis in protein arginine methyltransferase 1 (PRMT1)-deficient neural stem cells (NSCs). **(A)** Asymmetric dimethyl arginine levels in primary neurosphere at culture day 6 analyzed by Western blots using Asym26. **(B)** Expression of indicated proteins in primary neurosphere at culture day 6 analyzed by Western blots. **(C)** Relative expression of indicated genes normalized to *Actb* in primary neurosphere at culture day 6 analyzed by quantitative reverse transcription polymerase chain reaction (qRT-PCR). Data are shown as mean ± SEM (n = 6) and were analyzed by a two-tailed Student's t-test. $^{**}p < 0.01$, $^{***}p < 0.001$.

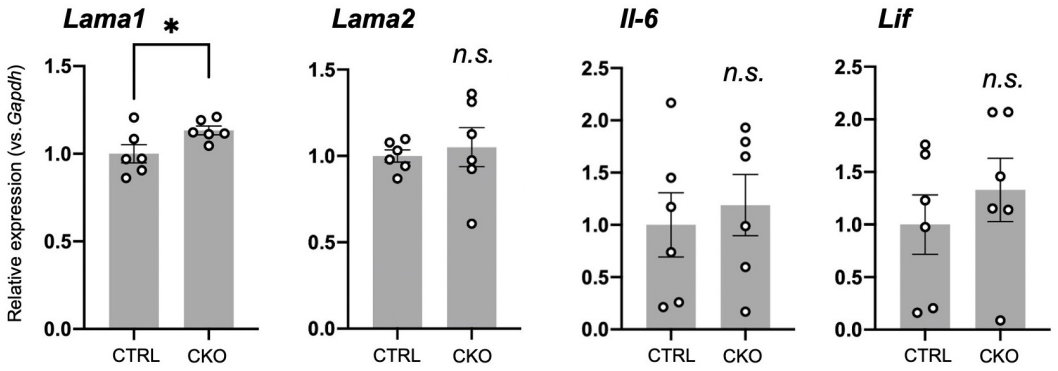

FIGURE 5
Potential extracellular factors supporting neural stem cell (NSC) proliferation and survival in protein arginine methyltransferase 1 (PRMT1)-deficient brains. Relative expression of *Lama1*, *Lama2*, *Il-6*, and *Lif* normalized to glyceraldehyde-3-phosphate dehydrogenase (*Gapdh*) in the forebrains of control and neural stem cell-specific protein arginine methyltransferase 1 knockout (CKO) E14 analyzed by quantitative reverse transcription polymerase chain reaction (qRT-PCR). Data are shown as mean ± SEM (n = 6 animals) and were analyzed by a two-tailed Student's t-test. *$p < 0.05$.

cell proliferation, apoptosis, and accumulation of p21 and p53. However, on the other hand, we found that PRMT1-deficient NSCs *in vivo* showed normal proliferation evaluated by BrdU incorporation, Ki67-positive cell number, and distribution of NSCs in the cerebral cortices at the same stage of embryonic development as preparation of NSC culture. To address this discrepancy, we tried culturing NSCs under hypoxic conditions, which are considered to be close to the physiological oxygen environment of embryonic brains. The primary neurospheres of the CKO brain increased the number and diameter of the sphere by lowering the oxygen concentration; however, hypoxia did not give enough recovery to the control level. Therefore, there may be some other *in vivo* factors necessary for the proliferation and survival of PRMT1-deficient NSCs.

In search for the reason for the discrepancy in PRMT-deficient NSC proliferation *in vivo* and *in vitro*, we focused on the possible upregulation of inflammatory signaling in the PRMT1-deficient brain. We have previously found that the aberrant increase and activation of astrocytes and microglia in the cerebral cortices of PRMT1-CKO after birth (Hashimoto et al., 2021b). In parallel, we have also shown the upregulation of various cytokine/chemokine-related genes and extracellular matrices in the neonatal CKO cortices (Hashimoto et al., 2021b). Previous research has demonstrated that astrocyte-conditioned media or IL-6 treatment induced NSC proliferation *in vitro* (Wang et al., 2011). Therefore, we sought to determine whether these cytokines from neighboring cells of NSCs, which are absent in culture systems, could be important for the proliferation of CKO NSCs. This prompted us to test the level of neurotrophic cytokines in the embryonic stages. However, we did not see higher trends of *Il-6* and *Lif* in the fetal brain of CKO (**Figure 5**). On the other hand, we found that *Lama1*, encoding α1 subunit of laminin, was significantly increased in the brain of CKO. Future rescue studies using adherent NSC culture over a laminin coat or the addition of laminin in a culture medium for CKO NSCs will be required to identify the precise mechanism. In addition, preliminary secretome analyses of embryonic brains are needed to fully cover the differences in extracellular signals that support the survival of CKO NSCs.

In addition to extracellular molecules, we should also consider the role of extracellular forces that are different between *in vitro* and *in vivo*. In the embryonic brain cortex, NSCs have a bipolar shape and are packed in the neurepithelium which has an apical–basal axis (Miyata, 2008). The mechanical tension in the environment to NSCs that are only emerged *in vivo* is suggested to be important for stem cell proliferation (Pathak et al., 2014; Kumar et al., 2017; Vining and Mooney, 2017). Thus, it is probable that PRMT1 deficiency using *Nestin-Cre* affects the extracellular forces, in addition to secretory molecules, from neighboring cells in the neurepithelium, leading to compensation of the NSC proliferation. While we have observed normal proliferation of NSCs in CKO cortices at E14, it is still possible that the proliferation potential changes during embryonic development due to the modification of both intracellular and extracellular signals by loss of PRMT1 *in vivo*.

Molecular control of survival and proliferation of neural stem cells by protein arginine methyltransferase 1

In our study, upregulation of the p53-mediated apoptotic pathway at least partially explains the increased cell death of PRMT1-deficient NSCs. A previous trial of inducible PRMT1 loss in mouse embryonic fibroblasts (MEFs) demonstrated spontaneous DNA damage and decreased proliferation without inducing apoptosis (Yu et al., 2009). Although our data did not show DNA damage in PRMT1-deficient NSCs by evaluating

γH2AX (**Figure 4B**), it would need more detailed chromosomal analyses. Therefore, it remains uncovered how PRMT1 loss leads to the accumulation of p53 in embryonic NSCs.

In terms of other members of the PRMT family and p53 signaling, a previous work demonstrated that PRMT1-p53 regulates epicardial invasion for normal heart development through PRMT1-mediated *Mdm4* splicing (Jackson-Weaver et al., 2020). Another study showed that PRMT5 is essential for NSC survival and proliferation through the generation of the functional *Mdm4* splicing variant which avoids aberrant accumulation of p53 (Bezzi et al., 2013). Our study found that p53 was accumulated at the protein level but not the mRNA level in CKO NSCs (**Figures 4B,C**), indicating that a similar p53 stabilization mechanism was activated by PRMT1 deficiency in NSCs. Therefore, our study highlights the importance of PRMT1 arginine methylation in NSCs in addition to PRMT5.

One limitation of our study is that we obtained the above data on p53 accumulation in primary neurospheres because we could not obtain enough secondary sphere population. Generally, neurosphere studies basically use secondary or tertiary neurospheres because they are groups of NSCs that have self-renewal capacity and are therefore suitable to NSC analyses. At least, we have confirmed that the primary neurospheres expressed relatively high levels of *Sox2* and *Nestin* both in CTRL and CKO (**Figure 3C**), suggesting that it would be meaningful to compare their proliferation capacity and molecular control.

In this study, we found arginine methylation of multiple proteins in primary neurospheres, and these were markedly suppressed by PRMT knockout (**Figure 4A**). These data suggest that PRMT1 is the major type I PRMT in NSCs. PRMT1 is also known as a popular epigenetic regulator because it methylates histone H4 arginine 3 (H4R3) (Wang et al., 2001). Meanwhile, asymmetrically methylated H4R3 (H4R3me2as) has not been detected in NSCs in the embryonic cortices (Chittka, 2010), implying that PRMT1 has non-histone targets in NSCs. While we did not focus here, NSC proliferation is essentially regulated by various growth signals, such as Wnt, MAPK, or Notch, as described elsewhere (Chenn and Walsh, 2002; Campos et al., 2004; Ables et al., 2011). Our previous data of RNA-seq of P0 cortices derived from CKO mice did not reveal any significant changes in these signals (Hashimoto et al., 2021b); however, it is possible that these signals are deregulated in cultured CKO NSCs because their proliferation is severely affected.

Roles of protein arginine methyltransferase 1 in the proliferation and differentiation of neural stem cells

A previous work has demonstrated that the knockdown of PRMT1 in NSCs reduced the potential for differentiation specifically in an astrocyte lineage through *Gfap* transcriptional repression, suggesting that PRMT1 is essential for the regulation of astrocytic differentiation (Honda et al., 2017). Although we have also tried differentiation assays using CKO NSCs, unfortunately, they did not survive well during differentiation (data not shown), so we could not collect enough data on differentiated cells. In our experiment, we found that PRMT1-deficient NSCs expressed the normal level of *Slc1a3* (GLAST) and *S100b*, which indicates an intact astrocytic differentiation potential after PRMT1 loss. Therefore, it is implied that the deregulation of astrocytic differentiation by loss of PRMT1 occurs in a setting in which NSC differentiation was strongly induced.

Our previous study has shown that OLIG2-positive oligodendrocyte precursor cells (OPCs) or immature oligodendrocytes were specifically reduced in PRMT1-deficient neonatal brains (Hashimoto et al., 2016). In the present study, CKO NSCs expressed a lower level of *Nkx2.2* and *Cnp* compared to control NSCs, in accordance with our previous findings. Therefore, it is implied that the oligodendrocyte differentiation potential was already affected in PRMT1-deficient NSCs. In addition to this, as we have previously suggested, brain inflammatory changes in CKO mice could have an additional negative impact on the survival and differentiation of OPCs (Hashimoto et al., 2021b).

Several recent studies are aimed at modulating NSCs for transplantation at neuronal injury sites (Yousefifard et al., 2016; Marsh and Blurton-Jones, 2017; Kitagawa et al., 2022). Therefore, it is of great importance to explore a novel molecular control of NSC proliferation, survival, and differentiation. Our findings that PRMT1 is essential for NSC survival and proliferation emphasize that arginine methylation is vital for NSCs. Furthermore, the unexpectedly normal proliferation of PRMT1-deficient NSCs *in vivo* prompts us to identify some extracellular factors that could support the survival of NSCs. Further molecular studies will pave the way for new therapeutic strategies for neuronal injury.

Data availability statement

The original contributions presented in this study are included in the article/**Supplementary material**, further inquiries can be directed to the corresponding author.

Ethics statement

This animal study was reviewed and approved by the Gifu University.

Author contributions

KT, AK, AY, and KI performed the experiments. MH and KT wrote the original manuscript. KM, CS-N, YK, AF, and TN

revised the manuscript. All authors contributed to the article and approved the submitted version.

Funding

This work was partially supported by the JSPS KAKENHI Grant-in-Aid for Research Activity Start-up (17H06730), Grant-in-Aid for Young Scientists (20K15913), Inamori Foundation Research Grants, the Gifu University, Yoshizaki Research Support Fund (YRSF), and the Cooperative Research Project Program of Life Science Center for Survival Dynamics, Tsukuba Advanced Research Alliance (TARA Center), the University of Tsukuba to MH, as well as Grant-in-Aid for Scientific Research (A) (17H01519), the Mitsubishi Foundation, and a grant from AMED-CREST, AMED (22gm1410010h0002) to AF.

Acknowledgments

We thank Swapna Paramanya Biswas (Gifu University) for the technical assistance.

Conflict of interest

The authors declare that the research was conducted in the absence of any commercial or financial relationships that could be construed as a potential conflict of interest.

Publisher's note

All claims expressed in this article are solely those of the authors and do not necessarily represent those of their affiliated organizations, or those of the publisher, the editors and the reviewers. Any product that may be evaluated in this article, or claim that may be made by its manufacturer, is not guaranteed or endorsed by the publisher.

Supplementary material

The Supplementary Material for this article can be found online at: https://www.frontiersin.org/articles/10.3389/fnins.2022.948517/full#supplementary-material

References

Ables, J. L., Breunig, J. J., Eisch, A. J., and Rakic, P. (2011). Not(ch) just development: Notch signalling in the adult brain. *Nat. Rev. Neurosci.* 12, 269–283. doi: 10.1038/nrn3024

Attardi, L. D., Reczek, E. E., Cosmas, C., Demicco, E. G., McCurrach, M. E., Lowe, S. W., et al. (2000). PERP, an apoptosis-associated target of p53, is a novel member of the PMP-22/gas3 family. *Genes Dev.* 14, 704–718. doi: 10.1101/gad.14.6.704

Bauer, S. (2009). Cytokine control of adult neural stem cells. *Ann. N. Y. Acad. Sci.* 1153, 48–56. doi: 10.1111/j.1749-6632.2009.03986.x

Bedford, M. T., and Clarke, S. G. (2009). Protein arginine methylation in mammals: Who, what, and why. *Mol. Cell* 33, 1–13. doi: 10.1016/j.molcel.2008.12.013

Bezzi, M., Teo, S. X., Muller, J., Mok, W. C., Sahu, S. K., Vardy, L. A., et al. (2013). Regulation of constitutive and alternative splicing by PRMT5 reveals a role for Mdm4 pre-mRNA in sensing defects in the spliceosomal machinery. *Genes Dev.* 27, 1903–1916. doi: 10.1101/gad.219899.113

Blanc, R. S., and Richard, S. (2017). Arginine methylation: The coming of age. *Mol. Cell* 65, 8–24. doi: 10.1016/j.molcel.2016.11.003

Bond, A. M., Ming, G. L., and Song, H. (2015). Adult mammalian neural stem cells and neurogenesis: Five decades later. *Cell Stem Cell* 17, 385–395. doi: 10.1016/j.stem.2015.09.003

Braunschweig, L., Meyer, A. K., Wagenführ, L., and Storch, A. (2015). Oxygen regulates proliferation of neural stem cells through Wnt/β-catenin signalling. *Mol. Cell Neurosci.* 67, 84–92. doi: 10.1016/j.mcn.2015.06.006

Campos, L. S., Leone, D. P., Relvas, J. B., Brakebusch, C., Fässler, R., Suter, U., et al. (2004). Beta1 integrins activate a MAPK signalling pathway in neural stem cells that contributes to their maintenance. *Development* 131, 3433–3444. doi: 10.1242/dev.01199

Chen, L., Zhang, M., Fang, L., Yang, X., Cao, N., Xu, L., et al. (2021). Coordinated regulation of the ribosome and proteasome by PRMT1 in the maintenance of neural stemness in cancer cells and neural stem cells. *J. Biol. Chem.* 297:101275. doi: 10.1016/j.jbc.2021.101275

Chenn, A., and Walsh, C. A. (2002). Regulation of cerebral cortical size by control of cell cycle exit in neural precursors. *Science* 297, 365–369.

Chittka, A. (2010). Dynamic distribution of histone H4 arginine 3 methylation marks in the developing murine cortex. *PLoS One* 5:e13807. doi: 10.1371/journal.pone.0013807

Gross, A., and Katz, S. G. (2017). Non-apoptotic functions of BCL-2 family proteins. *Cell Death Differ.* 24, 1348–1358. doi: 10.1038/cdd.2017.22

Hashimoto, M., Hirata, T., Yonekawa, C., Takeichi, K., Fukamizu, A., Nakagawa, T., et al. (2020). Region-specific upregulation of HNK-1 glycan in the PRMT1-deficient brain. *Biochim. Biophys. Acta Gen. Subj.* 1864:129509. doi: 10.1016/j.bbagen.2019.129509

Hashimoto, M., Kumabe, A., Kim, J. D., Murata, K., Sekizar, S., Williams, A., et al. (2021b). Loss of PRMT1 in the central nervous system (CNS) induces reactive astrocytes and microglia during postnatal brain development. *J. Neurochem.* 156, 834–847. doi: 10.1111/jnc.15149

Hashimoto, M., Fukamizu, A., Nakagawa, T., and Kizuka, Y. (2021a). Roles of protein arginine methyltransferase 1 (PRMT1) in brain development and disease. *Biochim. Biophys. Acta Gen. Subj.* 1865:129776.

Hashimoto, M., Murata, K., Ishida, J., Kanou, A., Kasuya, Y., and Fukamizu, A. (2016). Severe hypomyelination and developmental defects are caused in mice lacking protein arginine methyltransferase 1 (PRMT1) in the central nervous system. *J. Biol. Chem.* 291, 2237–2245. doi: 10.1074/jbc.M115.684514

Hirabayashi, Y., Suzki, N., Tsuboi, M., Endo, T. A., Toyoda, T., Shinga, J., et al. (2009). Polycomb limits the neurogenic competence of neural precursor cells to promote astrogenic fate transition. *Neuron* 63, 600–613. doi: 10.1016/j.neuron.2009.08.021

Honda, M., Nakashima, K., and Katada, S. (2017). PRMT1 regulates astrocytic differentiation of embryonic neural stem/precursor cells. *J. Neurochem.* 142, 901–907. doi: 10.1111/jnc.14123

Jackson-Weaver, O., Ungvijanpunya, N., Yuan, Y., Qian, J., Gou, Y., Wu, J., et al. (2020). PRMT1-p53 pathway controls epicardial EMT and invasion. *Cell Rep.* 31:107739. doi: 10.1016/j.celrep.2020.107739

Kazanis, I., and ffrench-Constant, C. (2011). Extracellular matrix and the neural stem cell niche. *Dev. Neurobiol.* 71, 1006–1017. doi: 10.1002/dneu.20970

Kim, H. J., Lee, E., Nam, M., Chung, J. K., Joo, S., Nam, Y., et al. (2021). Contribution of extracellular matrix component landscapes in the adult

subventricular zone to the positioning of neural stem/progenitor cells. *Exp. Neurobiol.* 30, 275–284. doi: 10.5607/en21012

Kitagawa, T., Nagoshi, N., Kamata, Y., Kawai, M., Ago, K., Kajikawa, K., et al. (2022). Modulation by DREADD reveals the therapeutic effect of human iPSC-derived neuronal activity on functional recovery after spinal cord injury. *Stem Cell Rep.* 17, 127–142. doi: 10.1016/j.stemcr.2021.12.005

Kumar, A., Placone, J. K., and Engler, A. J. (2017). Understanding the extracellular forces that determine cell fate and maintenance. *Development* 144, 4261–4270. doi: 10.1242/dev.158469

Li, X., Liu, X., Josey, B., Chou, C. J., Tan, Y., Zhang, N., et al. (2014). Short laminin peptide for improved neural stem cell growth. *Stem Cells Transl. Med.* 3, 662–670. doi: 10.5966/sctm.2013-0015

Mah, L. J., El-Osta, A., and Karagiannis, T. C. (2010). gammaH2AX: A sensitive molecular marker of DNA damage and repair. *Leukemia* 24, 679–686. doi: 10.1038/leu.2010.6

Marques, M. R., Horner, J. S., Ihrie, R. A., Bronson, R. T., and Attardi, L. D. (2005). Mice lacking the p53/p63 target gene Perp are resistant to papilloma development. *Cancer Res.* 65, 6551–6556. doi: 10.1158/0008-5472.CAN-05-0366

Marsh, S. E., and Blurton-Jones, M. (2017). Neural stem cell therapy for neurodegenerative disorders: The role of neurotrophic support. *Neurochem. Int.* 106, 94–100.

Miyata, T. (2008). Development of three-dimensional architecture of the neuroepithelium: Role of pseudostratification and cellular 'community'. *Dev. Growth Differ.* 50(Suppl. 1), S105–S112. doi: 10.1111/j.1440-169X.2007.00980.x

Mohyeldin, A., Garzón-Muvdi, T., and Quiñones-Hinojosa, A. (2010). Oxygen in stem cell biology: A critical component of the stem cell niche. *Cell Stem Cell* 7, 150–161. doi: 10.1016/j.stem.2010.07.007

Molofsky, A. V., Krencik, R., Ullian, E. M., Tsai, H. H., Deneen, B., Richardson, W. D., et al. (2012). Astrocytes and disease: A neurodevelopmental perspective. *Genes Dev.* 26, 891–907. doi: 10.1101/gad.188326.112

Mutoh, T., Sanosaka, T., Ito, K., and Nakashima, K. (2012). Oxygen levels epigenetically regulate fate switching of neural precursor cells via hypoxia-inducible factor 1α-notch signal interaction in the developing brain. *Stem Cells* 30, 561–569. doi: 10.1002/stem.1019

Ohtsuka, T., and Kageyama, R. (2019). Regulation of temporal properties of neural stem cells and transition timing of neurogenesis and gliogenesis during mammalian neocortical development. *Semin. Cell Dev. Biol.* 95, 4–11. doi: 10.1016/j.semcdb.2019.01.007

Pathak, M. M., Nourse, J. L., Tran, T., Hwe, J., Arulmoli, J., Le, D. T., et al. (2014). Stretch-activated ion channel Piezo1 directs lineage choice in human neural stem cells. *Proc. Natl. Acad. Sci. U.S.A.* 111, 16148–16153. doi: 10.1073/pnas.1409802111

Polager, S., and Ginsberg, D. (2009). p53 and E2f: Partners in life and death. *Nat. Rev. Cancer* 9, 738–748. doi: 10.1038/nrc2718

Qi, Y., Cai, J., Wu, Y., Wu, R., Lee, J., Fu, H., et al. (2001). Control of oligodendrocyte differentiation by the Nkx2.2 homeodomain transcription factor. *Development* 128, 2723–2733. doi: 10.1242/dev.128.14.2723

Takebayashi, H., Nabeshima, Y., Yoshida, S., Chisaka, O., Ikenaka, K., and Nabeshima, Y. (2002). The basic helix-loop-helix factor olig2 is essential for the development of motoneuron and oligodendrocyte lineages. *Curr. Biol.* 12, 1157–1163.

Tang, J., Frankel, A., Cook, R. J., Kim, S., Paik, W. K., Williams, K. R., et al. (2000). PRMT1 is the predominant type I protein arginine methyltransferase in mammalian cells. *J. Biol. Chem.* 275, 7723–7730.

Vining, K. H., and Mooney, D. J. (2017). Mechanical forces direct stem cell behaviour in development and regeneration. *Nat. Rev. Mol. Cell Biol.* 18, 728–742. doi: 10.1038/nrm.2017.108

Wang, F. W., Hao, H. B., Zhao, S. D., Zhang, Y. M., Liu, Q., Liu, H. J., et al. (2011). Roles of activated astrocyte in neural stem cell proliferation and differentiation. *Stem Cell Res.* 7, 41–53. doi: 10.1016/j.scr.2011.03.004

Wang, H., Huang, Z. Q., Xia, L., Feng, Q., Erdjument-Bromage, H., Strahl, B. D., et al. (2001). Methylation of histone H4 at arginine 3 facilitating transcriptional activation by nuclear hormone receptor. *Science* 293, 853–857. doi: 10.1126/science.1060781

Yao, Y., Chen, Z. L., Norris, E. H., and Strickland, S. (2014). Astrocytic laminin regulates pericyte differentiation and maintains blood brain barrier integrity. *Nat. Commun.* 5:3413. doi: 10.1038/ncomms4413

Yousefifard, M., Rahimi-Movaghar, V., Nasirinezhad, F., Baikpour, M., Safari, S., Saadat, S., et al. (2016). Neural stem/progenitor cell transplantation for spinal cord injury treatment; a systematic review and meta-analysis. *Neuroscience* 322, 377–397.

Yu, W. P., Collarini, E. J., Pringle, N. P., and Richardson, W. D. (1994). Embryonic expression of myelin genes: Evidence for a focal source of oligodendrocyte precursors in the ventricular zone of the neural tube. *Neuron* 12, 1353–1362. doi: 10.1016/0896-6273(94)90450-2

Yu, Z., Chen, T., Hébert, J., Li, E., and Richard, S. (2009). A mouse PRMT1 null allele defines an essential role for arginine methylation in genome maintenance and cell proliferation. *Mol. Cell. Biol.* 29, 2982–2996. doi: 10.1128/MCB.00042-09

Frontiers in Pharmacology

Explores the interactions between chemicals and living beings

The most cited journal in its field, which advances access to pharmacological discoveries to prevent and treat human disease.

Discover the latest Research Topics

See more →

Frontiers

Avenue du Tribunal-Fédéral 34
1005 Lausanne, Switzerland
frontiersin.org

Contact us

+41 (0)21 510 17 00
frontiersin.org/about/contact